AN ASSESSMENT OF THE PERFORMANCE OF HIGH DENSITY POLYETHYLENE COPOLYMERS FOR NATURAL GAS DISTRIBUTION PIPES

By: Paul Francis McNally

A thesis submitted for the degree of Doctor of Philosophy to the University of Aston in Birmingham.

March 1980

This work has been done independently as a full-time external student of the University of Aston in Birmingham, and has not been submitted for any other degree.

ACKNOWLEDGEMENT

I would like to offer my sincere gratitude to Professor G. Scott, firstly for accepting me as his post-graduate student and, secondly, for his constructive assistance given throughout the whole period of preparation of this work. I also gratefully acknowledge both the financial assistance and use of technical facilities given to me by the Phillips Petroleum Company.

Gratitude is also due to Stephen Franck for his help as external supervisor and to Valerie Evans for typing the thesis and correcting my spelling and punctuation.

Finally, I would like to express my sincere apologies to my family for the neglect that they have inevitably suffered over the past four years and, more importantly, during the very formative years of my two children. My family's understanding and consideration for me during this time must ever be remembered.

SUMMARY

AN ASSESSMENT OF THE PERFORMANCE OF HIGH DENSITY POLYETHYLENE COPOLYMERS FOR NATURAL GAS DISTRIBUTION PIPE

PhD submission by Paul Francis McNally, 1980

The total thermoplastics pipe market in West Europe is estimated at 900,000 metric tonnes for 1977 and is projected to grow to some 1.3 million tonnes of predominantly PVC and polyolefins pipe by 1985. By that time, polyethylene for gas distribution pipe and fittings will represent some 30% of the total polyethylene pipe market.

The performance characteristics of a high density polyethylene are significantly influenced by both molecular weight and type of comonomer; the major influences being in the long-term hoop stress resistance and the environmental stress cracking resistance. Minor amounts of hexene-1 are more effective than comonomers lower in the homologous series, although there is some sacrifice of density related properties. A synergistic improvement is obtained by combining molecular weight increase with copolymerisation.

The long-term design strength of polyethylene copolymers can be determined from hoop stress measurement at elevated temperatures and by means of a separation factor of approximate value 22, extrapolation can be made to room temperature performance for a water environment. A polyethylene of black composition has a sufficiently improved performance over yellow pigmented pipe to cast doubts on the validity of internationally specifying yellow coded pipe for gas distribution service.

The chemical environment (condensate formation) that can exist in natural gas distribution networks has a deleterious effect on the pipe performance - the reduction amounting to at least two decades in log time. Desorption of such condensate is very slow and the influence of the more aggressive aromatic components is to lead to premature stress cracking.

For natural gas distribution purposes, the design stress rating should be 39 Kg/cm^2 for polyethylenes in the molecular weight range of 150 - 200,000 and 55 Kg/cm^2 for higher molecular weight materials.

Pipe market, Ethylene Copolymers, Hoop Stress, Stress Cracking.

L I S T O F C O N T E N T S

CHAPTER 1: MARKET NEED FOR POLYETHYLENE GAS DISTRIBUTION SYSTEMS

CHAPTER 2: THERMOPLASTICS (POLYETHYLENE) IN ENGINEERING APPLICATIONS

CHAPTER 3: STRUCTURE AND PERFORMANCE OF PHILLIPS POLYMERISED POLYETHYLENE

CHAPTER 8: APPENDICES

L I S T O F T A B L E S

CHAPTER 3: STRUCTURE AND PERFORMANCE OF PHILLIPS POLYMERISED POLYETHYLENE

CHAPTER 5: PIPE HOOP STRESS PERFORMANCE OF ETHYLENE COPOLYMERS

CHAPTER 6: CHEMICAL ENVIRONMENTAL INFLUENCE ON HOOP STRESS

LIST OF FIGURES AND PHOTOGRAPHS

CHAPTER 1: MARKET NEED FOR POLYETHYLENE GAS DISTRIBUTION SYSTEMS

CHAPTER 3: STRUCTURE AND PERFORMANCE OF PHILLIPS POLYMERISED POLYETHYLENE

CHAPTER 5: PIPE HOOP STRESS PERFORMANCE OF ETHYLENE COPOLYMERS

CHAPTER 1. MARKET NEED FOR POLYETHYLENE GAS DISTRIBUTION SYSTEMS

INTRODUCTION

Transportation by pipeline represents the cheapest mode of transport today, as evidenced (1) by the data in Table 1.1. Plastic materials compete with other and more traditional materials in this market on the basis of cost effectiveness.

TABLE 1.1 Energy Content of Transportation:

Transport Mode	Ton-Miles/Gallon Fuel
Road	10
Rail	125
Sea	250
Pipeline	500

Pipelines and pipeline materials represent a very broad topic and thus, for the purpose of this thesis, consideration is restricted to the medium density and high density polyethylenes in the application areas of natural gas distribution systems since this market segment constitutes the most serious consequences should pipeline failure occur.

Many of the natural gas grids in Western Europe were designed and built for the transmission and distribution of manufactured town gas. The operating conditions for such a system are different from the requirements for natural gas. As a consequence, with the advent of natural gas from the Groningen, North Sea, Russian and Algerian gas fields, the gas grids of Europe will have to undergo drastic change to accommodate the drier, higher pressure gas of much higher calorific value. This will necessitate not only changes in the consumer's applications such as gas cookers and gas fires, but also changes in the transmission and distribution of the gas itself.

This thesis reviews the experience gained during these changes that are now taking place and presents the results and conclusions of a programme to support the use of hexene-1 copolymers of ethylene over the presently used propylene and butene-1 copolymers for plastic systems for the distribution of the natural gas from the transmission lines to the consumers.

1.1 NATURAL GAS IN WEST EUROPE

The relative importance of Natural Gas in relation to other energy sources (2) is shown in Table 1.2 together with the projection to 1985.

TABLE 1.2 Percent Distribution of West European Energy Sources:

	1960	1975	1980	1985
Coal	57.3	20.8	18.2	16.0
Oil	31.0	55.7	53.3	53.6
Natural Gas	1.7	13.4	16.3	15.5
Nuclear	0.1	2.3	5.7	8.9
Other	9.9	7.8	6.5	6.0

Natural gas will thus represent 16.3% of West Europe's 1500 million tons of oil equivalent energy demand by 1980 and 15.5% of the projected 1985 energy demand which is forecast to be almost 2000 million tons of oil equivalent energy.

Much of this gas, in comparison to manufactured gas, is relatively free of aggressive aromatic hydrocarbons (although some condensate is always present) is available at high pressure from the well head and has at least twice the calorific value as shown in Table 1.3.

TABLE 1.3 Calorific Value of Natural Gas

Average value for Town gas	4,000 Kcal/M^3 (3)
Natural gas from Groningen	8,400 Kcal/M^3 (4)
Nat. Gas from Ekofisk field	10,000 Kcal/M^3 (5)
Natural Gas from Algeria	10,600 Kcal/M^3 (3)

Prior to 1969, the countries having any experience of importance in the use of plastics materials for the distribution of gas were France, Italy, West Germany, the U.K. and Holland (9). A summary of these plastic pipe installations up to that date are shown in Table 1.4.

TABLE 1.4 Plastic Pipe Installations up to 1969

Country	Installed Length Km	Material	Years Experience
France	50	PVC	15
Italy	several hundred	PVC	10
Germany	1500	PVC	10
U.K.	300	PVC	10
Holland	7268	PVC	15

1.2 NATIONAL GAS GRIDS IN WEST EUROPE

Most European gas grids can be arbitrarily classified into three parts, a high pressure main, a district feeding system and the consumer service lines. A typical grid is that shown in figure 1.1 which relates to a town of population 20,000 in Holland (6).

The high pressure main is of steel and in pipe diameters ranging up to a maximum of 1,200 mm. Depending on the length of the pipeline, operating pressures

can be up to 60 Kg/cm^2. A pipeline of 1,220 mm diameter operating at 55 Kg/cm^2 internal pressure carries 10,000 million cubic metres of gas per year. A pipeline of 1,420 mm diameter and operating at 75 Kg/cm^2 pressure carries three times as much volume (7).

These lines, due to the high pressures involved, will remain the domain of steel. However, the four possible applications for polyethylene pipe in gas distribution are the renewal of old or installation of new services and the renewal of old or installation of new district lines.

The district feeding system was originally designed to operate at very low pressures, generally in the range of 0.5 Kg/cm^2. In certain instances the pressure from the main is reduced at a central regulator and the gas at 0.1 to 0.3 Kg/cm^2 pressure is distributed through the cast iron district feeding system into the service lines directly to the consumer. In order instances where the district system has been modernized, gas can be distributed throughout the district system and even into the service lines at pressures between 2 to 4 Kg/cm^2 with a regulator reducing the pressure to 0.3 Kg/cm^2 prior to the user's meter.

Thus no standardisation of distribution system exists and it is possible for pipes from 25 mm to 150 mm in diameter to be working at pressures ranging from 0.1 Kg/cm^2 to 4 Kg/cm^2 with gas from different origins and methods of manufacture.

A table of some of the pressure ranges found in European gas grids (8) is tabulated below in Table 1.5.

TABLE 1.5 Distribution of Gas Pressures in European Countries (Units Kg/cm^2)

	Belgium	France	Ireland	Holland	U.K.
Mains	67-15	67-4	1.4	8-1.5	25-2
Feed to District	15-4	16-4	0.3	3-0.8	2-0.5
District	4-0.4	4-0.4	0.025	1-0.2	2-0.5
Medium Pressure Net	0.4-0.05	0.4-0.05	0.025	0.1-0.04	2-0.5
Low Pressure Net	0.05	-	0.025	0.03	0.02

1.3 NATIONAL GAS INDUSTRIES STRUCTURE AND PIPE DEMAND

1.3.1 United Kingdom Industry Structure

In 1949, 275 municipal and 789 company owned gas distributors in the United Kingdom were grouped into 12 autonomous area boards which today are regionally responsibile for all gas sales. Natural gas accounts

for 83% of total sales and 76% of the total of 13,750,000 consumers have been converted from the older manufactured gas.

The gas system of transmission and distribution in the U.K. comprises approximately 195,000 kilometres of main and is largely of cast iron.

Transmission refers to the national grid carrying gas to the area boards at pressures up to 70 Kg/cm^2 and the super grids of the boards themselves carrying gas at pressures as high as 25 Kg/cm^2.

The distribution consists of feeder lines, district mains and services. Feeder lines carry gas from the producing plant, gasholder or from the super grid via a pressure reduction regulator and feed it into the district mains. District mains then carry the gas along the length of roads and, in turn, feed into services which carry the gas to the consumer's meter.

The mains vary in diameter from 1200mm for the large feeder lines to 75-150mm for the district mains. Services are usually between 20mm to 50mm in diameter.

With the advent of oil gasification and then in turn North Sea gas, pressures in the region of 25 Kg/cm^2

have become available to replace the low pressure coal gas of 0.1 Kg/cm^2 for which the bulk of the present day distribution system was designed and built.

The high pressures cannot, from strength considerations, be fed directly into the old mains but, where possible, pressure is kept as high as 0.1 - 0.3 Kg/cm^2 in the feeder mains and is then reduced to below 0.1 Kg/cm^2 before entering the district mains.

High pressure distribution is widely used although it seldom reaches all the way to the customer. New housing areas are crowded and might contain 10 to 30 homes per acre. The cost of a central pressure reduction service regulator tends to perpetuate low pressure distribution in such circumstances.

Furthermore, British customers are unused to and unwilling to accept outdoor pressure regulator sets. Older distribution systems may serve many streets of terraced property in which case the service pipes to the main are short, connections are numerous, and conditions again favour the continuance of low pressure distribution. However there are cases, especially in new installations, where distribution at 2 Kg/cm^2 with individual service pressure regulators

is well established.

U.K. Codes of Practice do not permit plastic pipe or compression joints to be laid closer than 1 meter from buildings unless they are installed within a gas-tight fireproof casing. The most common arrangement is to use a screwed steel service entry and riser within the house, and an end loading compression fitting for the steel/polyethylene connection outside the house wall. Another method, likely to grow in acceptance uses a 32 mm screwed steel casing and riser which is installed by the house builder. A 25 mm polyethylene service is later pushed through and fixed at the head of the casing by a fitting in which the compression joint is enclosed by screwed joints.

1.3.2 United Kingdom Pipe Demand

Prior to 1969 all plastics pipe gas distribution systems were in PVC, but this practice has since been discontinued and some of the 1200 kilometres of existing PVC lines, in pipe dimeter ranges varying from 16 mm to 200 mm, may have to be replaced due to the greater preoccupation with safety and concern over the relative fragility of PVC distribition systems.

The introduction of a complete integral plastics pipe system by du Pont marked the changeover from PVC to Medium Density Polyethylene and already by April 1974 approximately 8000 kilometres of various grades of polyethylene had been installed in diameters ranging from 16 mm to 150 mm. The annual growth of polyethylene services and mains installed per annum and an extrapolation of that growth is shown in Table 1.6 (12).

TABLE 1.6 Growth of U.K. Polyethylene Gas Distribution System

Year	Kilometres of Polyethylene	Cumulative Total
1971/72	800	800
1972/73	2,400	3,200
1973/74	4,000	7,200
1974/75	5,600	12,800
1975/76	6,400	19,200
1976/77	8,000	27,200
1977/78	10,000	37,200
1978/79	12,500	49,700
1979/80	15,600	65,300

The future potential for polyethyelene pipe systems in the U.K. is based on two factors:

1.3.2.1 Renewal and Extension of Exsiting Network

The existing network consists of 192,000 kilometres. The average annual renewal rate has been 1%, and 25% of this 1,920 Km is renewed using high density and medium density polyethylene pipes. Pipe diameter varies between 63 mm and 125 mm. This thus represents an annual demand of some 1000 metric tonnes. The British Gas Corporation intend that the renewal rate using polyethylene will triple to represent an annual demand of some 3400 metric tonnes.

The speciality large diameter relining of the existing network is estimated at a maximum of 2 Km per year of 315 mm diameter pipe, giving an additional annual requirement of 60 metric tonnes.

The extension of the existing network to feed new consumers is estimated at 130 consumers per Kilometer. A 25% polyethylene penetraction of new consumer lines gives an annual demand of 1200 metric tonnes.

1.3.2.2 Service Line Installations and Renewals

An average of 300,000 service renewals and the same number of new services have traditionally been installed yearly. However, in recent years, this figure has dropped dramatically to approximately

100,000. Pipe size lies between 25 and 32 mm in diameter and service line length between 8 and 16 metres. This represents an annual requirement of 1500 metric tonnes. This figure is based on achieving gas supply to 75% of the new housing starts in the public and private sector.

New housing starts in the past and those forecast (10, 11) for 1979 are:

TABLE 1.7 U.K. New Housing Starts

Year	New House Starts
1972	361,322
1973	337,214
1974	259,739
1975	310,168
1978	157,600
1979 Est.	137,800

In July 1976 the British Gas Corporation converted wholly to the metric system and the opportunity was taken to rationalise the range of metric systems and the four sizes adopted for mains distribution have been 63, 90, 125 and 180 mm to replace the previously used 2, 3, 4 and 6 inch equivalents. In addition to these sizes, 75 mm pipe has been specified for insert

renewal of deteriorating 4 inch cast iron mains. For services, the metric equivalents of 3/4 and 1 inch service systems, namely 25 and 32 mm, are specified.

1.3.3 Benelux Industry Structure

There are in the Benelux countries 150 gas distribution companies almost all municipally owned, who distribute gas in their supply area for domestic and smaller industrial use. Pressures in the distribution grid vary from 8 bar to 30 m bar and the practices employed are essentially the same as those outlined for the U.K.

The Dutch distribution grid was comprised of 60,200 Km in December 1974 and pipeline material distribution is shown by the following percentages:

TABLE 1.8 Distribution of Gas Distribution Pipe-Line Materials

	1971	1972	1973	1974
Steel	21.1	20.0	20.0	19.7
Ductile Iron	1.8	2.0	2.0	1.83
Cast Iron	38.1	29.8	27.7	25.7
HDPE	2.5	3.9	4.6	5.2
U. PVC	30.5	34.8	35.7	36.0

TABLE 1.8 (Cont'd)

	1971	1972	1973	1974
I. PVC	3.0	5.5	6.1	7.4
Asbestos Cement	3.0	4.0	3.9	4.1

The average annual growth rate calculated over the period 1971-74 for each of the pipeline materials is:

TABLE 1.9 Growth of Gas Distribution Pipeline Materials

	Annual Growth 1971-4	Trend for Future
Steel	6.5%	slight decrease
Ductile Iron	10 %	slight increase
Cast Iron	- 4.3%	definite decline
HDPE	54.7%	definite increase
U. PVC (unplasticised)	17 %	definite decline
I. PVC (Impact)	72 %	definite increase
Asbestos Cement	25.7%	decline

The declining trends for U PVC, cast iron and asbestos cement are due to two prime factors; firstly, the greater preoccupation with safety and the use of tougher pipeline materials, and secondly, the trend towards higher distribution pressures at which these materials are not authorised for use.

The percentage distribution of pressure is compared for 1971 and 1974 in the following table:

TABLE 1.10 Pressure Levels in Dutch Gas Distribution Grid

Pressure Level	Percentage of distribution grid		
Kg/cm^2	1971	1974	% Change
0.03	44.6	33	- 26
0.1	39.3	46.8	19
1	4.9	5.3	8
3	3.9	4.7	20.5
8	7.3	10.2	39.7

1.3.4 Benelux Pipe Demand

In Holland and Belgium there is a strong tendency towards the use of tougher materials for gas distribution purposes; toughness not only from the point of view of impact strength, but also chemical resistance, higher pressure resistance and overall greater safety possibilities. Thus there is a change from unplasticised PVC to higher impact resistant PVC grades and polyethylene. There is also concern over the effect of the gas constituents on the plastics pipelines and here the medium density and high density polyethyelenes have a big advantage.

1.3.4.1 Renewal and Extension of Existing Network

The programme of network renewal, specifically in Holland, centres on the replacement of the existing 21,700 Km of PVC and 15,500 Km of cast iron pipe over the next 10-15 year period. 60-70% of the PVC replacement will be with polyethylene, the remainder probably with impact modified PVC where pressure considerations will allow its use. Pipe diameters are between 63 mm and 125 mm, giving an annual requirement of 200 MT of polyethylene. (M.T. = Metric tonnes)

It is estimated that only 25% of the replacement of the cast iron lines will be with polyethylene, the main replacement material being ductile iron, due to the larger diameters involved.

Large diameter reline using HDPE is estimated at a maximum of 3 Km per year, giving an annual resin requirement of 100 MT.

TABLE 1.11 Pipe Diameters in Dutch Distribution Grid

	Pressure Level	
Pipe Diameter	> 0.1 Kg/cm^2	< 0.1 Kg/cm^2
Less than 110 mm	82.0%	16.8%
125-200 mm	15.7%	33.0%
Greater than 250 mm	2.3%	50.2%

In Belgium less than 0.8% of the 17,680 Km of gas distribution network is in plastics materials and of this total, 30 Km are in HDPE. For the immediate future, plastics pipe will be used only for service line connections and low pressure distribution mains. Some 500 MT is estimated for network renewal.

92% of the Dutch population is already served by gas, hence over the next five years very little new consumer connections need to be made. The number of housing starts is estimated by the gas companies to be 3.5% per year, giving an annual potential of 1000 Km of gas head-main per year for both distribution and service lines. 20% is estimated for the distribution network extension which at an average pipe weight of 2.079 Kg/m represents an annual requirement of 420 MT.

Network extension in Belgium is made using polyethylene coated steel, expect for low pressure distribution mains. Maximum potential for polyethylene pipe is thus only 500 MT.

1.3.4.2. Service Line Installations and Renewals

The standard for cost purposes is still PVC pipe with a rubber ring push fit joint. This sytem is cheap, easily and quickly made, and relatively fool

proof from the point of view of installation by the contractors. Thus impact modified PVC using chlorinated polyethylene as impact modifier is well placed as one of the preferred materials. The monolithic joint of polyethylene is psychologically good, but is approximately 40% more expensive. In many service line installations, the number of fittings and joints on a cost basis far outweighs the cost of the pipe.

Polyethylene for new service line installations in Holland is estimated at 80% of the annual 1000 Km of gas head-main which, at a pipe weight of 0.219 Kg/M, gives an annual requirement of 175 MT. A similar usage can be applied to Belgium.

1.3.5 West Germany Industry Structure

The gas manufacturing and distribution industry in Western Germany is composed of both public and privately owned companies, although in both cases the responsibility of distributing the gas to the final consumer rests with the municipal authorities.

At the present time the total gas grid consists of 99,500 Km, of which 70,925.6 Km is low pressure distribution network. 2.7% of the distribution grid is in plastics material and this predominantly in PVC. The only specification relating to plastics gas

distribution pipe is on PVC, although a specification for polyethylene is in the final stages of preparation and its publication would act as a spur towards a much greater use of polyethylene similar to that in Holland.

Most of the natural gas used in Germany originates from Holland and thus the same technical considerations for plastics gas pipe in Holland will apply in Germany.

There are a wide variety of trial lines under evaluation at pressure levels up to 8 Kg/cm^2. The favourable results being shown by polyethylene are in agreement with results obtained in other Western European countries.

The relation between the gas distribution grid and the pipe capacity is as follows:

TABLE 1.12 Relation Between Gas Grid & Pipe Capacity

Pipe Capacity (million m^3)	Pipe Length Kilometres	Private (mil. m^3)	Industrial (million m^3)
over 50	42,985.3	4,261	5,148.8
25 - 50	7,903.6	851.8	996.6
5 - 25	15,014.2	1,176.5	1,399
2.5 - 5	3,003.0	158.7	191.8
under 2.5	2,019.5	69.6	81.9
Totals	70,925.6	6,517.6	7,818.1

The yearly rate of pipe installation for the distribution grid is 2000 Km and the material distribution is:

TABLE 1.13 Pipe Material Distribution in W. Germany

	1974	1973
Cast iron	2.7%	3.3%
Ductile iron	13.1%	13.7%
Steel	68.0%	70.3%
Total Plastics	16.0%	12.6%

There is a wide divergence in the percentage use of pipe materials in the different regions of West Germany (13).

TABLE 1.14 Geographic Distribution of Plastics Gas Pipe Use in West Germany

Region	% metal (installed 1974)	% Plastics
Schleswig	42	58
Hamburg	100	-
Niedersachsen	73	27
Bremen	78	22
Norderheim - Westfalen	81	19
Hessen	82	18
Rheinland - Pfalz	94	6
Baden - Wurttenberg	97	3
Bayern	99	1
Saarland	100	-
Berlin	100	-

There are at present 6.5 million private consumers, of which 20% are still using coal gas. With the increase in the importation of natural gas, the number of consumers is projected to double. In addition, 50% of the new housing starts are expected to be supplied with natural gas. The number of housing starts dropped from 700,000 in 1974 to 400,000 in 1975.

1.3.6 West German Pipe Demand

No data are available pertaining to network renewal although, like Holland, the existing regid PVC and cast iron lines will need to be replaced over the next 10 years. It is assumed that the bulk of the cast iron will be replaced by ductile iron and that some 75-80% of the existing 2,700 Km of PVC will be replaced by polyethylene. This could provide a market requirement of 4,500 MT over the ten year period.

The present 320 Km of plastics gas pipe installed annually for network extension, will increase to 600 Km of which a minimum of 80% will be in polyethylene. At an average pipe weight of 2.097 Kg/m, this represents an annual resin requirement of 1010 MT.

The number of housing starts in Germany is now estimated at 350-400,000 and with the increasing importance of imported gas from Russia, the North Sea via the new Emden terminal and the Dutch gas, some 75% of the new housing starts can be expected to be new gas consumers. At an average of 2.5 Kg of polyethylene per consumer, the polyethylene pipe consumption for both new installations and service line renewals will amount to 875 MT.

1.3.7 Denmark Industry Structure

Until recently, no natural gas existed in Denmark. However, towards the end of 1978, 1.5 to 2 milliard (10^9) cubic metres of natural gas was delivered to the Jutland coast from the D.U.C. offshore fields. The completion of the planned trunk line from Norway will make available a further 3-4 milliard cubic metres. These deliveries will be monitored by the newly established state-owned oil and gas company and a subsidiary company, which will include representatives of the municipal authorities, will have the responsibility for building up the market, specifying materials and designing installation networks.

The distribution network is to be developed following the Dutch pattern and polyethylene will be used at pressures up to 4 Kg/cm^2.

Manufactured gas represents 1% of the total Danish energy requirement and a further 2% is given by LPG and butane. The state intends that, by 1985, manufactured gas will be phased out and that natural gas will represent 15% of the total energy requirement. The gas will be used at its full calorific value and will be distributed to both private and industrial consumers. None will be used for electricity generation.

The Danish gas network consists of 188.1 Km of transport line, 254.9 Km of medium pressure distribution line, and 4,245.2 Km of low pressure distribution line.

Approximately 60% of the population is served by gas and of the total of 616,017 gas consumers, 98.3% are private household.

Private gas consumption accounts for 80% of the total and the remainder is made up of industry with 19.7% and street lighting 0.3%.

The largest area of private consumption is Copenhagen with 58% of the total private use and it is intended that this will be fed with the Norwegian gas. The bulk of the industrial use is on the mainland and this will be supplied from the D.U.C. fields.

1.3.8 Danish Pipe Demand

The network renewal is estimated at 1% of the total medium and low pressure network. Since these lines operate at less than 3 bar pressure, 80% of the renewal would be in polyethylene, giving an annual requirement of 100 MT. The relining requirement is estimated at 0.5% of the existing medium pressure network and represents a nominal 30 MT.

With respect to the extension of the network, the conversion of 99% of the population to natural gas over the next 10 years would require, at a rate of 1 Km/300 persons, a further 3150 Km which, at penetration of polyethylene, yields an annual requirement of 540 MT.

For new service line installations and renewal of existing services, a further 60 MT is required annually.

1.3.9 Spain: Industry Structure

There are presently 28 companies distributing town gas and/or natural gas in Spain. The following table is a summarised analysis of the importance of the 5 largest plants in the country totals.

TABLE 1.15 Relative Importance of Major Distribution Companies

City	Distribution Grid (Km)	%	Customers ('000)	Gas Prod'n (MM thermias)	%
Barcelona	1,955	37	453	1,936	48
Madrid	1,173	22	268	1,219	30
Valencia	335	7	56	129	3
Sevilla	267	5	28	109	3
Palma	262	5	44	129	3
Sub-total	3,992	76	849	3,522	87
Other 23	1,268	24	137	549	13
Total	5,260	100	986	4,071	100
% of 5 largest	76%		86%	87%	

The above figures refer to the distribution lines for low and medium (4 Km/cm^2) pressure, and do not include the figures of Gas Natural S.A. which supplies natural gas to industrial customers in the Barcelona area at 10 Kg/cm^2 pressure.

Catalana de Gas is the largest gas distribution company in Spain. It directly operates the town gas plants in Barcelona, Sevilla, Mauresa, Reus, and Villanueva y Geltru; their affiliate CEGAS (Compañia Española de Gas) operates the plants in Valencia, Malaga, Cadiz, Murcia, and Santander. The group

CATALANA/CEGAS accounts for 3,129 Km or nearly 60% of the total distribution grid, and for 2,357 million thermias or 58% of the total.

Natural gas was introduced in Spain late in the 1960's, when Gas Natural's LNG regasification plant started up. Catalana de Gas distributes it through their grid and uses it for town-gas production. Natural gas already accounts for 35% of Catalana's gas supplies, and the company plans to convert all its customers to natural gas in three years.

Spain's Energy Plan calls for the following use of natural gas:

TABLE 1.16 Spanish Energy Plan (14)

	1973	1980	1985
Total Energy $10^9 M^3$	68	105	140
Natural Gas $10^9 M^3$	0.9	7	15
Natural Gas share %	1.4%	6.8%	10.6%

The above plan is, however, considered as very optimistic by most experts. The $7.2 \times 10^9 M^3$ consumption in 1980 is practically impossible to reach and a more realistic figure is $5.5 \times 10^9 M^3$, provided the projected gas pipelines to Bilbao and Valencia are in full service, and the areas of Valencia, Tarragona, Zaragoza, and Bilbao are converted to natural

gas by then. The 1985 figure is very speculative; to reach it, a new large regasification plant or the gas pipeline from Algeria would be needed.

The Barcelona-Bilbao (646 Km) and Gandesa-Valencia (213 Km) gas lines will be 500-750 mm in diameter, and bids for their construction have already been asked for by ENAGAS, company responsible for the projects. Through these gas lines, natural gas regasified in Barcelona will be sent to Bilbao, Valencia and intermediate cities. For the increased needs of natural gas, ENGAS has signed a contract with SONATRACH for the supply of $4.5 \times 10^9 m^3$/Year from Skidda, Algeria.

The other gas line is a major international project, which is in the early phases of development and is not expected to materialise before 1982. Its feasibility has been studied by William Bros. and it would be operated by an international consortium (SONATRACH, Gas de France, ENAGAS, and others). It would carry $40 \times 10^9 m^3$/Year, of which $5\text{-}10 \times 10^9 m^3$ would be for Spain's consumption, and the rest would proceed to Portugal, France, Benelux, Switzerland, and possibly, Italy. The main technical difficulty being encountered is the crossing of the sea from Africa; the projected layout would run across Spain from South

to North through Madrid. Should this project materialise, several other regions of Spain would certainly be converted to natural gas during the period 1982-85.

1.3.10 Spain Pipe Demand

Catalana uses low pressures distributed through steel pipe in densely-populated areas and medium pressures distributed through plastics pipe in the new areas. Plastics pipe (PVC) is limited to 80% of the new installations and 25% of replacement lines.

The annual requirements for the distribution grid of Catalana de Gas can be summarised as:

TABLE 1.17 Catalana Distribution Grid in Plastics

	Total Km		
Area	1976	1980	Approx. breakdown
Barcelona city	22	24	100% low pressure
Barcelona area	76	105	50% low 50% medium
Reus, Manresa, Villanova	10	12	90% low 10% medium
Seville	20	21	90% low 10% medium
New Areas	9	9	100% medium
	137	171	

Assuming a low pressure pipe diameter of 110 mm at a pipe weight of 2 Kg/m and a medium pressure pipe diameter of 50 mm of pipe weight 0.7 Kg/m, the projected

total Spanish polyethylene requirements can be given as:

TABLE 1.18 Projected Spanish Polyethylene Gas Pipe Demand

Dist. Company	Km	MT
Catalana	171	267
Cegas	20	30
Others	64	100
	255	397

1.4 TOTAL EUROPEAN MARKET DEMAND

The greatest potential for gas distribution systems based on polyethylene is to be found in the Central West European area, comprising the Benelux countries, West Germany, France and the U.K. These countries already have a significant supply of natural gas. Areas of future new demand for polyethylene gas distribution systems will be Spain and the Scandinavian countries, principally Denmark.

Between 1976 and 1980 the requirement for natural gas distribution pipe and fittings based on polyethylene is estimated at a total of 58,000 metric tonnes (MT) for the five-year period, increasing from 6,000 MT in 1976 at an average annual growth rate of 25.9% to reach 19,000 MT by 1980.

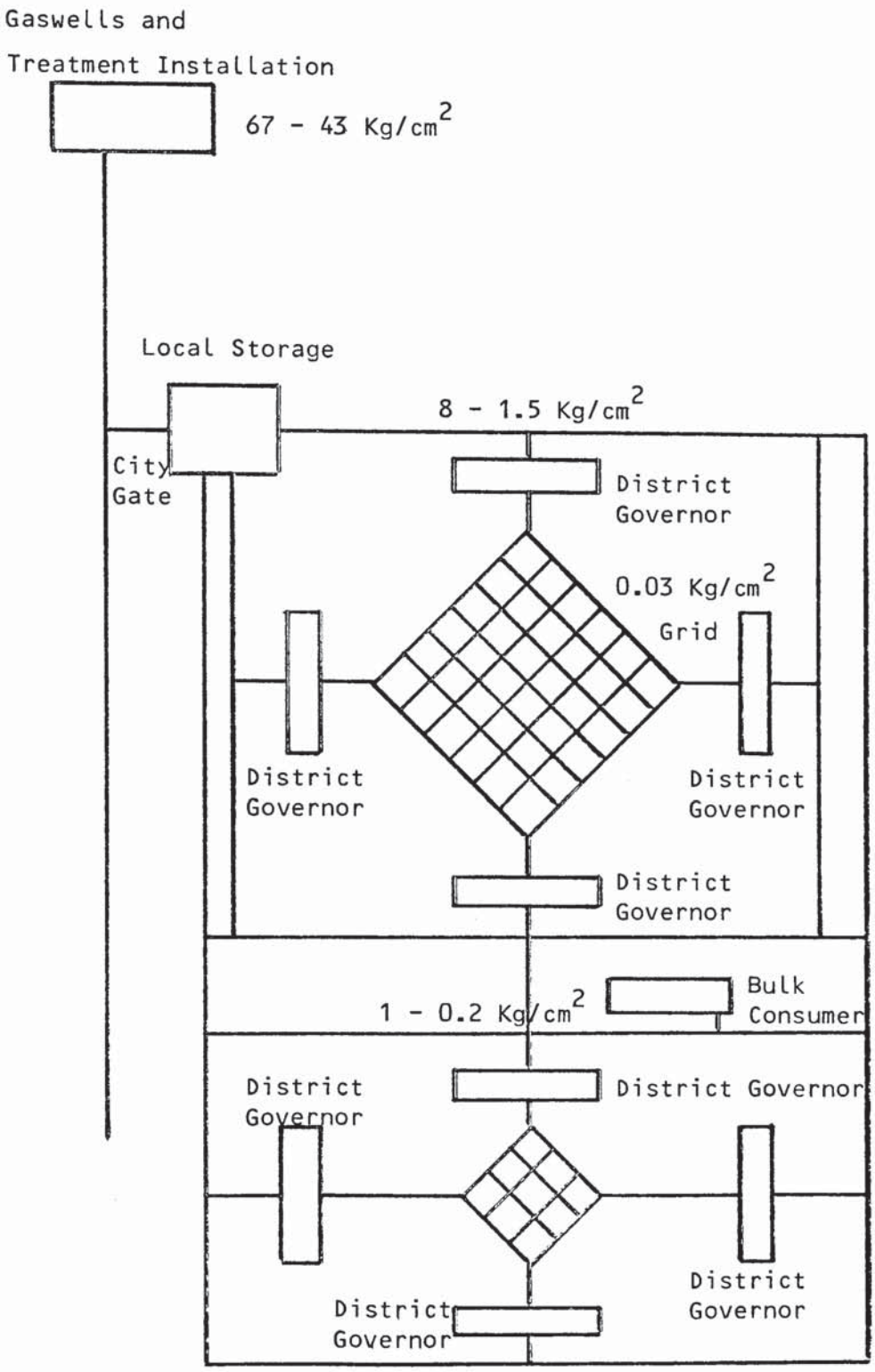

Fig. 1.1 SCHEME OF TYPICAL GAS GRID

Although it is unlikely that such growth rates can be maintained throughout the next five year period, the projected demand by 1985 in the European Economic Community area of 43,000 MT (15) will represent 30% of the total high density polyethylene pipe consumption at that time.

It is important that with such a projection of significant usage, the material be adequately researched as to its long-term suitability with respect to all the applicable safety aspects concerning the distribution and supply of a dangerous explosive substance such as natural gas.

CHAPTER 2. THERMOPLASTICS (POLYETHYLENE) IN ENGINEERING APPLICATIONS

INTRODUCTION

"Plastics" like "metals" denote a broad variety of engineering materials that must be carefully selected for the particular application. The family of thermoplastics has over the past decade been the fastest growing group of materials, and in important technical fields the more traditional materials are being increasingly replaced at a very fast rate by these thermoplastics which, no more than 30 years ago, were considered as curiosities. The reasons for this growth and replacement are that plastics possess a unique combination of design freedom, ease of fabrication and end product properties not offered by other materials that make them ideal candidates for the application of pipe.

2.1 COMPARISON OF PLASTICS WITH METALS

The proposed use of thermoplastics in general, and polyethylene in particular, as an engineering material invariably demands the comparison of polymeric materials with the more traditional engineering materials, such as metals. In the application being considered, namely gas distribution systems, the

comparison between polyethylene and the traditionally used steel and cast iron, reveals several major advantages for the polymerics. These can be summarised as (16, 17, 18, 19):

i: Resistance to a wide range of chemicals, corrosive acids, oils, petrols fats, fungi and bacteria, which more specifically is resistance to the chemical and physical aggression of the natural environment (20).

ii: Lightness and sufficient flexibility to be coiled for convenience in storage, shipping and installation, giving a reduction in carriage costs, ease of handling and a reduced number and size of support fixtures for above ground installation (21).

iii: Improved internal smoothness and low coefficient of friction, giving better flow properties and absence of scale formation (22,23). This generally results in the use of plastics pipe of smaller internal diameter.

iv: Simple jointing techniques of thermoplastics and fitting either by heat welding (24, 25, 26) or application of suitable solvent cements (27, 28). In addition, compatibility with metal or other plastics systems already installed (29).

v: Excellent electrical insulating properties (30). A point of no minor concern in the distribution of natural gas.

vi. Absence of maintenance and decoration costs (31)

vii: Rapid installation by less skilled personnel (32).

viii: Strength and durability to provide long service under the normal internal and external stresses at economical cost (33).

However, in a plastics gas distribution system comprising pipe, fittings and various valve assemblies three distinct disadvantageous situations of great practical importance could occur (34).

i: A component stressed for a period of time (not necessarily long) may cease to function properly because of changed dimensions.

ii: A component, as in (i) may fail, either by a cracking process or by a process analogous to tertiary creep in metals.

iii: A component stressed rapidly may fail, more or less immediately, in either a brittle or a ductile manner.

Some of the usually published property data purporting to indicate these particular modes of behaviour are often inadequate since they are based on "hand-me-down" tests of older technologies with only minor regard to the viscoelastic nature of plastics materials.

Metals are fundamentally composed of atoms arranged in specific geometric lattices, most common metals having either a body centred cubic crystal structure as in the case of alpha-iron, chromium, and tungsten, or a face centred cubic crystal structure such as aluminium and nickel (35). The metal structure is made up of an aggregate of crystal grains having different properties in different crystallorgraphic directions. However, the equations of strength of materials describe the behaviour of real metals, because in general the crystal grains are so small that for a specimen of any macroscopic volume the materials are statistically homogeneous and isotropic (36).

Plastics, unlike metals, are organic materials and as such differ markedly in structure and behaviour from metals; moreover, plastics materials have a much greater sensitivity to environmental conditions than metals and their mechanical properties are therefore more dependent on time and temperatures.

2.2 STRUCTURE AND PROPERTIES OF POLYMERS

2.2.1 Level of Organisation

Bawn (37) defines and distinguishes three levels of organisation of the structure:

i: Chemical: The chemicals nature of the repeating unit.

ii: Macromolecular: The molecular structure and the properties of the assembly of polymer molecules in terms of stiffness, size, shape and length distribution.

iii: Super-molecular. The structural features, including the nature and extent of interactive forces.

The physical and mechanical properties of a polymer are determined to a large extent by the detailed structure and properties of the chain molecules and manner in which they aggegate together in the solid state. On cooling from the molten state, polymers form either a hard rigid solid, which may be of a crystalline nature and thus characterised by a melting point - Tm or melting point range, or a glassy amorphous solid with one or more well-defined glass transition temperatures - Tg. The stereochemical configuration of the polymer chain is the major factor determining the degree of crystallinity, the size and

orientation of the crystallites and the mechanical and thermal characteristics of the polymer.

Thus, although chains based on the aliphatic C-C and C-O bonds are generally considered quite flexible, the introduction of ring structures into the main chain, such as in the case of polyethylene terephthalate or bisphenol A polycarbonate will have a marked stiffening effect and give rise to a higher glass transition than the aliphatic counterparts.

Polarity increases the modulus in the glassy region and both the glass transition temperature and the temperature of secondary transition are increased by polarity. Thus the presence of the polar group chlorine accounts for the higher transition point of polyvinyl chloride compared to polyethylene. However, it is to be noted that the presence of two identical symetrical polar groups will reduce the transition point, due to a reduction in dipole moment. This is the case for polyvinylidene chloride compared to polyvinyl chloride.

The structure and steric configuration of side groups attached to the main chain exert a considerable influence on both physical and mechanical behaviour.

2.2.2 Interactive Forces

Structural regularity and strong intermolecular interaction between adjacent polymer chains are the two main features which lead to a high tendency towards crystallization and high-melting point.

The valency forces which bind together the atoms of the polymer are quite strong as shown by the considerable energy required to break such bonds, for example: the relatively high temperatures required for decomposition of polymers. The bond energy lies in the range of 50 - 150 Kcal/mole and bond length is 1-2Å (38). The forces between adjacent molecules of the polymer are generally much smaller than the interatomic forces and are due to exchange forces between electrons (dispersion or london forces). The interaction energy for two $-CH_2-$ groups in neighbouring molecules is only 0.68 Kcal/mole with a distance of 2-5Å (38). However, these intermolecular forces can operate over a very much greater length of the polymer chains and in this way their effect is enhanced by a very large factor. The force required to separate polymer chains from each other may in fact exceed the strength of the covalent bonds in the main chains.

The most favoured energetic state of the simpler linear chains such as polyethylene, PVC, polyoxy-

methylene (polyformaldehyde) is to adopt a fully-extended trans-planar zig-zag conformation (39). In contrast, a polymer chain which consists of asymmetric units such as polypropylene will have a favoured rotation in one direction over the opposite direction leading to an energetic preference for a helical chain formation mainly because of the steric interaction which would occur between the closely spaced pendant methyl groups if the backbone was planar.

The polymer chains thus tend to fall into a fit largely determined by shape factors to give maximum filling of space and the largest interaction of dispersion forces.

Structurally regular polar groups exhibit interaction between dipoles or induced dipoles (Polar forces) as in the case of the pendant groups of acrylonitrite (-CN) or PVC (-Cl). The dipole-dipole interaction becomes the dominant influence and the polymers are more rigid and less soluble than the unsubstituted counterparts.

In some polymers, hydrogen bonding becomes the major determinant in the lattice structure as in the (-CO-NH-) polyamides where the bonding occurs intramolecularly between the carbonyl oxygen atoms and immino hydrogens in adjacent chains.

2.2.3 Chain Flexibility

The most important factor determining the temperature at which molecular motion becomes frozen - the glass transition temperature - is the flexibility of the polymer chain. Flexibility is a consequence of the properties of internal rotation about the bond links of the polymer chain. The ease with which and the rate at which orientation of segments occurs, depends on the energy barriers between the different geometric arrangements of the connecting bonds in the molecule.

Low values of glass transition temperatures are shown by polymers having highly flexible chains (low energy barriers for rotation) such as those with oxygen backbone linkage (polysiloxane, polyformaldehyde). The influence of steric hindrance is to restrict internal rotation along the main chain, thus increase the energy barrier for rotation and thus increase the Tg value. However, the transition temperature depends not only on the size of the side group, but also on its inherent flexibility. In general, provided more compact arrangements are not possible, then as the length of the side group increases, the molecule becomes more mobile, less thermal energy is needed to cross the energy barriers and the temperature of the main transition decreases.

2.2.4 Copolymerization

The main structural characteristics of a polymer are altered by copolymerization. A comonomer will be an irregularity in the structure supermolecular organisation and will thus influence those characteristics dependent on the structure organisation. Thus, random copolymerization will disrupt crystallisation and therefore influence crystalline properties such as melting point and modulus, but will not influence the transition temperature since this is determined not by the ability of the polymer chains to pack together into a lattice,but by average chain stiffness and average molecular forces.

Block copolymers (40) are formed by the chemical combination of homopolymer units which are themselves sufficiently large to ensure that the chemical integrities are maintained. Thus these copolymers are heterogeneous, although the two or more phases of the separate homopolymers are chemically connected.

Typical examples are the Phillips Petroleum Butyl lithium polymerised styrene-butadiene-styrene and styrene-isoprene-styrene linear and branched block copolymers (41, 42). The molecular weights of the middle and end blocks are sufficiently high to ensure the formation of a discrete polystyrene phase

which behaves as both a thermally reversible cross linking agent and reinforcing filler for the polybutadiene matrix. As the ratio of styrene to butadiene or isoprene is increased, it becomes more and more difficult for the polybutadiene or polyisoprene to envelop the polstyrene phase and it is possible to define a series of micro-composite morphologies ranging from spherical particles of polystryene in polybutadiene through fibrous and laminar structures to the other extreme, spherical polydiene phase dispersed in a polystyrene matrix (43, 44).

2.2.5 Influence on Mechanical Properties

In order to perform service as engineering materials, the desirable properties of any polymer are the combination of a high level of rigidity and low creep with a high resistance to impact. These properties are clearly in conflict in that impact strength requires that the material easily deforms to take up energy.

Stress-strain measurements give information on the ductility and stiffness of the material. Stress-strain behaviour depends on a number of structural factors. Increase in cyrstallinity raises the modulus and decreases the elongation at break, since crystalline polymers exhibit brittle properties.

The amorphous form of a polymer will be less brittle and thus will be more resistant to fracture. Control of crystallinity by branching or copolymerization or blending with elastomers is thus used to lower the brittle temperature of a polymer below room temperature.

The spherulitic structure of crystalline polymers influences properties over and above the influence of crysallinity. Large spherulitic structures promoted by slow cooling and annealing are generally more brittle in nature than small spherulites and exhibit lower toughness and tensile elongation due to the high crystallisation creating structural irregularities which tend to promote fracture by stress concentration.

Impact performance is stress-strain behaviour at very high rates of strain. The frequency distribution of segmental rotation controls the ability of a polymer to dissipate impact energy (45). If the majority of the energy is concentracted in the frequency band corresponding to the segmental roation frequency, then the maximum energy absorption will take place without fracture. However, if only a small amount of energy is concentrated in the segmental rotation frequency band then fracture occurs, ductile fracture if the test frequency lies below the segmental rotation frequency, brittle fracture if it lies above.

The requirements for a tough rigid polymer are a high modulus with a high yield stress, which is less than the fracture stress, since if the fracture intervenes before any appreciable deformation occurs, the material is brittle. Modifications to the polymer nature to reduce the yield stress below the fracture stress, include plasticisation as in PVC, blending with elastomers as in polystyrene, and polymer grafting as in ABS.

Plasticisation reduces the interaction between chain forces and as a consequence, reduces the properties dependent on the pendant group polar forces (46).

The effect of introducing rubber particles into a polymer by blending, is to lower the craze initiation stress relative to the fracture stress, thereby prolonging the crazing stage of deformation (47). In glassy polymers the stress required to form a craze is so close to the rupture stress that very little crazing occurs in the specimen before fracture intervenes. In rubber modified polymers, the gap between these two critical stresses is greater and very dense crazing occurs at lower stresses, before rupture occurs. This is because the Young's Modulus of the rubber is about 10^3 times lower than that of the surrounding resin and the applied stress is therefore concentrated in the resin.

Blending with block polymers of the type styrene - butadiene or styrene-isoprene with high polystyrene block sequence (thermoplastic rubbers) has a more pronounced effect on impact performance. The crystalline regions in these polymers act in the same manner as chemical crosslinks in preventing slippage of chain molecules over one another. In blends with polystyrene, the styrene blocks attached to the rubbery domains in the copolymer act as anchors to the polystyrene continuum, performing the role of the grafts in conventional impact polystyrene or ABS (48).

Grafting procedures tend, in general, to increase the volume fraction of the rubber and to shift its glass transition to higher temperatures (49), the volume of the rubber depending upon the total weight of grafted chains, the transition temperature depending upon the number of points at which these chains are attached. A small number of long side chains has less effect on the mobility of a rubber molecule than a large number of short ones.

2.3 BASIC ASSUMPTIONS OF ELASTICITY THEORY

The analysis of any problem describing the behaviour of a continuum, may be divided into three distinct steps: equilibrium, compatibility and a stress-strain relationship. The first two are independent of the

nature of the material and are basic to the solution of all problems (50). The time dependency of polymers requires modification of the standard elasticity theory in the following areas.

2.3.1 Strains

The strains are assumed to be small which in practice limits strain to less than 1%. For the elastic deformations of metals this is usually the case, whereas in the case of plastics, strains are often in excess of this figure. It has in fact been shown (51) that it is strain rather than stress which dominates non-linear behaviour.

2.3.2 Isotropy and Homogeneity

The material is assumed to be isotropic and homogeneous. This assumption is valid for metals but for plastics variations in properties both with direction and position are more common.

2.3.3 Reversibility and Time Dependence

Stresses in elastic materials are assumed to be completely and immediately reversible and the times for which the stresses are applied have no influence on the deformations. For metals, these are accurate assumptions, but for plastics, the properties are time dependent.

2.3.4 Linearity and Superposition

The material is assumed linearly elastic and to obey Hooke's Law.

$$e_x = \frac{1}{E} s_x$$

Where e is Strain

s is Stress

E is constant (Young's Modulus)

The strains at right angles to e_x are fixed proportions of such that:

$$e_y = e_z = ve_x = -v/Es_x$$

Where v is Poisson's Ratio

As a consequence of the linearity and reversibility, these stresses may be superimposed (Boltzman Superposition Principle) since the order and duration of loading have no effect. Also, since the shear strains are related to the shear stresses by modulus of rigidity G, it can be shown that the rigidity modulus is a function of Young's Modulus and Poisson's ratio given by: $G = E/2\ (1+v)$
and thus, the complete behaviour is described by two constants, namely E and **v**. The main characteristic of thermoplastics which is of fundamental importance to designers, whether deformation or ultimate failure is the main criterion, is that without exception they are non-linear viscoelastic materials (34, 52) the

non-linearity between stress and corresponding strain persisting to quite small strains (53). They exhibit either a time dependent response in strain when exposed to a constant applied stress or a time dependent response in stress when held under conditions of constant strain. The visco-elastic properties thus need to be characterised by a stress-strain-time-temperature relationship.

2.4 CONCEPT OF VISCOELASTICITY

In order to provide reliable information on plastics, entirely new concepts have to be introduced, concepts which must take into account the wide differences which exist between the organic and inorganic materials, particularly under dynamic stress and fatigue conditions.

The general design approach to most metal and other structural materials is based on the assumption of Hookean behaviour where the relationship between stress and subsequent deformation is determined by a material constant that is independent of the duration or rate of loading. Thus material constants such as tensile, compressive or shear modulus can be determined by relatively simple tests and used in a variety of design equations for specific situations such as bending of beams or loads on columns (54).

Polymeric materials are viscoelastic in that when stressed they respond in two ways, by viscous flow which dissipates energy and by an elastic displacement which stores free energy (55).

Properties of strength and rigidity depend on the amount of stress, the rate of loading and the length of time that the stress is applied, as well as the temperature at which it is applied. Thus many of the short time tests such as those for tensile and flexural strength, modulus and impact resistance, which have been inherited from metals technology, are severely limited in usefulness because they do not take into account the fact that viscoelastic behaviour requires performance tests to measure time dependence.

Hookean materials, including metals, concrete, wood and ceramics, respond to load in a predictable manner. In the case of plastics under stress, deformation occurs instantaneously upon loading (elasticity) then continues at a decreasing rate for a time (delayed elasticity and early stages of creep) followed by a small but continuous deformation with time (creep). Removal of the load produces some instantaneous recovery, some more gradual recovery and some permanent deformation.

The time dependence of the mechanical properties of plastics arises because the molecular movements which constitute the strain, are opposed by frictional resistance due to the close proximity of neighbouring molecules. The molecular segments vibrate continuously in a random fashion by reason of their thermal energy, but when an external stress is applied, some movements become more likely than others and this change of probabilities for particular movements leads to the observed time dependence (51).

2.5 POLYMER VISCOELASTICITY

The deformation of a solid body may cause a change in its internal energy due to the changes in the intermolecular distances. It may also cause a change in its entropy due to a change from a more probable atomic distribution to a less probable one. These two possibilities plus a combination of both gives rise to three possible types of deformation (56).

2.5.1 Entropy Change at Constant Internal Energy

This type of deformation occurs in gases and to a large extent in amorphous plastics at temperatures above their main transition. Treloar (57) gives as the prime reason why plastics in the soft elastic region (rubbery region) deform with entropy changes is that under the influence of thermal vibrations,

the very long flexible molecules change their shape continually by rotation about the covalent bonds.

Thus to develop entropy elasticity, a body needs long flexible molecules. If these molecules have strong forces connecting them at many points along the length the movement is restricted and as a consequence there is insufficient flexibility to take up all the configurations demanded by entropy elasticity. If the molecules are not sufficiently long, then under stress the molecules slide past each other without any change in entropy.

2.5.2 Internal Energy Change at Constant Entropy

Under the conditions of low temperature and high frequencies the thermal motions of the molecular segments are not large enough to overcome the energy barriers of the secondary valence forces and the molecules are effectively rigid. Consequently, there is no change of entropy on deformation and in the hard elastic region (Glassy State) the response to deformation is governed only by changes in internal energy. A similar situation occurs at higher temperatures with cross-linked polymers where the high covalent bond density effectively renders the thermal motion as negligible.

2.5.3 Internal Energy and Entropy Change

In the viscoelastic region, the thermal energy is sufficiently large to permit atoms to cross barriers. Under these conditions, some of the atoms or groups of atoms rotate about covalent bonds, causing the molecules to change their shapes. With this type of molecular movement, the material is more easily deformed.

The transition region between the hard glassy state and the soft rubbery state is influenced by the side groups attached to the main chain. Bulky inflexible side groups increase the temperature of the main transition. As the size of the rigid side group increases, the mobility of the molecule is reduced. This means that more thermal energy is needed to overcome the energy barriers and the temperature of the transition is increased. More compact arrangements reduce the flexibility of the molecule and the transition temperature is markedly increased (58).

Increasing the length of flexible side groups reduces the temperature of the main transition (59). Thus as the length of the side group increases, the molecule becomes more mobile, less thermal energy is needed to cross the energy barriers and the temperature of the main transition region decreases.

Many polymers have secondary transitions at temperatures other than the main transition (60, 61). In these regions small parts of the molecule are considered to become free to move over energy barriers although complete mobility is not attained until the main transition is reached.

The factors that influence the main transition of amorphous polymers are the same factors that influence that of crystalline polymers. However, in crystalline polymers an additional transition, the crystalline melting point, is principally influenced by (62) cohesive energy density, molecular rigidity or flexibility, molecular shape and sequential order of methylene groups.

Crystalline polymers show several transitions provided that a sufficiently high proportion of their molecular segments are in crystalline regions. However, until they melt, the crystalline regions hold the polymer together as a solid.

CHAPTER 3. STRUCTURE AND PERFORMANCE OF PHILLIPS POLYMERISED POLYETHYLENE

3.1 PROCESS DISCOVERY AND DEVELOPMENT

The Phillips Polyolefins process today accounts for 1.9 million metric tonnes or 30.5% of the worldwide HDPE capacity (63).

The discovery, made only a little over two decades ago, by J.P. Hogan and R.L. Banks, that ethylene could be converted to solid polymers over a chromium oxide-silica alumina catalyst, had as its genesis an earlier discovery at Phillips by Bailey and Read, that ethylene could be converted to liquid polymers over certain nickel oxide-silica alumina catalysts (64).

The initial polymerisation system used a fixed bed of catalyst but the process was limited to relatively low molecular weight (5,000-20,000) brittle polymers with hydrocarbon solvent containing no more than 2-4% ethylene (65).

Within two years a more promising system involving polymerisation as a polymer solution in a stirred reactor was developed. Pilot plant studies progressed from laboratory batch operation to an integral, continuous flow system permitting, by 1954, the commence-

ment of commercial process design. In April 1955, based on recommendations of technical and market evaluation groups, Phillips' Management approval was obtained to construct a 35,000 MT polymerisation unit which began operations in Pasadena, Texas, in December 1956 (66).

The first commercial grades of polyethylene produced were high density homopolymers of various melt indices. Ethylene 1-Butene copolymers were introduced in 1958, which together with other polymerisation factors, enabled an extension in the choice of polymer type.

The process used up until 1960 (polymer in solution process) was entirely based on the utilisation of a hydrocarbon which was a good solvent for the polyethylene at the polymerisation temperatures of 150-180°C. Molecular weights were thus limited to the range of 10,000-140,000 depending on the reaction temperature control.

Research and development in the intervening period, led to the commerical operation in 1961, at Pasadena, of the Particle Form Process where the hydrocarbon used was a poor solvent for polyethylene and was used as liquid diluent in which to suspend the catalyst. Refinements of this latter process now account for

the vast bulk of the production of HDPE following the Phillips Petroleum Polymerisation Process.

The most recent significant contribution to the extension of the Phillips process capability, has been the copolymerisation of ethylene with 1-hexene and the possibility to produce polymers in the range of density 0.923-965 g/cc and molecular weights up to one million and above (66).

3.2 POLYMERISATION PROCESS

3.2.1 Introduction

The polymerisation of ethylene using the Phillips Petroleum Catalyst is performed over a general temperature range of 65° to 180°C, with the higher temperatures favouring lower molecular weight polymers, due to the decreasing catalyst activation and/or chain transfer reaction (67, 68).

Rate of ethylene polymerisation depends on catalyst activity, ethylene concentration in the reaction medium, reaction temperatures and polymerisation time. Co-polymerisation with alpha-olefins results in the formation of short branches which interrupt crystallisation and alter significant characteristics.

3.2.2 Catalyst

The two important features of the hetergeneous catalyst system are chromium in the Cr-6 state and the silica-alumina powdered substate. Typically the concentration of the total chromium is 0.5 to 2%, since no increase in activity is observed above this level (65, 69). Silica-alumina ratio in the base has not been found critical over a wide range, but is generally of the order of 90:10 silica to alumina (65, 69).

Catalyst activation is achieved by heating in air fluidised beds at temperatures in the range 500-1000°C. In the dehydration process, the chromium ions, regardless of the starting valence, largely combine with the silica substrate in the Cr-6 state to form surface silyl chromate or dichromate (65).

In the polymerisation reaction, the monomer is physically adsorbed onto the high surface area silica alumina and are held there by Weak Van der Waals forces and ion-dipole interreactions. Some of the molecules undergo chemisorption-adsorption with an energy of activation which leads to chemical bonding between the adsorbent and surface. The process of adsorption changes the bond energy of the adsorbed molecule, concentrates the molecules in a condensed layer and holds them in a fixed position.

The chromium content of the catalyst appears to be in intermediate valence state during the polymerisation. Differential thermal analysis (70) and electron spin resonance (65, 71) have shown the formation amongst others of chromic decachromate $Cr_2(Cr_{10}O_{31})_3$ with chromium having an average valence state of 5.8 (72), chromic bichromate $Cr_2(Cr_2O_7)_3$ of valence 5.25 and chromic chromate $Cr_2(CrO_4)_3$ of valence 4.8.

These intermediate valence states have unpaired electrons which are available for chemisorption of the monomer, for reaction with the monomer and for linking of the monomers together.

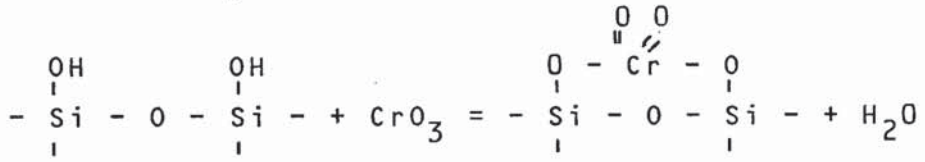

3.2.3 Homopolymerisation

The molecular structure of ethylene homopolymer made by Phillips process is that of a very high molecular weight alpha-olefin.

$$CH_2 = CH - (CH_2 - CH_2)_n - CH_2 - CH_3$$

The product produced in the solution form polymerisation differs markedly with respect to branching and unsaturation depending on whether the fixed bed or slurry variation of the process is used (69, 72, 73).

The product from the fixed-bed reaction has approximately 16 methyl groups per 1000 carbon atoms and about 4.8 double bonds per 1000 carbon atoms, of which 93% is of the internal-trans type and 7% is of the terminal-vinyl type. The currently used slurry process product has about 2 methyl groups per 1000 atoms and about 1.5 double bonds per 1000 carbon atoms, of which 94% is of the terminal-vinyl type and 6% is of the internal-trans type. The differences are considered due to isomerisation occuring at higher temperatures that were used in the older fixed-bed process.

Ethylene homopolymer produced in the particle form porcess is also linear although in certain fractional melt index particle form polymers there is circumstantial evidence that a minimal amount of long chain branching is present. The melt viscosity is higher than would be predicted from the solution viscosity and the melt elasticity is high, suggesting the presence of long chain branching (66).

3.2.4 Copolymerisation

The Phillips polymerisation system will polymerise all 1-olefins with no branching closer than the 4-position to the double bond and containing eight carbon atoms or less (65). Copolymers of ethylene with 1-olefins such as propylene, 1-butene and 1-hexene contain branches, the number of branches per molecule and the

number of carbon atoms per branch depending on the amount and nature of the comonomer used. Copolymerisation results in formation of branches on average two carbon atoms shorter in length than the alpha-olefin comonomer. Thus comonomer 1-hexene will produce butyl branches. The addition of a few branches per 1000 carbon atoms in the backbone lowers the density of the polymer by disrupting crystallisation. Research has shown that incorporation of 21 methyl branches per 1000 carbon atoms in a propylene-ethylene copolymer (6.25% weight propylene) lowers the crystallinity by approximately 20%. Similarly, incorporation of 14 ethyl branches per thousand carbon atoms in a copolymer of 1-butene and ethylene (corresponding to 5.6 weight % 1-butene) also lowers the crystallinity by about 20%. This suggests that one ethyl branch is equivalent to about 1.5 methyl branches in so far as lowering of crystallinity is concerned.

3.3 MOLECULAR STRUCTURE OF POLYETHYLENE

The polymerisation of the monomer unit ethylene results in the simple structured monomer units being connected to each other by chemical covalent bonds in which the bonding electrons are shared equally between the bonded atoms. The end groups of the polymer chain may or may not be indentical but, because of valency requirements, must differ structurally from the repeat

unit. The linear polyethylene molecules possess a considerable degree of flexibility in that the groups that the single covalent bond connects can rotate with respect to each other about the axis of the bond with the constraint of the inter-action between the repulsive force fields of the substituent atoms in the two groups. The ease or frequency with which rotations occur in molecules depends on the height of the rotational energy barriers in relation to the thermal energy possessed by the molecules and is thus temperature-dependent.

As a result of random thermal motion (Brownian Movement) of the polymer chain segments, the conformation of an individual molecule changes at a rate depending upon the inherent rotational energy barriers of the polymer, as well as upon the environmental factors such as temperature or imposed mechanical stress. When bulk flow of the polymer takes place under the influence of stress, bodily movement of the molecules relative to each other proceeds by a succession of loosely co-ordinated local changes in the conformation of chain segments. However, in the case of high molecular weight polymers, the molecules, being looped or intertwined with each other to some extent and being in such intimate contact, such entanglements act as temporary cross-links during deformation of the polymer.

Polyethylene molecules possess a sufficient degree of chemical and geometric regularity, that on slow cooling from the molten state, small regions of local molecular order (crystallites) appear. The partial crystallisation does not proceed to completion because the average length of the polymer chains far exceeds the size of the crystallisation nuclei and the same molecule may participate simultaneously in crystallite growth at different points along its length. Since the growth directions of the nuclei are randomly orientated, it becomes increasingly difficult, as crystallisation proceeds, for uncrystallised portions of the molecule to enter a crystal lattice because their motion becomes increasingly restricted.

The configurational regularity of isotactic polymers, such as P.P., facilitates their entry into a crystal lattice in which the molecules generally assume a spiral form and thus they attain higher degrees of crystallinity than the chemically identical but atactic counterparts which are more amorphous. The better mechanical, physical and chemical characteristics are attributable to higher crystallinity.

3.3.1 Structural Model

In the solid state, the mass of molecules are heavily entagled but, whereas in the ideal amorphous polymer the individual molecules take up a modified random

coil configuration, the crystalline polymers have regions in which polymer chains are perfectly aligned into crystalline lattice order. However, X-ray diffraction of ideal crystallised polymer samples always yields a combination of crystalline and amorphous patterns (74). This fact led to the conclusion that the partially crystallised polymer contains very small crystals embedded in an amorphous matrix. This idea was embodied in the structural model of the "fringed micelle concept" and assumes a random arrangement of long linear macromolecules which, in regions of sufficient chain alignment, are able to form a crystal lattice (75).

3.3.2 Fringed Micelle Concept

The model assumes that the polymer is a non-stationary two-phase, system. In the amorphous phase, chain entanglement and partial inclusion in more than one crystal prevent the transformation into a stable crystalline phase. The individual molecules extending from one crystallite to another, pass through amorphous regions and thus hold the polymer together and yield the elastic restoring forces. The small crystallites act as physical cross-links and are responsible for the shape and conservation of the sample. Fig 3.1 is an illustration of the model showing the chains forming short bundles within which they are parallel

over a short portion of their lengths. Within these parallel portions, they are in crystallographic register giving rise to a crystal lattice, but they sprout into an amorphous tangle at both ends, producing a network of amorphous chains with the crystallites acting as junction points.

However, photomicrographs from study of spherulites using polarising optics (76) show a uniform orientation over extended area and spherical symmetry, neither of which can be accounted for by the fringed micelle model. The argument that the micelles could be visualised as lying circumferentially within an overall spherical entity is not tenable with the fact that spherulites are common amongst all crystallising substances and are the results of radiating growth of fibril-like entities from a common centre of nucleation. The periodic organisation is not a periodic alternation of crystalline and amorphous regions accommodated within spherical symmetry, but more due to a periodic orientation variation of the radially growing fibrils from the nucleus as shown schematically in Fig. 3.2

3.3.3 Folded Chain Concept

The discovery of spherulites in solid polymers and polymer crystals together with the discovery of crystalline lamellae with a thickness in the region of

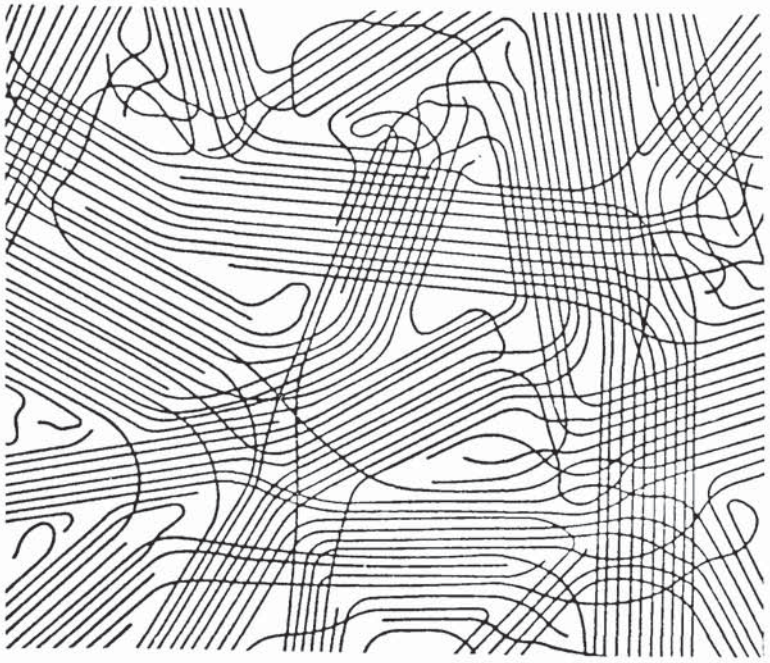

Fig. 3.1 REPRESENTATION OF FRINGED MICELLE CONCEPT

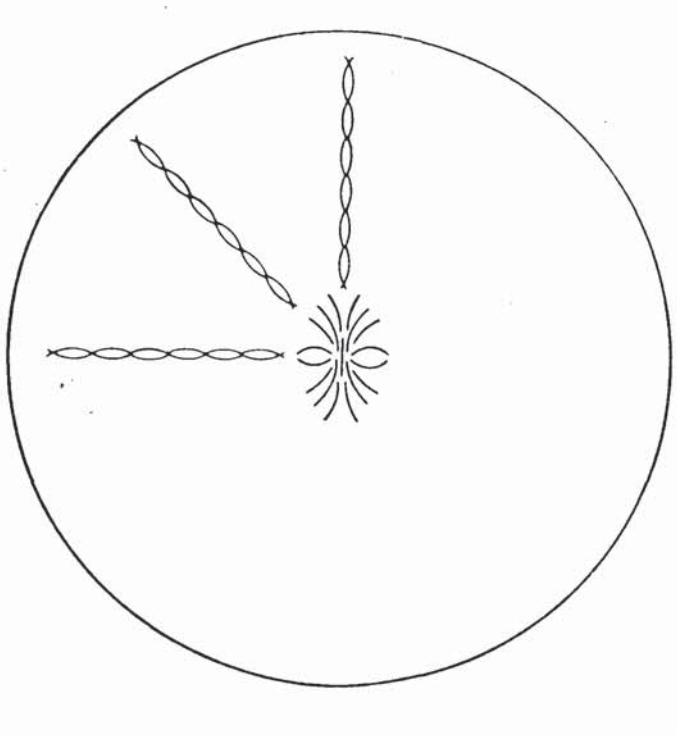

Fig. 3.2 ESSENTIAL STRUCTURAL FEATURES OF A TYPICAL SPHERULITE

100Å led to the concept of chain folding.

This model considers the polymer solid to be a polycrystalline one-phase system, and the existence of lamellar crystals with chain folds at the surface and only very few chains going through more than one crystal.

The individual polymer molecules within a crystal are considered to fold back and forth upon themselves. X-ray evidence (77) indicates that the polymer chains are arranged with their axes perpendicular to the principal faces of the crystal or parallel to its thinnest dimension, usually of the order of 100-200 Å. Since this is only a small fraction of the total length of a high polymer chain, it follows that the molecule is folded into the crystal platelet. The fold length and therefore the thickness of the crystal is a function primarily of the temperature at which crystallisation takes place, with folds occurring at regular intervals along the chain as dictated by thermodynamic considerations. An entire molecular chain, many such chains in fact, can thus be encompassed completely by a single crystal and the cohesive forces between adjacent crystals must, in the absence of disturbing forces, be largely secondary in nature. A diagrammatic representation of chain folding is shown in Fig. 3.3.

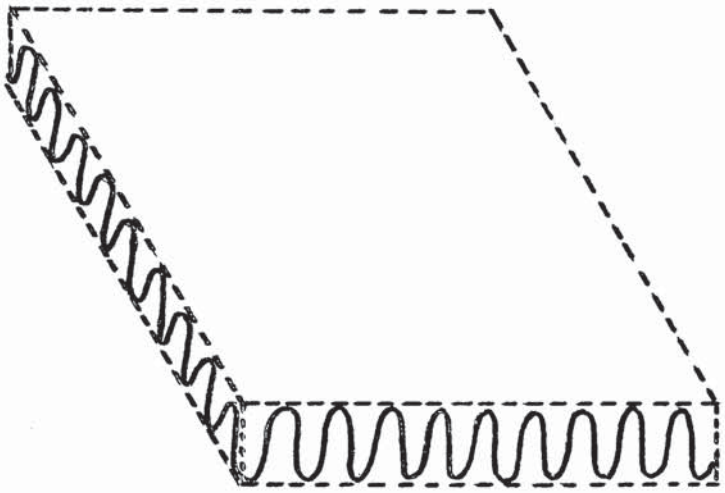

Fig. 3.3 DIAGRAMMATIC REPRESENTATION OF CHAIN FOLDING

(After A. Keller)

It follows from the chain folding concept that the crystal thickness is identical or closely-related to the fold length which itself is dependent on crystallisation temperature, higher temperatures leading to longer fold lengths. When a crystal already formed is heated beyond its crystallisation temperature, it thickens. In molecular terms, this corresponds to a refolding to greater fold lengths and is the molecular basis of effects which occur on heat annealing.

Although this concept explains the structure of highly crystalline polymers, it is not so satisfactory for semi-crystalline materials or polymers showing low crystallinity.

3.3.4 Intermediate Micelle-Folded Chain Concept

A more satisfactory approach is a model intermediate between the fringed micelle and the extreme folded chain concept in that many of the chains become independently included in two or more different crystals or in two or more places in the same crystal and hence cannot be fully incorporated into a single folded crystal. Such tie molecules contribute the amorphous content, together with contributions from lattice defects, uncrystallisable components and impurities rejected by crystallisation. There are several reasons for departures from the extreme folded chain model.

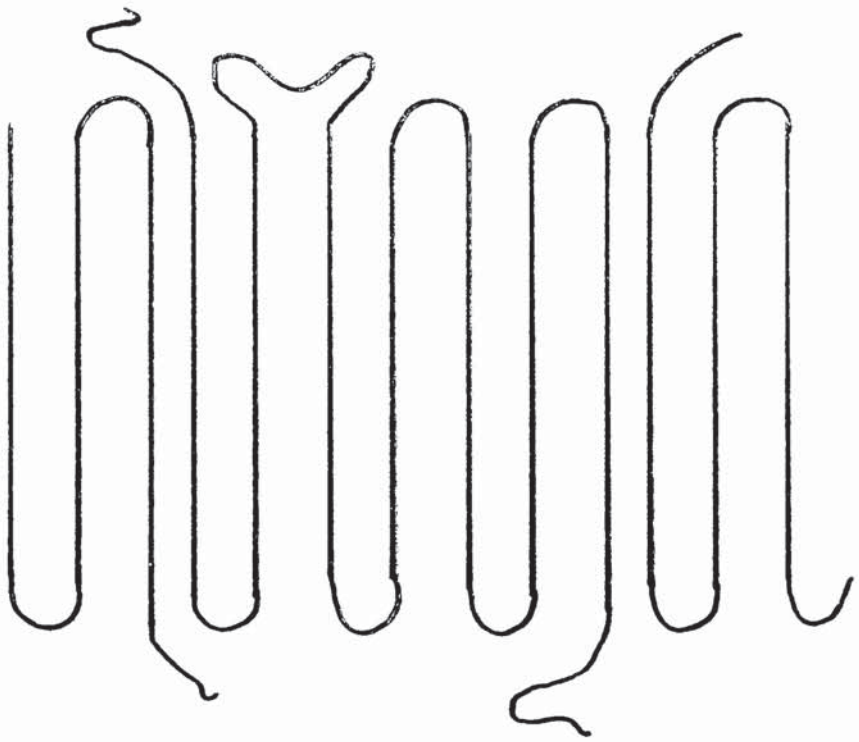

Fig. 3.4 SCHEMATIC REPRESENTATION OF CILIA AND LOOSE LOOPS

One reason is that of the finite length of the polymer chains, the ends of which give rise to loose chain portions which either stay excluded giving rise to cilia (78) or fold in later producing large loose loops, which may or may not produce protruding folds. Schematic representations of cilia formation and loose loops are shown in Fig. 3.4. The loose cilia can become incorporated in consecutive overlying layers to constitute the tie molecules. The occurrence of a branch at a near an intended fold point on the polymer chain should result in a dislocation at that point, since the chain could no longer fold in the manner necessary to accommodate itself into the crystal. Consequently, the remainder of that chain should find itself excluded from the crystal into which part of its length has already been incorporated. If the excluded portion is of sufficient length and appropriate constitution it could accommodate itself into another growing crystal nearby. These two crystals would then be tied together by the primary valence bonds of the polymer chain. Repetitions of the process lead to a crystalline mass securely interconnected by polymer chain bridges and is characterised by superior properties.

This concept accounts for the strength properties of crystalline polymers and is substantiated in practice by the remarkable increase in creep resistance bestowed

upon otherwise linear ethylene polymers by the branches introduced through copolymerisation with minor amounts of butene or hexene (79).

3.4 STRUCTURAL INFLUENCE ON PROPERTIES AND PERFORMANCE

3.4.1 Introduction

As a generalisation, a polyethylene resin can be adequately described, regardless of the process used to produce it, if its density, molecular weight and molecular weight distribution are known. These three parameters determine the properties a resin will have (80, 81). In relating physical and chemical properties, it is an over simplification to state that a property is dependent entirely on any one parameter. Although many properties are more dependent on one than the other two.

A fourth parameter is short chain branching. Short branches of less than 10 carbon atoms are incorporated during polymerisation by the introduction of minor quantities of an alpha-olefin comonomer. Both the type and concentration of branching can exert a pronounced effect on performance. Thus, when hexene-1 is introduced as a comonomer in place of butene, the relationship between density and certain physical properties is altered; specifically the stress-cracking

re Sistance and hoop stress performance.

3.4.2 Crystallinity

3.4.2.1 Features

Crystallinity is a very important structural feature in determining the basic properties of the polymer and is determined, to a large extent, by the number of branches along the chains (82), although this is strictly true only from an equilibrium crystallisation viewpoint.

The branch structure of small pendent groups will not conveniently fit into the regular array of chains in the crystal lattice and thus, some disruption of crystallinity occurs around the branch site. As more and more branches are introduced into the chain, the disruption becomes progressively more until there is insufficient regularity of structure to permit a regular crystalline array to form and the eventual product is a gummy elastomeric material. Low density polyethylene is characterised by having about 20 branches per 1000 carbon atoms with degrees of crystallinity between 40-70%, whilst high density polymer varies in branching from 5 to essentially zero with resultant crystallinity between 60-90%.

Crystallinity is directly propertional to density:

$$C = \frac{P_c}{P} \circ \frac{P - P_a}{P_c - P_a} \times 100$$

Where C is weight per cent crystallinity

P is the measured density

P_a is the amorphous density

P_c is the crystalline density

In some cases, the equilibrium degree of crystallinity is not attained either because the rate of cooling is too fast (quenching) or the molecular chain length is too long (83).

3.4.2.2 Density Range of Phillips Polymers and Dependent Properties

The density of Phillips-type polyethylene homopolymer can be altered from 0.965 g/cc for a high melt index low molecular weight polymer, to about 0.960 g/cc for a melt index polymer of 0.3-0.5 dg/min., to as low as 0.94 g/cc for an ultra high molecular weight polymer. The density decrease with molecular weight increase is related to chain entanglement. Because of entanglement, the long polymer chains inhibit the movement necessary to the formation of ordered crystalline structure (84).

Broad molecular weight distribution polymers tend to be slightly higher in density than narrow molecular

weight distribution polymers, because the short molecules can align with segments of long molecules to increase crystallisation.

The major properties which are density dependent and increase with increasing density are:

Stiffness
Hardness
Softening temperature
Chemical resistance
Tensile yield stress

Dependent properties which decrease with increasing density are:

Tensile elongation
Low temperature impact
Permeability

For density control in Phillips polymerised polymers of various melt indices, an alpha-olefin such as propylene, 1-butene, or 1-hexene, is employed. The resultant copolymerisation results in the formation of branches two carbon atoms shorter in length than the comonomer, the inclusion of these branches lowering density by disrupting crystallisation.

The effect of such density changes at constant melt index on some general physical properties are summar-

ised in Table 3.1. The methods of test employed are summarised in Appendix 1.

TABLE 3.1 Density Dependent Properties of Ethylene-Butene-1 Copolymers of Melt Index 0.3 dg/min.

Density g/cc	0.96	0.95	0.94	0.925
Flexural Modulus kg/cm	15.5	11.6	9.8	4.7
Tensile Strength km/cm	310	265	230	125
Tensile Elongation %	25	70	280	600
Bell ESCR (F-50) hrs	30	150	600	1100

(Environmental Stress Crack Resistance)

3.4.3 Molecular Weight

3.4.3.1 Features

During the synthesis of high polymers, not all the molecules grow to the same size. Because of this size variation, high polymers do not possess a specific molecular weight in the usual sense of pure compounds, but an average value. The mixture of homologous compounds of different molecular weights, although rarely affecting the chemical properties, has an important influence on the physical, mechanical and rheological behaviour of the polymer.

The number average molecular weight M_N as measured by osmotic pressure, cryoscopic or ebulliometric methods, is in every sense the mean molecular weight

of the molecules in a sample of polymer. This value is appropriately used when the property is a function of molecular weight and when the value of the property depends on the number of molecules in a unit weight of polymer. One such property is the glass transition temperature, the explanation being that the greater concentration of chain ends and the associated increase of space accompanying a low molecular weight, results in a greater facility for the chains to rotate and hence the value of Tg is low. It is the number of chain ends that control the variation from the ultimate Tg value and this is related to the number average molecular weight (84).

The weight average molecular weight Mw as measured by light scattering or sedimentation techniques, is appropriately used when the polymer property is dependent on the weight of polymer in a molecular weight range. Such properties are those that depend on the movement of chains relative to others, so that chain entanglement is dominant. This includes, for example, most mechanical properties and intrinsic viscosity.

The determination of the viscosity average molecular weight is by a more simple means and yields a value which is between number average and weight average, but closer to weight average, since it is influenced by the same factors.

3.4.3.2 Molecular Weight Range of Phillips Polymers and Dependent Properties

Molecular weight when measured in the form of melt index, can be varied in the Phillips process within the range 0.2 dg/min to 35 dg/min in solution polymerisation and from 15 dg/min down to melt index values corresponding to molecular weights of 750,000 in the particle form polymerisation.

The major properties which are molecular weight dependent and which increase with increasing molecular weight are:

- Melt Viscosity
- Ultimate Tensile Strength
- Ultimate Tensile Enlongation
- Resistance to creep
- Impact Strength
- Environmental Stress Cracking Resistance

The physical properties of linear polyethylene which are most sensitive to melt index or molecular weight are correlated in Table 3.2.

TABLE 3.2 Molecular Weight Dependent Properties of Ethylene Homopolymer

Molecular Weight Mw x 10^{-3}	175	140	125	95	85
Melt Index dg/min	0.2	0.9	1.5	3.5	5
Tensile Impact Kg cm/cm^2	215	135	125	85	65

TABLE 3.2 (Cont'd)

Izod Impact Kg cm/cm Notch	75	20	10	8	6
Tensile Elongation %	30	25	20	15	12
Bell ESCR (F-50) hrs	60	14	10	2	1
Brittleness temp °C	-118	-118	-118	-101	-73

The ability to resist breaking under tensile impact declines with increase in melt index, the Izod strength of notched specimens declining more rapidly indicating an increase in notch sensitivity as well as a decrease in impact strength. Ultimate tensile elongation increases with increasing molecular weight since cold drawing occurs.

3.4.4 Molecular Weight Distribution

3.4.4.1 Features

During polymerisation the molecules grow to different sizes. The terms most frequently used to describe this size variation are molecular weight distribution, polydispersity and heterogeneity. The molecular size can be shown by several ratios. The hetergeneity index H.I is defined as the ratio of the average molecular weight to the number average molecular weight.

An indication of the molecular weight distribution may also be obtained by measuring the slope of the plot of shear rate to shear stress. A good approxi-

mation of this slope may be obtained by making two flow measurements at different shear stresses and dividing the flow obtained at the higher stress by the flow at the lower stress. In general the low stress value is the standard melt index value and the higher stress a high load melt index value at 21.6 Kg or a 1500 psi pressure on a high shear viscometer.

Although flow ratios are good approximations of molecular weight distribution, other polymer structural properties such as long chain branching can also affect the flow ratio and must be taken into account.

Morgan (66) compares two Phillips homopolymers of similar weight average molecular weight, but where the long chain branching increases the melt viscosity of the particle form polymer at very low shear rates by restricting flow. The viscosity studies demonstrate the increase in the elasticity of the polymer melt of particle form resins as shown in Table 3.3

TABLE 3.3 Effect of Long Chain Branching on Viscosity

Polymerisation Method	Polymer Properties			
	(N)(1)	(N)(2)	Mw(3)	Mw/Mn
Phillips Solution Process	2.1	3.4	169,000	11
Phillips Particle Form Process	2.0	5.6	169,000	7

(1) Inherent Solution Viscosity. ASTM D 1601 in Tetalin

(2) Melt Viscosity in poise x 10^{-5}, shear rate 10^{-1} sec^{-1}

(3) Gel Permeation Chromatograph

3.4.4.2 Molecular Weight Distribution & Dependent Properties

The molecular weight distribution of both the solution and particle form Phillips polymerised polymers is normally fairly broad and can be altered by catalyst and process modifications.

Typical weight average to number average molecular weight ratios (Mw/Mn) vary from as low as 3 for narrow distribution resins, to as high as 20 for very broad distribution resins. In general, the broad molecular weight distribution polymers of higher molecular weight are used in applications requiring good environmental stress cracking resistance and fast processing, properties which result from the increased shear response of the broad molecular weight distribution.

A comparison of the two HDPE polymers of different molecular weight distribution show a marked difference in shear response when the shear stress is increased tenfold.

TABLE 3.4 Influence of shear stress on shear response

Polymer	Mw/Mn	MI(1)	HLM1(2)	HLMI/MI
Narrow MWD	6	0.3	180	60
Broad MWD	20	0.3	330	110

(1) Melt index in dg/min at 2.16 Kg/cm^2 load

(2) High load melt index in dg/min at 21.6Kg/cm^2 load

The molecular weight distribution of a resin affects both the processing and the product performance, as well as influencing the resin properties. In general, as distribution is broadened, the overall processability is improved in both extrusion and injection moulding application. However, the ease of flow through the processing equipment is obtained at the expense of finished product properties; namely, warpage in injection moulded items and shrinkage and retraction in extruded items.

Molecular distribution has no signficant influence on stress-strain properties, but broader distributions increase creep resistance, softening temperature and environmental stress cracking resistance, but decrease overall toughness.

3.5 PHYSICAL and MECHANICAL PROPERTIES

3.5.1 Melting Range

In the process of crystallisation and subsequent melting, equilibrium is seldom attained with the result that linear polyethylene melts over a range of 120-130°C. Melting range and final melting point are influenced by both the amount and randomness of branching which then causes significant differences in the modulus/temperature characteristics.

The melting point of a polymer varies with the regularity of structure and to a less extent with how close to equilibrium the polymer has been permitted to crystallise. Reasonable agreement with measured values is obtained with the use of Flory's (85) melting point depression equation:

$$\frac{1}{T_m} - \frac{1}{T_m^o} = - \frac{R}{H} \ln Na$$

Where Tm is final melting point in ^oK

T_m^o is melting point of completely linear resin

R is the gas content

H heat of fusion per repeating unit

Na is mole fractions of $-CH_2$ units

This relationship is strictly true only for statistically random copolymers whereas many polyethylene copolymers are not statistically random. This leads to a lesser melting point depression at a given disruptive comonomer concentration than predicted. Thus, in non-random copolymers it takes more of the disruptive comonomer to lower the melting point to any given temperature because there is a smaller composition range over which the copolymers are amorphous. Where the variation from randomness is great, the copolymers show crystallinity over the whole composition range.

It has been shown (86) that propylene is less

effective in disrupting crystallinity in ethylene copolymers than the higher normal alpha-olefins such as butene, pentene or hexene. This is because the small methyl pendant groups can, to a large extent, be accommodated in the expanded crystal lattice.

3.5.2 Glass Transition

Whereas glass temperatures Tg are known for hundreds of simple and complex polymers, the glass temperature of the simplest organic polymer $-(CH_2)-$ is still the subject of a widespread controvesy (89). The confusion in the literature which covers a range of about 100°C was such as to cause McCrum, Read and Williams to state (90): "It is by no means certain that the assignment of a Tg in polyethylene is a meaningful activity".

Boyer (89) postulates a double glass transition - an upper figure which varies with fractional crystallinity, a lower figure which corresponds to the classical transition of Amorphous Polymers - together with the gamma relaxation temperature $T\gamma$. From the morphological point of view, tie molecules and loose loops become longer with decreasing crystallinity, thus influencing the upper Tg value, whereas the dangling chain ends or cilia together with polymer chains not incorporated into the spherulites, influence the amorphous transition.

Of the two main transitions, the lower figure is associated with straight chain C - C motion and the upper figure is associated with motion of groups adjacent to the branch site. (91).

3.5.3 Mechanical Behaviour of Polethylene

The outstanding mechanical properties of polyethylenes are due very largely to their high crystallinity. The presence of the crytalline phase tends to retain mechanical strength over a large temperature range and give rise to the relatively high melting point despite the relatively low glass transition. (92).

3.5.3.1 Modulus

There is a linear relationship between stiffness and density and also the crystallinity since this latter is directly proportional to the density:

$$C = \frac{Pc}{P} \circ \frac{P - Pa}{Pc - Pa} \times 100$$

However, it is strictly density or specific volume which is the determining factor and the modulus reflects simply the free volume whether it comes from thermal expansion or decrease in crystallinity when temperature is increased. Both torsional stiffness and modulus measurements are measures of crystallinity, but torsional stiffness reflects more the minor changes in density. A composite plot is given in Fig 3.5 showing the linear relation of stiffness,

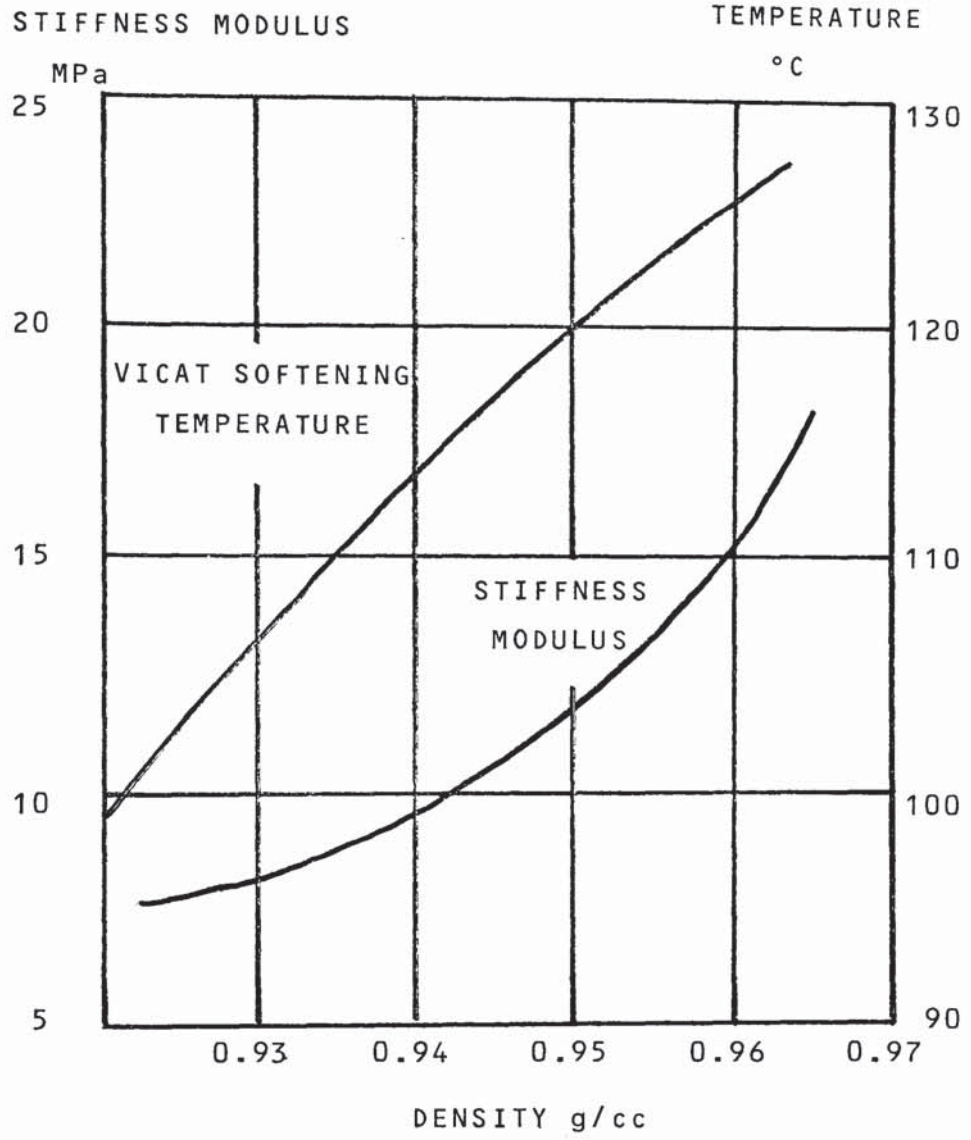

Fig. 3.5 RELATION OF SOFTENING TEMPERATURE AND MODULUS WITH DENSITY

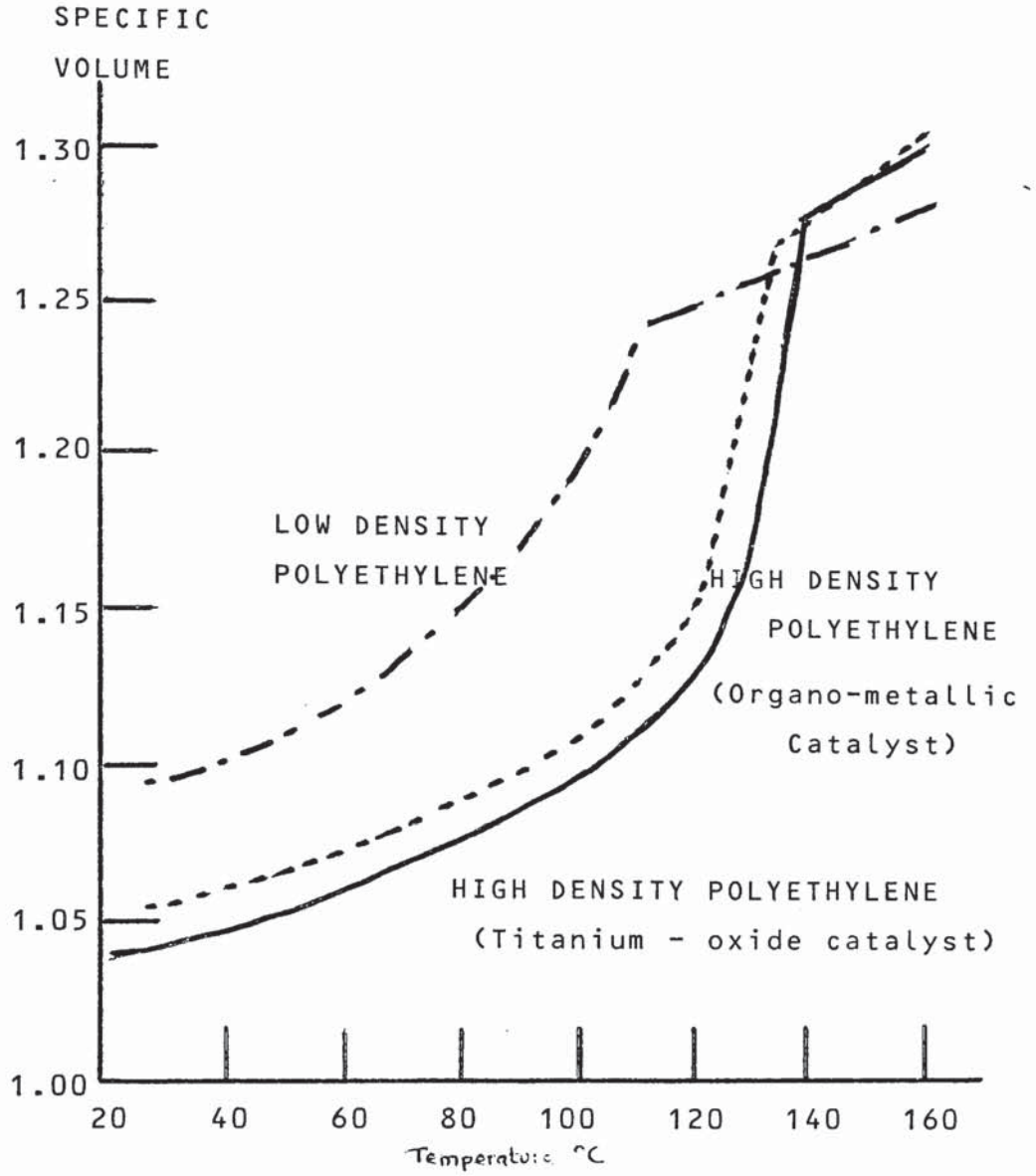

Fig. 3.6 SPECIFIC VOLUME - TEMPERATURE RELATIONSHIP FOR VARIOUS POLYETHYLENES

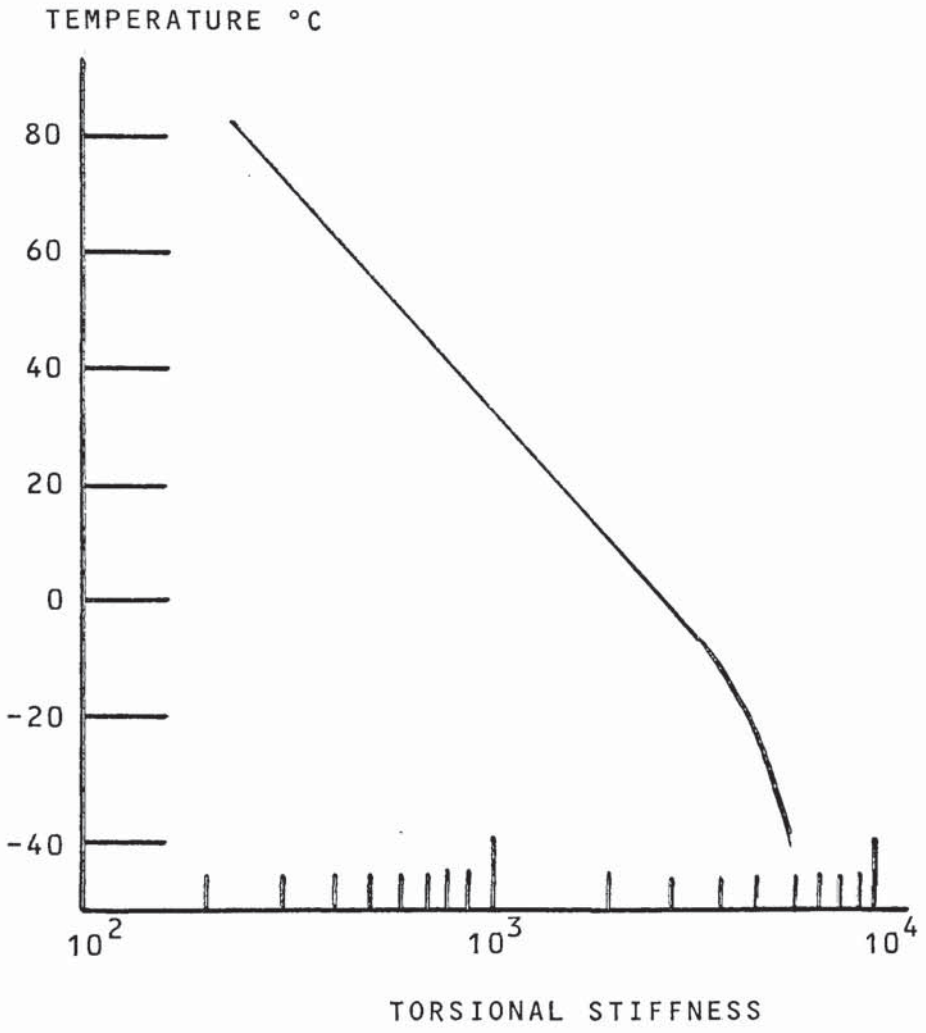

Fig. 3.7 EFFECT OF TEMPERATURE ON TORSIONAL STIFFNESS OF A 0.94 g/cc DENSITY ETHYLENE-HEXENE COPOLYMER

temperature and density. The specific volume-temperature relationship for various polyethylenes is shown in Fig. 3.6 and the effect of temperature on torsional stiffness of an ethylene-hexene copolymer in Fig. 3.7

3.5.3.2 Tensile Properties

Tensile properties depend on a number of variables, including temperature, density, molecular weight and rate of loading.

Increasing density increases tensile properties due to the greater modulus of higher density resins which effectively shifts the stress-strain curve upward along the stress axis and the increased crystallinity which helps to hold the polymer together. Increasing temperature causes an increase in elongation at first, but as the melting range is reached, the crystallites which hold the polymer together start to disappear and elongation drops. Ultimate tensile strength is not only density dependent, but is also affected by molecular weight. As the molecular weight is increased, cold drawing of the specimen occurs and ultimate tensile strengths significantly higher than the yield strengths are obtained. With low molecular weight resins, the ultimate strength is lower than the yield strength, especially at high rates of loading. Ultimate tensile strength like yield strength is also

affected by temperature and rate of loading as shown in Fig. 3.8

Increasing strain rate causes an increase in tensile strength, although there is a maximum in tensile strength at some particular high strain rate since elongation is reduced to such an extent that the material sample breaks before the yield point. Thus tensile strength is critically dependent upon elongation.

The influence of straining rate is illustrated in Table 3.5 and 3.6 for two resins of equivalent molecular weight, but different density.

TABLE 3.5 Influence of Straining Rate on Tensile Properties

Strain rate mm/min	50	100	500
Yield Strength Kg/cm^2	225	230	255
Ultimate Strength Kg/cm^2	215	190	155
Ultimate Elongation %	650	615	105

Test Specimen ISO R 527 type 2

Polyethylene density 0.950 g/cc

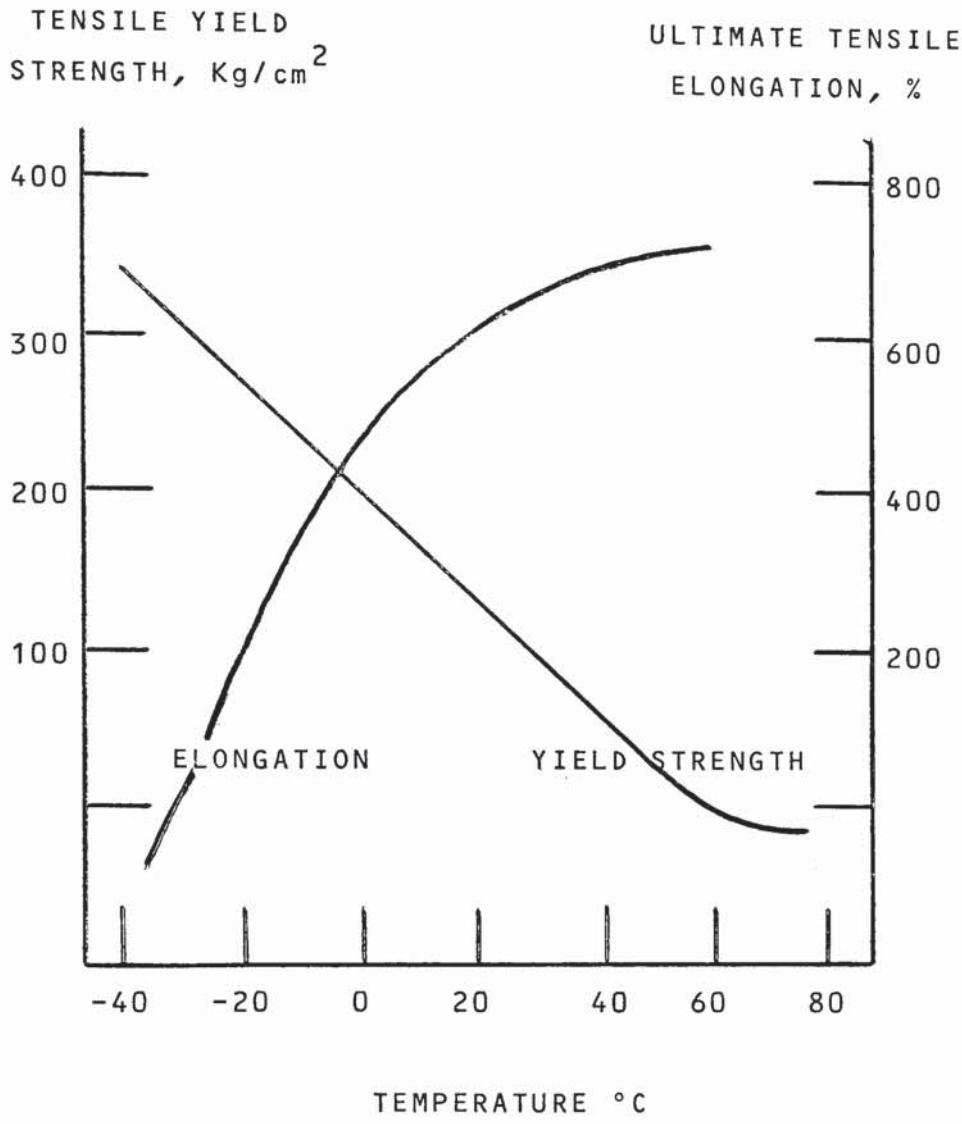

Fig. 3.8 INFLUENCE OF TEMPERATURE ON THE TENSILE PROPERTIES OF A 0.94 g/cc DENSITY ETHYLENE-HEXENE COPOLYMER

TABLE 3.6 Influence of Straining Rate on Tensile Properties

Strain rate mm/min	50	100	500
Yield Strength Kg/cm^2	195	200	220
Ultimate Strength Kg/cm^2	240	240	160
Ultimate Elongation %	705	700	550

Test Specimen ISO R 527 type 2

Polyethylene density 0.939 g/cc

3.5.3.3 Impact Strength

Qualitatively the impact strength of a plastic material is the amount of energy it can take up before some permanent damage is done. Arbitrarily, the area under the stress-strain curve carried out to break can be taken as the impact strength. Thus, approximately, impact strength is the product of tensile strength and elongation and as such it is influenced by the same parameters, these being molecular weight and molecular weight distribution, although molecular weight is the dominating factor.

In general, the copolymer resins yield impact values according to the Izod test that are lower than for homopolymer of similar melt index. A partial explanation for this is that melt index does not have the same signficiance for different polymers as shown from a study of flow rates under high shear '94).

At high shear the flow of the copolymer resins is much higher than would be expected from the standard melt index values. When comparison is made on the basis of high shear flow, the impact strength (95) results of the copolymers are in good agreement with those of the higher density polymers. This fact is further illustrated in Tables 3.7 and 3.8 which give comparative data for various melt index and high shear flow index materials of both a 0.96 g/cc homopolymer polyethylene and a butene copolymer of 0.95 g/cc density.

The CIL flow index is the measured weight of flow in grammes per ten minutes through an orifice of 0.5mm under a pressure of 105.5 Kg/cm^2 at 190°C.

TABLE 3.7 Impact Strength of Homopolymer Polyethylene

Melt Index dg/min	0.2	0.9	1.5	3.5	5.0
CIL Flox Index dg/min	1.2	3.4	5.6	10.0	12.5
Izod Impact J/m	750	210	105	80	65
Tensile Impact J/m	5400	3400	3150	2200	1600

TABLE 3.8 Impact Strength of Copolymer Polyethylenes

Melt index dg/min	0.3	0.5	1.2	4.0	6.5
CIL Flow Index dg/min	1.8	2.5	7.0	17.0	24.0
Izod Impact J/m	210	105	55	43	37
Tensile Impact J/m	4300	3400	2500	2000	1700

3.5.4 Chemical Properties

There are several chemical factors which affect the use of a plastics material for any specific application. These include chemical attack, environmental stress cracking resistance (ESCR) and permeation. With respect to general chemical properties, polyethylene holds a very strong position since it is one of the most chemically resistant plastics materials commercially available. However, certain substances present from time to time in some gas lines can and do have a profound effect on polyethylene and this topic is considered in more detail in the relevant section in Chapter 6.

3.5.4.1 Environmental Stress Cracking Resistance

The environmental stress cracking phenomenon exhibited by polyethylene, continues to be an area of widespread research. Two distinct types of cracking have been reported (96, 97, 98, 99). Cracking exhibited by polyaxially stressed polyethylene in the presence of a surface active environment is generally the phenomenon referred to as ESCR. Thermal stress cracking or thermal embrittlement (100) is exhibited by some polyethylene when held in a stressed condition at elevated temperatures for a period of time and is considered as being of more relevance to wire and cable applications. Stress cracking is the short time brittle failure of a material under tensile

stress appreciably below the limits of its long term strength. The distinguishing characteristic is a time-load dependence, the stress responsible for the ultimate catastrophe being the resultant of the concerted action of all the stress components present, those externally applied as well as those internally contained or arising from the product or sample preparation (101).

Increasing average molecular weight and narrowing molecular weight distribution improve the resistance to stress cracking. Increasing crystallinity can have either a beneficial or detrimental effect, depending on whether the circumstances involve constant load or constant deflection, but in the ultimate increased crystallinity provides increased opportunity for brittle fracture.

Stress failures may be initiated in or near the surface layers of polymer or deep within the mass of the material. Those developing on the surface are abetted by the presence of an agent, such as a typical surfactant, which has the ability to adsorb on and to lower the surface energy of the polymer. Swelling agents and partial solvents can also induce cracks.

Rebinder (102) in studying stress cracking in metals observed that a surface fracture environment tends to adsorb onto all available surfaces and decrease the surface energy level. This resulted in a sharp decrease in plastics flow and a lowering of the level of stress necessary to cause fracture. Gilroy (103) found that when a surfactant is applied to polyethylene during a standard tensile test an abrupt change occurs in the modulus and ease of extensibility at the moment of application and a pronounced inflection appears in the stress-strain curve.

These findings indicate that the ease of environmental failure ought to be proportional to the lowering of the surface energy of the material by the adsorbed environment in the material surface flaws. This in turn is related to the surface energy characteristics of the adsorbing agent. This has been confirmed by Howard (104) who found the time to crack to vary in roughly inverse proportion to the surface tension of the cracking agent solution, the critical variable being the interfacial tension between the solution and the polymer substrate.

From the stress cracking viewpoint, it is the size and perfection of the crystalline aggregates or spherulites that control the material properties. The process by which fibrils grow to form the spherulite

is a very selective one which permits the incorporation into the growing structure of only selected components and rejects as impurities all other species. The rejected material is continually pushed ahead of the growing crystal face and eventually is distributed between inter-spherulitic boundries. The volume decrease which must accompany the crystallisation process must result in stresses on the remaining non-crystalline areas which provide sites, especially in the surface layers of the material, for the operation of a Griffith type mechanism. Distribution of the rejected impurities between interspherulitic boundries and intraspherulitic entrapments provide an explanation of the observed randomness of the fracture path, sometimes between, sometimes through spherulites. It similarly accounts for the beneficial effects of narrowed molecular weight distribution or disastrous effects on crack resistance of small concentration of low molecular weight fractions (101).

The influence of molecular weight (measured as melt index) on the environmental stress cracking resistance as measured by the Bell test is shown for a 0.960 g/cc density homopolymer in Table 3.9 and for a 0.95 g/cc butene copolymer in Table 3.10. The influence of density of ethylene-butene copolymers of melt index 0.3 dg/min on ESCR is tabulated in Table 3.11.

TABLE 3.9 Influence of Molecular Weight on ESCR of Ethylene Homopolymer

Molecular Weight Mw	175,000	140,000	125,000	95,000	85,000
Melt Index dg/min	0.2	0.9	1.5	3.5	5.0
ESCR-F50 hrs	60	14	10	2	1

TABLE 3.10 Influence of Melt Index on ESCR of Ethylene-Butene Copolymer

Melt Index dg/min	0.3	0.5	1.2	4.0	6.5
ESCR-F50 hrs	350	175	55	20	10

TABLE 3.11 Influence of Density of Ethylene-Butene Copolymers on ESCR

Density g/cc	0.96	0.95	0.94	0.925
ESCR-F50 hrs	30	150	600	1100

The ESCR of these polymers can be further increased by the use of 1-hexene in place of 1-butene as co-monomer, at the same density. The trend in improved ESCR performance by the use of a higher member of the homologous series as comonomer is adequately shown in Table 3.12.

TABLE 3.12 Effect of Comonomer on ESCR

Comonomer	Melt Index	Density	ESCR
Propylene	0.32	0.937	500
1-Butene	0.31	0.937	870
1-Pentene	0.27	0.940	> 1000
1-Hexene	0.30	0.940	> 1000

3.5.4.2 Permeation

Primarily, permeation is considered a physical migration of a product through the walls of the container and a subsequent vaporisation process once the product reaches the outside surface. Also to be considered is the possibility that outside elements may permeate into the container. One such example would apply when natural gas and potable water pipes are laid side by side. Any permeation of gas out through the plastics walls of the gas pipe and in through the plastic walls of the water pipe would cause tainting of the water.

In a city or industrial gas distribution system, wherever there is a possibility of a dead air space, gas permeation would be aproblem because of the explosive mixture that could be created.

The theoretical gas permeation can be expressed as:

$$q = \frac{PA}{t}$$

Where q = quantity transmitted/area/time

p = pressure difference

A = permeability coefficient

t = pipe well thickness

Permeation measurements (105) of a gas mixture through actual pipe specimens using a gas chromatography analysis technique established for a series of thermoplastic pipe materials for different pipe wall thicknesses and different gas pressures that -

i: Gas permeation is inversely proportional to pipe wall thickness and directly proportional to the pressure in the pipeline - Fig. 3.9.

ii: Gas permeation rates decrease as the homologous hydrocarbon series increased in carbon atoms - Fig. 3.10

The transmission mechanism of the gas constituents through the pipe wall is through a process in which the gas dissolves at one surface, diffuses through the pipe wall under a concentration gradient and evaporates from the other surface at the lower concentration. Transmission rate is therefore dependent on the solubility of the natural gas constituents at a specific pressure and on the diffusion constant of the dissolved gas in the respective polymer. The activation energy for diffusion is the energy required

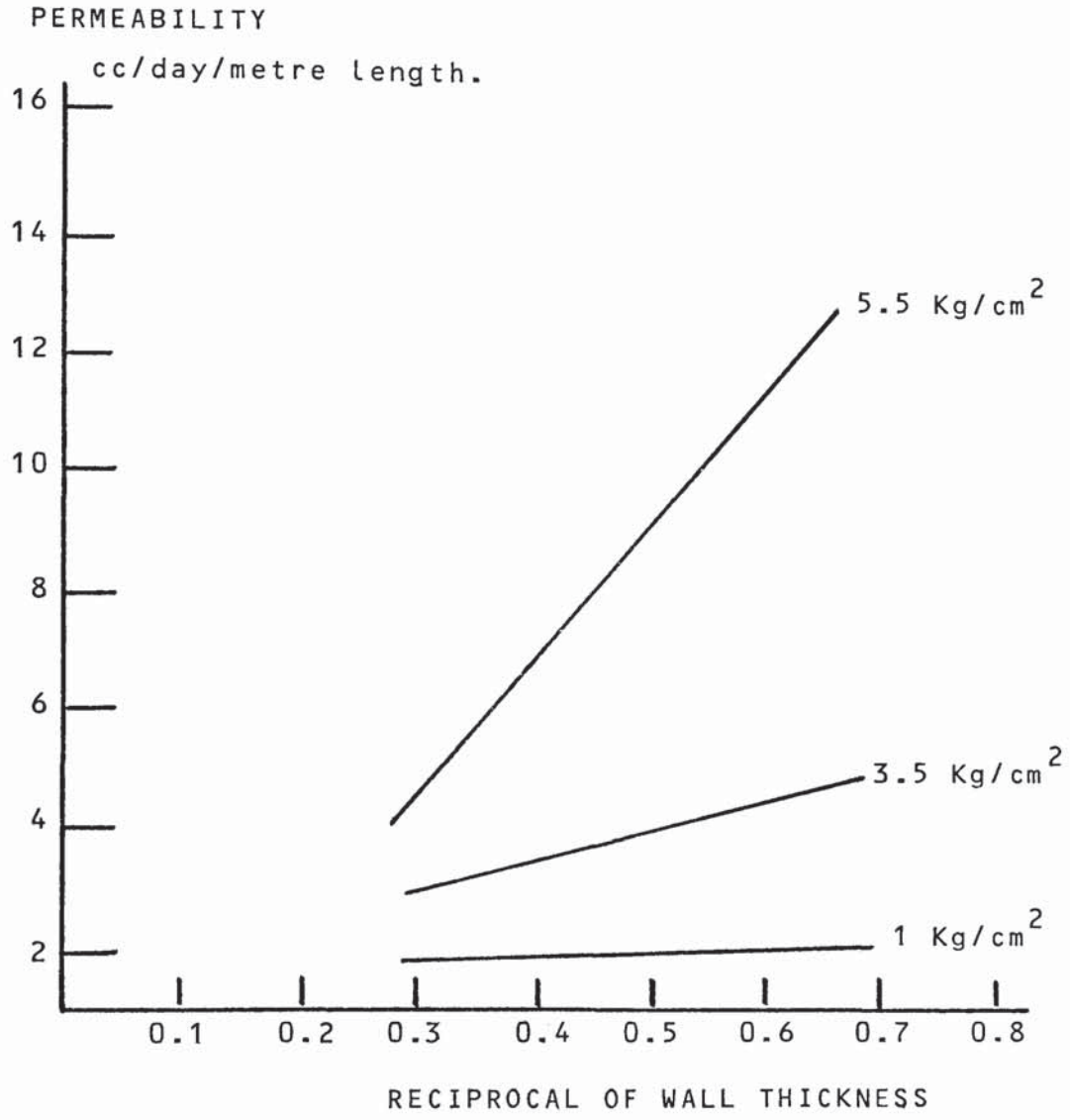

Fig. 3.9 Influence of Pipe Wall Thickness and Pressure on Gas Permeation

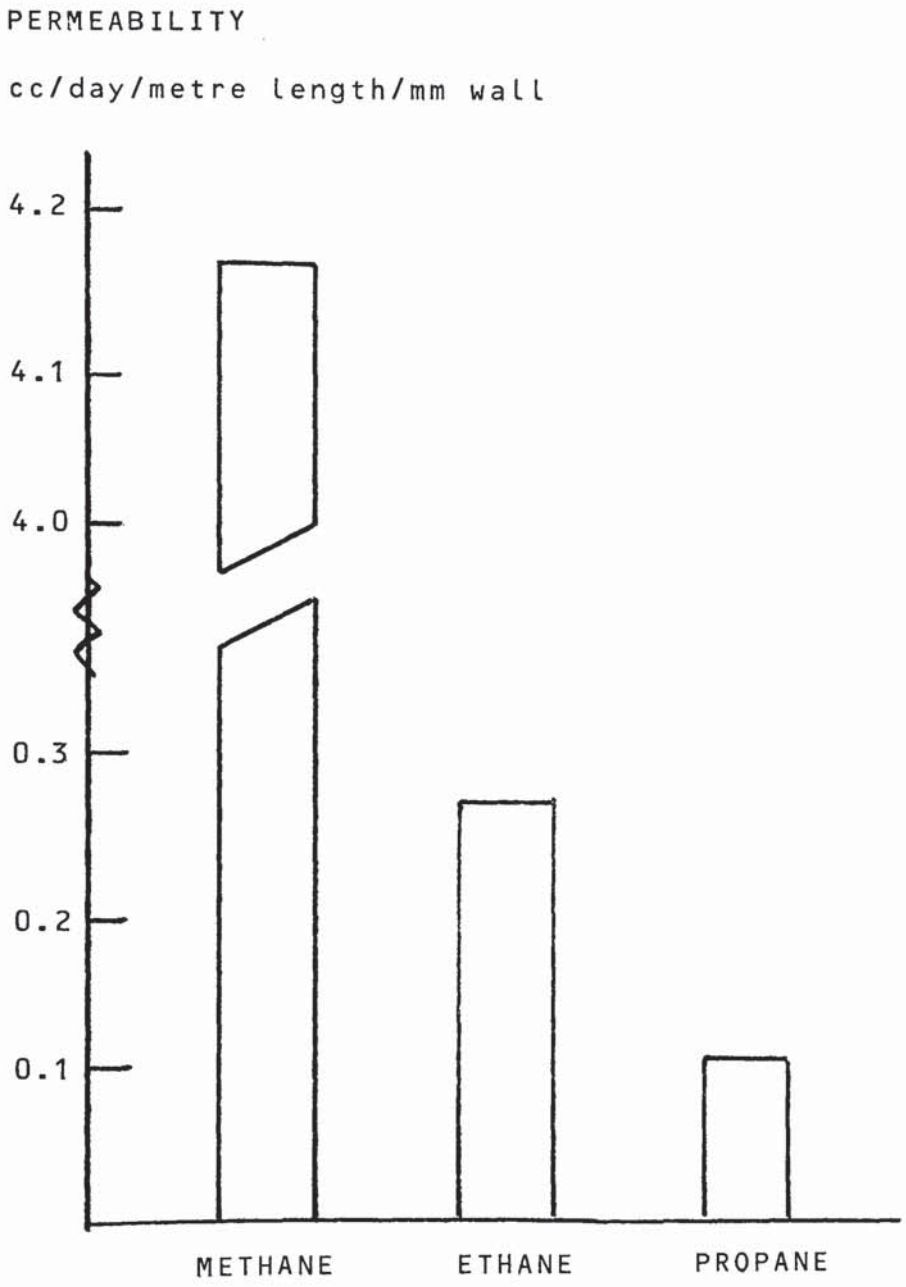

Fig. 3.10 Permeation of Gases Through HDPE Pipe

for separation of the polymer chain segments against the cohesive forces of the polymer chain to allow the passage of the diffusing gas molecule (106). The polyolefin materials have low cohesive energies and thus high diffusion constants. However, as shown in Fig. 3.11, which is calculated from the previous data, permeability decreases with increasing density or degrees of crystallinity due to the impedence to flow due to bypassing impenetrable crystallites. The crystallinity serves to reduce the permeability by the combined effects of reduction of volume available for flow, diffusional impedence by the crystallites and restriction of polymer chain mobility.

Plastics materials in general have relatively high permeability co-efficients especially with a first comparison to the more traditional metal materials. A comparison of permeability through the most common plastics gas distribution materials as calculated from the above data is shown in Fig. 3.12.

It is noteworthy to compare that whereas permeability through metal is zero, many national gas authorities suffer up to an 11% loss representing £21 million for the U.K. in the total gas transmitted through cast iron mains due to dried out joint seals and corroded lines (107).

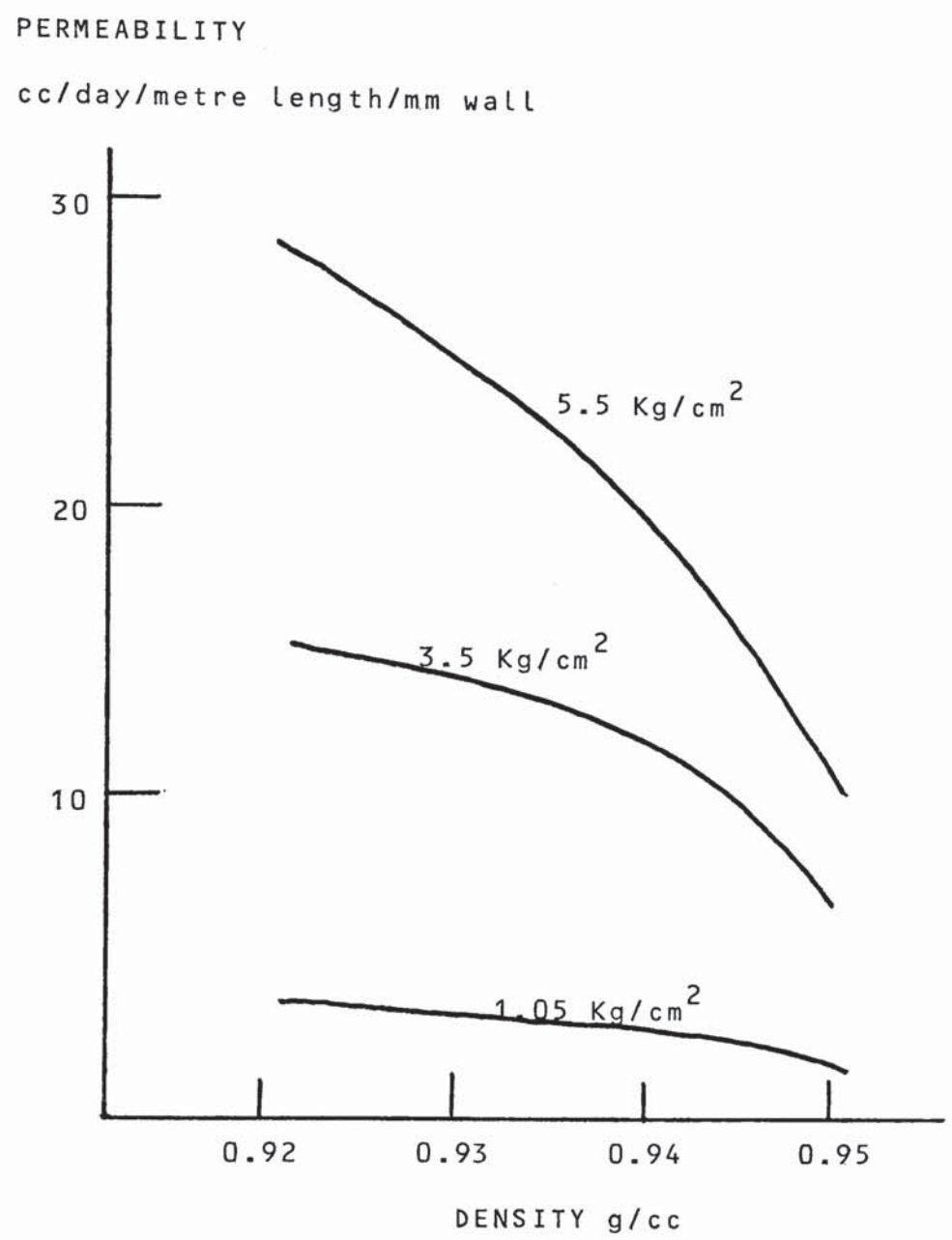

Fig. 3.11 Relation Between Permeability and Pipe Density

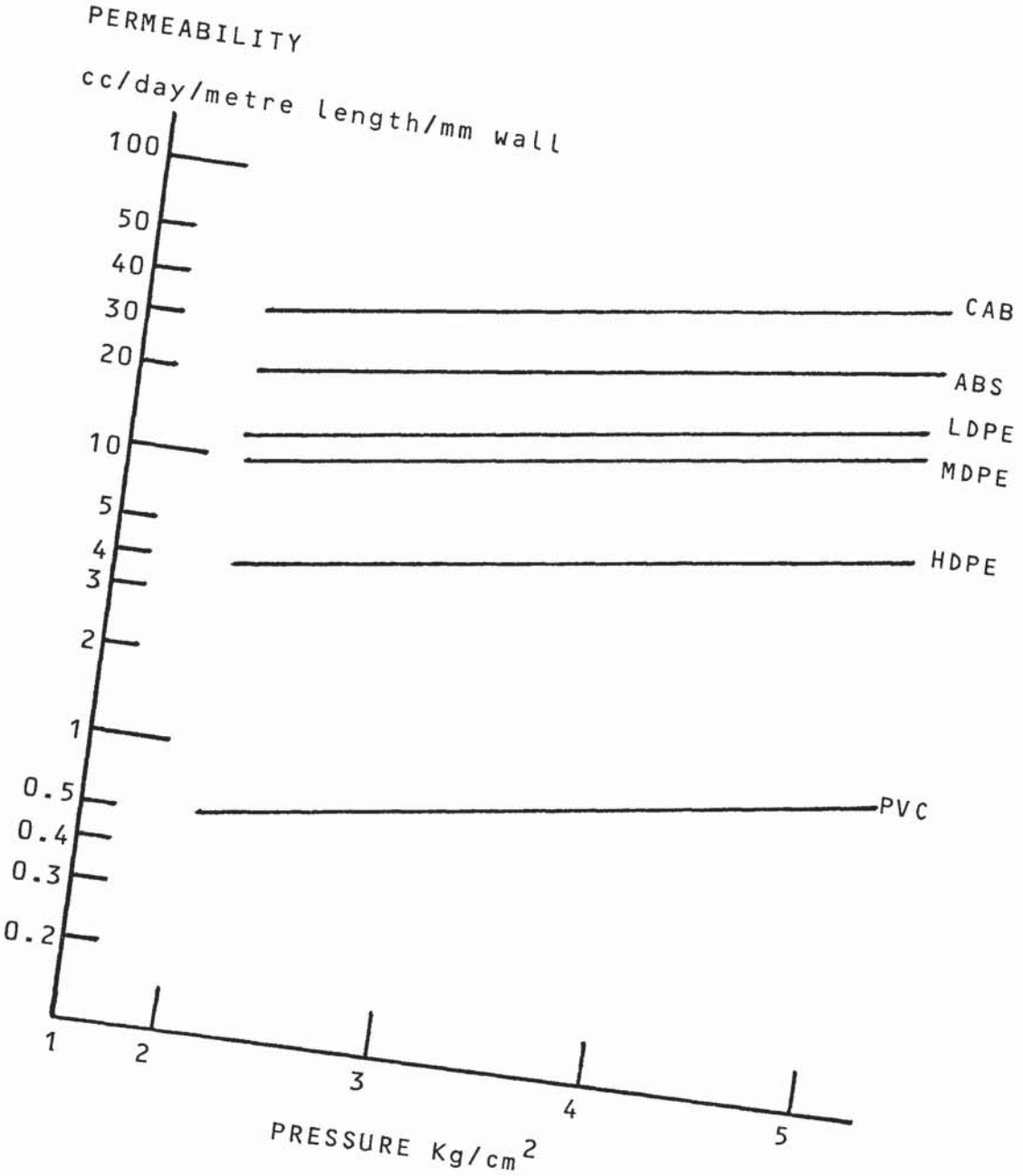

Fig. 3.12 Relative Permeability Through Plastics Pipes

Calculation of the above data as shown in Fig. 3.12 shows that under the normal prevailing gas line pressures up to and including 4 Kg/cm^2, the loss of natural gas by permeation through a medium density ethylene-hexene copolymer pipe wall will be insignificant and amount to no more than 5 litres per day per kilometre of 50 mm diameter pipe.

Apart from economic loss, the main concern of gas permeation in a natural gas distribution line is the safety aspect of the creation of an explosive mixture of gas in dead air space. Fig. 3.13 represents the time in months for such an explosive mixture to be created by gas permeation through the pipe walls. For the purposes of this hypothetic case, these times are based on a 70 litre space with an exposed length of 3 metres of 32mm diameter pipe. An explosive atmosphere is created with the permeation of 3.5 litres of gas.

3.5.5 Stability

In the presence of air, polyolefins degrade slowly by an oxidative process which becomes quite rapid when promoted by ultra-violet radiation or heat. The degradation manifests itself in a gradual loss in flexibility until the sample becomes so brittle that it fractures under very slight stress. Both thermal and photo-oxidation degradation proceeds via a free

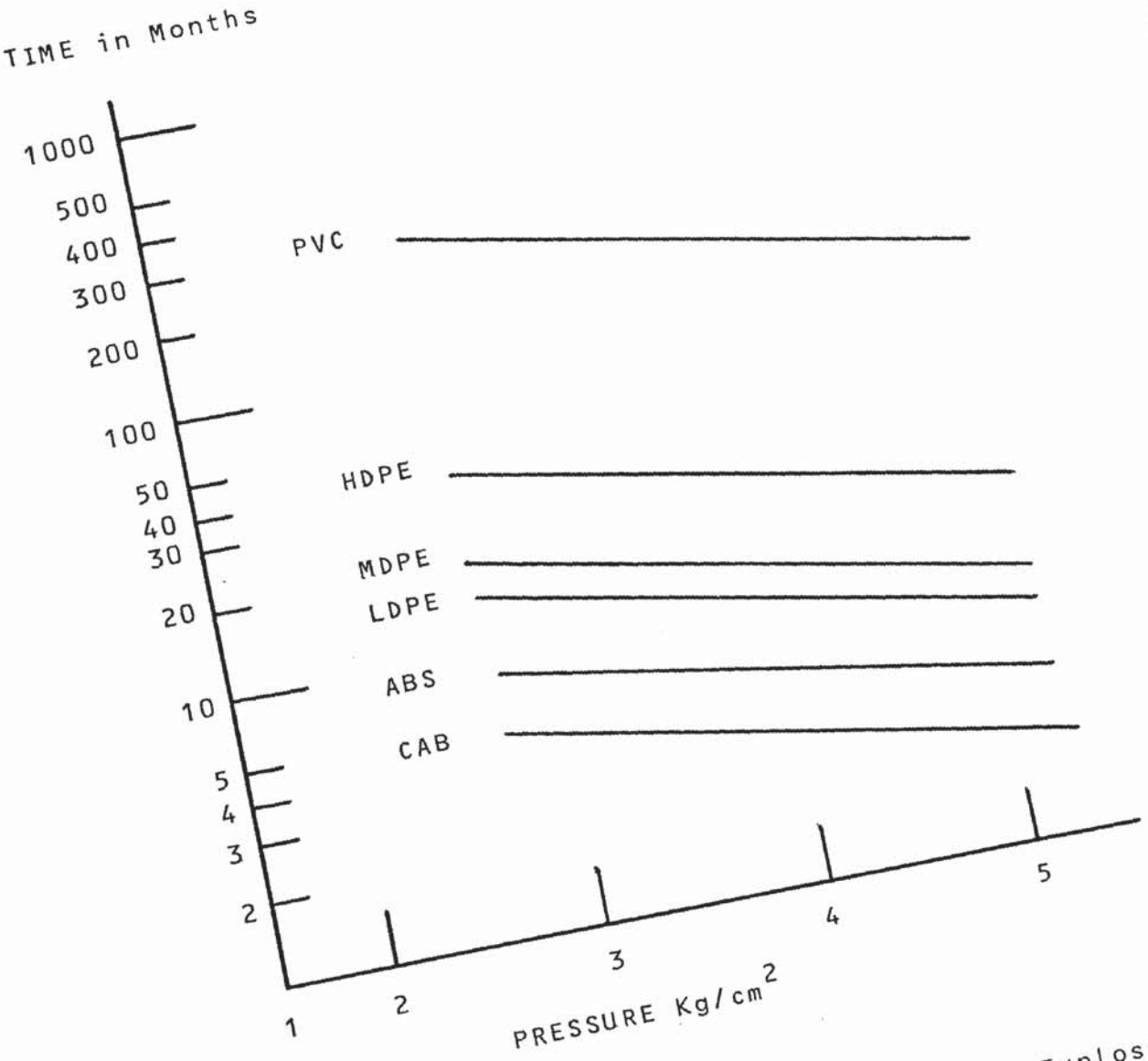

Fig. 3.13 Time Before Permeation Causes an Explosive Mixture

radical chain reaction (108, 109) and in both cases is due to the presence of peroxides (110). The rapid initial formation of carbonyl compounds occurring during thermal and photo-oxidation is associated with thermolysis and photolysis of peroxide compounds respectively with the formation of initiating free radicals and carbonyl compounds, the rate of carbonyl generation being directly proportional to the initial peroxide concentration present (111).

3.5.5.1 Thermal and Mechanical Degradation

The thermal and mechanical forces which act upon the macromolecules when the polyolefins are processed above their melting points, can cause molecule cleavage. These molecular cleavages initiate chain reactions via a radical mechanism which either reduce the molecular weight via chain scission or increase the molecular weight via branching and crosslinking. In practice, both mechanical and thermal degradation processes are always induced simultaneously in the presence of oxygen. The possible reactions are shown schematically in Fig. 3.14.

At high melt temperatures an overall reduction in molecular weight occurs, whereas at lower melt temperatures, the formation of long chain branching is favoured leading to molecular weight increase. The

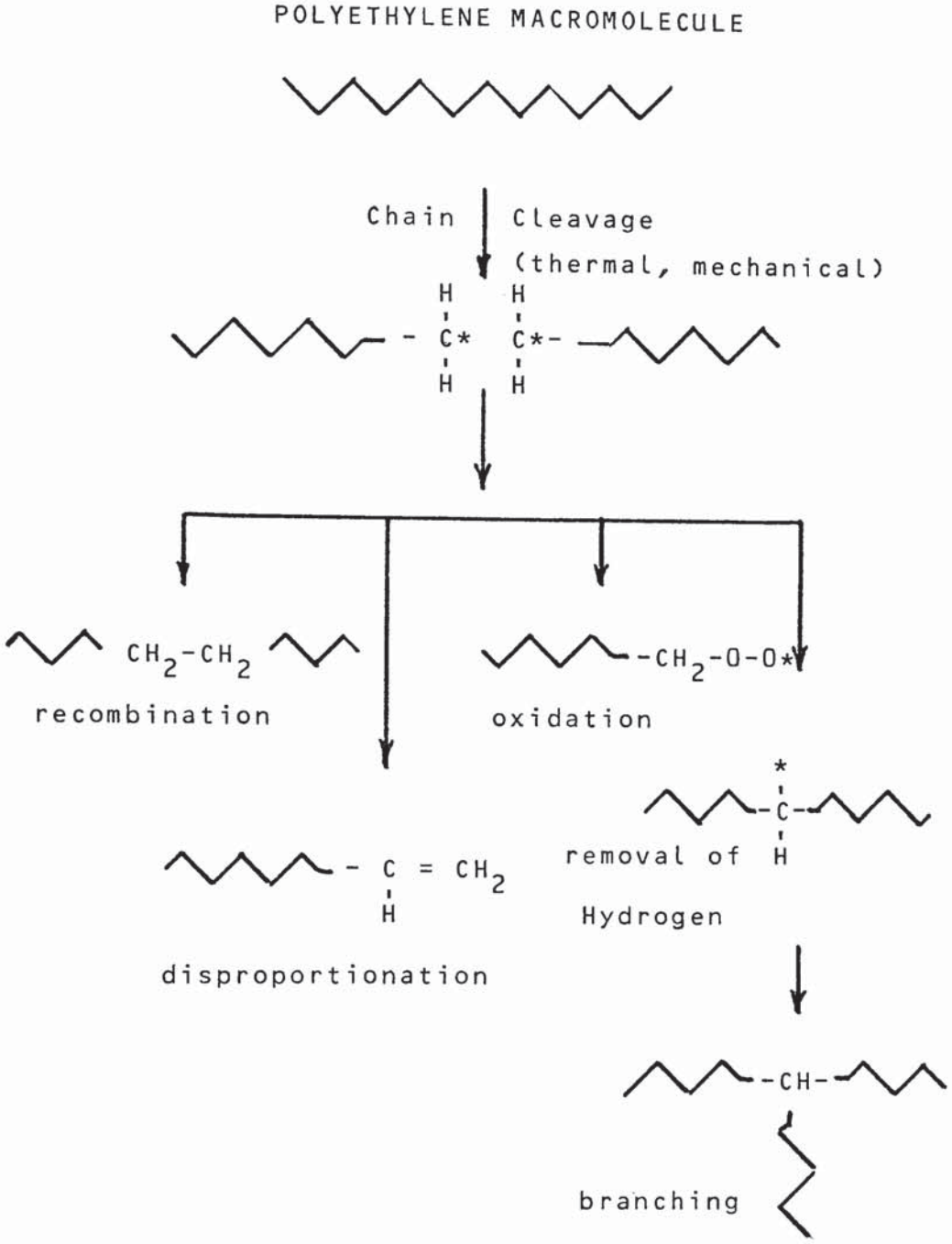

Fig. 3.14 Reaction Possibilities Under the Influence of Mechanical and Thermal Stress

presence of oxygen leads to peroxy radical (ROO°) formation which propagates the reaction by abstraction of hydrogen to form hydroperoxides (112). Additional oxidation chain reactions may be initiated by radicals formed by homolytic cleavage of these peroxides. Terminal vinyl groups can also influence the reaction and will lead to molecular weight increase via a branching process.

These reactions can also lead to changes not only in the molecular weight, but also in the molecular weight distribution. Schaaf (113) has shown that, under mechanical and thermal stress, high density polyethylene homopolymer suffers a reduction in both molecular weight Mw and molecular weight distribution MWD as reproduced in Table 3.13.

(113)

TABLE 3.13 Thermal Mechanical Degradation of HDPE

	Polymer A	Polymer B
Orignal Mw	139,000	194,000
Final Mw	105,000	122,000
Original MWD	9.2	15.2
Final MWD	5.1	10.1

This fact has been practically applied in the earlier days of polyethylene development to economically produce high melt index narrow molecular weight distri-

bution resins for injection moulding applications by "vis-breaking" more easily polymerisable high molecular weight extrusion resins.

Stablization against thermal degradation depends, in part, on reactions which remove the propagating radicals from further reaction, the stablizers functioning in a sacrificial role.

One mechanism for stablization is based on peroxy radical extraction of a labile hydrogen from a hydroxyl or an amine group of the stabilizer. When the protectant has been consumed in its sacrifical role, oxidation becomes autocatalytic and eventually the rate approaches that of the uninhibited polymer. Types of antioxidants other than phenols and amines, achieve their effect by decomposing hydroperoxides into inactive products without the intervention of free radicals. In this way, they destroy the initiators of oxidation chain reaction. Thus, phosphites or sulphides reduce peroxides to alcohols.

The ethylene copolymers are inherently more thermally stable than homopolymers. The higher molecular weight polyethylene in any series of resins where density is constant have the best thermal stability. A several-fold improvement is obtained by lowering the

density or decreasing the modulus of the resins (114). This is illustrated in Table 3.14 which shows the failure times for a 0.2 dg/min melt index homopolymer and 0.3 dg/min melt index ethylene butene copolymer at strain reates between 5-40% at 71°C. These data were determined by bending 6.35mm wide 0.15mm thick strips around mandrels of varying radii to impose known strain on the outer surface and noting the time for cracking to develop. With the copolymer resin, the critical strain may be increased to over 40%.

TABLE 3.14 Comparison of Homo- and Co-Polymer Thermal Stability

Strain %	0.3 m.i. Copolymer hours	0.2 m.i. Homopolymer hours
40	> 1000	1
30	> 1000	1
20	> 1000	1
10	> 1000	7
5	> 1000	> 1000

3.5.5.2 Photodegradation

All organic polymers undergo degradation on exposure to sunlight and in the presence of oxygen, but the extent of this varies markedly with the structure of the polymer. Thus the relatively high stability of polytetrafluoroethylene is due to the constituent

carbon - carbon (C - C) and carbon - fluorine (C - F) bonds being stable with bond energies exceeding the light energy. Conversely the tertiary hydrogen atom in the polypropylene and polybutent-1 backbone is easily abstracted by radicals and more strikingly the conjugated double bonds in the recently commercially introduced syndiotactic 1, 2 - polybutadiene enable absorption to take place even in the visible range.

For practical purposes, photodegradation usually results in embrittlement of the polymer followed by loss of tensile properties. Discolouration accompanies the degradation depending on the level of dehydrochlorination to produce a conjugated double bond polyene structure. Longer polyenes are capable of forming cabonium salts which lead to a further deepening of colour (115).

3.5.5.2.1 Light Energy

The deterioration of plastics in outdoor weathering is caused predominantly by sunlight, especially ultra violet radiation. Ultra-violet radiation is defined (116) as electromagnetic radiation of wavelength between 4 and 400 nanometers (nm = 10 angstroms $=10^{-9}$m) and as such constitutes the radiation between X-rays and the violet end of the visible spectrum. Sunlight

is filtered through the atmosphere removing the shorter wavelengths up to 280-310 nm before it reaches the earth (117). Thus the ultra violet effects on plastics result primarily from wavelengths of 290 - 400 nm which represents approximately 5% only of the radiation incident on the earth's surface. In energy terms, this wavelength range corresponds to 100 - 70 Kcal/mol. This energy range is sufficient to cause dissociation of many bonds and hence the quanta present in the U.V. spectrum have the potential to cause chain scission in many polymer types.

Typical indoor lighting, both fluorescent and incandescent, have U.V. wavelengths of much lower intensity and with a sharp cut-off at 330 nm (90 Kcal/mol). Furthermore, window glass does not transmit significantly below 330 nm and thus, in an indoor environment, the critical portion of the sun's spectrum between 290 - 330 nm (erythermal region) is essentially absent (118).

3.5.5.2.2 Process

A sequence of reactions is normally entailed in any photodegradive process. A prerequisite is that the polymer be able to absorb light having sufficient energy to activate the constituent groups. Secondly,

mechanisms must exist whereby this excitation then leads to a chemical reaction instead of degradation of the energy via some photophysical process such as fluorescence, phosphorescence, or loss of energy as heat.

Theoretically, a distinction may be made between photoinitiation and photosensitisation. A group that is excited by absorbed light and subsequently decomposes into free radicals, which may then initiate oxidative degradation, is defined as a photoinitiator. A photosenitiser is defined as a group or compound which is excited by absorbed light, but subsequently transfers its excitation energy to other groups which then initiate the actual degradation. However, under different conditions, a given group can act as both initiator or sensitiser and, hence, it is not possible to make this distinction 'a priori'.

The mechanism of degradation usually proceeds via a mechanism of free radical formation and abstraction of hydrogen followed by chain scission and crosslinking reaction (119). These photolysis mechanisms are normally complicated by the diffusion limitations of the free radicals and thus polymers with a glass transition below ambient temperature will be degraded more readily because of the increased radical mobility.

Chain reactions involving peroxy radicals formed by interaction with oxygen dominate the overall degradation process. Hydrogen abstration by the peroxy radical forms weak hydroperoxide bonds with a dissociation energy of only 42 Kcal/mol and these can be further photolysed by U.V. as well as by catalytic action of metals.

3.5.5.2.3 Photo-initiation Mechanism for Poly-Ethylene

Polyethylene as a high molecular weight aliphatic hydrocarbon should be transparent and therefore stable to ultra-violet radiation. In practice, this is not the case; the explanation being the presence in the polymer of very small but significant amounts of photosensitive groups (108, 113). Such groups are peroxide groups, carbonyl structures, aromatic rings, conjugated double bonds, hydroxyl groups and certain solvent and catalyst residues all of which can become incorporated during the polymer synthesis, processing or subsequent storage or use.

Scott (109, 110) has demonstrated that the chromophore primarily responsible for the photo-initiation process is the hydroperoxide group and that this photo oxidative reaction precedes that of the macrocarbonyl group which had long been regarded (120) as the major photo-initiation mechanism. The hydroperoxides and

peroxides are formed during the polymer drying and processing steps by thermal oxidation. The macro carbonyl group becomes more important in the later stages of the photo-initiation process when, under the influence of U.V., they further dissociate via a Norrish reaction. Photo-initiation then continues by further reactions of the primary alkoxy and hydroxyl radicals (121) with chain scission through allylic hydroperoxide breakdown predominating over crosslinking through vinyl addition. These reactions are schematically illustrated in Figure 3.15

3.5.5.2.4 Weathering Resistance of Polyethylene

The extent to which photo-oxidative degradation will occur in polyethylene, will depend on several factors such as molecular structure, location and duration of exposure (122), geometry of sample and type and concentration of stabilizers employed (123). Photo-degradation, for the most part, manifests itself in a reduction in the molecular weight of the resin with a corresponding increase in brittleness (124).

The process of ultra violet degradation differs from thermal oxidative breakdown in that it occurs initially only at the surface of the sample and then progressively attacks the underlayers. The depth of degradation depends upon the oxygen pressure and is

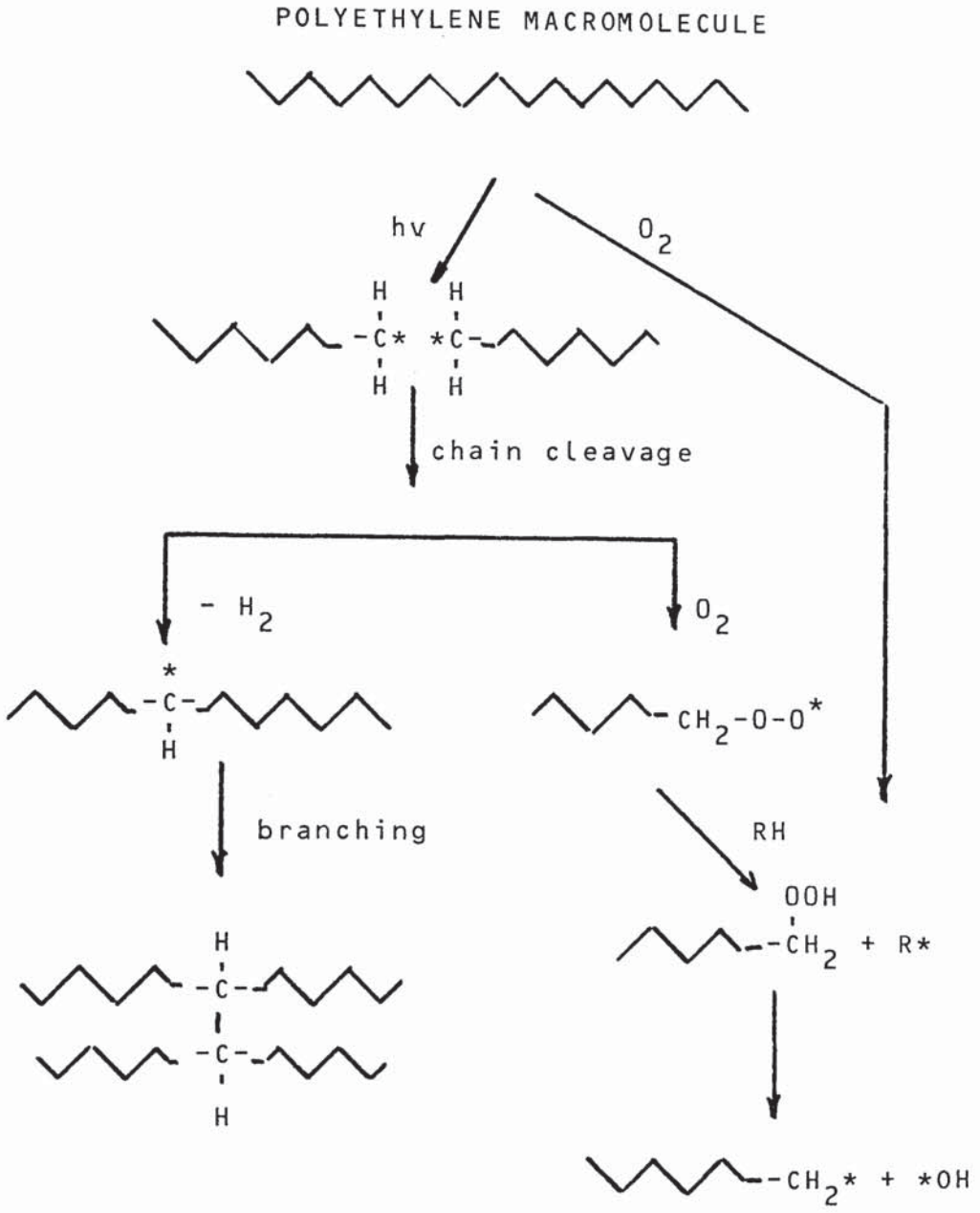

Fig. 3.15 Photoinitiation Mechanisms for Polyethylene

typically 700 microns thickness at twice the atmospheric pressure (125).

Owing to the high degree of polymerisation associated with polyethylene, it is only necessary for one in a thousand of the bonds to be broken in order to cause an appreciable fall in molecular weight (126) with a consequent deterioration in mechanical properties. Thus it will require a longer time for a high molecular weight resin to embrittle in the presence of ultra-violet light, than a resin with a lower molecular weight. This is illustrated in Figs. 3.16 and 3.17, which plot respectively the percentage tensile strength and elongation retained against melt index for a 0.955 g/cc stabilised ethylene-butene-1 copolymer after one year of exposure in Arizona.

In addition to molecular weight, Martinovich (127) has investigated the influence of copolymerisation and the comparative data for a 0.96 g/cc density ethylene homopolymer and a 0.95 g/cc density ethylene butene-1 copolymer, both of 0.3 dg/min melt index, are illustrated in Fig. 3.18. The tensile samples were exposed to a carbon arc illumination in a weatherometer and the exposure time determined for an absolute value of tensile elongation of 10%. The influence of pigment on the stabilised materials is also illustrated.

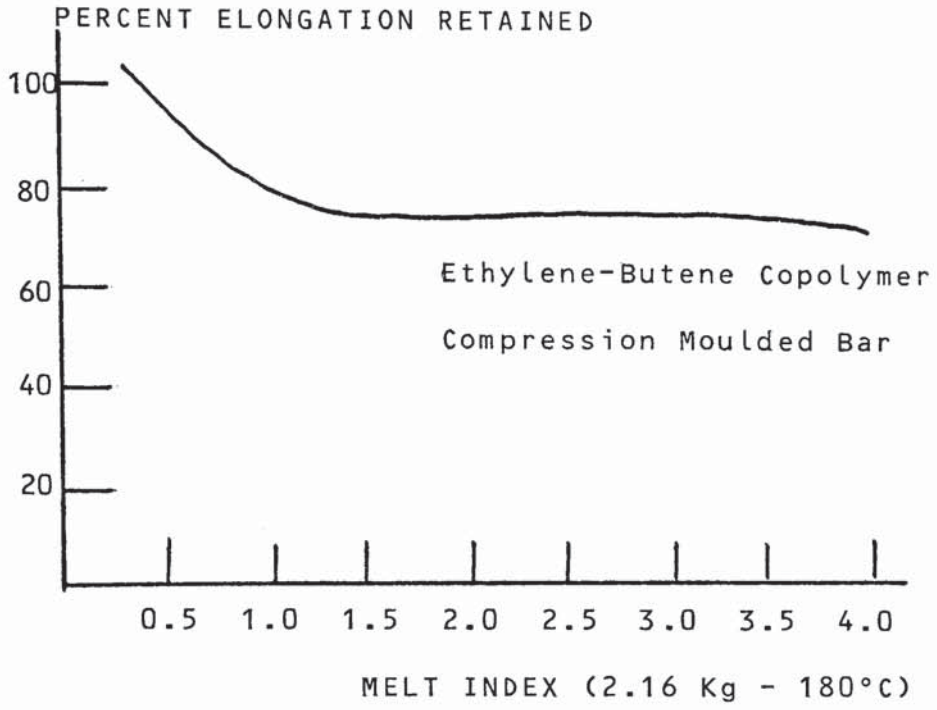

Fig. 3.16 Percent Elongation Retained After One Year Exposure in Arizona

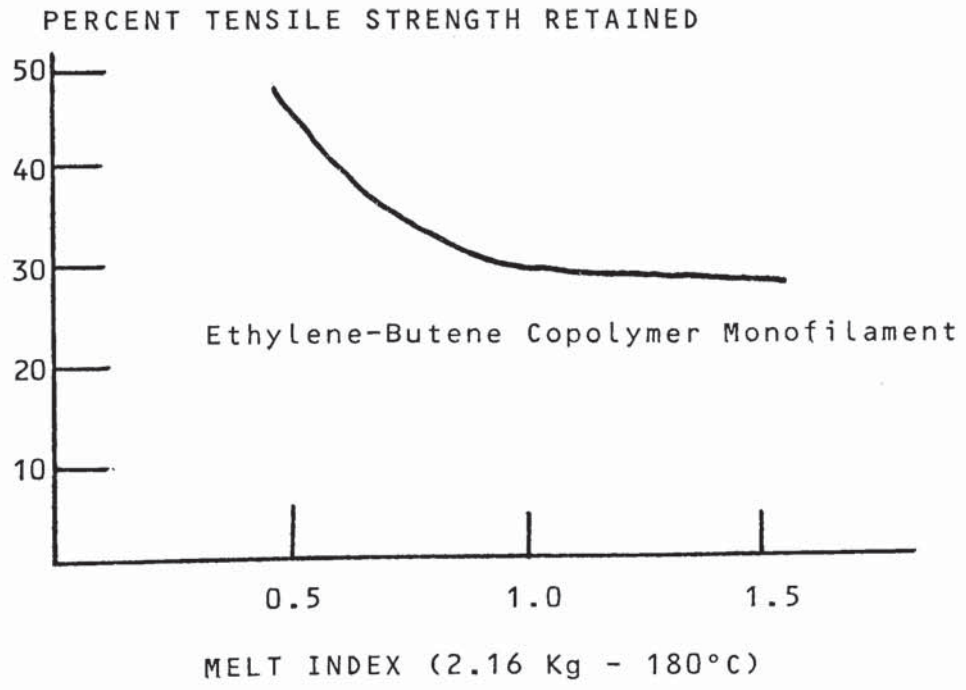

Fig. 3.17 Percent Tensile Strength Retained After One Year Exposure in Arizona

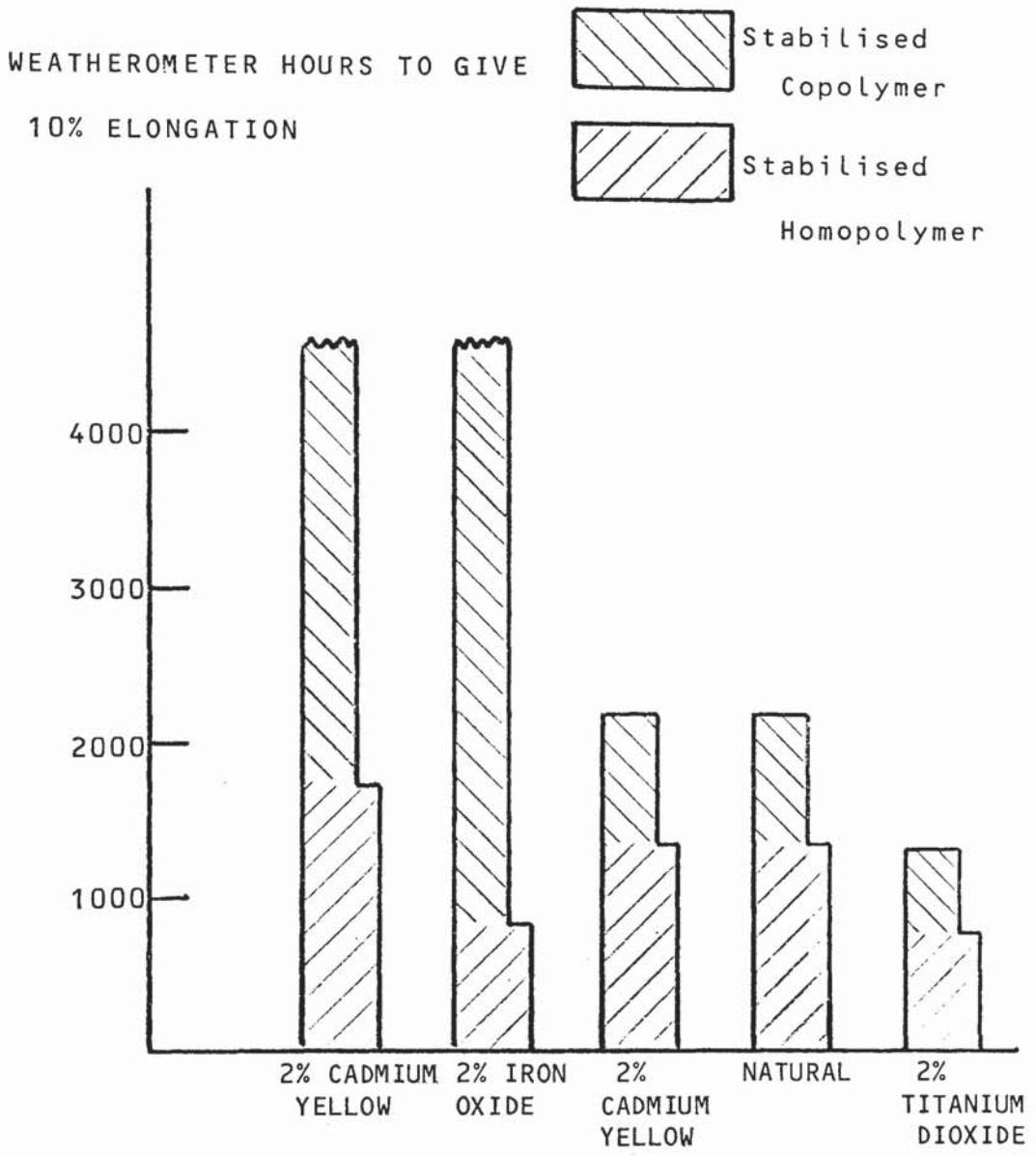

Fig. 3.18 Comparative Weatherometer Data for Ethylene Homopolymer and Ethylene-Butene Copolymer

Pigmentation, in practice, has a pronounced effect on U.V. protection, the pigment either absorbing strongly in the U.V. region while exhibiting very little or no absorption in the infra-red, such as the channel types of carbon black, or actually accelerating degradation as in the case of titanium dioxide. Figure 3.19 illustrates this influence of pigments (124, 127) on a 0.95 g/cc density stabilised ethylene butene-1 copolymer subjected to 4000 hours in a weatherometer.

Not only does the protection offered by pigments against U.V. degradation depend on the type of pigment, but also on the concentration, assuming that dispersion is adequate in all cases. Fig. 3.20 shows the effect of red iron pigment concentration on outdoor ageing of ethylene homopolymer monofilaments after one year of exposure in Arizona.

Under international colour code rules for dangerous products, pipe systems carrying natural gas are colour coded yellow and, specifically in the U.K., are coloured within the range 10E.53 to 08E.51 of B.S. 4800 (128). There is much data (122 - 129) to suggest that from a U.V. stability viewpoint, a yellow system is far from ideal and legislation should be promoted for a black pigmented system with a yellow line or lines for identification purposes.

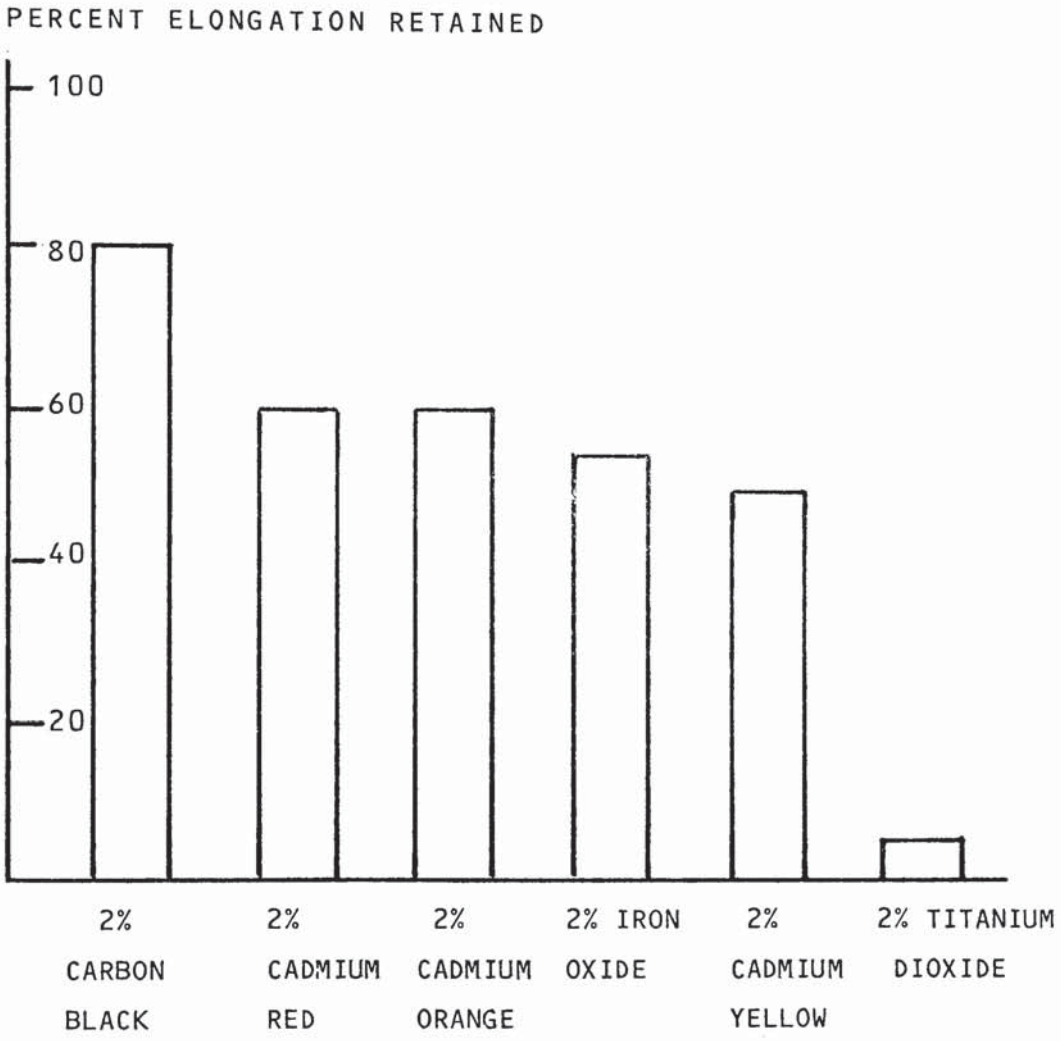

Fig. 3.19 Pigment Effect on Elongation of Ethylene-Butene Copolymer Subjected to 4000 Hours Xenon Lamp Exposure

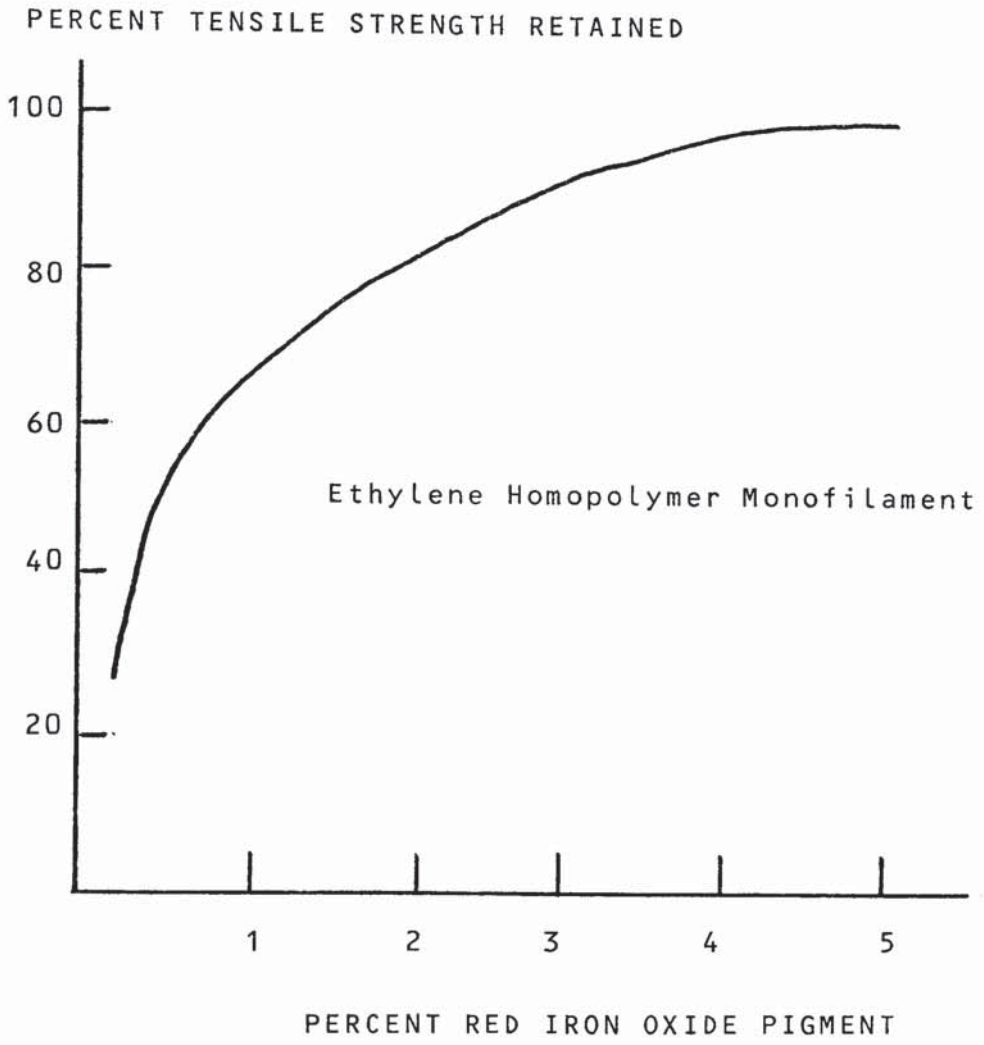

Fig. 3.20 Effect of Pigment Concentration on Tensile Strength After One Year Ageing in Arizona

The yellow pigments cadmium yellow, lithopone yellow and coated molybdate have been evaluated in both stabilised ethylene homopolymers and copolymers at both 1% and 2% concentration under Xenon lamp weatherometer exposure up to 8000 hours (129). These results are reproduced in Fig. 3.21. Increasing the concentration of the coated molybdate and lithopone yellow improves weathering performance, whereas the cadmium is reduced in effectiveness. That there is some interaction between cadmium yellow and the hyroxybenzophenone stabiliser is further illustrated in Fig. 3.22, which shows that in the absence of any stabiliser, the high concentration of pigment gives the better weathering performance. Nickel complex light stabilizers do not exhibit this phenomenon (127).

Photodegradation starts at the illuminated surface and progressively invades the underlying areas. It has been demonstrated (124) that the effects of weatherability can be partly nullified for a non-stressed specimen at specimen thickness greater than 2.5 mm.

Correlatory evidence for both artificial and natural weathering (Fig. 3.23) shows that below 2.5 mm the effects of weathering are very pronounced. This is added weight to the stipulation for a pipe minimum

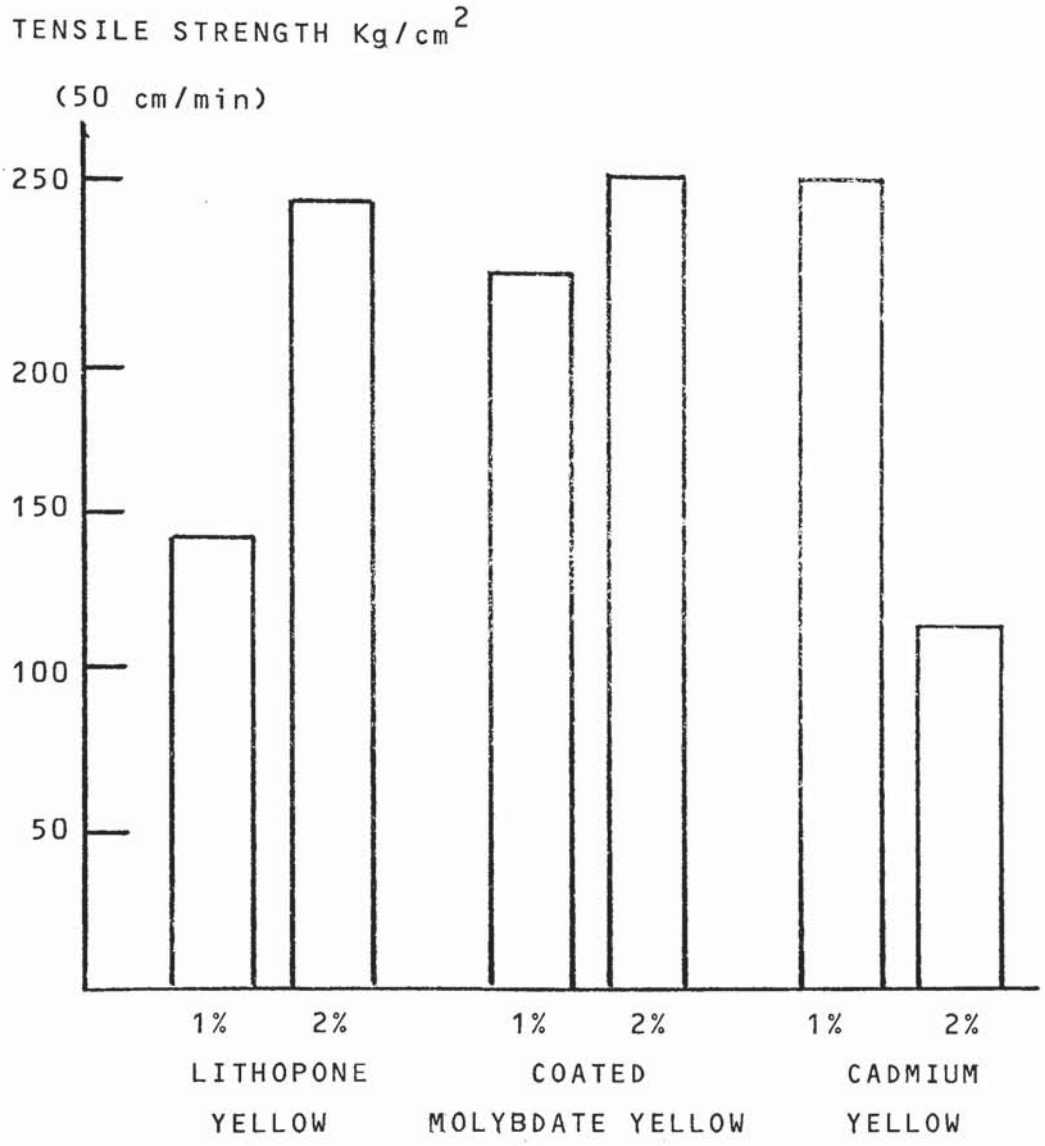

Fig. 3.21 Influence of 8000 Hours Weatherometer Exposure on Yellow Pigmented, Stabilised Ethylene-Butene Copolymer

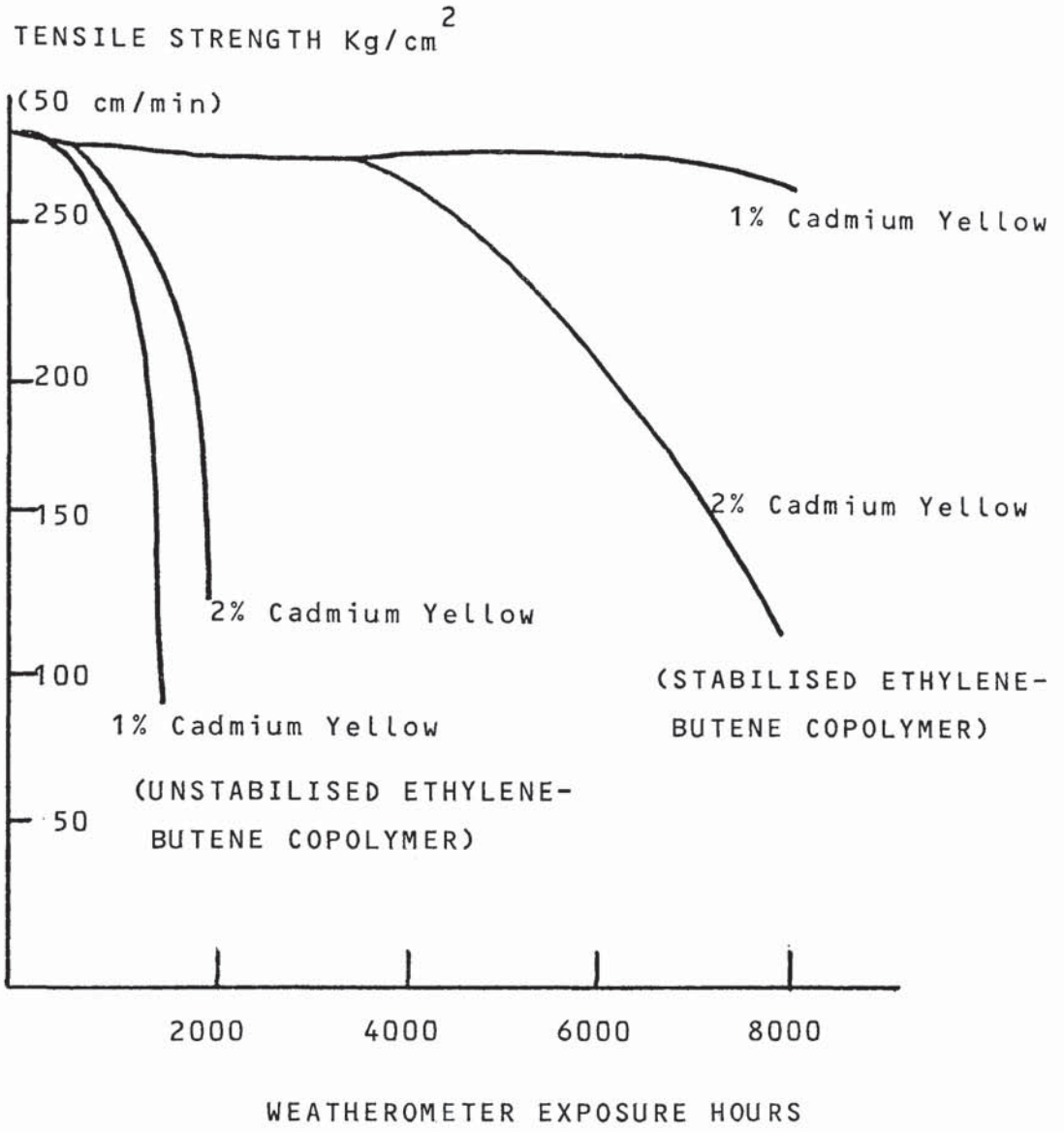

Fig. 3.22 Effect of Cadmium Yellow Pigment on Exposure Resistance

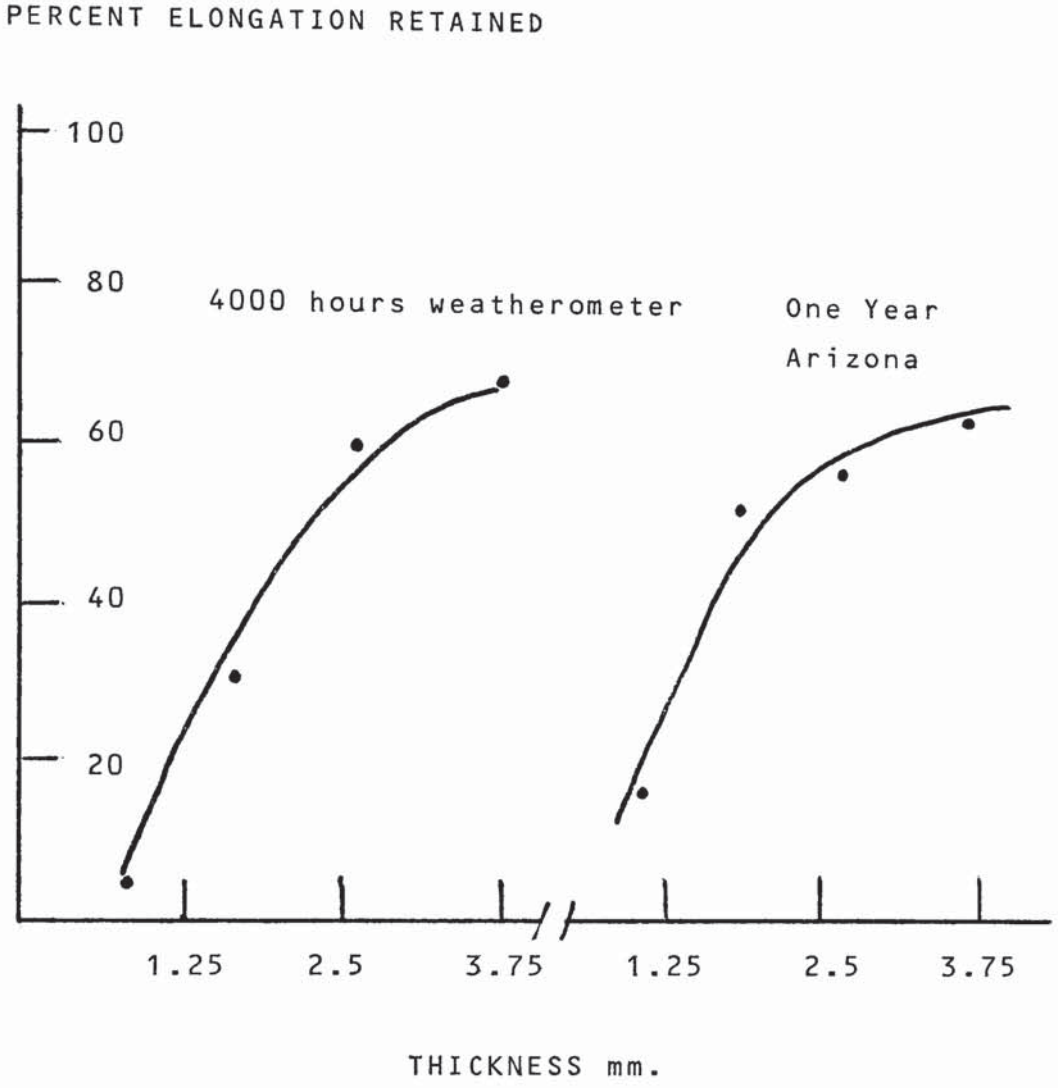

Fig. 3.23 Effect of Sample Thickness on Weathering Resistance of Stablised Ethylene Homopolymer

wall thickness of 2 mm irrespective of diameter or pressure rating when the pipe is to be used for natural gas transmission and distribution.

Previous data (122, 123, 124) have indicated a correlation between artificial weathering with a Xenon lamp and actual weathering at different climatic locations such that:

One year in Phoenix, Arizona, is approximately equivalent to at least two years in Bartlesville, Oklahoma, and to greater than 3.5 years in Akron, Ohio. Whilst there is scattering of data, the weatherometer results indicated that 1000-2000 hours exposure are approximately equivalent to 12-24 months in Arizona, 3000-4000 hours compare to 24-36 months, and over 5000 hrs compare to greater than 42 months with the same relationship holding for Arizona and the other two locations.

However, a "round robin" programme conducted between the International Standards Organisation Task Group members from D.S.M., Hoechst, Solvay, Unifos and Phillips Petroleum, was unable to come to any such conclusion for Northern Europe. The programme evaluated both yellow and black pigmented, stabilised ethylene butene and ethylene-hexene copolymers in both compression moulded sheet and extruded pipe form.

Under the recommended procedure (128, 129) 2 mm thick sheets were compression moulded from both virgin pipe resin and granulated extruded pipe. I.S.O. type 2 tensile specimens were cut from the pressed sheets and subjected to Xenon lamp exposure in a weather-ometer before being tensile tested in accordance with ISO R 527 (130) using a grip separation rate of 5 cm/min. The weatherometer used was an Atlas type 25/18 WT conforming to type AH of ASTM D 2565 (131, 132) with a continuous light cycle without water spray (133)

A duplicate evaluation was performed using outside exposure for one year (8,760 hours). The number of direct sunlight hours recorded was 1,614 hours (134).

These results, tabulated in Tables 3.15 and 3.16, as part of the input to the "round robin" programme, show that neither Xenon lamp exposure up to 2000 hrs nor one year outside ageing have any significant influence on the tensile characteristics of either the hexene-1 or butene-1 copolymers of ethylene when exposed as a black formulation containing 2.5% of fine particle size carbon black.

Exposure, however, does have a significant detrimental effect on the aging of the cadmium pigmented samples. Table 3.17 illustrates the inferior resis-

tance of the butene-1 copolymer to Xenon lamp exposure as measured by the ultimate tensile properties. The effect of prior processing is adequately demonstrated in Table 3.18, which shows that the inherent resistance to exposure, both Xenon lamp and direct sunlight is considerably diminished. Again, the relative stability of the hexene-1 copolymer over that of the butene-1 copolymer, is shown by the less severe reduction in ultimate tensile properties. Similar results were found by Cartier (135) and Tansley (136) but under different exposure conditions (137).

These results also serve to demonstrate the potential danger in the continuation of the practice by many authoritative bodies (138) to specify yellow pipe for gas distribution purposes, when a black pipe with a yellow code would be a much safer proposition. Muller (139) has shown that, after 14 years continuous outside exposure, the average time for hoop stress failure for black compounded butene-1 copolymer pipe samples was still approximately twice the specification value of 48 hours, when tested at 80°C.

TABLE 3.15 Xenon Lamp Exposure Study on Black Virgin Polymer

	Medium M.Wt Hexene Copolymer		High M.Wt Butene copolymer	
	Av.value	St.dev.	Av.value	St.dev.
Unaged Control:				
Yield Stress Kg/cm^2	214	2	250	4
Yield Elongation %	8.7	0.5	8.6	1
Ultimate Stress Kg/cm^2	307	14	332	18
Ultimate Elongation %	708	26	880	38
1000 hours Exposure				
Yield Stress Kg/cm^2	210	4	246	7
Yield Elongation %	8.5	0.2	9.1	0.3
Ultimate Stress Kg/cm^2	315	21	318	26
Ultimate Elongation %	825	38	880	74
2000 hours Exposure				
Yield Stress Kg/cm^2	215	3	252	3
Yield Elongation %	6.5	0.5	6.9	0.3
Ultimate Stress Kg/cm^2	320	7	321	32
Ultimate Elongation %	810	16	900	47

TABLE 3.16 AGEING STUDY ON BLACK GRANULATED PIPE

	Medium M.Wt Hexene Copolymer		High M.Wt Butene Copolymer	
	Av.value	St.dev.	Av.value	St.dev.
Unaged Control				
Yield Stress Kg/cm^2	214	2	254	1
Yield Elongation %	7.7	0.4	7.3	0.3
Ultimate Stress Kg/cm^2	297	12	326	15
Ultimate Elongation %	770	30	870	20
1000 hours Xenon Exposure				
Yield Stress Kg/cm^2	217	1	266	3
Yield Elongation %	6.8	0.1	6.5	0.3
Ultimate Stress Kg/cm^2	324	15	320	40
Ultimate Elongation %	805	20	850	60
2000 hours Xenon Exposure				
Yield Stress Kg/cm^2	217	3	266	5
Yield Elongation %	6.7	0.1	6.0	0.3
Ultimate Stress Kg/cm^2	296	11	261	56
Ultimate Elongation %	765	22	770	105
One Year Outside Exposure				
Yield Stress Kg/cm^2	225	1	272	3
Yield Elongation %	7.0	0.2	6.1	0.2
Ultimate Stress Kg/cm^2	303	6	273	43
Ultimate Elongation %	770	20	790	15

TABLE 3.17 XENON LAMP EXPOSURE STUDY ON YELLOW VIRGIN POLYMER

	Medium M.Wt Hexene Copolymer		High M.Wt Butene Copolymer	
	Av.value	St.dev.	Av.value	St.dev.
Unaged Control				
Yield Stress Kg/cm^2	218	2	245	3
Yield Elongation %	8.7	0.4	8.5	0.5
Ultimate Stress Kg/cm^2	315	10	325	10
Ultimate Elongation %	810	30	860	15
1000 hours Exposure				
Yield Stress Kg/cm^2	226	2	260	2
Yield Elongation %	8.4	0.3	8.2	0.3
Ultimate Stress Kg/cm^2	312	11	201	21
Ultimate Elongation %	820	17	680	25
2000 hours Exposure				
Yield Stress Kg/cm^2	223	1	259	2.6
Yield Elongation %	6.8	0.1	7.0	0.4
Ultimate Stress Kg/cm^2	314	18	176	-
Ultimate Elongation %	825	30	455	85

TABLE 3.18 AGING STUDY ON YELLOW GRANULATED PIPE

	Medium M.Wt Hexene Copolymer		High M.Wt Butene Copolymer	
	Av.value	St.dev.	Av.value	St.dev.
Unaged Control				
Yield Stress Kg/cm^2	224	2	243	5
Yield Elongation %	7.9	0.3	8.1	0.2
Ultimate Stress Kg/cm^2	247	7	317	36
Ultimate Elongation %	695	25	865	55
1000 hours Xenon Exposure				
Yield Stress Kg/cm^2	228	1	251	3
Yield Elongation %	6.8	0.1	6.7	0.1
Ultimate Stress Kg/cm^2	252	46	314	29
Ultimate Elongation %	690	103	885	50
2000 hours Xenon Exposure				
Yield Stress Kg/cm^2	233	2	246	6
Yield Elongation %	6.4	0.4	6.0	0.1
Ultimate Stress Kg/cm^2	174	10	Brittle	
Ultimate Elongation %	570	15	Brittle	
One Year Outside Exposure				
Yield Stress Kg/cm^2	242	3	262	5
Yield Elongation %	6.6	0.4	6.0	0.1
Ultimate Stress Kg/cm^2	172	13	415	-
Ultimate Elongation %	505	75	175	11

CHAPTER 4: ANALYSIS OF METHODS TO PREDICT LONG TERM PIPE HOOP STRESS RESISTANCE

INTRODUCTION

The most important engineering aspect of pipelines is their behaviour when subjected to internal stresses arising from the transport of gases and fluids under pressure. Although a universal consideration with all materials in pipe form, this aspect is one of particular interest for pipe made from plastics because:

a) They show plastic flow behaviour under stress
b) They have relatively low strength compared to that of steel
c) They have been known and used for a relatively short time.

Other materials such as steel are less plastic in nature at ordinary temperatures and a highly significant point is the fact that they were widely used before engineering properties and design criteria were developed.

The knowledge of long term failure stress of plastic pipe materials is very important, both to engineering design as well as to theoretical understanding.

However, the time region of interest - about 10^5 hrs, is impractical for actual measurement of the failure stress under ambient conditions. From the application point of view, the experiment time should not be too long because a long time interval before obtaining the experimental data would reduce drastically the value of the data. The dangers then are that either practice anticipates (wrongly) the expected results which come a little late for action or, alternatively, practical development is slowed down waiting for research to confirm that it would have been perfectly justified.

The search for methods to predict long term failure stress has received much attention in the past and with the increasingly wide application of plastics pipes in various industries and the building trade, the need for a method to predict the long-term bursting stress of plastics pipes is also growing. Although a method (140) has been recommended and is widely used in commercial literature, the validity of its prediction has not been proven and the various safety factors applied have been no more than arbitrarily chosen when the method is used to predict a long-term safety stress for gas distribution piping.

In this section, several published correlations between failure stress and time to failure are re-

viewed as to their suitability for pipe burst stress prediction and a method finally advocated for the prediction when water is considered as the environment. Hoop stress data experimentally determined in environments other than water, show that such an advocated method still requires considerable modification prior to its satisfactory use as a method for predicting the long-term safe stress of polyethylene materials used for the distribution of natural gas in Western Europe.

4.1 DEFINITIONS

For the purpose of clarity and uniformity, the following definitions when expressed with reference to pipe are adhered to throughout this report. It is a fact that not only within Western Europe, but also within the North American Continent, there is some considerable misuse and/or lack of uniformity of terminology.

4.1.1 Stress

The force per unit in the wall of pipe in the circumferential orientation due to internal hydrostatic pressure in units of kilogrammes per square centimetre.

4.1.2 Pressure

The force per unit area exerted by the medium in the pipe in units of kilogrammes per square centimetre.

4.1.3 Design Stress

The estimated maximum tensile stress in the wall of the pipe in the circumferential orientation due to internal hydrostatic pressure that can be applied continuously with a specified degree of certainty that failure of the pipe will not occur.

4.1.4 Long Term Strength (LTS)

The estimated tensile stress in the wall of pipe in the circumferential orientation that when applied continuously will cause failure of the pipe at a specified time.

4.1.5 Pressure Rating (Pnom)

The estimated maximum pressure that the medium in the pipe can exert continuously with a specified degree of certainty that failure of the pipe will not occur.

4.1.6 Stress/Pressure Relation

The relation between the pressure applied and the resultant stress is given by the Lamé formula for stressed thin walled pipe.

i. Radial Stress $= \frac{Pr_1^2}{r_2^2 - r_1^2}\left(1 - \frac{r_2^2}{r^2}\right)$

Where r is the average radius of the pipe

r_1 is the inside radius of the pipe

r_2 is the outside radius of the pipe

P is the pressure applied

For a thin walled pipe

$r = r_1$ approximately

hence:

$$\text{Stress} = \frac{Pr_1^2}{r_2^2 - r_1^2}\left(\frac{r_1^2 - r_2^2}{r_1^2}\right)$$

that is, the radial stress varies between - p and zero between the inside pipe wall and the outside pipe wall respectively.

ii. Axial Stress $= \frac{Pr_1^2}{r_2^2 - r_1^2}$

$$= \frac{Pr_1^2}{(r_2 - r_1)(r_2 + r_1)}$$

$$= \frac{Pr_1^2}{t\,(2r)}$$ where t is the wall thickness

$$= \frac{P\,(D-t)}{4t}$$

Which in practice is a very small value.

iii. Circumferential Stress =

$$\frac{Pr_1^2}{r_2^2 - r_1^2} \left(1 + \frac{r_2^2}{r^2}\right)$$

$$= \frac{Pr_1^2}{(r_2 - r_1)(r_2 + r_1)} \left(1 + \frac{r_2^2}{r^2}\right)$$

For a thin walled pipe $r = r_1 = r_2$ approximately.

Hence:

$$\text{Stress} = \frac{2\,Pr_1^2}{t\,(2r)} = \frac{P\,(D-t)}{2t}$$

4.2 REVIEW OF LITERATURE

4.2.1 Semi-Logarithmic Methods

Several relations, which are found to be satisfactory for correlating the rupture stress and time to failure of metals, are borrowed to predict the long term stress of glass laminates and are considered here as to their suitability to the application to plastics pipe rupture strength.

Taylor (141) suggested an empirical equation of the following form: $\log t = a + \frac{b}{s}$ 1

where $b = EA \cdot \frac{1}{kT}$

and t is time to failure

S is hoop stress

E is Young's modulus

A is the activation energy

T is the absolute temperature

a and k are constants.

However, Machlin and Norwick (142) correlated the rupture stress itself with the logarithm of time.

$$\text{Log } t = a + bS \quad \ldots\ldots \; 2$$

and specified that ...

$$a = \frac{A}{T} + B$$

$$b = \frac{-D}{T}$$

where A, B and D are constants

Both equations are of the semi-log form and very similar, but Machlin takes log time as a linear funtion of stress, whilst Taylor takes log time as linear to the reciprocal of stress. Clearly both equations cannot be correct, otherwise equating both to eliminate log time will give an expression predicting rupture stress independent of time.

The Machlin equation has been found to be workable for glass laminates by Ratner (143) whilst Carey and Oskin (144) made the comparison and preferred the equation suggested by Larson and Miller (145) who

started with the basis that creep appears to obey rate process theories (146 - 149) which state that the rate at which certain processes progress is related to temperature by the expression:

$$r = Ae^{-Q/RT} \quad \ldots\ldots 3$$

where r is the rate

A is a constant

Q is the activation energy for the process under the conditions considered

R is the gas constant

T is the absolute temperature

Several investigators (150 - 152) have demonstrated that, for a constant stress, creep rate data fit this equation providing the rate taken is either the minimum rate or the rate at a constant strain. Since the time to rupture depends on the summation of creep rates until rupture, the equation may be rewritten:

$$\frac{1}{t} = Ae^{-Q/RT} \text{ for constant stress } \ldots\ldots 4$$

where t is the time to rupture

This equation can be reduced to:

$$T = (C + \log t) = \frac{Q}{2.3R} = \text{Constant} \quad \ldots\ldots 5$$

where $C = \log A$

and, at a constant stress:

$$T_1 (C + \log t_1) = T_2 (C + \log t_2) \text{ ..... } 6$$

which is the Larson-Miller equation.

Similarly, Holloman and Jaffe (153) have shown that the relation between the rate process for tempering of steel alloys and temperature for a given hardness could be expressed by:

$$T (C + \log t) = \text{Constant} \text{ ..... } 7$$

where T is the absolute temperature
c is a material constant
t is the time

Equations (5) and (6) imply that the constant C is constant only for constant stress, whereas Larson and Miller assert that C is independent of stress and possibly of material and was shown to be so for a wide range of steel alloys when log t was plotted against the reciprocal of the absolute temperature for constant stress at a series of stress levels.

Values of C obtained varied from 18 to 22 and were explained by Kanter (154, 155) on the basis of dislocation theory.

The fundamental principle of the procedure proposed by Larson and Miller is that time and temperature

may be equated by employing the constant C. Thus, the correctness of the method is predicted on an accurate value of constant which is assumed to have an average value of 20. In cases where the value differs appreciably from 20, it is assumed that other factors are involved, such as a phase change and that the relationship is invalidated.

If there is actually a variation in the constant C, then the error in time, introduced by using the wrong value, can be determined by differentiating log t with respect to C, holding T1, T2 and t2 constant in equation (6):

Thus, $T_1 (C + \log t_1) = T_2 (C + \log t_2)$

differentiates to $$\frac{d (\log t_1)}{dC} = \frac{T_2 - T_1}{T_2} \quad \ldots\ldots 8$$

and thus errors in log t, will be proportional to the difference in temperatures considered and will be negligible if the temperatures are not too widely separated as in the case of plastics pipe testing.

Carey and Oskin (144) have also demonstrated that the parameter C, which is dependent on the stress applied, is a linear function of the rupture stress S but that the plot was shown as a straight line of two segments since the constants d and c change their

values in different regions of the hoop stress plot.

$$S = d + cK \quad \ldots\ldots \quad 9$$

If equations 9 and 5 are combined and the terms transported

$$\log t = -C + (S-d)cT \quad \ldots\ldots \quad 10$$

and this is the same form as proposed by Machlin and Norwick (equation 2) except that it specified that:

$$a = -C - \frac{d}{cT} \quad \text{and} \quad b = \frac{1}{cT}$$

4.2.2 Initial Conclusions

All of the previously considered proposals are based on the assumption that there exists a linear relationship between the logarithm of time to failure and the failure stress or its reciprocal. Further proposals are the interpretation of the correlation constants in terms of experimental temperature.

In order to determine the validity of any of these equations, for use in the prediction of the long term burst strength of polyethylene pipes, experimental data for time to failure at various stress levels and temperatures were plotted both as log time to hoop stress and log time to the reciprocal of hoop stress. The resulting hoop stress plots are reproduced in Figures 4.1. and 4.2. as illustrated examples of the data tabulated in Table 4.1.

TABLE 4.1 Representative Sustained Hoop Stress Data Points for Phillips Polymerised Ultra High Molecular Weight Ethylene - Butene Copolymer

Time t-hours	Log t	Hoop Stress Kg/cm^2	Reciprocal $\frac{1000}{\text{Stress}}$
26	1.41	127.6	7.84
28	1.45	127.6	7.84
136	2.13	121.3	8.24
208	2.32	121.3	8.24
189	2.28	118.6	8.43
281	2.45	118.6	8.43
859	2.93	117.9	8.48
953	2.98	117.9	8.48
674	2.83	115.5	8.66
1053	3.02	115.5	8.66
1151	3.06	114.8	8.71
1364	3.13	114.8	8.71
1101	3.04	112.4	8.90
1313	3.12	111.7	8.95
1512	3.18	111.7	8.95
3120	3.49	109.3	9.15
2350	3.37	108.3	9.23
2281	3.46	108.3	9.23
3240	3.51	106.9	9.35
4632	3.67	106.9	9.35

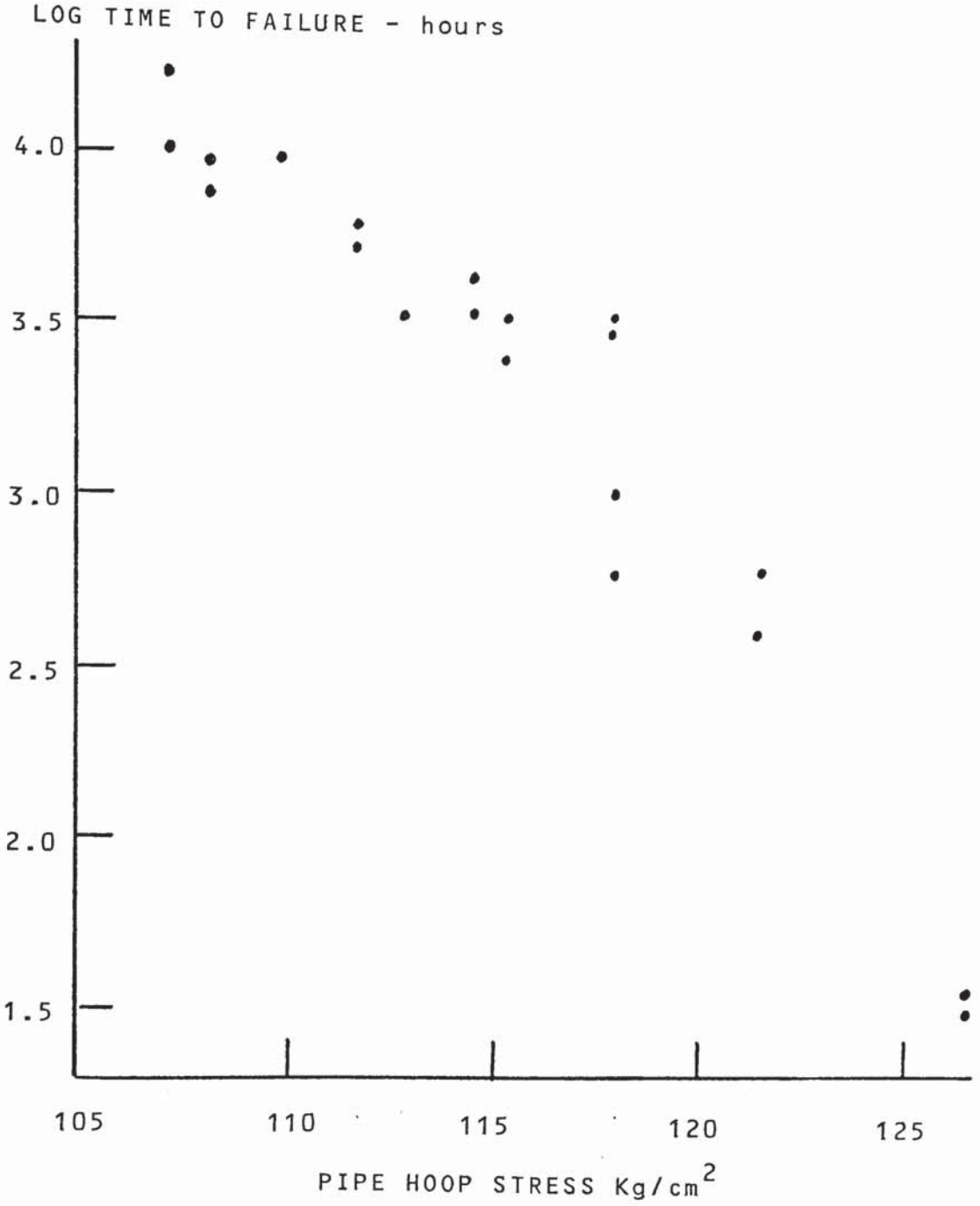

Fig. 4.1 Log Failure Time to Hoop Stress Plot of Table 4.1 Data

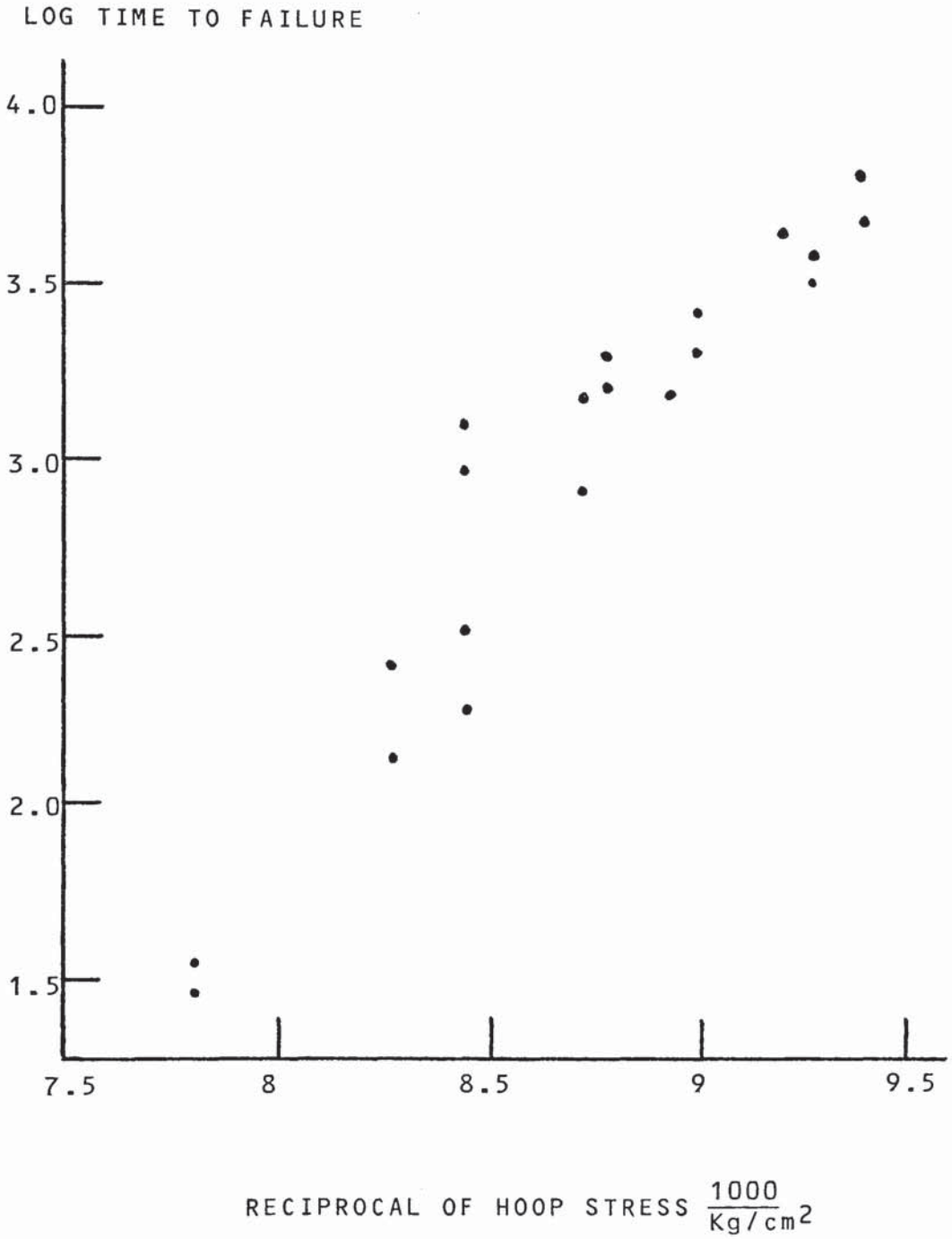

Fig. 4.2 Log Failure Time to Reciprocal of Hoop Stress Plot of Table 4.1 Data

It is evident that these data are not represented by a straight line. Thus the relation between the logarithm of time to failure of a polyethylene pipe and the stress applied or its reciprocal is not linear. Thus the previously considered proposals cannot be considered as such for use in the prediction of the long term hoop stress for polyethylene pipe.

4.2.3 Methods using a Shift Factor

4.2.3.1 Reduced Variables

The method of reduced variables, which is widely accepted and successfully applied to stress relaxation (156) creep (157) and ultimate strength (158, 159) of viscoelastic materials employs the temperature effect on stress or strain to prolong the experiment time range. The basic assumption of this method is that temperature has the same effect on all the mechanisms involved. Hydrostatic pipe testing is primarily a constant load process carried to the point of rupture and as such this method is applicable.

The basic equation has the form

$$So\ (\frac{to}{A}) = S\ (t) \quad \ldots\ldots\ 11$$

Where So is hoop stress at the reference temperature

λ °Kelvin

S is hoop stress at the experiment temperature

λ °Kelvin

to is time to failure at the reference temperature °Kelvin

t is time to failure at the experiment temperature °Kelvin

A is the shift factor

The equation states that the hoop stress at temperatures T and at time t is equal to the hoop stress of the same material at the reference temperature To and time to/A. Thus, hoop stress data obtained at different temperatures can be combined into one composite curve at one reference temperature by applying the shift factor "A". A value of "A" determined from one stress level can be applied to all stresses at the same temperature "T" when being referred to the same reference temperature To.

Chang (160) has illustrated the applicability of this reduced time method to ABS pipe. Pipe failure times of less than 1000 hours at a series of temperatures were used to predict failure stress at 30,000 hours with percentage errors between -1.6% to +1.6%.

4.2.3.2 Williams-Landel-Ferry Equation

Visco-elastic properties depend strongly on temperature. If the creep behaviour of a polymer at different temperatures is plotted against the logarithan

of time then, since the curves obtained at each temperature will have the same general shape, the curves can be made to superimpose on a master curve at some arbitrarily chosen reference temperature by a horizontal shift in which each value on the abscissa is corrected by a factor (log time- log shift factor). In other words, a time temperature superposition is applicable.

The Willaims-Landel-Ferry (WLF) equation, which is based on the temperature dependance of viscosity, gives good prediction of the shift factor "A" for linear amorphous polymers when the reference temperature is taken as the glass transition temperature Tg in degress Kelvin (161):

$$\text{Log } A = \frac{-17.44\ (T-Tg)}{51.6 + (T-Tg)} \quad \ldots\ldots\ 12$$

An important aspect of the concept of time temperature superposition is that the shift factor applies to a particular polymer regardless of the nature of the mechanical response. Therefore, a shift factor determined for stress relaxation is applicable for predicting time - temperature behaviour in creep or dynamic testing. Using this technique, it is possible to predict the properties of a polymer at a variety of temperatures when experimental data is available at only a few temperatures. However, more

reliable results are obtained when interpolating between temperatures with known data than when extrapolating to temperatures outside the range of the data. A further limitation is that the WLF equation is not applicable near and below the glass transition temperature. Chang (162) in work on stress relaxation found that the shift factor at temperatures below the glass transition is related to the reciprocal of temperatures in the following manner:

$$\text{Log } A = B\left(\frac{1}{T} - \frac{1}{To}\right) \quad \ldots\ldots \quad 13$$

Where B is a constant, characteristic of the polymer.

4.2.3.3 Goldfein Equation

A mechanical chemical equation of state based on the Arrhenius relationship in its differential form, has been developed by Goldfein and applied to stress rupture data for plastics pipe (163):

$$K = \frac{T\,To}{To - T}\,(C + \log t) \quad \ldots\ldots \quad 14$$

where T is the test temperature

To is a temperature defined for the material under evaluation, as the temperature at which it has no strength. It is analagous to minimum moulding temperature.

C is a constant that assumes values in the range 20 for plastics materials.

The experimentally determined time to failure at different stress levels and temperatures can be combined to obtain a master curve of stress versus K. The prediction is made by calculating a value of K from the time and temperature desired and reading off stress from the master curve.

If To >> T, the equation is reduced to that of Larson and Miller

If equation 14 is rewritten:

$$K = (\log t - \log to)/(\frac{1}{T} - \frac{1}{To}) \quad \ldots\ldots \quad 15$$

then the quantity in the first pair of parentheses is exactly the logarithm of shift factor log A. Therefore, the parameter K is nothing but the slope of the log A versus 1/T curve, which is constant for the material and independent of the stress.

4.2.4 Conclusions

Methods of prediction of long term hoop stress, which are based on the power law or the Arrhenius approach, depend upon the exponent (the slope of the line on the log time to failure against log failure stress

plot) or the activation energy (the slope in the log time to failure against reciprocal absolute temperature plot) remaining constant. Experience shows that the failure mode at high stresses and short times is different from that at lower stresses and longer times. This change in mechanism of failure results in a change in slope of the plot and would also involve a change in activation energy.

4.2.5 Double Logarithmic Plots

4.2.5.1 U.S. Plastics Pipe Institute Method

The procedure for estimating long-term hydrostatic strength by this method is essentially an extrapolation with respect to time of tests made in accordance with ASTM D 1598-63T. The procedure was originally developed by the Plastics Pipe Institute (164) of the U.S., working with Batelle Memorial Institute in Columbus, Ohio. It is now recognised by the American Society for Testing and Materials as ASTM method D 2837. Stress-failure times are plotted on logarithmic co-ordinates and an extrapolation is made in such a manner that the long-term hydrostatic strength is obtained.

In the extrapolation, the regression equations are developed by the method of least squares with stress as the independent variable. Data for test periods less

than 10 hours are not used because firstly, the excessive scatter in this region which creates considerable bias in the least squares calculation and, secondly, because of the sharp upturn of the data in this region which is a marked departure from linearity and again creates a strong bias in the least squares calculation.

In establishing this empirical method, the PPI analysed over 350 sets of data on a stress-log time basis with linear and quadratic equations and on a log stress-log time basis with linear and quadratic equations. Initially the sets of data were also analysed on a normal stress-time basis, but the results deviated so much from known behaviour that this basis of calculation was abandoned. For polyethylene pipe materials, the linear stress-log time calculations gave essentially the same results as the linear double logarithmic calculations in half the number of cases. In the case where there was not agreement, the semi-log calculations gave abnormally low results or a low confidence limit.

This method proposes that the effective scatter of the data points is evaluated by calculating the 95% two-sided confidence limits at 100,000 hours. When the lower confidence limit (LCL) for a particular

set of data is less than 25% of the predicted 100,000 hours hydrostatic strength, the data are judged to have too much scatter to be useful. In addition, the calculation procedure for the long-term strength gives a plot which appears to have an abnormally high slope when examined by eye for data that has a wide scatter. This selection is made to provide a reproductible means for making the lower reliability inherent in this wide scatter effective in reducing the long-term strength to such an extent that it would be satisfactory as a basis for engineering design, on the conservative side.

A minimum requirement was specified by 18 data points distributed in a specified manner in the various time regions from 10 to beyond 10,000 hours, including at least one point beyond 10,000 hours. It is also essential that these data be plotted on the same basis as the calculations are made, if a reasonably true visual representation is desried. The spacing should be such that each stress unit is equivalent to each time unit on a log-log basis. The straight line which is fitted to the data and extrapolated to 100,000 hours, represents the mean of the data on a logarithmic basis. From the intercept of this line at 100,000 hours (the long-term strength) a hydrostatic design basis is selected from tables.

The U.S. PPI method delineates an accepted practice for examining data when all physical evidence indicates that the relationship can be represented by a single straight line. Even though the log-log plot will give a flatter appearance than a semi-log plot, the hoop stress versus time relationship is not a straight line in either scale over a wide range of time. This is in fact accepted by the PPI when consideration is given to extrapolating the least squares line to shorter periods to determine a method of test for water-hammer strength. On a log-log equiscaler basis, the actual test results for periods less than 10 hours are greater than the extrapolation predicts. The actual plot in this region has a sharp upturn or elbow which varies in shape and intercept with the type of thermoplastic material and with commerical products of the same general type.

Although there is a straight line portion of the curve for a relatively short time range, the arbitrary appli-cation of a linear equation in either semi-log or log-log scale, without any knowledge of the location of this straight line portion, which varies from resin to resin, will lead to inaccurate estimation of the long-term stress.

Evidence from other test methods indicates that at room temperature, a fall off from the predicted line

will occur beyond 10,000 hours, due to a change in failure mechanism from a ductile nature to a brittle nature. Field experience shows that the life of a pipe is governed by this brittle failure mechanism. Because of the length of time involved, and the sheer mechanical problem of maintaining uniform pressures over such extended periods, it is difficult to observe this transition in laboratory testing at room temperature. The extrapolation between 10,000 and 100,000 hours appears to be a small step on a logarithmic scale, but it represents 90% of the expected life. Furthermore, if the test data suggest a virtually horizontal characteristic curve, the method of least squares will become very difficult to use. The resulting fit would produce a high standard deviation in the time co-ordinate and would tend to reduce confidence in the extrapolation.

The inclusion of long-term experimental data beyond 10,000 hours and nearer the time of interest (100,000 hours) will render the extrapolation extending to a shorter distance outside the experimental time range and will improve, to a slight extent, the accuracy fo the estimated value as originally anticipated; but the long wait for these last data points to become available reduces the value of the experiment to the investigator.

Theoretically speaking, if the linear equation is a true representation of the hoop stress-time relation, the requirement of a specific distribution of data points over the time scale is not necessary, regardless of the scattering of points. Thus, the specified distribution admits that the relation is not linear.

4.2.5.2 European Graphical Method

When a series of pipes are stressed at different stress levels and the corresponding failure times plotted on a double logarithmic plot then, during extended tests, the regression line shows a sudden change in slope becoming much steeper than originally. The change in slope is associated with a change in failure mechanism from ductile to brittle. Failure in practice at working pressures can be expected to be of the brittle nature and, as a consequence, the first part of the regression curve loses its value entirely with respect to service life prediction. A sufficiently accurate determination of the steeper slope would take too long a time and thus another basis of extrapolation is required.

The European double logarithmic method is based on the hypothesis developed by Richard and Gaube (165) who found that rupture data determined at tempera-

tures above 20°C, and plotted as log stress against log time, followed a curve that appeared to be made up of an initial low slope section followed by a steeper straight portion. At different temperatures these curves were found to have a correlative shape and thus hoop stress data developed at the higher temperatures could be used to help complete the data at lower temperatutes by extrapolation, as illustrated in Figure 4.3.

Assuming that the velocity of cracking in the burst strength test is a function of the energy of activation, as is the velocity of a chemical reaction Gloor (166) apparently successfully applied the Larson and Miller relation to Richard and Gaube's results, using a value of 22 for the constant C. However, Whyman and Szpak (167) plotted the behaviour of an ethylene - butene copolymer and found that the behaviour was unlike that of metals in that the failure points did not initially fall on a common line regardless of the temperature, but followed a specific pattern for temperature down to a point of convergence where they then formed a single master curve.

Following the European Graphical method as proposed by Richard and Gaube, the characteristic curves are

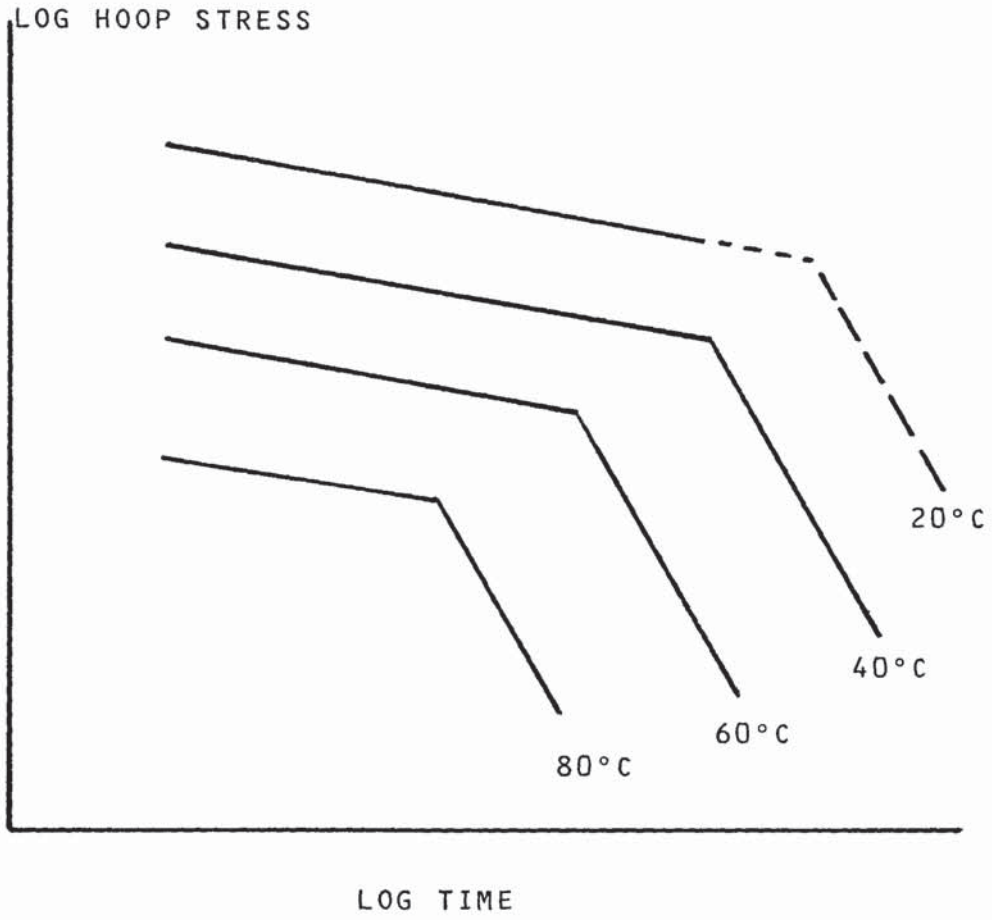

Fig. 4.3 Representative Double Logarithmic Hoop Stress to Failure Time Plots

plotted through the 95% lower confidence limit points and the hydrostatic design stress level is established from a maximum allowable expansion for the pipe to maintain permanent deformation within reasonable limits. In the case of high density polyethylene and medium density polyethylene, this allowable expansion is related to the micro-structure of the finished product such that microfractures remain too small to allow propagation. This corresponds to a critical strain level of between 1.5 and 3.5%. All European pipe specifications are now standardised on 3% for polyethylene and 0.5% for PVC.

The European Graphical method has the definite advantage that since the minimum values of rupture strength at room temperature and those at high temperatures are interrelated, test for quality control purposes may be carried out at the higher temperature. At these higher temperatures e.g., 80°C a test time of 200 hours is sufficient for controlling the position of the steep branch of the rupture strength curve at room temperature. Testing stresses and times of 40, and 30 Kg/cm^2 for 96 and 168 hours respectively, are now official standards in all European countries without exception, and many others outside Europe.

4.2.6 Methods of Accelerating Test Time

Increase in test temperature is only one, albeit by far the most common, possibility of accelerating deformation-free fractures during the rupture strength test for pipe. By combining higher temperatures with the action of detergents, the test time can be further reduced.

4.2.6.1 Detergents

It is accepted that detergents act as stress cracking agents and can cause brittle failures in relatively short time. Van der Vegt (168) demonstrated the influence of a detergent solution on the pipe bursting characteristics at a temperature of 95°C. He showed that the data for ductile failures obtained with the detergent coincided with those obtained in water, but that the brittle mode fractures were considerably accelerated by the presence of detergent by a factor of about 9. The steeper parts of the curve were approximately parallel (Fig. 4.4) and the appearance of the fractures themselves in water and detergent were identical.

Test results in detergent solution at five different test temperatures gave curves analogous to those obtained in water, but for the fact that brittle failures also occurred at lower temperatures. It is

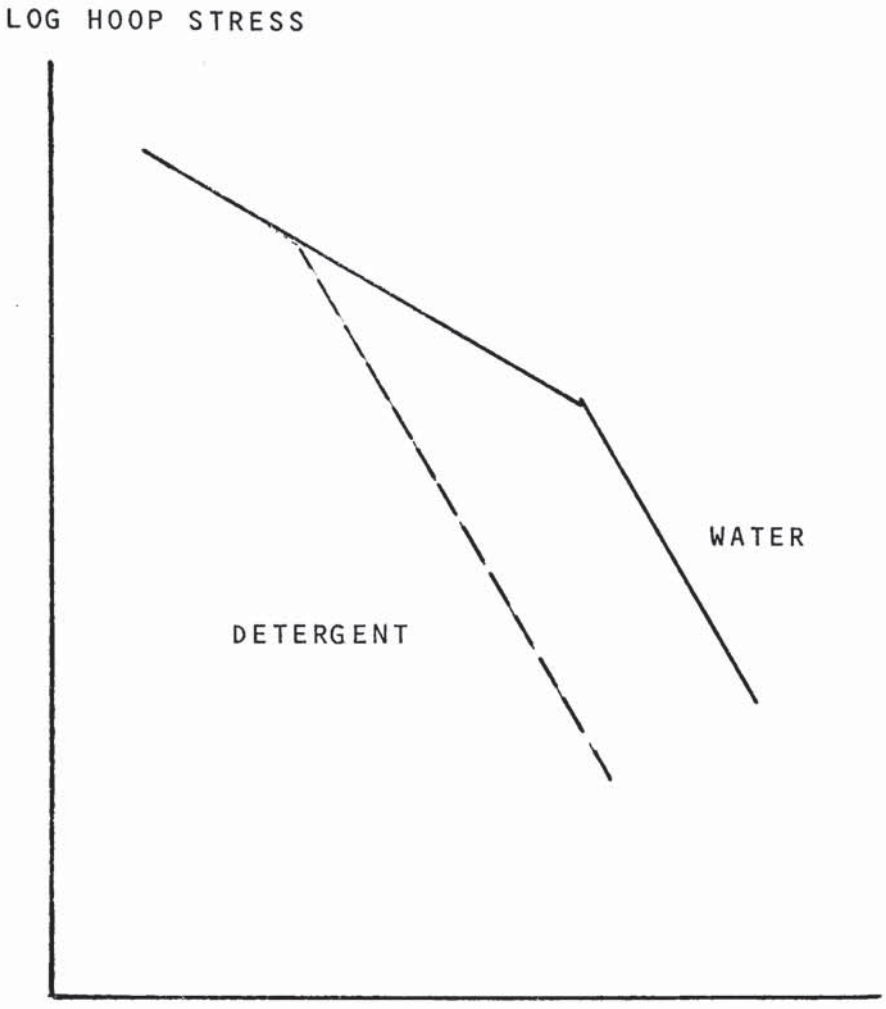

Fig. 4.4 Accelerating Influence of Detergent on Hoop Stress Failure

thus evident as shown by Dukes (169) in studying the effect of high temperature durability of pipe in a surface active agent environment, that the accelerating effect of the detergent increases as temperature decreases (Fig. 4.5). Data determined in this manner can be extrapolated to give a prediction of service life, if the position of the brittle fracture characteristic at room temperature can be ascertained.

As a first approximation, the brittle fracture characteristic may be represented by nearly parallel straight lines. This enables each line to be related to a single parameter viz. distance measured horizontally. Since the lines are situated on very different stress levels, these distances cannot simply be measured along a single horizontal line; the mutual position of neighbouring lines has to be considered. A reference line is selected and the distances from this line obtained, expressed in decades on a logarithmic scale. These values are plotted against temperature for both water and the detergent solution. From the extrapolation, the values obtained give an indication of the estimated distance of the room temperature water curve data points with respect to the high temperature detergent curve points.

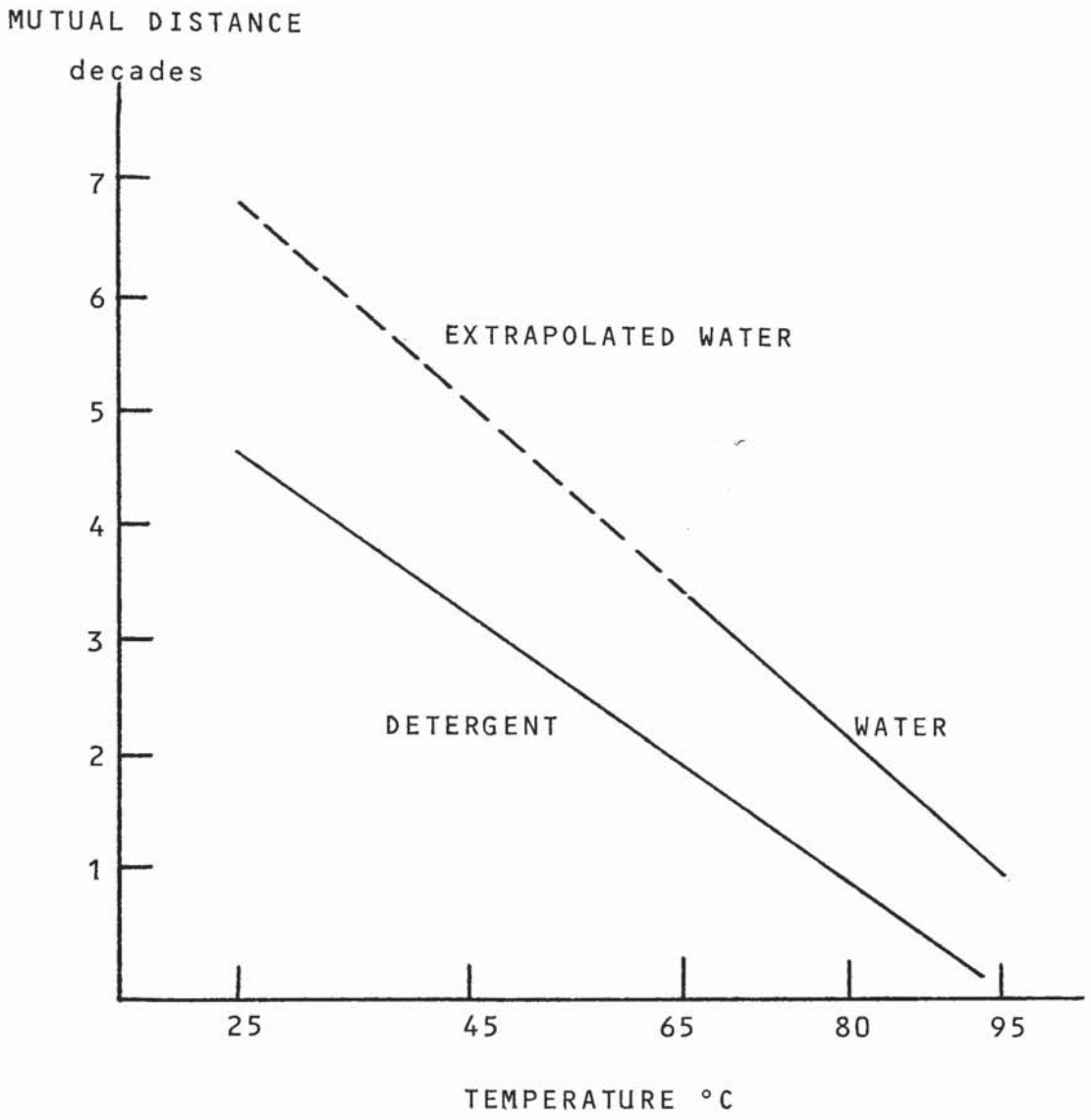

Fig. 4.5 Mutual Distance Between Brittle Fractures

4.2.6.2 Intermittent Stressing

A further method of accelerating testing conditions is the alternate application of two stress levels, one of which is zero. From tests performed in both the region of ductile failure and brittle failure, Van der Vegt (168) concluded that ductile failure does not occur when the load is applied intermittently during suitably chosen periods. This fact suggests that deformation of the pipe wall, which ultimately leads to fracture, is initially entirely recoverable and disappears when the load is removed. However, on the contrary, brittle fracture is effected by continuously built-up material damage, consisting of the propagation of cracks in the wall of the pipe, which, with each application of the load, get progressively worse.

Considering these two conclusions together, then at the bructile transition zone of the hoop stress curve the two different characteristics intersect,each of which denotes a mechanism of failure. There is thus a conflict between these two mechanisms as to which of them will cause the ultimate fracture. At stresses higher than the transition level, this conflict is won by the flow mechanism; at the lower levels by the crack propagation. It is to be expected that, at the higher stresses, brittle cracks are also initiated,

but they do not get the time to develop completely because the flow will cause ductile fracture in a shorter time. By suppressing this flow, namely by applying the load intermittently, the situation changes because crack propagation is not abolished by resting periods.

The variation in the conditions prevailing during such a test show that, as a first approximation, the brittle fracture mechanism is governed by Miner's hypothesis of the linear superposition law of damage.

This law can be formulated mathematically as:

$$\sum \frac{ti}{ri} = 1 \ldots\ldots 24$$

Where ti denotes the time of exposure to the i.th set of conditions

ri denotes the time to failure for constant exposure to these conditions.

A practical consequence of the knowledge of the superposition law is the possibility of prediction of service life under varying circumstances. If, for all the prevailing temperatures, the brittle fracture characteristics should be known, not only in the region of the brittle failure, but also for their extension into the upper region, the behaviour of the

pipe under each given spectrum of stresses and temperatures could be calculated on the basis of the law. Even the effect of short high stress pulses could be taken into account, since these, although too short to cause ductile fracture, contribute to brittle crack propagation.

However, two serious practical limitations to this procedure are firstly, that the time to ductile failure decreases so very rapidly at increasing stress that the permissable periods for an intermittent test become too short, and secondly, the continuous monitoring of the pressure levels limits its applicability for greater time periods.

4.2.7 Stress Propagation Method

4.2.7.1 Introduction

Fracture of a plastic gas distribution system can be defined as any loss of integrity which results in the escape of gas into the environment. In polyethylene pipe and fittings, there are four distinct processes which relate to the final mode of failure (170) namely: yielding, crack initiation, crack growth and crack propagation. Crack propagation occurs when a crack has grown beyond a critical length, becomes unstable and rapidly extends. Failure initiation may result from external interference, such as mech-

anical diggers or may arise spontaneously, induced by the action of stress on the small intrinsic defects inevitably present in polyethylene fusion systems.

The vulnerability of pipelines to the propagation of brittle fracture, simply depends upon the magnitude of the hoop stress generated within the pipe wall. A propagating fracture will occur if the strain energy within the pipe is in excess of that energy needed to propagate failure. From the energy balance a simple relationship (171) between the stress in the pipe G, the diameter of the pipe D and the fracture toughness of the material Kc, is given by:

$$G^2 > 2Kc^2 \frac{(1 - v^2)}{\pi D} \quad \ldots\ldots 16$$

Where v is Poisson's Ratio.

Cracking of this nature proceeds longitudinally along the pipe in a characteristic sinusoidal pattern at speeds approaching 338 m/Sec (172) until arrested within some area of local stress reduction. Propagation is sustained because the gas contained in the pipeline does not decompress fast enough to reduce the stresses existing at the crack tip. The moving crack, in effect, continually senses the full pipe-

line pressure stresses and in theory will travel over an infinite length. Water and other incompressible fluids decompress rapidly, leading to a state of sub-critical stress at the crack tip and a consequent crack arrest close to the initiation source.

4.2.7.2 Derivation of Fracture Mechanics Parameters

The ability of a polyethylene pipeline to sustain brittle fracture propagation is dependent upon both the level of stress generated within the pipe wall, due to internal pressure, and also the intrinsic resistance of the pipe material to brittle fracture propagation. The stresses at the crack tip cannot be quantified in absolute terms, but can be characterised in fracture mechanics terminology by a stress intensity factor Ki. The critical factor Kic associated with the moving crack condition is a material property usually defined as "fracture toughness" and can be determined experimentally from instrumented Charpy and Izod type impact tests (173).

Assuming that elastic deformation of a test specimen containing a crack occurs, since short time durations are involved, then linear elastic fracture mechanics can be applied (174)

With elastic deformation, the compliance C is a funtion only of crack length, 1, and specimen geometry. Thus for an applied load P resulting in a deflection x:

$$\frac{x}{p} = Ca \qquad \ldots\ldots 17$$

The energy absorbed, W, for purely elastic deflection is:

$$W = \frac{1}{2} Px$$

$$= \frac{1}{2} P^2 C \qquad \ldots\ldots 18$$

The strain energy release rate G for specimen of uniform thickness t during deflection is:

$$G = \frac{1}{t} \frac{dw}{da} \qquad \ldots\ldots 19$$

Unstable fracture occurs and crack propagation contintinues unaided when G reaches a critical value Gc given by:

$$Gc = \frac{p^2}{2t} \cdot \frac{dC}{da} \qquad \ldots\ldots 20$$

The critical strain energy Gc is related to the critical stress intensity factor (fracture toughness parameter) Kc by:

$$Kc^2 = f.E.Gc \qquad \ldots\ldots 21$$

Where f is a factor for plain strain or plain stress conditions and E is the short term dynamic modulus.

Indefinite brittle propagation will occur in a unit length of pipe when the strain energy S is greater than the energy required for fracture; i.e.:

$$S > Gc.t. + H \qquad \text{..... 22}$$

Where H is the sum of the secondary effects including damping and Kinetic energy.

The strain energy around the pipe of diameter D and wall thickness t is given by:

$$S = \frac{\sigma^2}{2E} \pi (D-t).t \qquad \text{..... 23}$$

Where σ is the nominal hoop stress.

Thus, from equations 21 and 23, the energy balance for indefinite propogation is:

$$\frac{\sigma^2}{2E} \pi (D-t)t > f.\frac{Kc^2}{E} .t + H \text{ ..... 24}$$

The damping term is a function of volume and is related to the circumference $\pi(D-t)$. For small diameter pipe this term can be neglected and if the hoop stress is sufficiently high both the damping and Kinetic energy terms (H) will be small in comparison to Kc^2.

The relationship thus simplifies to:

$$\sigma^2 > \frac{2Kc^2}{\pi(D-t)} . F \qquad \text{..... 25}$$

For pipe where the wall is sufficiently thin to allow the material to deform, the stress through the thickness will be zero and plane stress conditions will apply thus:

$$Kc^2 = EGc \qquad \ldots\ldots 26$$

For pipe with a thick wall no such deformation can occur, strain through the pipe wall will be zero, and plain strain conditions will apply where:

$$Kc^2 = \frac{E}{1-v^2} .Gc \qquad \ldots\ldots 27$$

Where V is Poisson's Ration.

4.2.7.3 Determination of Fracture Toughness Data

An assessment of the parameter Kc and the associated parameter Gc can be arrived at by different means; the simplest, in that it avoids difficult experimentation and results complicated by dynamic effects and recording measurement problems, involves the measurement of the absorbed energy of a conventional impact test.

From equations 18 and 20:

$$W = Gct.D.\emptyset \qquad \ldots\ldots 28$$

Where the calibration factor $\emptyset = \frac{C}{dc/d(\frac{a}{D})}$ 29

calibration factors (174, 175) and compliance functions (176) for various types of test specimen geometry are available. The impact energy for a series of impact specimens of varying notch depth are determined using the standard pendulum method, such as is specified in BS.2782: method 306,ISO R 179 and ASTM D 256. When plotted as a function of tDØ a straight line plot results with slope of Gc (Fig. 4.6).

The analysis of impact data depends on whether crack propagation is stable or unstable. If the fracture is unstable, it will proceed unaided once initiation has occurred, implying that the energy to propagate is less than the initiation energy. Plasticity effects can occur, which, if small, can be corrected for by the addition of a plastic zone correction factor to the calibration factor Ø. Large-scale plastic deformation which results in stable crack growth, cannot be corrected with an additional factor and Gc must be determined from a ligament area calculation. Although no correction is required for medium density and high density polyethylene resins, it is required for example for rubber modified polystyrene.

4.2.7.4 Application of Fracture Toughness Data

The critical stress condition which defines the transition between the propagation and arrest of brittle

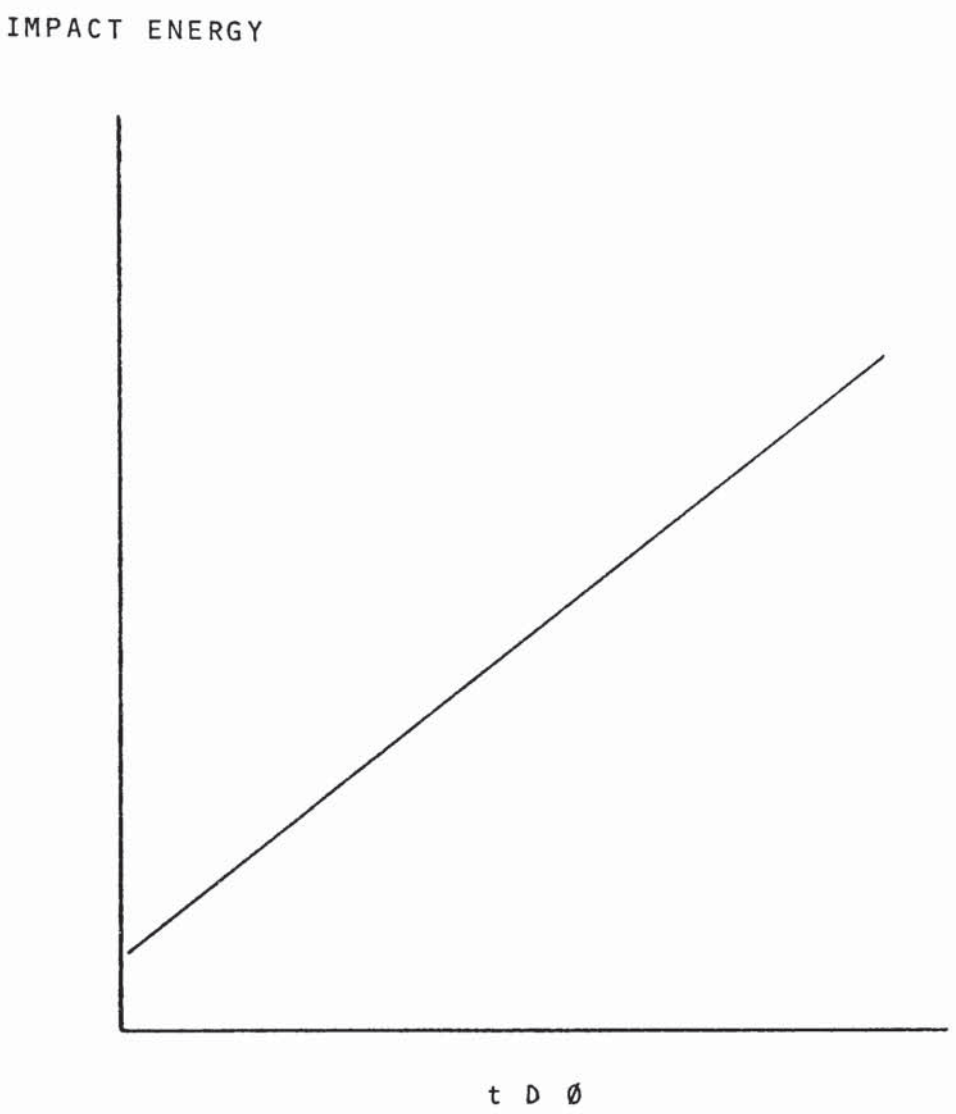

Fig. 4.6 Representative Plot of Impact Energy versus tDØ

cracks in polyethylene pipe can be expressed in terms of internal pressure Pc by:

$$Pc = Kic\sqrt{\frac{8}{\pi}} \cdot \frac{D/t}{D(^{D}/t-1)^{3}} \qquad \ldots\ldots 30$$

Using a value of Kic = 2.0 $/\overline{m}$. MN/M^2 a relationship between critical internal pressure and pipe outside diameter has been obtained (171).

Strain energy in the pipe has been found to be only marginally affected by a surface defect such as that obtained during the handling and pipe laying operations. However, the area of fracture may be significantly reduced, thus altering the energy required to propagate failure. The relationship for indefinite propagation where x is the ratio of defect depth to wall thickness, is:

$$G^2 > \frac{2Kc^2\ (1-v^2)(1-x)}{\pi\ (D-t)} \qquad \ldots\ldots 31.$$

CHAPTER 5: PIPE HOOP STRESS PERFORMANCE OF ETHYLENE COPOLYMERS

INTRODUCTION

The internal pressure (Fig. 5.1) in a pipe produces polyaxial stresses (177) at the inner and outer sides of the pipe wall which are of the most interest. At the inner wall, stress is triaxial with three principal normal stresses: the tangential, the axial, and the radial. At the outer wall, the radial stress is zero and hence stress here is biaxial with the principal normal stresses being tangential and axial (178).

If the individual principal normal stresses are not equal, which is the case with most technical structural members, shearing stresses are produced in addition to normal stresses. As soon as the shearing stresses have reached a certain critical value, they produce plastic deformation.

Pipes made from thermoplastics are always in a mixed elastic-plastic range, due to the so-called cold flow. Tests on polyaxial stressed specimens are therefore indispensible since a strength hypothesis to satisfactorily describe the plastic behaviour is not available.

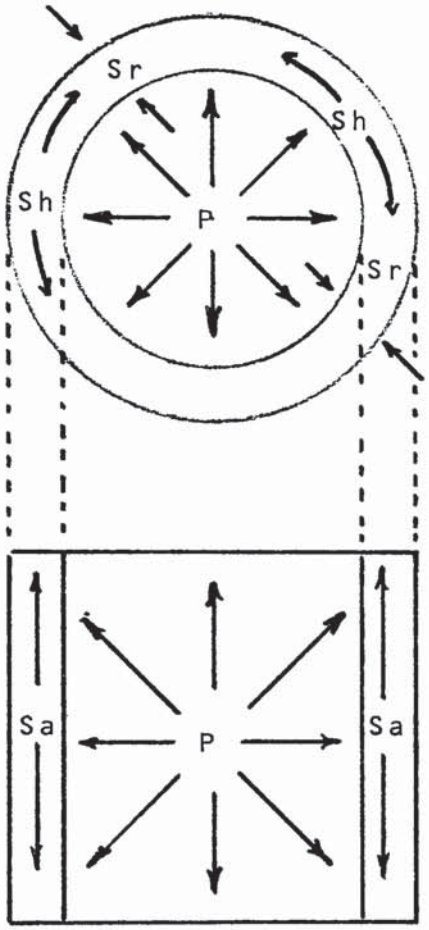

Sh = Tensile stress in the circumferential direction

Sr = Compressive Stress across the Pipe Wall

Sa = Tensile Stress in the Longitudinal direction

P = Pressure in the pipe

Fig. 5.1 Stress System in Thin Walled Pipe Under Pressure

Evaluations made with uniaxially stressed test bars, although easily and inexpensively performed, suffer from the disadvantage that the stress in the test bar constitutes an ideal case which does not exist in practice. In considering thermoplastics pipes, and especially those made from polyethylene, an account must be taken of the fact that the method of pipe manufacture imparts different properties in a longitudinal and a circumferential direction dependent, amongst other factors, on linear rate of extrusion, method of pipe sizing, and the extruder die and mandrel configuration. Thus, for a proper determination of the strength properties, it is advantageous to use annular circumferentially stressed pipe sections rather than test bars which have been cut from the pipe in a longitudinal direction, since in the annular sections, the direction of force coincides with the direction of the maximum stress exerted by the internal pressure. Such annular sections, however, suffer from the disadvantage that stress is only uniaxial and partially only at the periphery, so that the deformation-impeding influence of polyaxial stress cannot become effective.

It therefore follows that evaluation of a complete pipe specimen is indispensible to fully characterise the properties of the material for the appli-

cation. Plastics pipes are an ideal example of a structural element of which the deformation and strengh behaviour can only be determined by imitating, to a great extent, the conditions prevailing in practice.

In addition to the uncertainty in the calculation of the pipe strength, there are other difficulties which are encountered which are related to the quantitative estimation of changes in the properties of the pipes occurring during service. In this category are changes due to factors that appear only to a limited extent, if at all, in short-term tests and therefore, necessitate long time tests. One such factor is that, since the loading capaicty of thermoplastics decreases when the time of leading is increased, the dependance on time has to be quantitatively determined. Another important factor is the action of gases or liquids which gradually swell the pipe material or, in combination with tensile stress, may initiate evironmental stress cracking. Other factors include ageing due to the influence of oxygen, light or temperature which occur and which need to be known quantitatively.

The three most important considerations from the point of view of pipe design, remain the time, the temperature, and the pressure. The use of a variety of

co-efficients can then be applied to derive an overall degree of safety, depending upon the degree of safety required for the final application. Considerations as to quality necessitate, above all, an agreement on the necessary minimum lifetime. Gas distribution pipe lines and, for that matter, potable water distribution lines are generally amortized over a period of 50 years, by community and municipal authorities in Europe. It is therefore to be expected that the life time of the piplines be not shorter than 50 years. Viewed from the angle of durability, the 50-year limit is arbitrarily chosen. It is known, for example, that water conduits installed in Roman times are still in use in Europe, and that in Paris, lines dating from the times of Louis XIV are still being used. However, on the other hand, it is known that the durability of iron pipes in aggressive soils, for example in coastal regions, is only a few years.

A reference temperature for the strength of a pipeline is arbitrarily chosen as 23°C. This temperature is chosen more from the point of view of ease of room temperature testing than any application point of view, since in actual service, the medium being transported through the line will not exceed 8-10°C for six months of the year and for a period of no more

than 2-3 months will the temperature reach 15°C during the Summer time. An average annual temperature for Europe (179) can thus be calculated within the range 10-12°C. However, the selection of a reference temperature in this range would markedly increase the cost of standard testing for all plastics pipe materials for all applications and a correlation with other physical and mechanical testing of plastics in general would be required.

Some agreement with regard to nominal gas-line pressure is also difficult within Europe, due to the wide variety of pipe line materials and types of gas used. Larger municipalities take the view that it is of advantage to design the pipe lines uniformally for a nominal pressure of 4 Kg/cm^2, even if the normal conduit pressure is only half of this figure, since the steady growth of towns often requires a subsequent increase in the conduit pressure in order to ensure a sufficient gas supply at the end of the pipe line. However, smaller communities often prefer the less expensive pipe designed for a nominal pressure of 2 Kg/cm^2. The range of pressure used by the major gas using countries in Western Europe, which are applicable to plastics gas distribution pipe (180, 181) are tabulated in Table 1.5 of Chapter 1.

5.1 RUPTURE MECHANISM

Uniaxially strained tests bars of high density polyethylene and medium density polyethylene give values of a tensile elongation at break of 500-1000%. Strain is at first uniform over the entire test length. When the tensile force exceeds a maximum value, then a more localised reduction in cross-section occurs, which gradually spreads over the whole test length.

When a polyethylene pipe is subjected to a burst stress, the high stresses which lead to rapid destruction of the pipe produce firstly an initial uniform expansion of the pipe, followed by a localised formation of a blister, which finally bursts in a circumferential direction. The total elongation at the burst position is of the order of only 100% in the circumferential direction. At the position of failure, the wall thickness is reduced to a very small fraction of the original value. When compared to the elongation at break of a uniaxially stressed test specimen, a considerable loss of elongation has occurred, owing to the deformation-impeding effect of polyaxial stress.

When pipe is loaded with a constant internal pressure which is only a little below the bursting pressure, the pipe will fail within a short time after blister

formation at the position of fracture. Tests with lower internal pressures yield longer times for rupture and reduced total expansion of the pipe, but the blister formation still occurs. When the stress is still further reduced, ductile failure is replaced by brittle failure in that the pipes are uniformly expanded over their entire length, but local blister formation no longer occurs. In these cases, the pipe cross-section remains relatively unchanged even at the position of failure. In the brittle failures, the surfaces of the fracture generally exhibit a punctiform spot where the fracture started and concentric marks which are arranged around this spot in the form of angular rings and from which the growth of the fracture can be seen.

The ductile and brittle modes of failure indicate that the destruction of polyethylene pipes is due to two different mechanisms of deformation or rupture. Ductile failure is due to shearing stress and occurs when the latter exceeds a limiting value. With ductile failure, the molecules disunite and slide past one another with continuous new formation of crystallites.

A high degree of deformation is therefore necessary for a complete separation of the material.

In the case of brittle failure, the degree of deformation preceeding failure is small.

Cooney (182) has shown the location of incipient microfractures between polymer spherulites in specimens of high density polyethylene and, by direct measurement, related the size of these fissures to a critical level of overall strain and to the nature of the surrounding fluid. If the size of the microcracks exceeded this level, they began to propagate and extend themselves perpendicular to the direction of applied stress. Eventually, through a mechanism of coalescence, these fissures formed a brittle failure.

The rupture strength curve is therefore composed of two branches as shown diagrammatically in Fig. 5.2. The flat portion is formed by the action of shearing stresses and the steep one normal stresses (183). In the range of the bend of the curve - the so-called "knee" - the transition zone, mixed fractures referred to as "bructile" failures occur due to the action of both kinds of stress. The three types of failure mode are shown in the photographs of Figs. 5.3 and 5.4.

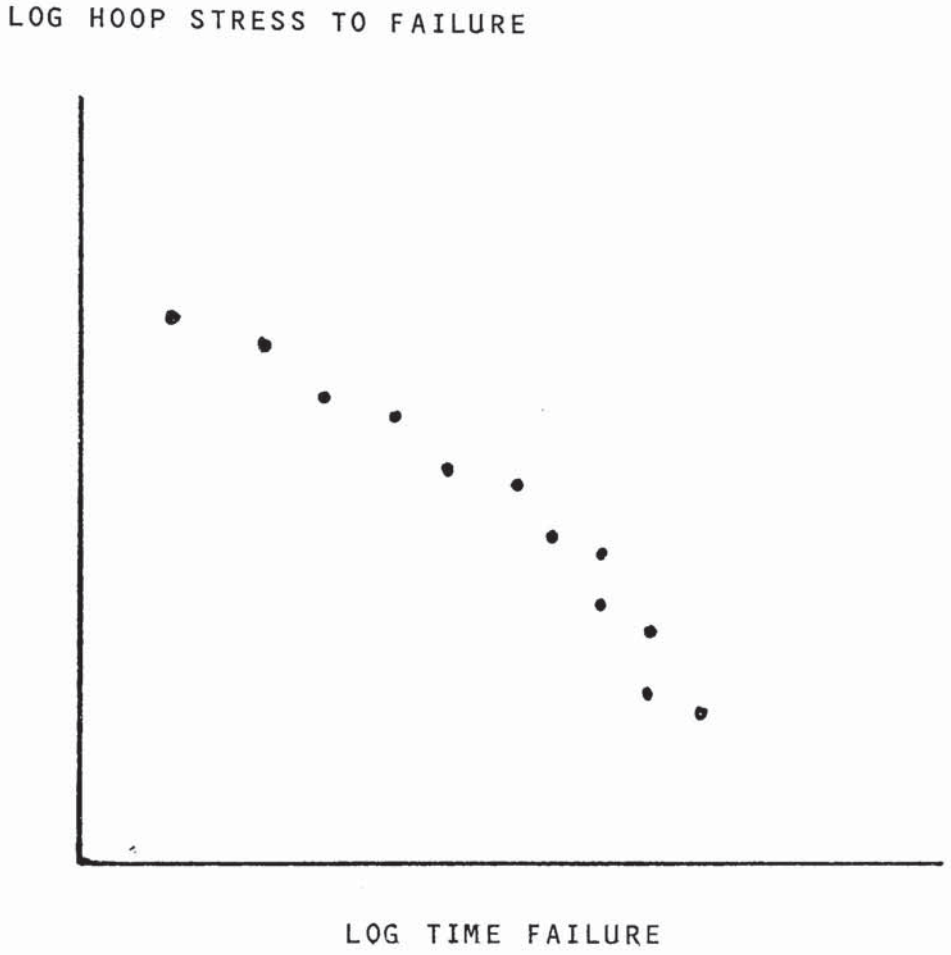

Fig. 5.2 Typical Polyolefin Stress Rupture Curve

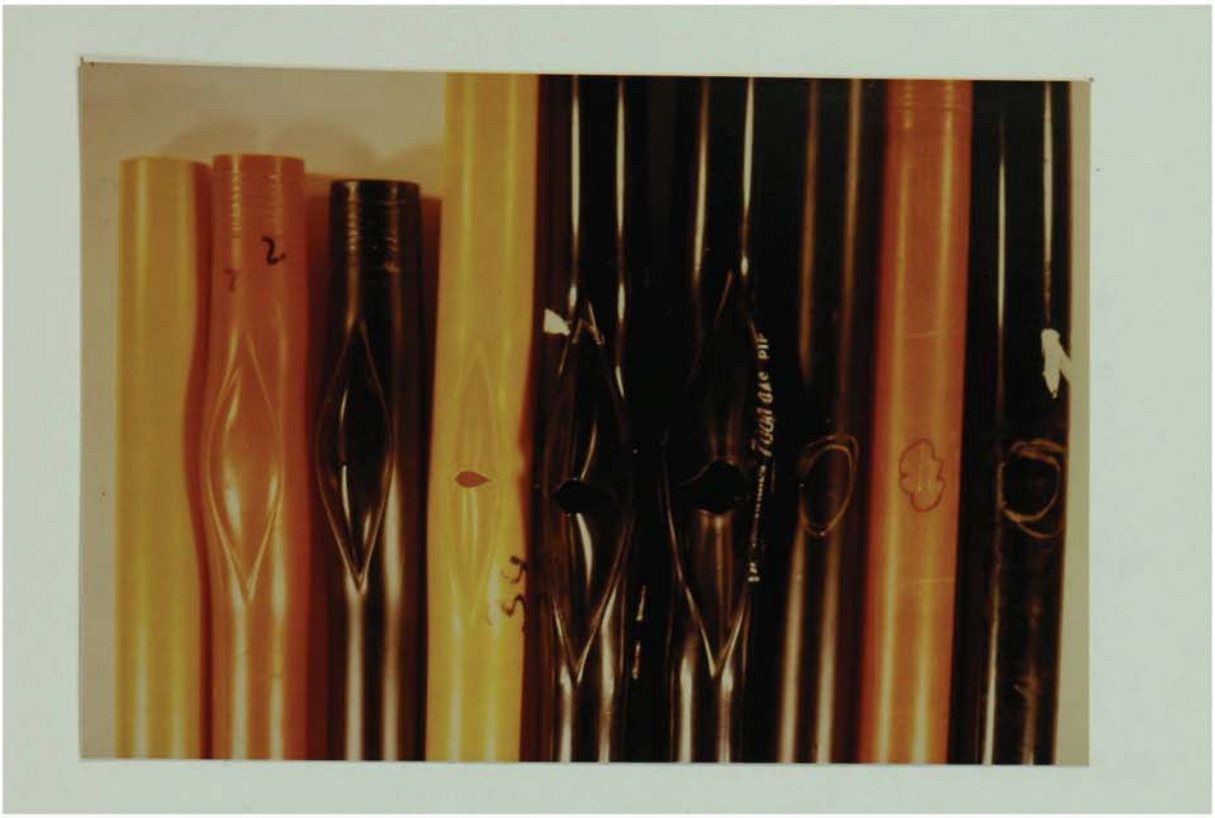

Fig. 5.3 Photograph of Types of Pipe Failure Observed

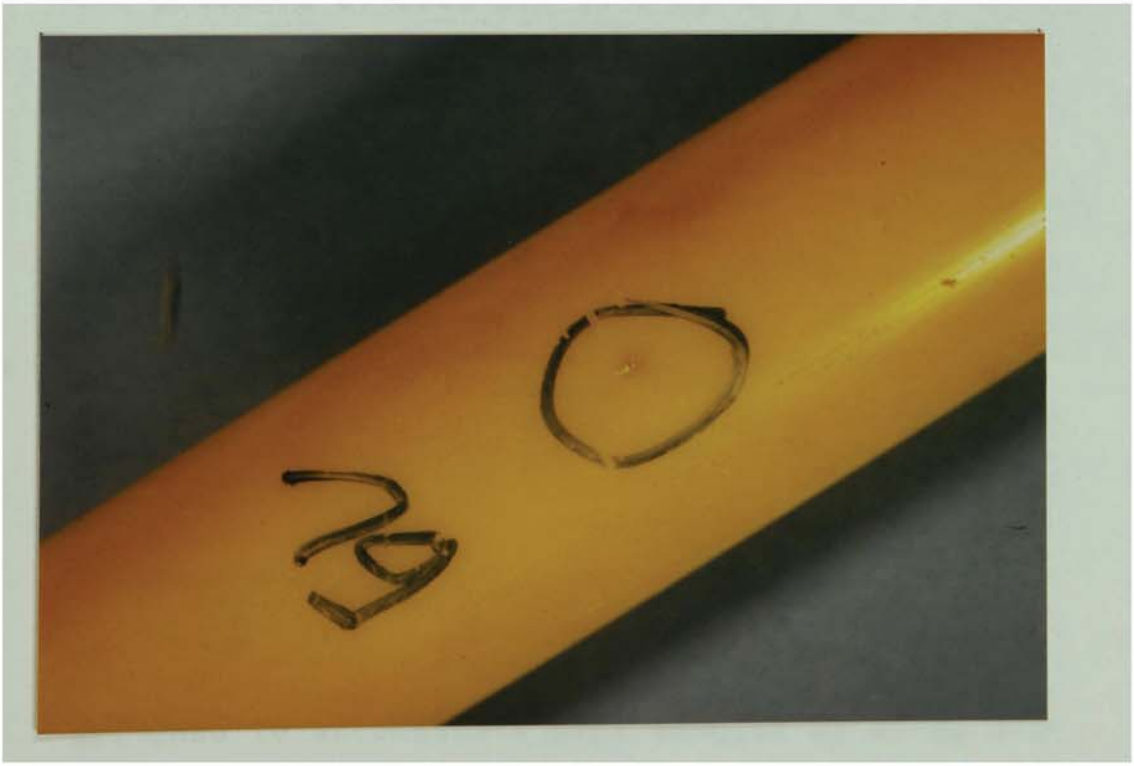

Fig. 5.4 Photograph of Typical Brittle Failure Point

5.2 EVALUATION PROCEDURE

5.2.1 Hoop Stress Test Equipment

The long-term pipe bursting apparatus designed for the Phillips Petroleum Technical Centre by Yarsley Research Laboratories Limited, applies a constant hydraulic internal pressure to pipe samples and records the time to failure. This equipment is diagrammatically shown in Fig. 5.5.

The hydraulic pressure is applied via a Greer-Mercia accumulator; the pressure being exerted by nitrogen supplied from a commerical gas cylinder. The test rig has been designed to accommodate a maximum cylinder pressure of 2500 psi (170 Kg/cm^2) and a maximum test pressure of 30 Kg/cm^2.

The test pressure is kept constant within the specified limits by connecting the gas cylinder side of the Greer-Mercia accumulator to a large reservoir, so that the changes in pipe volume, due to expansion under pressure, do not form a significant proportion of the volume.

Although the test apparatus has been specifically designed to accommodate pipe samples of 32 mm diameter, by reducing the number of samples under test a maximum diameter of 225 mm can be accommodated.

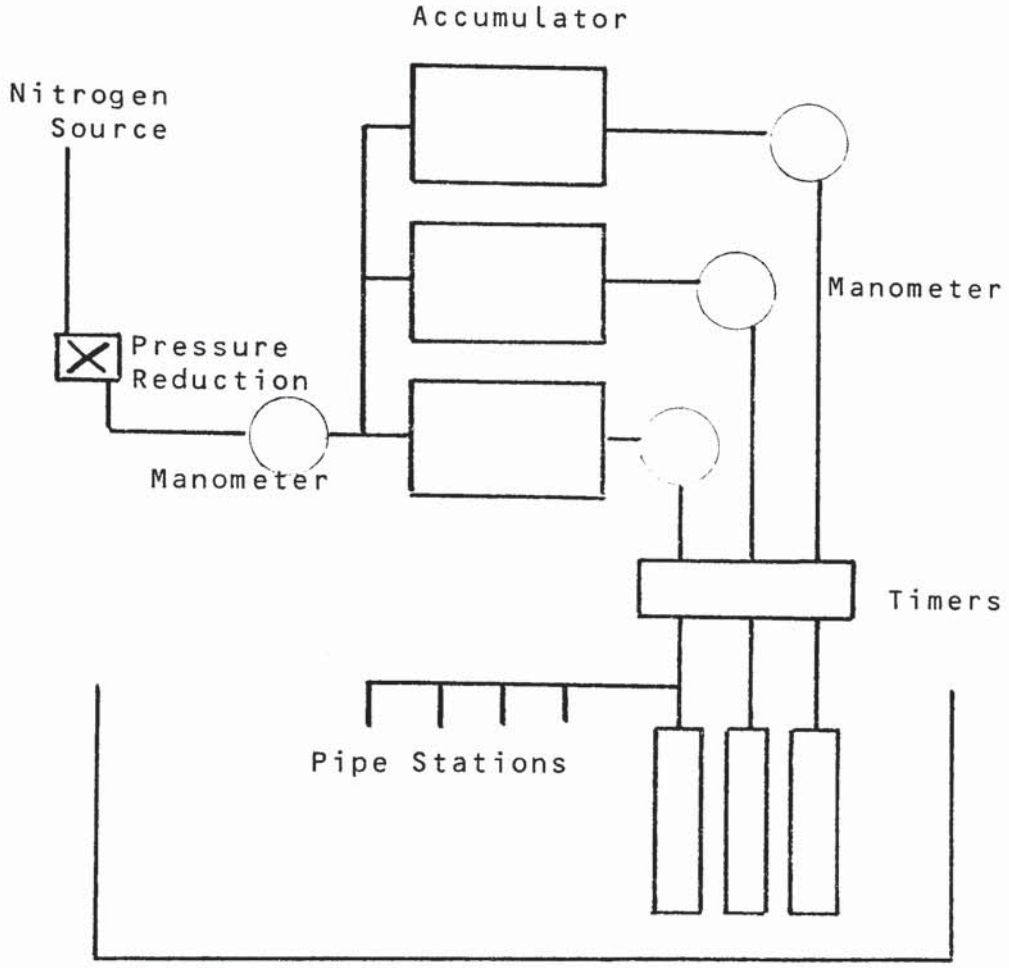

Fig. 5.5 Simplified Form of Hoop Stress Test Equipment

The pipe stations are divided into convenient banks and all pipe stations on a bank must be the same pressure, although different banks can be at different pressures. When a sample fails, the pressure fuse in the circuit prevents any loss of pressure from the other stations under test in the same bank.

The apparatus has been designed to perform tests in accordance with B.S. 4728:1971 (184) and other equivalent specifications usch as ASTM D 1598-63 (185) and DIN 8075 (186).

5.2.2 Sample Preparation

The materials under investigation were extruded into 32 mm diameter pipe of 2.8 mm wall thickness. Pipe calibration was by means of a Floataire combined vacuum calibration-cooling bath.

The extruded pipe was cut into 35 cm lengths in accordance with the minimum length relation:

25 cm + (3 x diameter) + end fitting allowance

The pipes were then marked, measured for minimum wall thickness and diameter, and the end-fixture fitted (Fig 5.6). Prior to pressurisation, the pipes were filled with water and allowed to rest in the temperature controlled water bath of the test rig for 24

Fig. 5.6 Photograph of Pipe Sample with End Fitting

hours. The specimens at each stress level were then pressurised and the pressure adjusted periodically to take into account the expansion of the pipes. The time to failure for each specimen at each stress level was recorded.

Test data originating from other laboratories were obtained in a similar manner.

5.2.3 Processing of Data

The failure stress-failure times were plotted on double logarithmic plots. The procedure (187) for estimating long-term hydrostatic strength is essentially an extrapolation with respect to time. In the extrapolations, the regression equations are developed by the method of least squares with stress as the independent variable. It is to be noted that the common practice in plastics pipe technology is to plot time on the X-axis. This plotting practice is maintained, but the variables in the least square regression equations are reversed so that the calculations are correct according to the mathematical principles.

Because of the large number of data points and the tedious calculation procedure, a computer programme (188) written in Fortran 1V for the G.E.-205 computer

was used. This programme was modified (189) to permit the estimation of the long-term burst strength of thermoplastics pipe, when the pipe has been subjected to varying internal hydrostatic pressures. The programme determines, by least squares analysis, the best fit between log rupture time and log working stress. It estimates the rupture time for three predetermined pressures to aid in plotting the best fit relation. It then estimates the working stress which the pipe has a 95% chance of withstanding, for 100,000 hours and 50 years.

This programme is reproduced as Appendix 2 at the end of the thesis. Rather than interrupt the text of Chapter 5 with several consecutive pages of illustrations, it was considered preferable to locate the Tables of the applied hoop stresses and the corresponding failure times for each pipe sample, together with the computer print-out data, at the end of this Chapter.

5.2.4 Mathematical Discussion

Given, from Chapter 4, that there are "a priori" reasons, from the theory of the process, to suspect that the relationship between two variables:

h, logarithm of failure time in hours

f, logarithm of failure stress in Kg/cm^2

should have the form:

$$h = af^b$$

Where b can have any value

Then this has the linear form

$$\log h = \log a + b \log f \quad \ldots\ldots \text{(i)}$$

Where the definition of the best straight line to the data is that line which makes a minimum the sum of squares of the deviations from the line of the measurements of "h". The independent variable "f" is assumed to be free of error.

In order to predict values of "f" from known values of "h", where "n" is the number of data points, then the equation for the regression line is calculated where:

$$F = \frac{\Sigma f}{N} \quad \ldots\ldots \text{(ii)}$$

$$H = \frac{\Sigma h}{N} \quad \ldots\ldots \text{(iii)}$$

$$W = \Sigma (fh) - \frac{(\Sigma f)(\Sigma h)}{N}$$

$$= \Sigma (fh) - NFH \quad \ldots\ldots \text{(iv)}$$

$$V = \Sigma h^2 - \frac{(\Sigma h)^2}{N}$$

$$= \Sigma h^2 - NH^2 \quad \ldots\ldots \text{(v)}$$

$$U = \Sigma f^2 - \frac{(\Sigma f)^2}{N}$$

$$= \Sigma f^2 - NF^2 \qquad \ldots\ldots \text{(vi)}$$

$$b = \frac{W}{U} \qquad \ldots\ldots \text{(vii)}$$

$$a = H - bF \qquad \ldots\ldots \text{(viii)}$$

The formula to deduce the most probable value of "f" corresponding to a given value of "h", that is, the regression of "f" upon "h" is:

$$f = a + b\,(h-H) \qquad \ldots\ldots \text{(ix)}$$

This regression line of "f" upon "h" is the line which gives the squares of the deviation of every point measured parallel to the "f" axis in units of "f" summed for all points, as a minimum. It gives the best estimate of stress "f" from known value of time "h".

Similarly, to predict the value of "h" from a known value of "f"

$$a^1 = \frac{\Sigma h}{N} = H$$

$$b^1 = \frac{\Sigma (f-F)(h-H)}{\Sigma (f-F)^2} = \frac{W}{u}$$

$$F = \frac{\Sigma f}{N}$$

$$h = a^1 + b^1\,(f-F)$$

The correlation coefficient "r" is calculated in order to test for the significance of an apparently linear relation.

$$r = \frac{\Sigma (h-H)(f-F)}{\sqrt{\Sigma (h-H)^2 \Sigma (f-F)^2}}$$

$$= \frac{W}{\sqrt{Vu}}$$

If the relationship between the data can be represented exactly by a straight line, then:

$$r = \pm 1$$

The standard deviation "s" is calculated from the relationship

$$S = \sqrt{\frac{1}{N-2} (V - \frac{W^2}{u})}$$

and the minimum and maximum data lines at 95% confidence limit are obtained from:

$$h \text{ min} = (a+b\ f) - st$$

$$h \text{ max} = (a+b\ f) + st$$

Where t is the factor for testing and estimating of means, corresponding to N-2 degrees of freedom at the two-sided level of significance obtained directly from Tables (190).

5.3 EXTRUSION CONDITIONS

Several preliminary extrusion trials were performed to determine the range of conditions at which a consistent quality of pipe could be produced from the materials under investigation.

By variation of the extruder barrel temperature profile, the melt temperature was varied in three steps within the range of 185°C to 235°C. At each melt temperature, three extruder screw speeds: 20, 40 and 60 rpm, were used. The tensile elongation of pipes produced under this range of conditions showed no appreciable differences and thus from the point of view of conserving material and ease of the extrusion operation, the following conditions were set as a standard:

Screw speed:	20 rpm
Melt temperature:	205°C
Extruder Cylinder temperature	Zone 1: 190°C
	Zone 2: 200°C
	Zone 3: 185°C
	Zone 4: 180°C
Extruder Adaptor temperature	Zone 5: 160°C
Die Head temperature	Zone 6: 170°C
	Zone 7: 170°C
	Zone 8: 190°C
Die Tip temperature	Zone 9: 235°C

Extruder Motor Power:	14 amps
Die Head Pressure:	65 Kg/cm^2
Linear Output:	0.66 M/min
Weight Output:	11 Kg/hour

Under these processing conditions, the pipe reversion (191) measured in Glycol at 120°C was between 0.1 to 0.3% a figure well below the maximum allowable specification level of 3.0%.

5.3.1 Extruder and Screw Design

The extruder used was a Reifenhauser S-60-11, manufactured by Reifenhauser KG, Troisdorf, West Germany. The barrel length to diameter ratio is 24:1 and there are four barrel resistance - heating and water-cooling zones, and five die head heating zones. The breaker plate at the die head adapter has 2 mm diameter holes and a triple screen pack of 20/80/20 mesh is used to provide back pressure.

The screw used throughout the evaluation was a 60 mm, 24:1 length to diameter, two-stage screw, of design for polyethylene. The design dimensions of the screw are: Feed section 445 mm of depth 9.6 mm

Compression section 180 mm, conical

First metering section 360 mm of depth 2.4 mm

Decompression section 24 mm, conical

Second feed section 180 mm of depth 9.6 mm

Compression section 120 mm, conical

Final metering section 300 mm of depth 3.2mm

Pitch equal to diameter, 60 mm

5.3.2 Die and Calibration Design

The die was designed to produce a pipe of 32 mm outside diameter, class C, in accordance with the GIVEG specification (192). A diagrammatic representation of the die head is illustrated in Fig. 5.7.

The die diameter was designed 10% oversize at 36.60mm to allow for drawdown and shrinkage to the correct size. Land length of 73.8 mm gave a ratio of 2:1 to the diameter. The die mandrel diameter of 30.60 mm for an annular gap of 3.0 mm, is a land length to thickness ratio of 24:6. This design allows for a drawdown of 16% which is considered normal in European pipe production but considerably lower than that used in the United States.

$$\frac{\text{Cross section of die}}{\text{Cross section of pipe}} = \frac{316.5\ \text{mm}^2}{273.2\ \text{mm}^2}$$

A Floataire vacuum calibration system was used, the calibrating diameter of 33.28 mm being deliberately oversized to take into account a 4% shrinkage. The calibrating length was 95 mm. The calibration system is diagrammatically represented in Fig. 5.8.

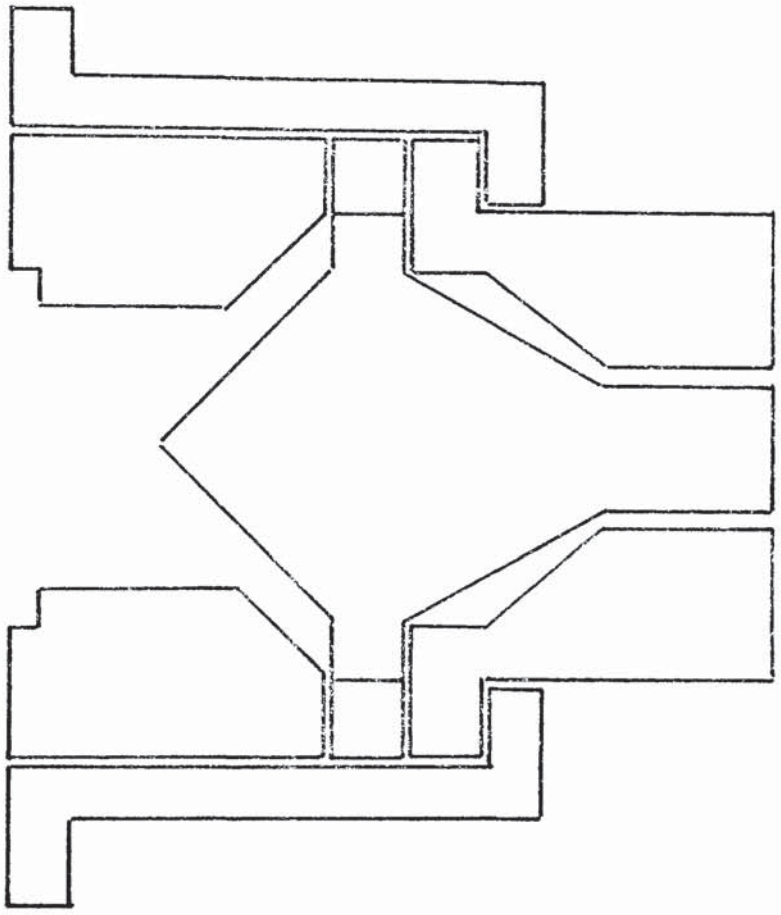

Fig. 5.7 Illustration of Extruder Die-Head for Pipe

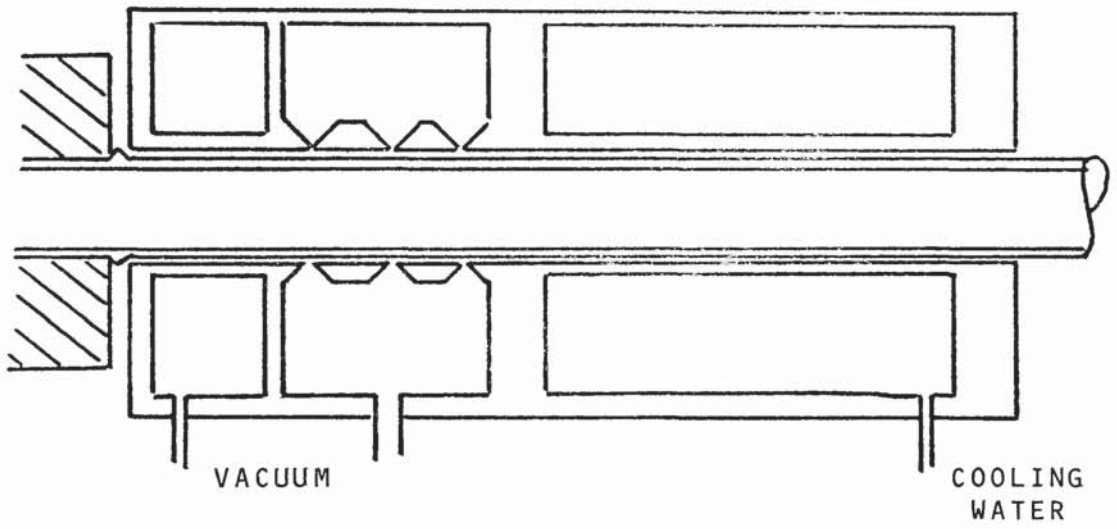

Fig. 5.8 Illustration of Pipe Calibration System

Due to the high melt viscosity of the ultra high molecular weight copolymers, calibration was effected under pressure in the die head. Numerous trials with more conventional polymers have shown that such calibration does not significantly alter the extruded pipe characteristics and thus all the pipe samples were considered to have been produced under similar conditions.

5.4 PRELIMINARY DATA

McGlamery (193) studied some of the earlier homopolymers and copolymers of ethylene in an effort to predict hoop stress performance. These data, plotted as Barlow hoop stress and reproduced in Figs. 5.9 to 5.11 demonstrate the improved hoop stress performance by increasing the molecular weight of the homopolymer or introducing 1-butene as a comonomer in the Phillips S.F. polymerisation process. These data are plotted as average lines (50% lower confidence limit) and the Larson-Miller correlation factor shows a very wide variance at different stress levels between 9.6 to 17.4 for the lower molecular weight homopolymer; 13.1 to 15.6 for the higher molecular weight homopolymer, and between 17 to 23 for the copolymer.

An additional point is that the actual data points do not progress further than approximately 5000 hours,

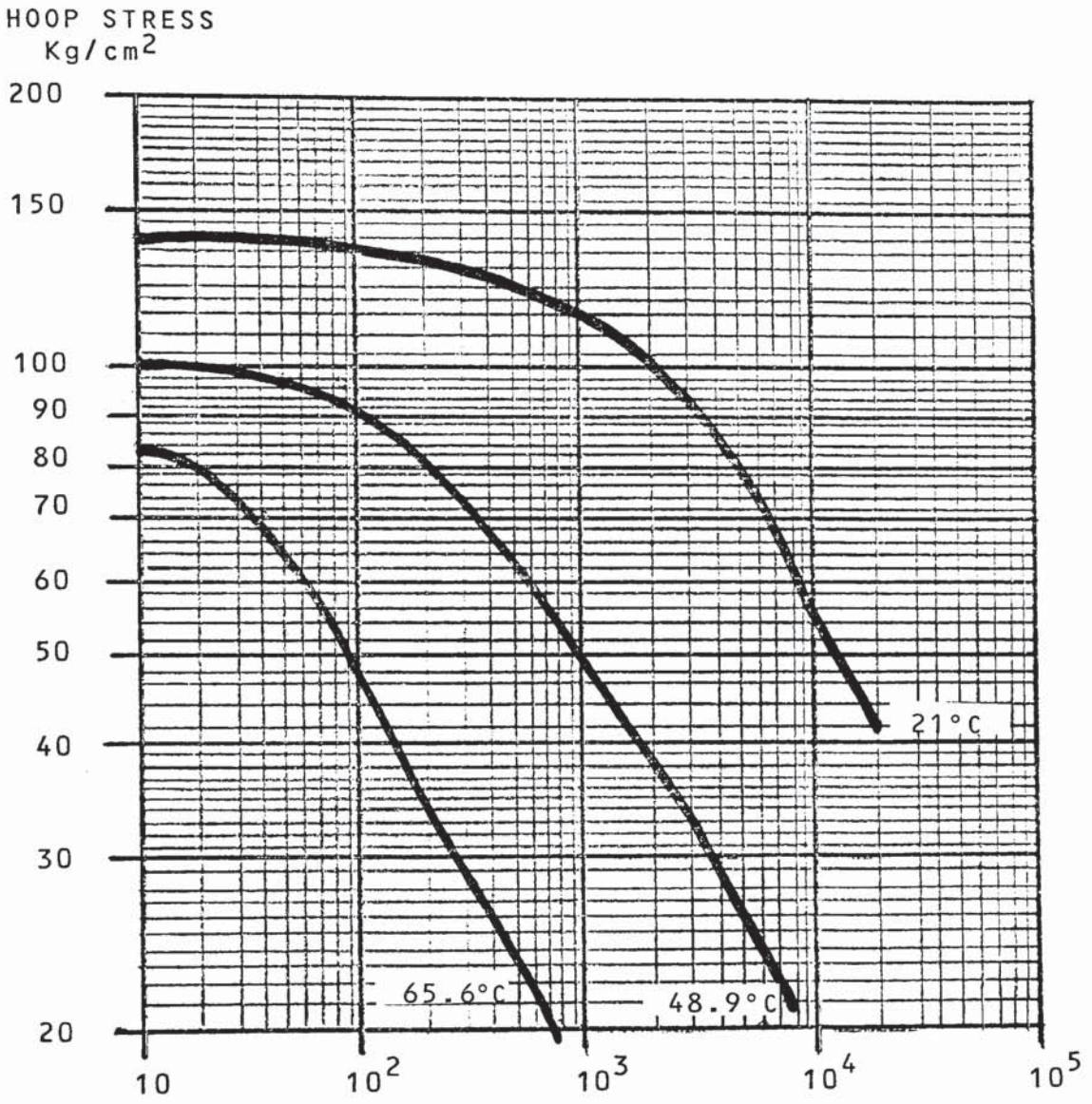

Fig. 5.9 Hoop Stress Performance of Phillips Low Molecular Weight Homopolymer

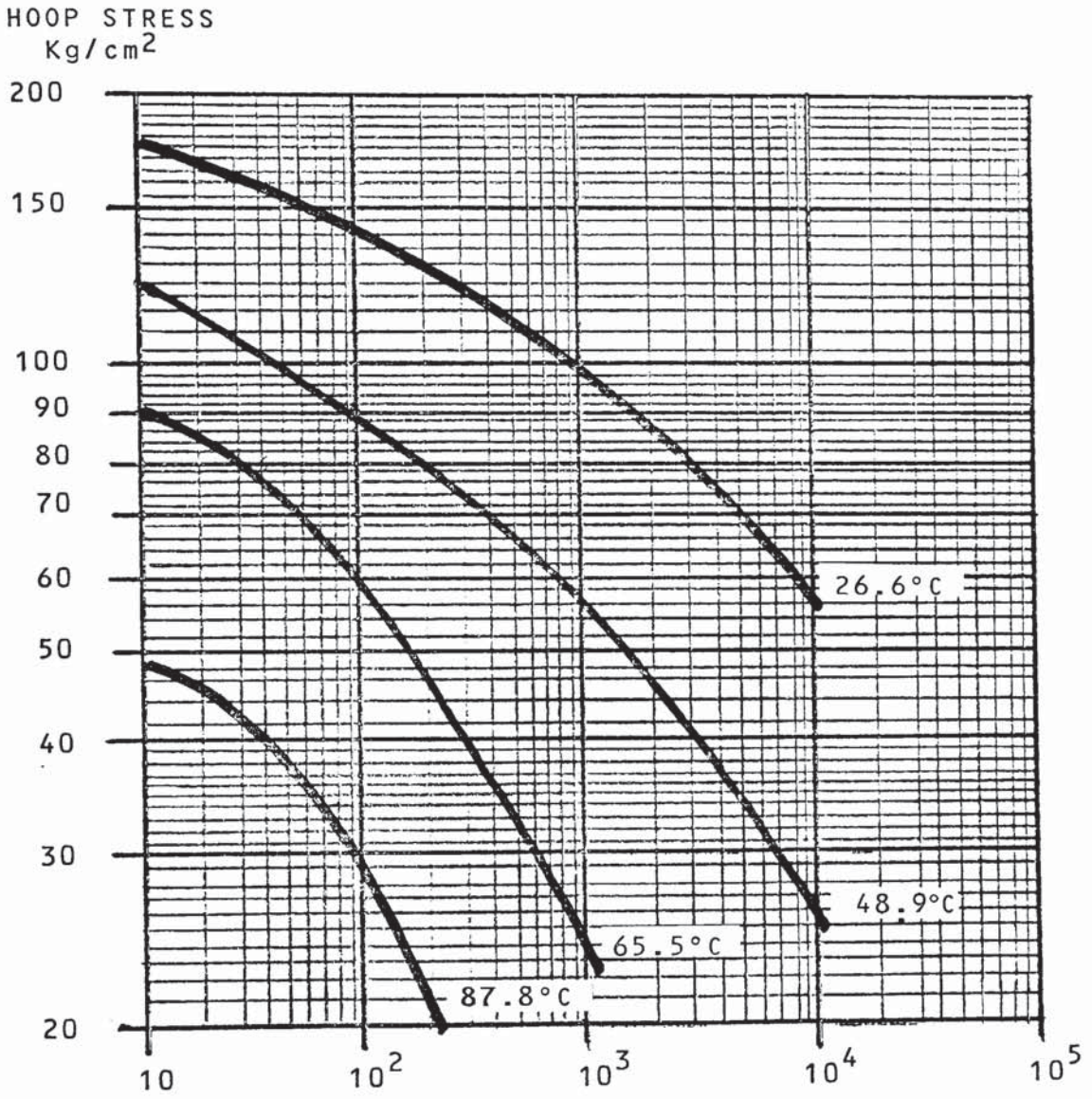

Fig. 5.10 Hoop Stress Performance of Phillips Medium Molecular Weight Homopolymer

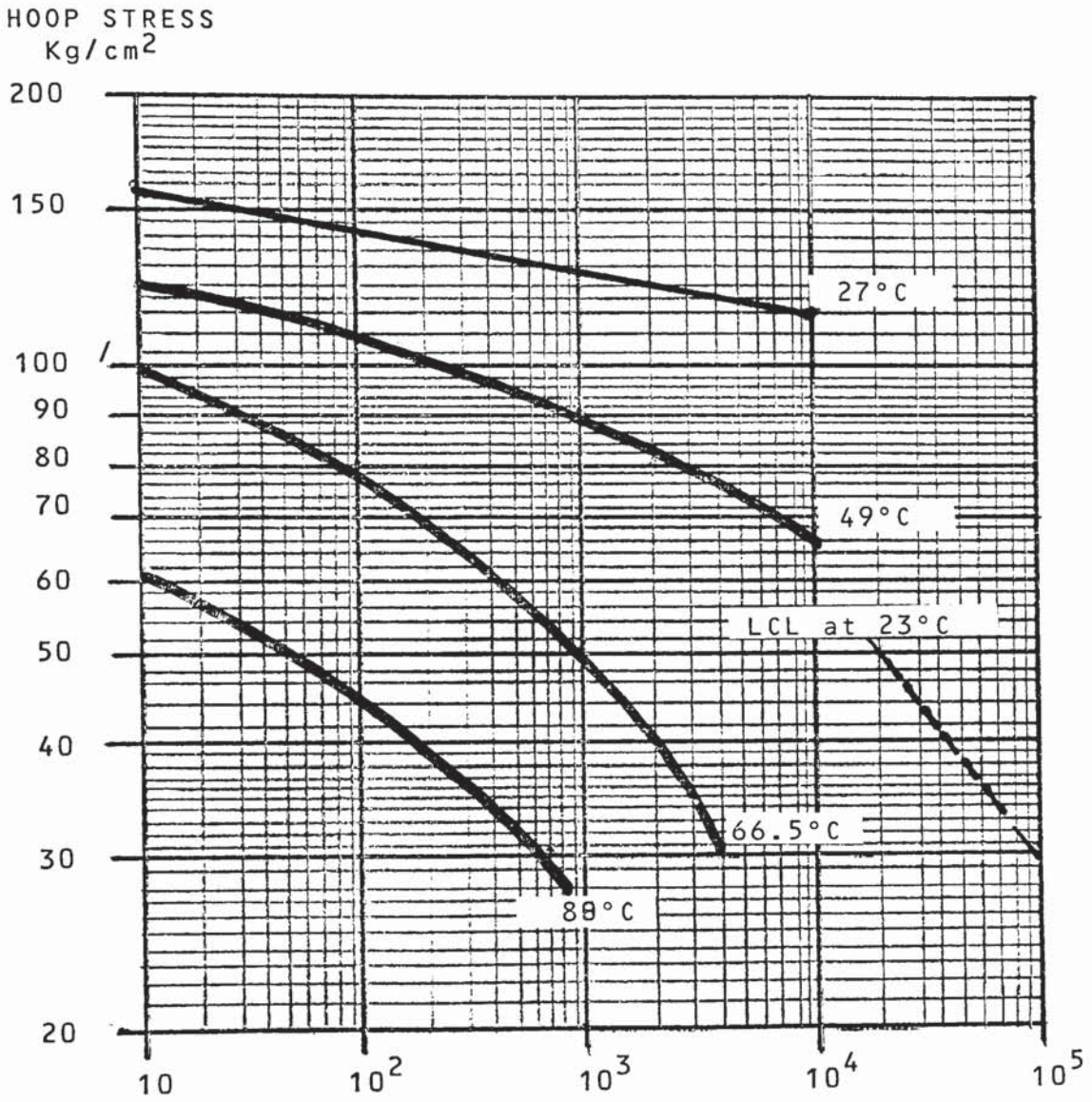

Fig. 5.11 Hoop Stress Performance of Phillips Medium Molecular Weight Ethylene-Butene Copolymer

and thus, there is likely to be a significant influence on the shape and direction of the curves from the ductile-brittle (Bructile) transition failures.

More recent data (194) relating to the Ziegler high molecular weight ethylene-butene copolymer has been substantiated by further testing during the course of this work and the I.S.O. hoop stress is plotted as the 95% Lower Confidence Limit in Fig. 5.12. Gaube, Diedrich and Müller (194) maintain Richard's (177) findings that these data follow Arrhenius's Law and thus allow the extrapolation from short-term data at elevated temperatures to more long-term data at room temperature. The Larson-Miller Constant (separation factor) for these data is 47.5 for the horizontal portion of the curve, where the mechanism of failure is creep and ultimately ductile failure, and a constant of 22 in the more vertical portion of the curve where brittle failure predominates. Barton and Cherry (195, 196) using the same data, arrive at a Larson-Miller type constant having the value:

$$C = 7.1 \times 10^{16}\ T^{-5.3}\ (1.12 \times 10^{4}\ T^{-1} - 13.45)$$

which, over the temperature range of 23°C to 80°C, varies between 18.5×10^4 to 4×10^4 respectively. Both methods predict brittle failure at 20°C at about 10×10^4 hours although Gaube predicts a smaller slope

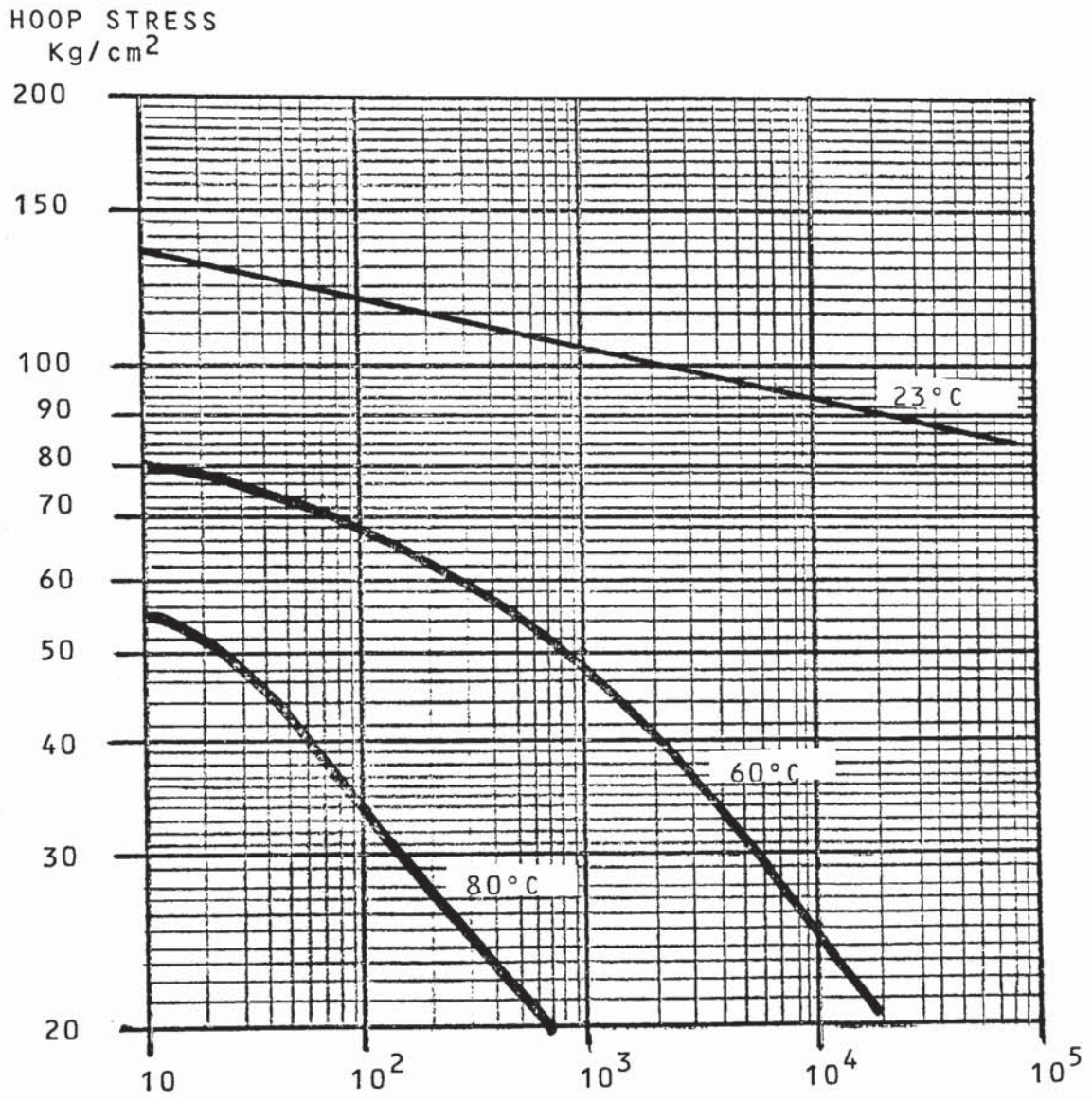

Fig. 5.12 Hoop Stress Performance of Ziegler High Molecular Weight Ethylene-Butene Copolymer (95% LCL)

after the ductile - brittle transition "knee-point".

5.5 TEST PROGRAMME RESULTS

5.5.1 Polyethylene Homopolymers

The relevant properties of the two homopolymers are:

	Low Molecular Weight	Medium Molecular Weight
Polymerisation Process	Phillips S.F.	Phillips S.F.
Density g/cc	0.960	0.962
Melt Index dg/cc	0.8	0.2
Separation factor:		
at hoop stress 56.25 Kg/cm^2	13.3	-
35.15 Kg/cm^2	-	13.8 - 17.4
28.12 Kg/cm^2	14.6	-
14.06 Kg/cm^2	15.6	9.6
Extrapolated LTS Kg/cm^2	14.5 approx	18.0 approx.

The Larson-Miller constants (separation factors) are those determined by McGlamery (193) on the average Barlow hoop stress (Fig. 5.9 and 5.10).

The extrapolated long-term hoop strength (LTS) value at 50 years for the low molecular weight homopolymer was determined as 14.5 Kg/cm^2 and for the medium molecular weight homopolymer as 18.0 Kg/cm^2.

In view of the uncertainty surrounding the testing of these materials, it is not intended to offer these

values as absolute figures but to show, in the subsequent sections, the degree of improvement obtainable by copolymerisation. The influence of molecular weight is already demonstrated by the 24% improvement in extrapolated long-term strength.

5.5.2 Ethylene-Butene Copolymers

The relevant properties of the medium, high and ultra high molecular weight (M.Wt) ethylene-butene copolymers are:

	Medium M.Wt	High M.Wt	Ultra High MWt
Polymerisation Process	Phillips SF	Ziegler SF	Phillips PF
Density g/cc	0.490	0.947	0.943
Melt Index dg/min	0.3	-	-
High Load Melt Index dg/min	-	14.0	2.0
Separation factor	16.3 (22.2)	22.0	21.55
Extrapolated LTS Kg/cm^2	51 (19.0)	65.0	89.84

The original data on the Phillips SF medium molecular weight copolymer originates from McGlamery's work (193) and the so-derived separation factors are reproduced from the plot of Fig. 5.11.

The same comments apply here as proposed in section 5.6.1, relative to ethylene homopolymers. The validity of these separation factors is not substantiated by a separate recent series of test data obtained at

80°C performed in the course of this work. In all cases, the failure times at 80°C were less than the average times obtained by McGlamery at 88°C. The additional test results at 80°C are tabulated below together with the 95% lower confidence limits and additionally shown in Fig. 5.11.

Hoop Stress Kg/cm^2	Failure time-hours	95% LCL
41.1	24, 36, 48, 65, 76	2.34
40.9	24	
35.3	47, 65, 95, 133	3.49
30.2	39, 175	5.0

Curve equation $h = (5.88 - 2.626\ f) - 1.2717$

Applying the 80°C standard deviation to the extrapolated 23°C average curve, yields an estimate of the 95% lower confidence limit at 23°C and gives an extrapolated lower confidence limit long-term strength value at 4.368×10^5 hours (50 years) of 19 Kg/cm^2. Recalculation of the separation factor at this stress level, using the lower confidence limit data at 80°C and 23°C, yields a value of 22.2 for the Phillips SF medium molecular weight ethylene-butene copolymer.

The extrapolated average long-term strength value of 51 Kg/cm^2 compares to the figure of 18.0 Kg/cm^2 for the Phillips SF medium molecular weight homopolymer

of equivalent melt index and demonstrates the degree of improvement achievable by copolymerisation with butene-1. The long-term strength value estimated with a 85% lower confidence limit, is still higher than the average figure for the homopolymer.

The data determined at 80°C to substantiate that published by Hoechst for their Ziegler SF polymerised ethylene-butene copolymer, Hostalen G M 5010, agrees very closely when using the 95% lower confidence limits.

From the data tabulated in Table 5.1 and plotted in Fig. 5.12, the computer-derived equations are:

Ductile region:

$$h = (52.146926 - 28.271292\ f) - 0.40003\ t$$

Brittle region:

$$h = (8.49895 - 3.77134\ f) - 0.52815$$

Applying the brittle region equation at 80°C to obtain the separation factor and taking the published 95% lower confidence figure of 65 Kg/cm^2, hoop stress at 50 years at 23°C, the factor is determined as:

$$\text{Temp °C } (C + \log h_1) = \text{Temp °C } (C + \log h_2)$$

$$C = 22.28$$

This figure is 1.2% higher than that proposed by Gaube (194) and is most probably due to the relatively small number of samples taken with the consequent necessity

of using a relatively high students 't' distribution vamue in the brittle region equation.

From the data (Tables 5.3 - 5.12, and Figs. 5.13-5.17) developed on the Phillips PF polymerised ultra high molecular weight high density ethylene-butene copolymer, the computer-derived equations are:

Ductile Region:

at 23°C $h = (65.51111 - 30.21613\ f) - 0.31268\ t$

at 60°C $h = (60.706325 - 30.494517\ f) - 0.378556\ t$

at 66°C $h = (43.82000 - 22.130495\ f) - 0.3824598\ t$

at 80°C $h = (82.56844 - 43.75093\ f) - 0.31803\ t$

Brittle Region:

at 60°C $h = (10.621223 - 3.694487\ f) - 0.12500\ t$

at 66°C $h = (11.017409 - 4.143500\ f) - 0.114826\ t$

at 80°C $h = (8.48415 - 3.21670\ f) - 0.20526\ t$

at 90°C $h = (7.97447 - 2.96335\ f) - 0.15559\ t$

The brittle region equations were applied to selected stress levels of 65, 60 and 55 Kg/cm^2 respectively. These stress levels were chosen on the basis of the range over which the majority of the test results were obtained. The corresponding time values calculated from these equations are tabulated below.

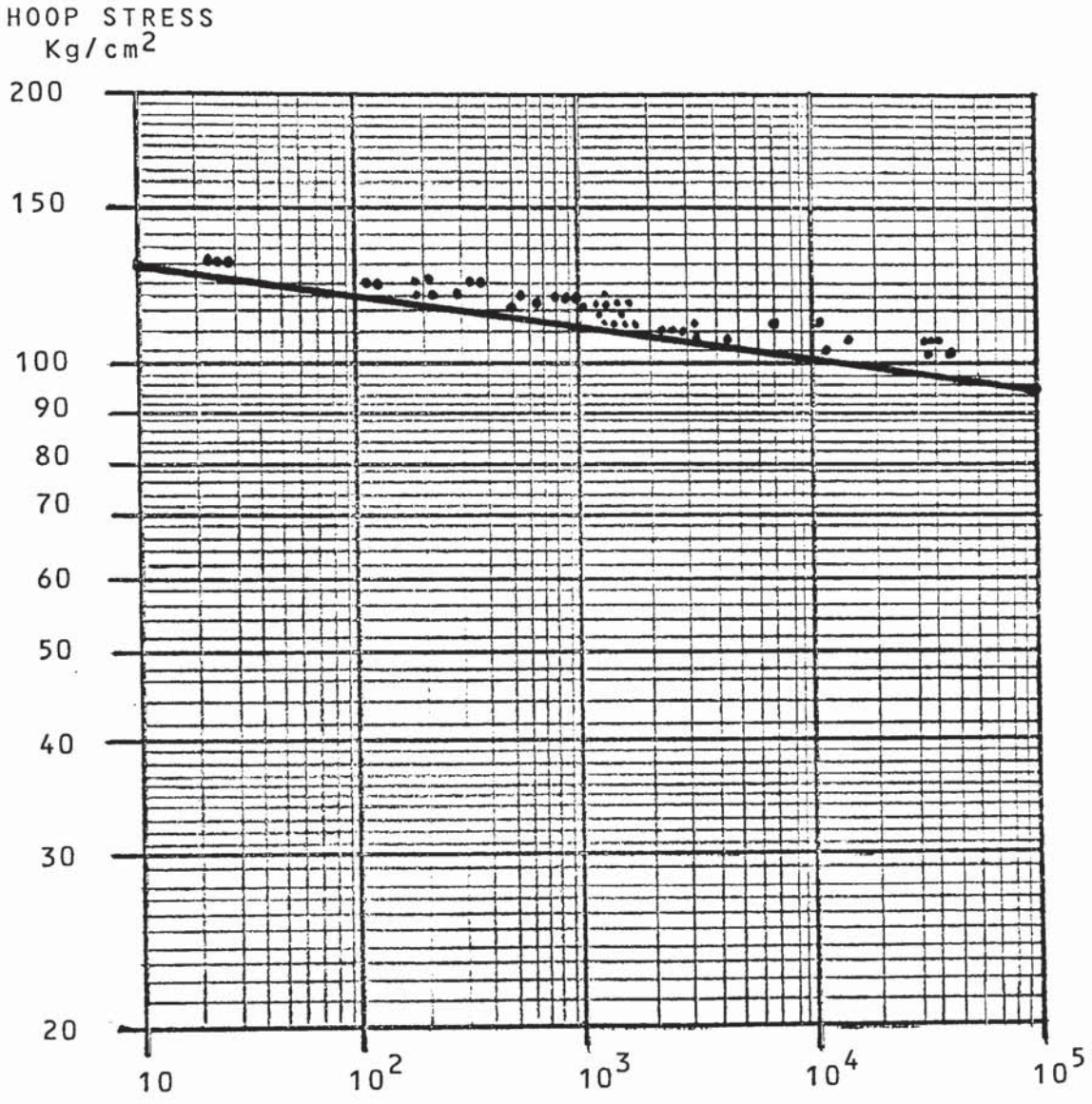

Fig. 5.13 Data Points and 95% LCL Plot for Phillips Ultra High Molecular Weight Ethylene-Butene Copolymer at 23°C

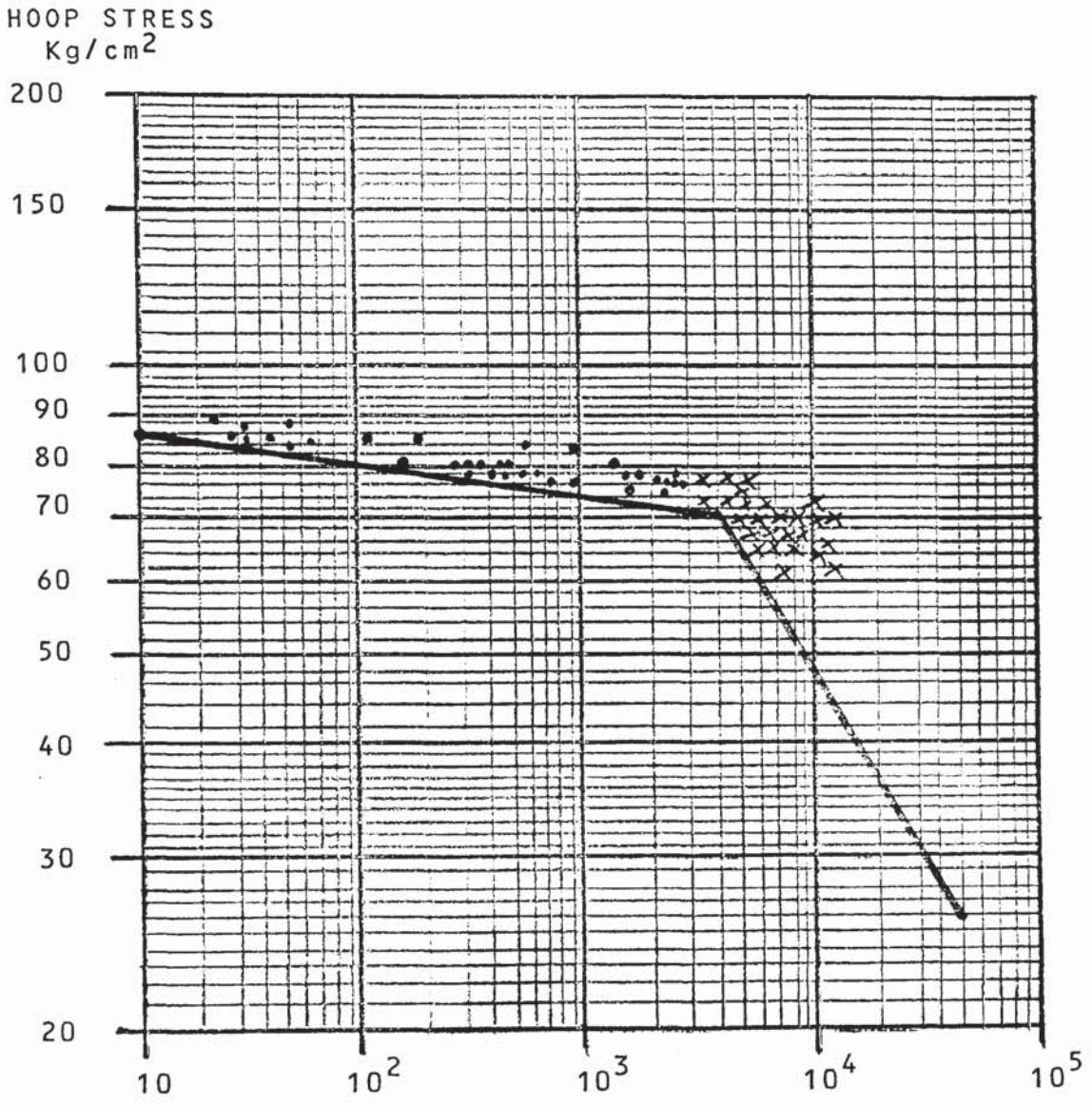

Fig. 5.14 Data Points and 95% LCL Plot for Phillips Ultra High Molecular Weight Ethylene-Butene Copolymer at 60°C

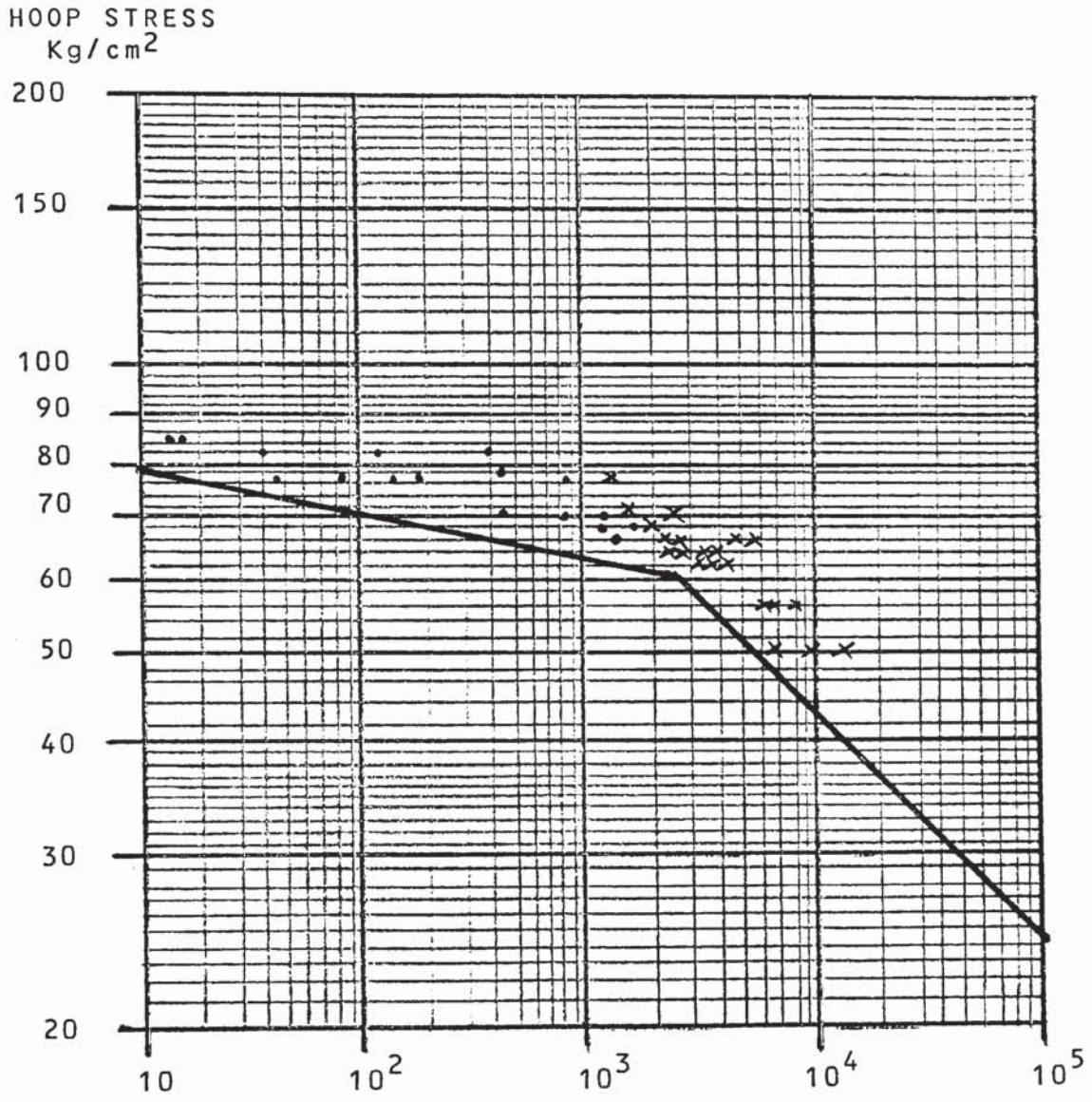

Fig. 5.15 Data Points and 95% LCL Plot for Phillips Ultra High Molecular Weight Ethylene-Butene Copolymer at 66°C

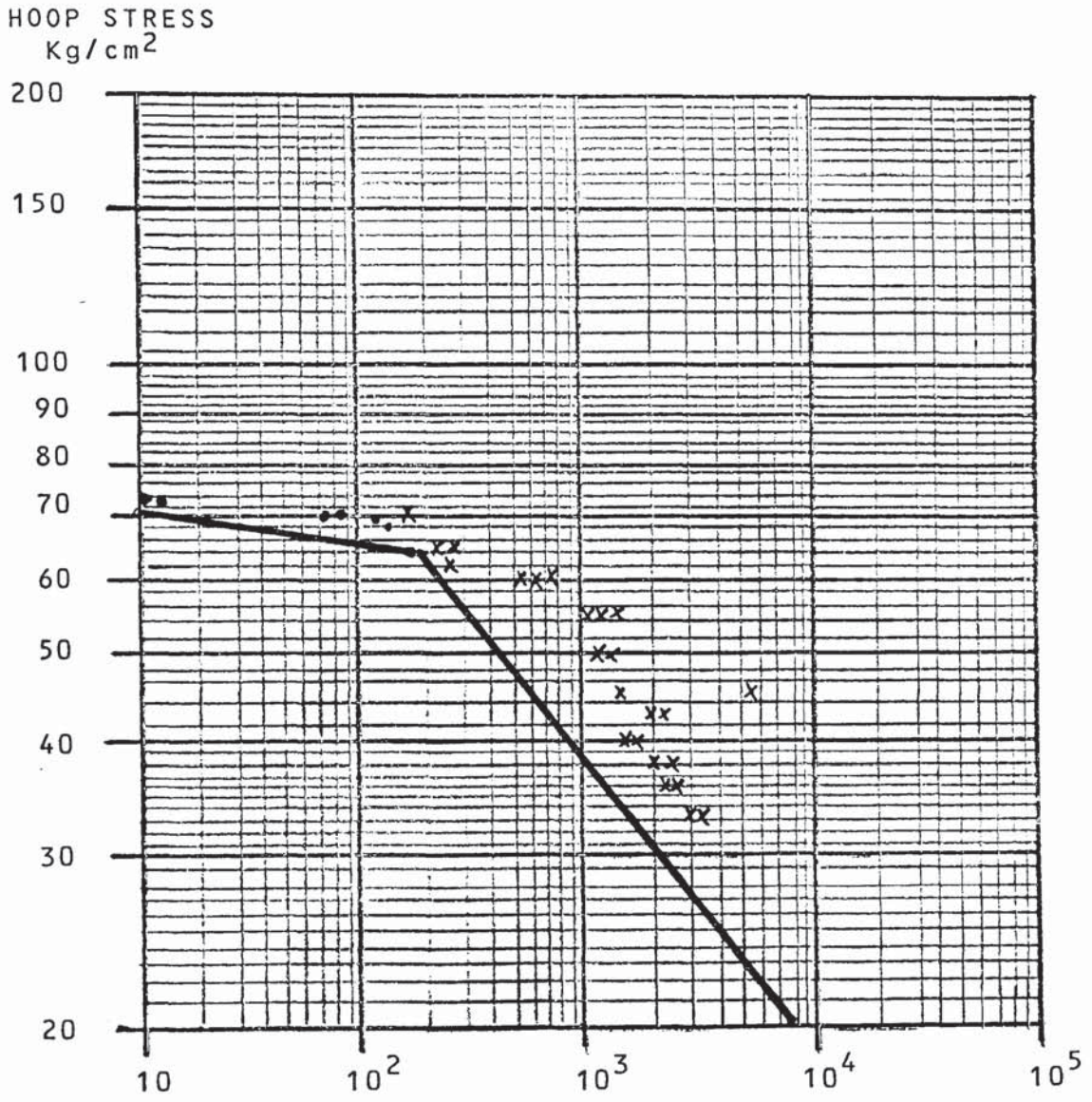

Fig. 5.16 Data Points and 95% LCL Plot for Phillips Ultra High Molecular Weight Ethylene-Butene Copolymer at 80°C

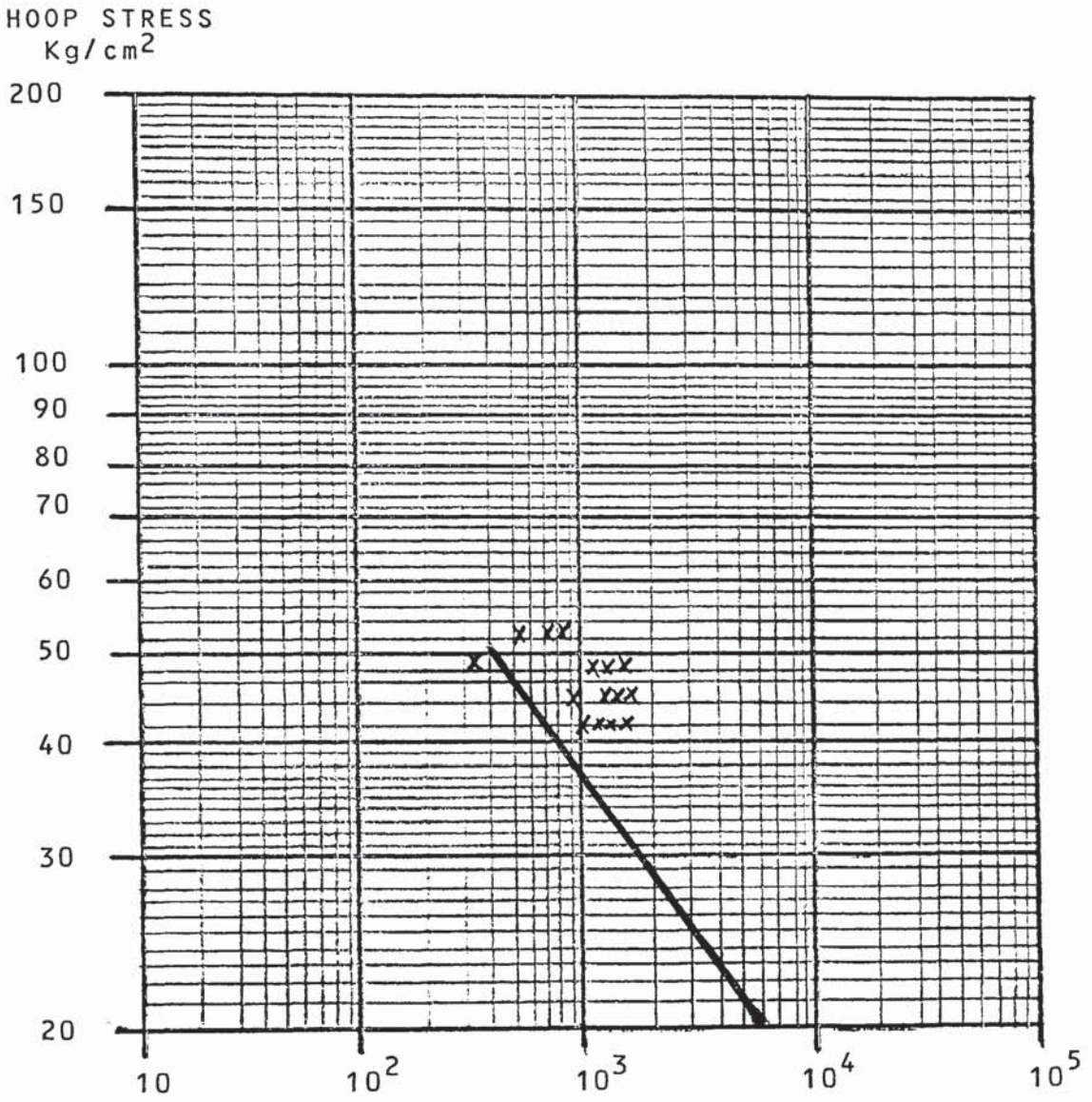

Fig. 5.17 Data Points and 95% LCL Plot for Phillips Ultra High Molecular Weight Ethylene-Butene Copolymer at 90°C

Stress Level Kg/cm^2	65	60	55
95% LCL Time - hours			
at 60°C	5154	6928	9555
at 66°C	2027	2825	4051
at 80°C	199	258	341
at 90°C	212	269	348

At a hoop stress level of 65 Kg/cm^2, the relationship between the computer-derived time values and the different temperature levels, and thus the separation factor is:

Temperature Range	Calculated Times	Factor Derived
60°C/66°C	5154/2027	19.20
66°C/80°C	2027/199	22.12
80°C/90°C	199/212	-
60°C/80°C	5154/199	21.24

At a hoop stress level of 60 Kg/cm^2, the derived factors are:

Temperature Range	Calculated Times	Factor Derived
60°C/66°C	6928/2825	18.18
66°C/80°C	2825/258	22.77
80°C/90°C	258/269	-
60°C/80°C	6928/258	21.39

At a hoop stress level of 55 Kg/cm^2, the derived factors are:

Temperature Range	Calculated Time	Factor Derived
60°C/66°C	9555/4051	17.08
66°C/80°C	4051/341	23.50
80°C/90°C	341/348	-
60°C/80°C	9555/341	21.58

The factors so derived can be rearranged into the following Table:

Stress Level Kg/cm^2	Temperature Range °C		
	60/66	66/80	60/80
70	20.14	21.49	21.08
65	19.2	22.12	21.24
60	18.18	22.77	21.39
55	17.08	23.50	21.58
50	15.88	24.30	21.74
40	13.46	26.16	22.23

From these results it may be concluded that there is a very close relation between the lower confidence limit data at 60°C and that at 80°C, whereas the data at 66°C converges on that of 60°C and diverges from the lower confidence line at 80°C. It is submitted that the least squares analysis at 66°C is heavily influenced by the small number of data points at stress levels below 62 Kg/cm^2, giving rise to a less steep slope than would be expected with a greater amount of samples tested in the brittle region. The number of

data points at 90°C are insufficient to give any consistent lower condifence limit value.

The average factor determined over the stress level range of 70 - 40 Kg/cm^2 is 21.55, and if this factor is used to determine the long-term strength at 23°C from the data at 60°C and at 80°C, the following is obtained via the Larson-Miller relation:

Stress Level Kg/cm^2	Failure Time at:		
	60°C	80°C	23°C
65	5154	-	7.4×10^6
	-	199	7.7×10^6
60	6928	-	1.0×10^7
	-	258	1.0×10^7
55	9555	-	1.5×10^7
	-	341	1.5×10^7

These data are used to establish the brittle region equation at 23°C for the ultra high molecular weight high density ethylene-butene copolymer. Using the method of least squares, this equation is determined to be:

$$h = 14.33731665 - 4.11859644\ F$$

Using this equation, the commencement of brittle failure is predicted to be at a stress level of 129.33 Kg/cm^2 after a time period of 50 years. This is clearly a higher stress level than that predicted by

the ductile region equation and thus a 50 year long-term strength value for this copolymer can be safely predicted by the ductile equation which with a 95% lower confidence limit is 89.84 Kg/cm^2. The complete hoop stress-failure time characteristic for this co-polymer is shown in Figure 5.18.

This value of 89.84 Kg/cm^2 for Phillips polymerised ultra high molecular weight high density ethylene - butene copolymer is 38% higher than that of the Ziegler polymerised high molecular weight high density ethy-lene-butene copolymer and demonstrates the degree of improvement attainable by increasing the weight average molecular weight approximately two-fold.

5.3.3 Ethylene-Hexene Copolymers

Two hexene copolymers of ethylene were studied; the essential difference between them being the molecular weight. The data relating to the medium molecular weight material were determined on both a cadmium pig-mented composition and a carbon black composition. These data were separated to determine whether there was any reinforcing influence derived from the carbon black.

The relevant properties of the two copolymers are:

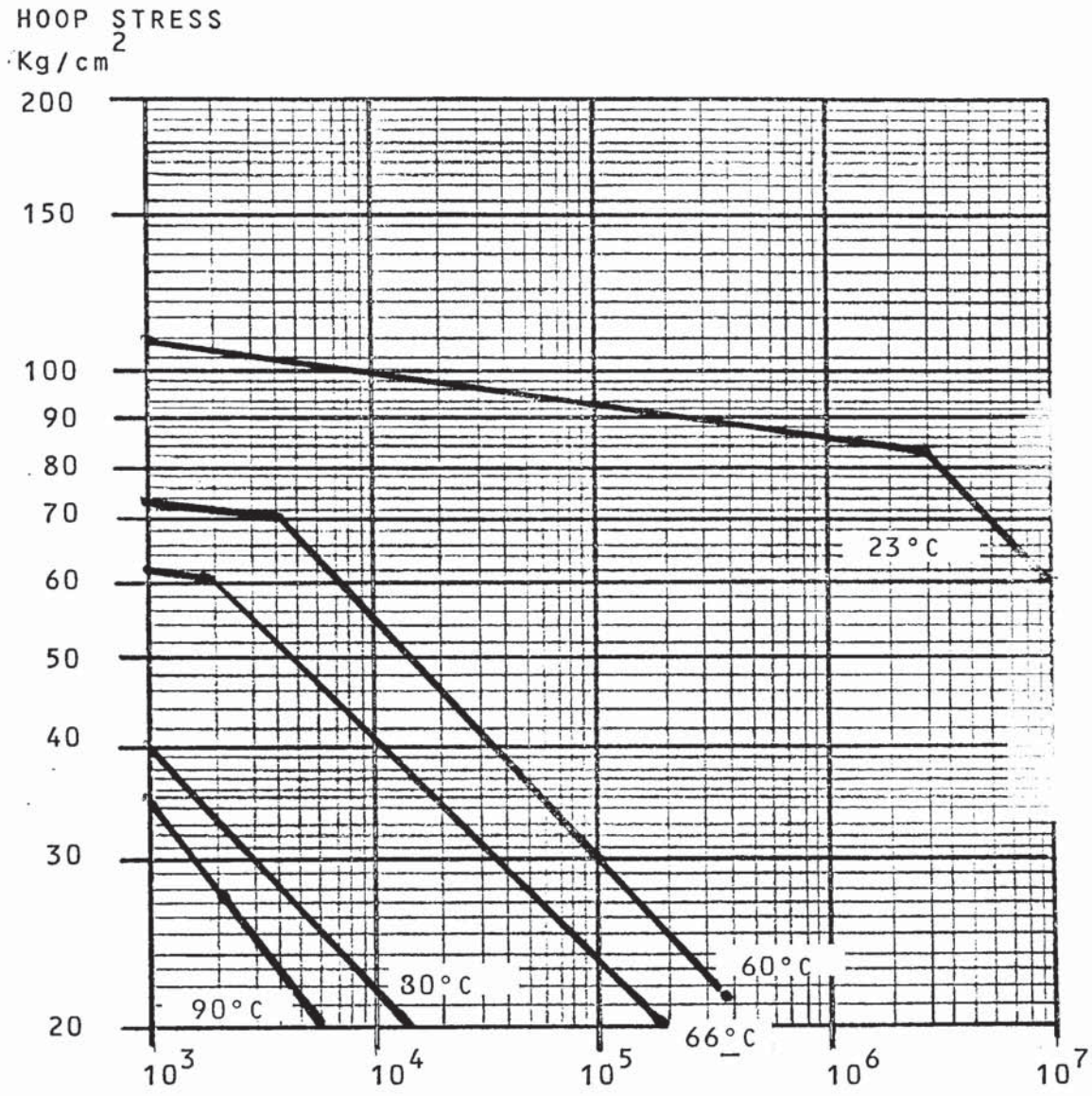

Fig. 5.18 Complete Hoop Stress - Failure Time Characteristic for Phillips Ultra High Molecular Weight Ethylene-Butene Copolymer

		Medium Molecular Weight	Ultra High Molecular Weight
Polymerisation Process		Phillips P.F.	Phillips P.F.
Base Denisty g/cc		0.939	0.943
Melt Index dg/min		0.18	-
High Load M.I. dg/min		-	2.0
Separation Factor:	Pigmented	21.94	-
	Black	23.01	22.25
Extrapolation LTS Kg/cm^2:			
	Pigmented	88.91	-
	Black	93.21	101.95

5.5.3.1 Data on Pigmented Composition Pipe

The hoop stress data on the cadmium pigmented, Phillips P.F. medium, molecular weight ethylene-hexene copolymer, are tabulated in Tables 5.13 to 5.22, together with the computer-dervied data. The respective plots of these data are shown in Figs. 5.19 to 5.23.

In summary, the computer-derived equations are:

Ductile Region

At 23°C $h = (67.72331 - 31.53527\ f) - 0.31031\ t$

At 60°C $h = (91.41214 - 47.60843\ f) - 0.53185\ t$

At 66°C $h = (65.58778 - 33.68402\ f) - 0.35041\ t$

At 80°C $h = (71.94832 - 40.72997\ f) - 0.38261\ t$

At 90°C $h = (63.575265 - 37.633029\ f) - 0.47202\ t$

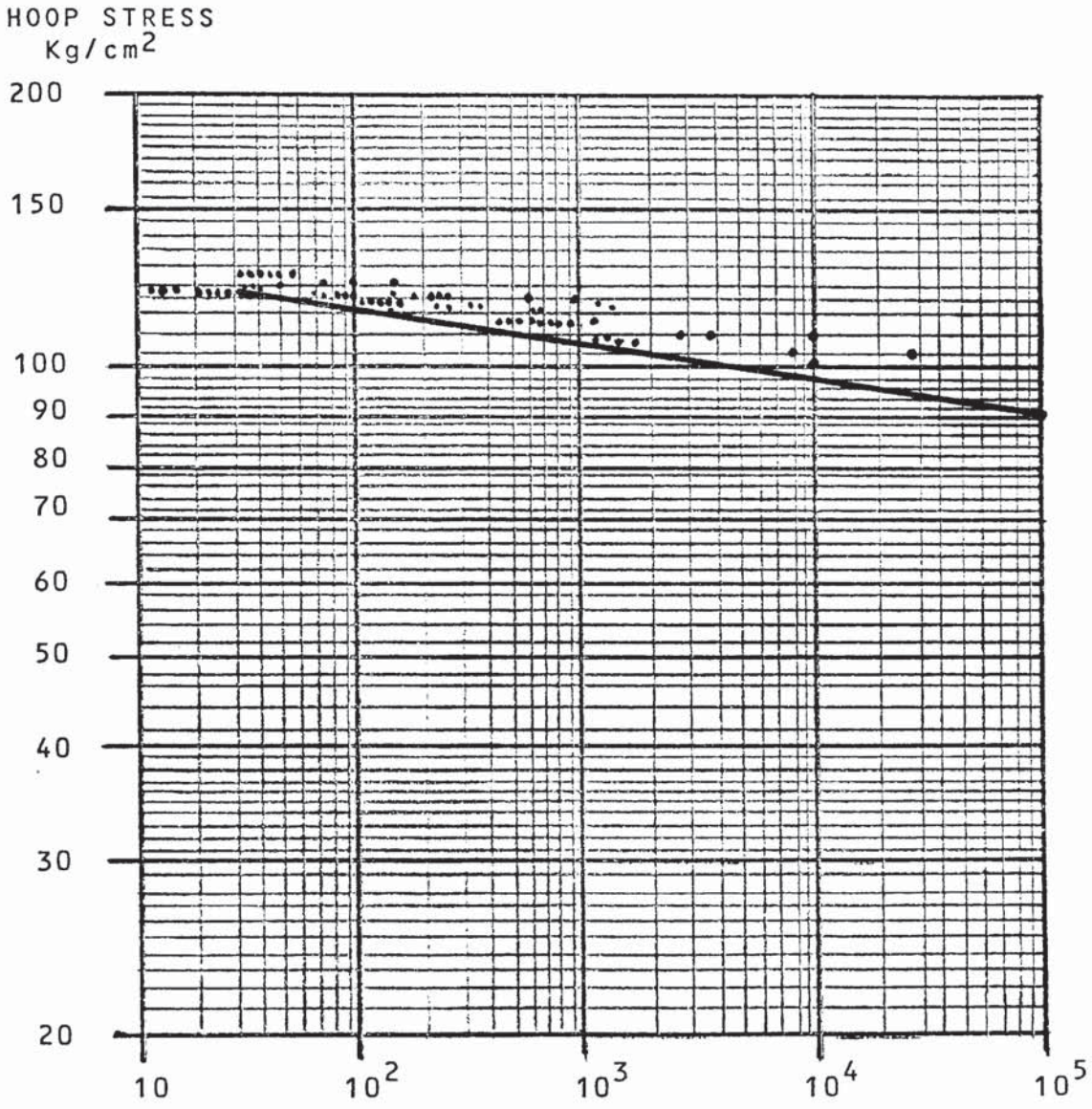

Fig. 5.19 Data Points and 95% LCL Plot for Phillips Pigmented Medium Molecular Weight Ethylene-Hexene Copolymer at 23°C

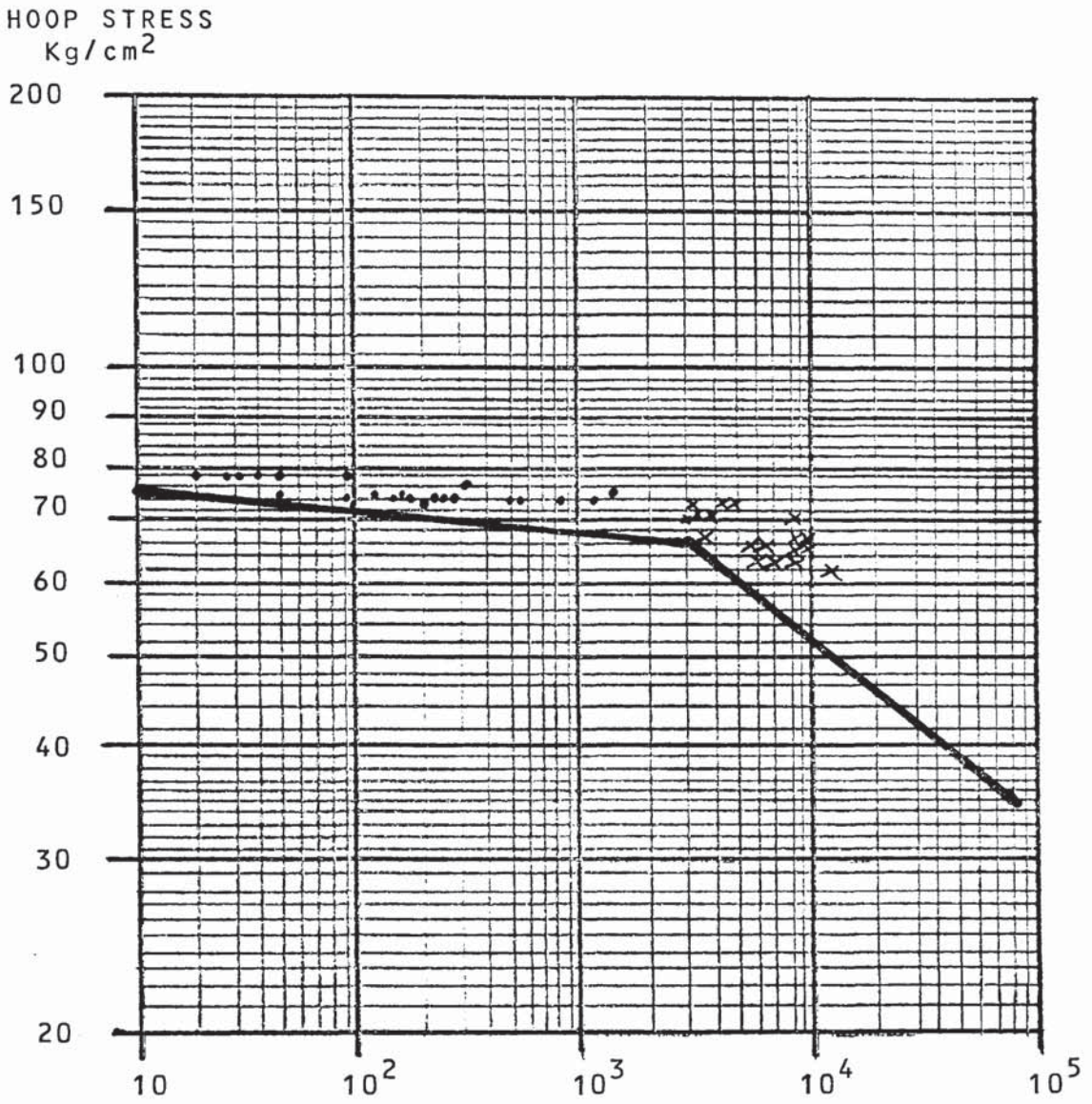

Fig. 5.20 Data Points and 95% LCL Plot for Phillips Pigmented Medium Molecular Weight Ethylene-Hexene Copolymer at 60°C

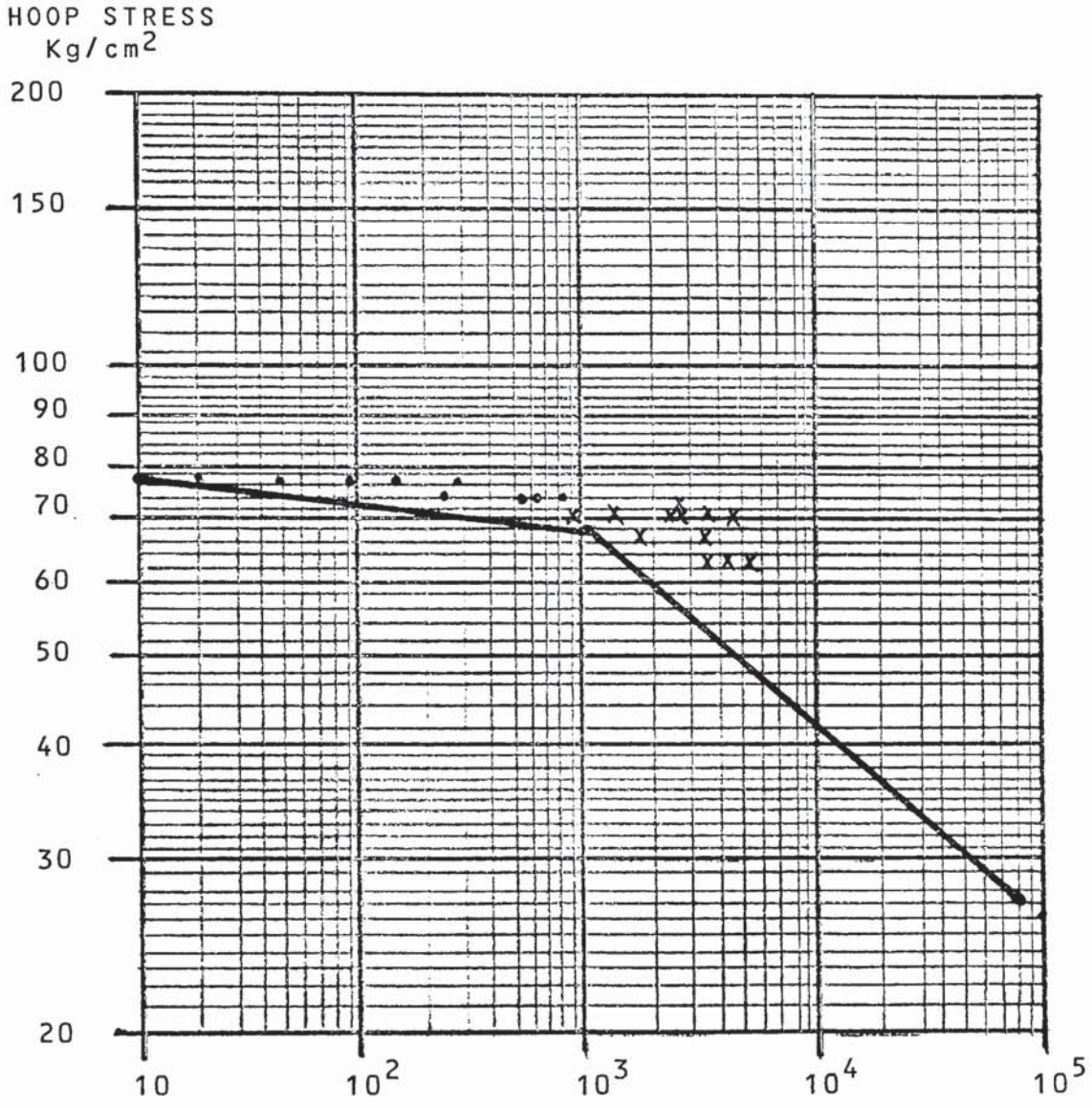

Fig. 5.21 Data Points and 95% LCL Plot for Phillips Pigmented Medium Molecular Weight Ethylene-Hexene Copolymer at 66°C

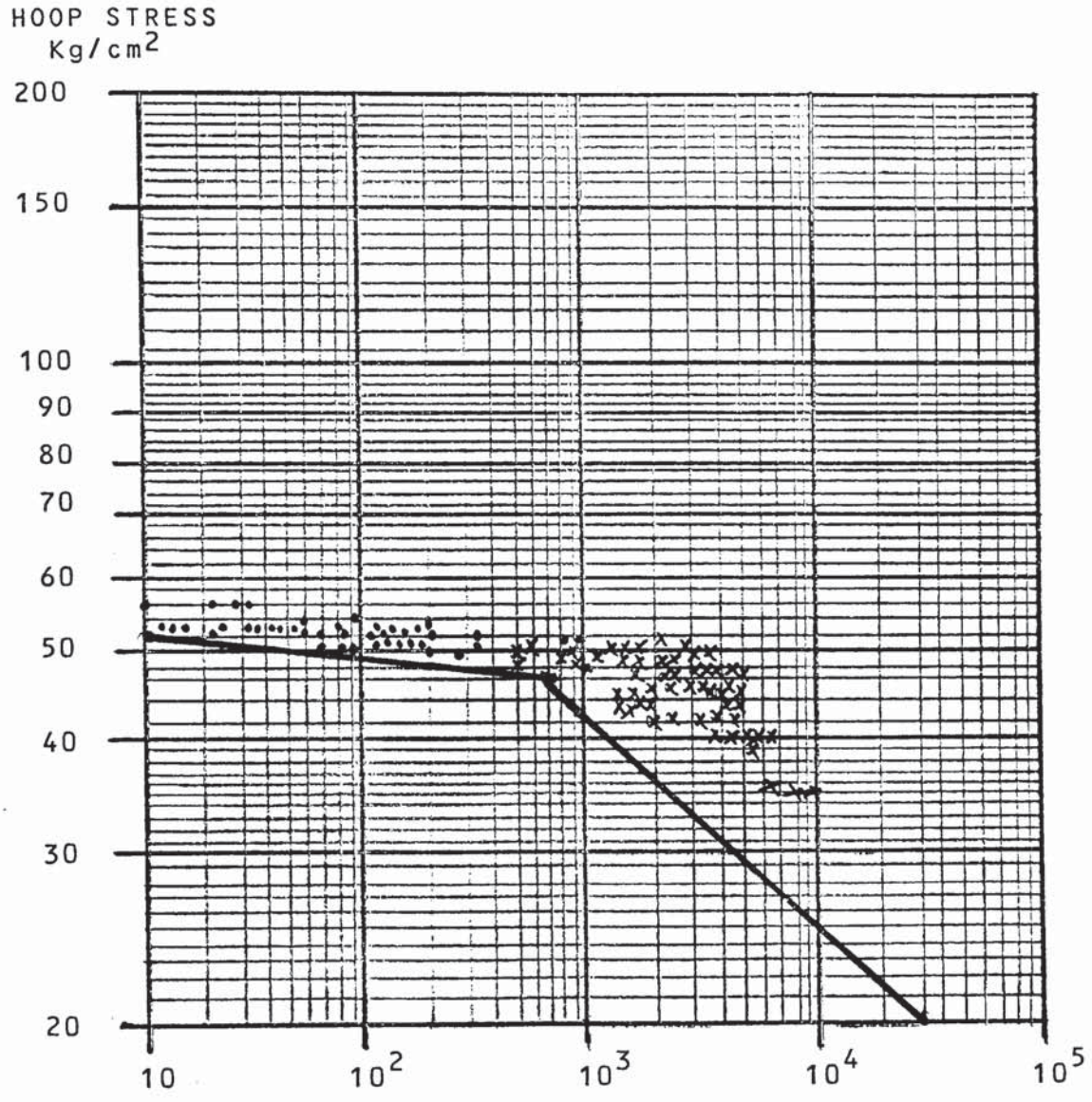

Fig. 5.22 Data Points and 95% LCL Plot for Phillips Pigmented Medium Molecular Weight Ethylene-Hexene Copolymer at 80°C

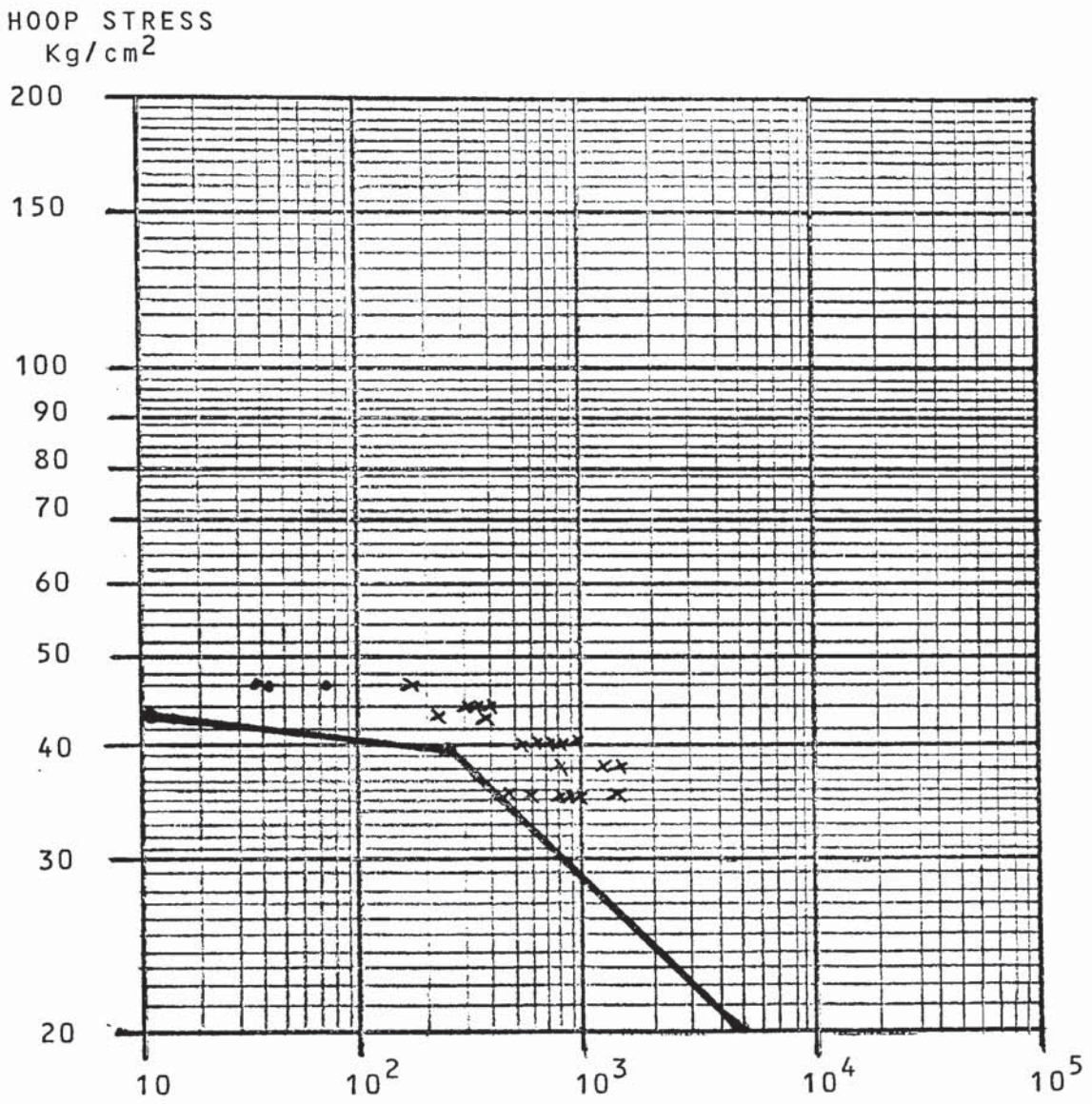

Fig. 5.23 Data Points and 95% LCL Plot for Phillips Pigmented Medium Molecular Weight Ethylene-Hexene Copolymer at 90°C

Brittle Region

At 60°C $h = (13.026467 - 5.061226\ f) - 0.152333\ t$

At 66°C $h = (12.396427 - 4.878645\ f) - 0.206052\ t$

At 80°C $h = (11.321287 - 4.766791\ f) - 0.296432\ t$

At 90°C $h = (10.226699 - 4.658235\ f) - 0.173999\ t$

The brittle region equations were applied to selected stress levels of 65, 40 and 30 Kg/cm^2. These stress levels were chosen on the basis of being representative of the range over which the majority of the test results were obtained. The corresponding time values predicted by these equations are tabulated below:

Stress Level Kg/cm^2	65	40	30
95% LCL Time - hours			
At 60°C	3373	39367	168840
At 66°C	1237	13214	53775
At 80°C	122	1235	4867
At 90°C	26.4	253.4	967.7

At the selected hoop stress level of 65 Kg/cm^2, the relationship between the computer-derived 95% lower confidence limit time values and the different temperature levels, and thus, the separation factor, is:

Temperature Range °C	Calculated Times hours	Factor Derived
90/80	26.4/122	22.05
90/66	26.4/1237	22.19
90/60	26.4/3372.5	21.97

Temperature Range °C	Calculated Times hours	Factor Derived
80/66	122/1237	22.28
80/60	122/3372.5	21.93
66/60	1237/3372.5	21.09

At hoop stress level of 40 Kg/cm^2 the derived factors are:

Temperature Range °C	Calculated Times hours	Factor Derived
90/80	253.4/1235	21.89
90/66	253.4/13214	21.86
90/60	253.4/39367	21.93
80/66	1235/13214	21.84
80/60	1235/39367	21.95
66/60	13214/39367	22.20

At hoop stress level of 30 Kg/cm^2 the derived factors are:

Temperature Range °C	Calculated Times hours	Factor Derived
90/80	967.7/4867	21.79
90/66	967.7/53775	21.67
90/60	967.7/168840	21.91
80/66	4867/53775	21.59
80/60	4867/168840	21.97
66/60	53775/168840	22.86

The factors so derived can be rearranged into the following Table:

Stress level Kg/cm^2	Temperature Range °C					
	90/80	90/66	90/60	80/66	80/60	66/60
70	22.08	22.24	21.97	22.35	21.92	20.92
65	22.05	22.19	21.97	22.28	21.93	21.09
60	22.05	22.14	21.97	22.20	21.93	21.28
55	22.02	22.08	21.95	22.12	21.92	21.47
50	21.97	22.01	21.95	22.04	21.94	21.69
40	21.89	21.86	21.93	21.84	21.95	22.2
35	21.85	21.77	21.92	21.72	21.96	22.51
30	21.79	21.67	21.91	21.59	21.97	22.86

These results show a very close relationship at all temperature ranges except that at 66°C, this latter line converging to the 90°C and 80°C lines and diverging away from the 60°C as stress level is reduced. The 66°C brittle data is suspect in that the least squares analysis is made over only three hoop stress levels.

The average factor determined over the stress level range of 70-30 Kg/cm^2 is 21.936 and if this average factor is used to determine the long-term strength at 23°C from the data at higher temperatures, the following is obtained via the Larson-Miller relation.

Predicted Failure 23°C	At stress level of 65 kg/cm^2	40 Kg/cm	30 Kg/cm^2
from 90°C	5.081×10^6	8.135×10^7	4.207×10^8
80°C	5.128×10^6	8.105×10^7	4.159×10^8
66°C	5.326×10^6	8.025×10^7	4.004×10^8
60°C	5.122×10^6	8.125×10^7	4.180×10^8

These data are used to establish the brittle region equation at 23°C for the cadmium pigmented medium molecular weight ethylene-hexene copolymer which is:

$$h = 16.990988 - 5.669356\ f$$

This equation predicts the commencement of brittle failures at 50 years to be at a stress level of 100.44 Kg/cm^2. This value is clearly in excess of the ductile strength of the material of 88.91 Kg/cm^2 given by the ductile region equation. This copolymer can therefore withstand a 50-year long-term strength, without exhibiting brittle failure. The complete hoop stress-failure time characteristic for this copolymer is shown in Fig. 5.24.

5.5.3.2 Data on Black Composition Pipe

The hoop stress data on the carbon black composition of Phillips P.F. medium molecular weight ethylene-hexene copolymer are tabulated in Tables 5.23 to 5.30 together with the computer derived data. The respective plots of these data are shown in Figs. 5.25 to 5.28. In summary the computer-derived equations are:

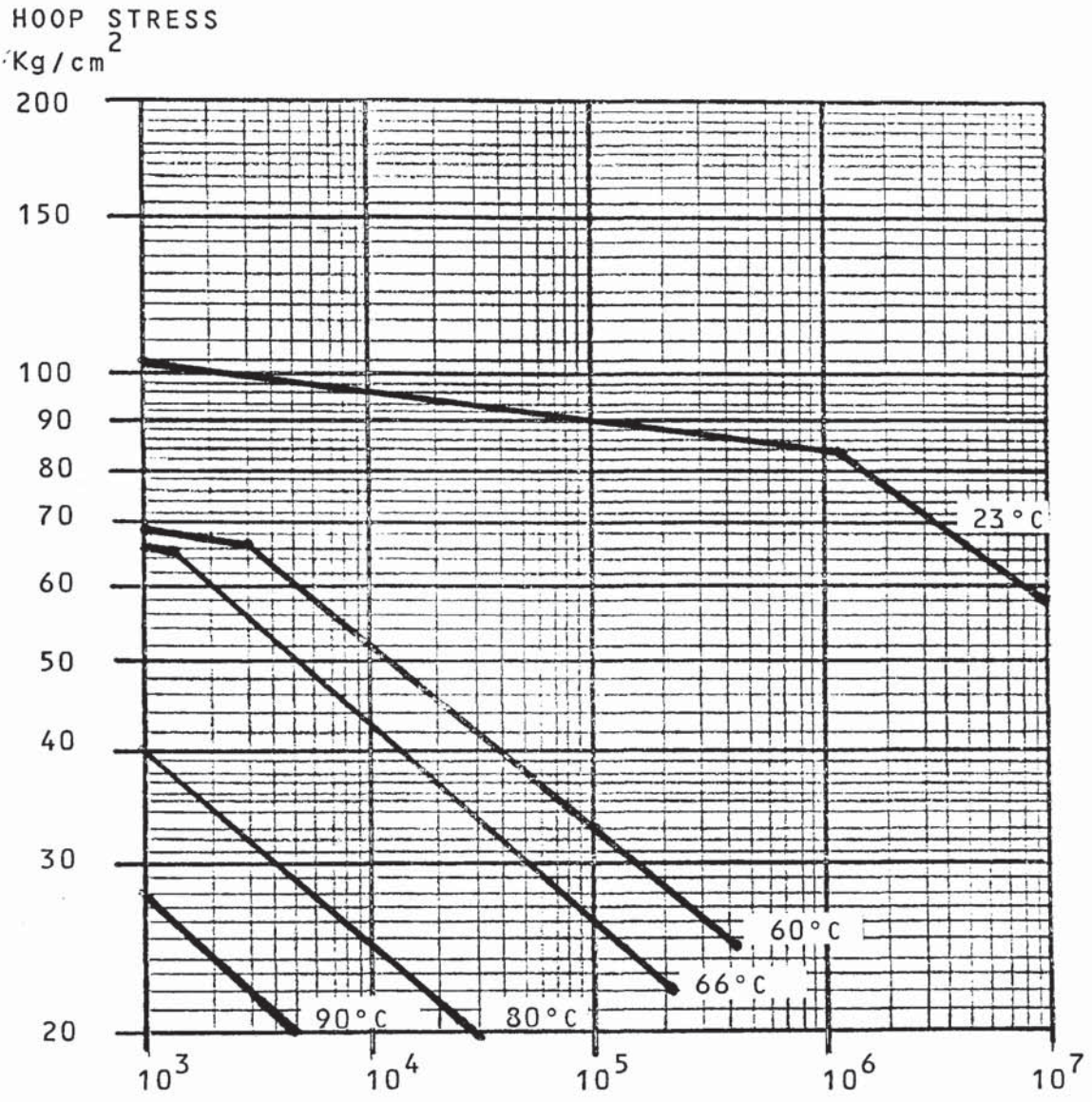

Fig. 5.24 Complete Hoop Stress - Failure Time Characteristic for Phillips Pigmented Medium Molecular Weight Ethylene-Hexene Copolymer

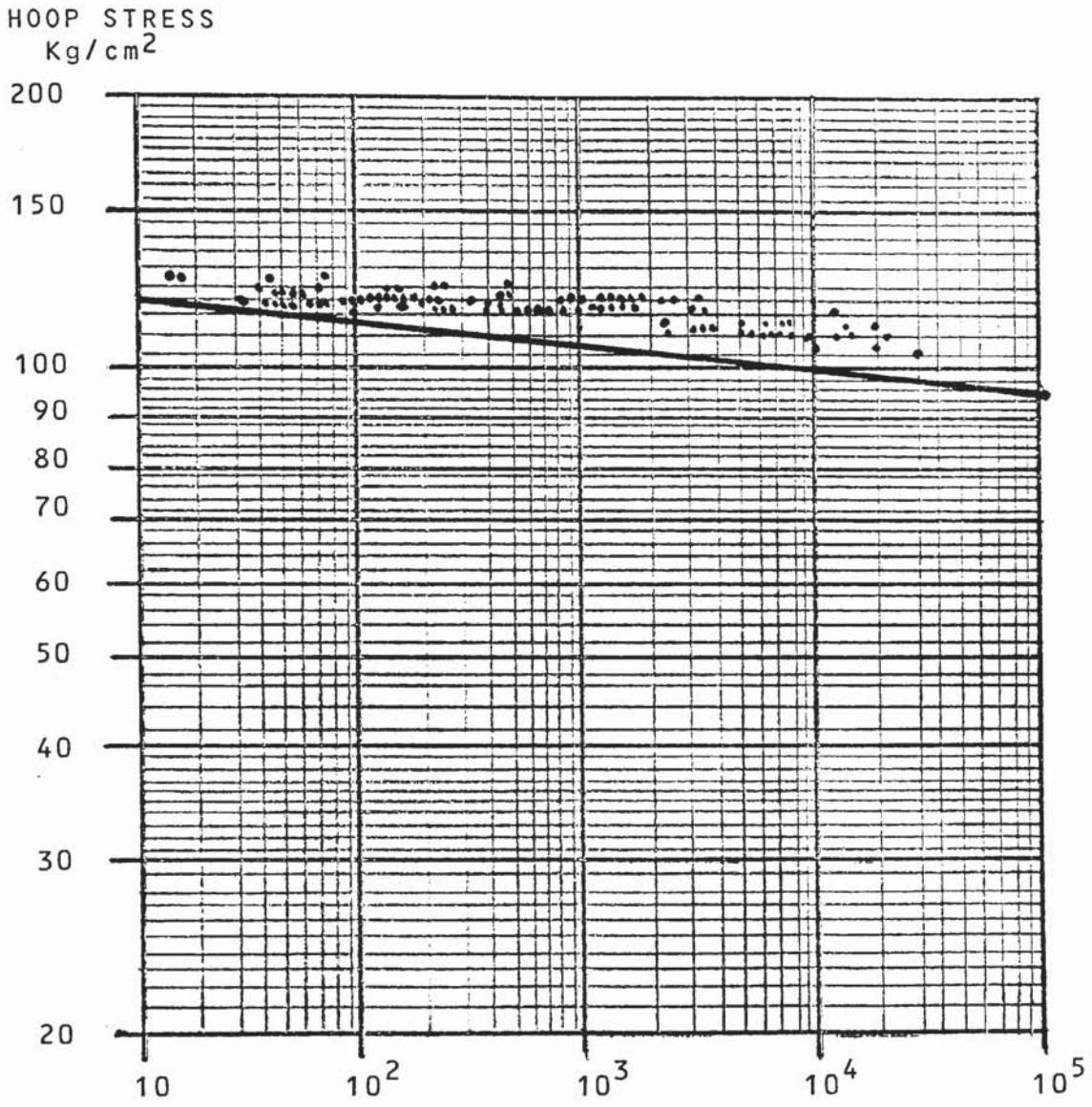

Fig. 5.25 Data Points and 95% LCL Plot for Phillips Black Medium Molecular Weight Ethylene-Hexene Copolymer at 23°C

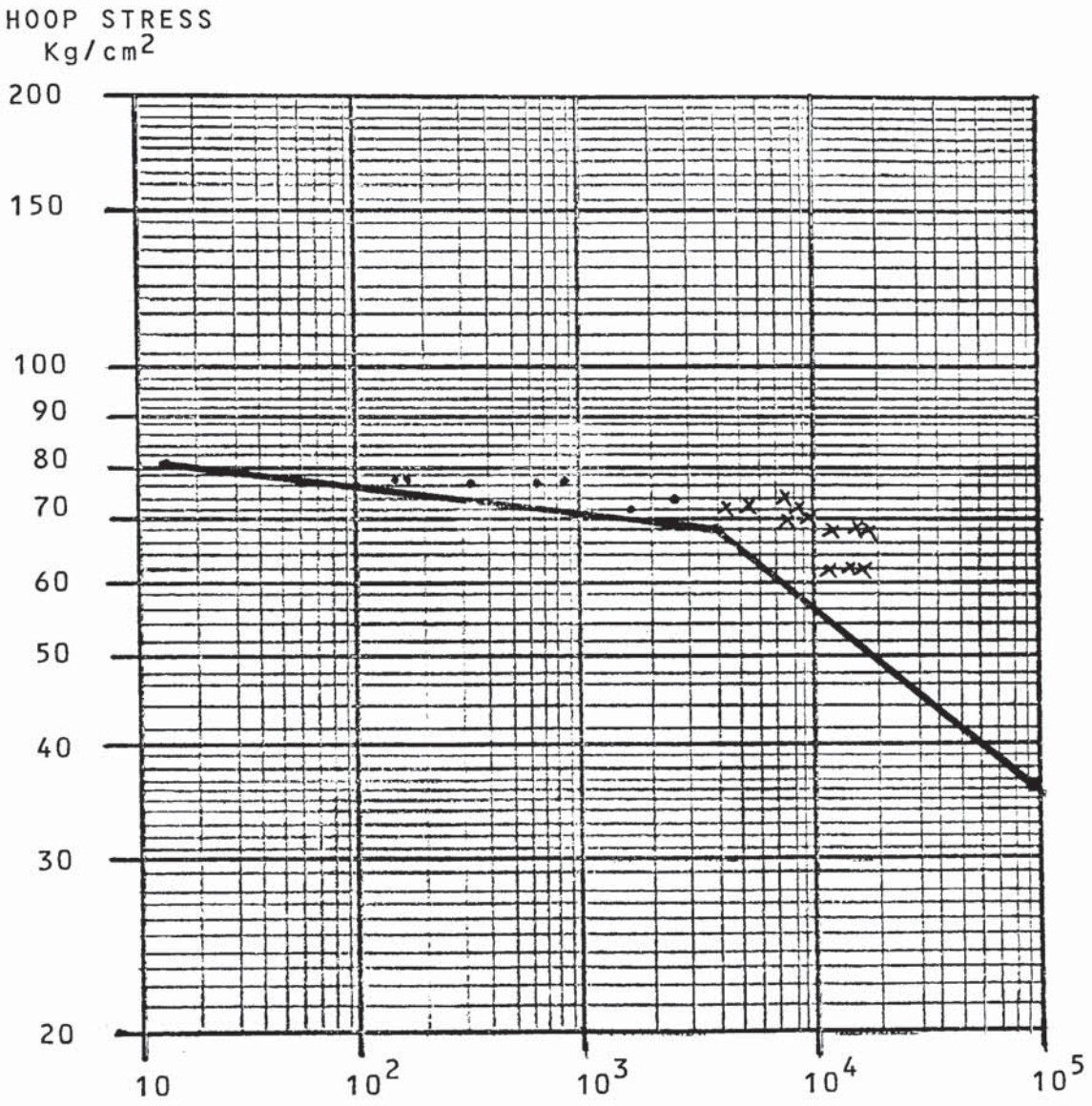

Fig. 5.26 Data Points and 95% LCL Plot for Phillips Black Medium Molecular Weight Ethylene-Hexene Copolymer at 60°C

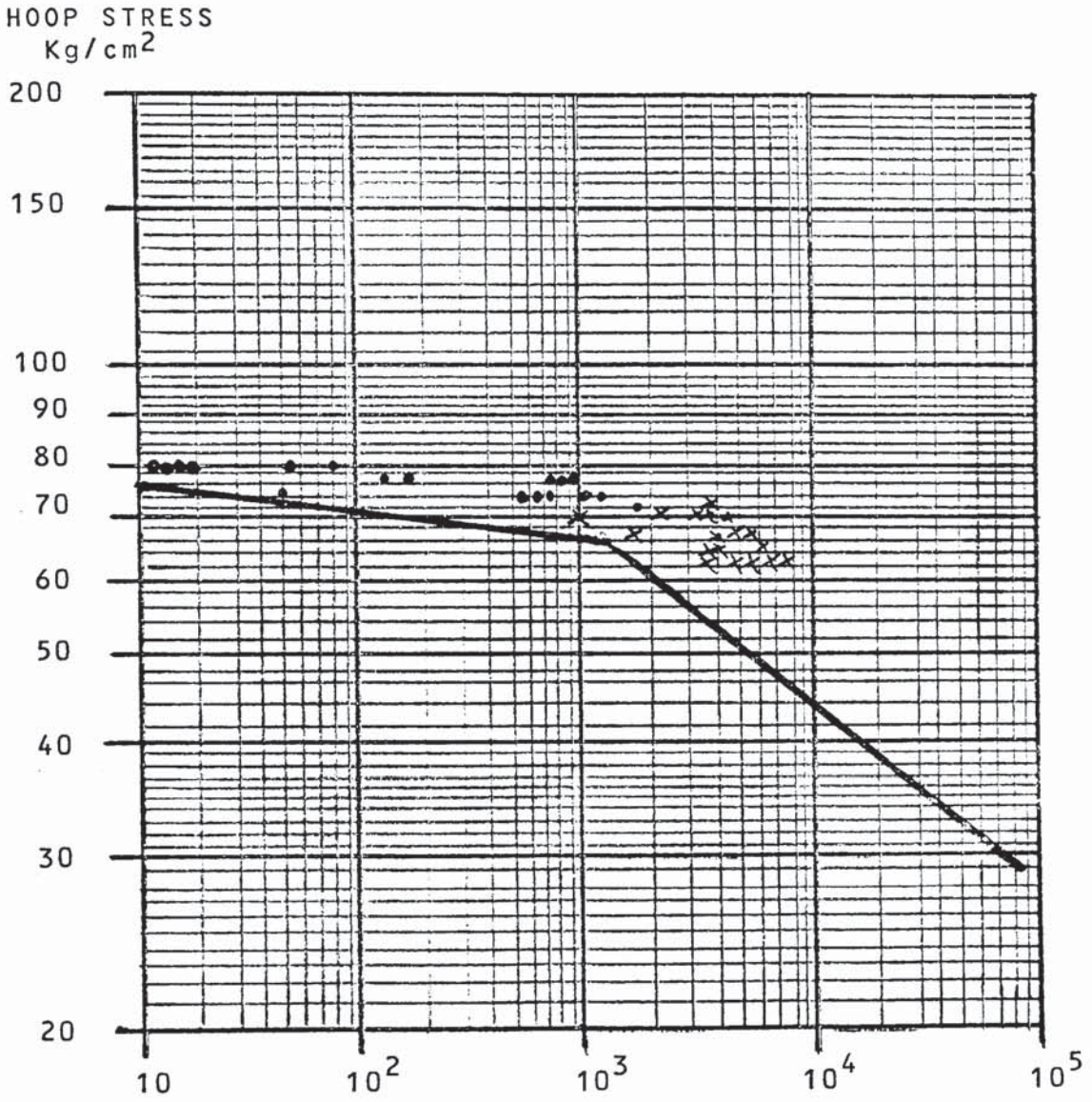

Fig. 5.27 Data Points and 95% LCL Plot for Phillips Black Medium Molecular Weight Ethylene-Hexene Copolymer at 66°C

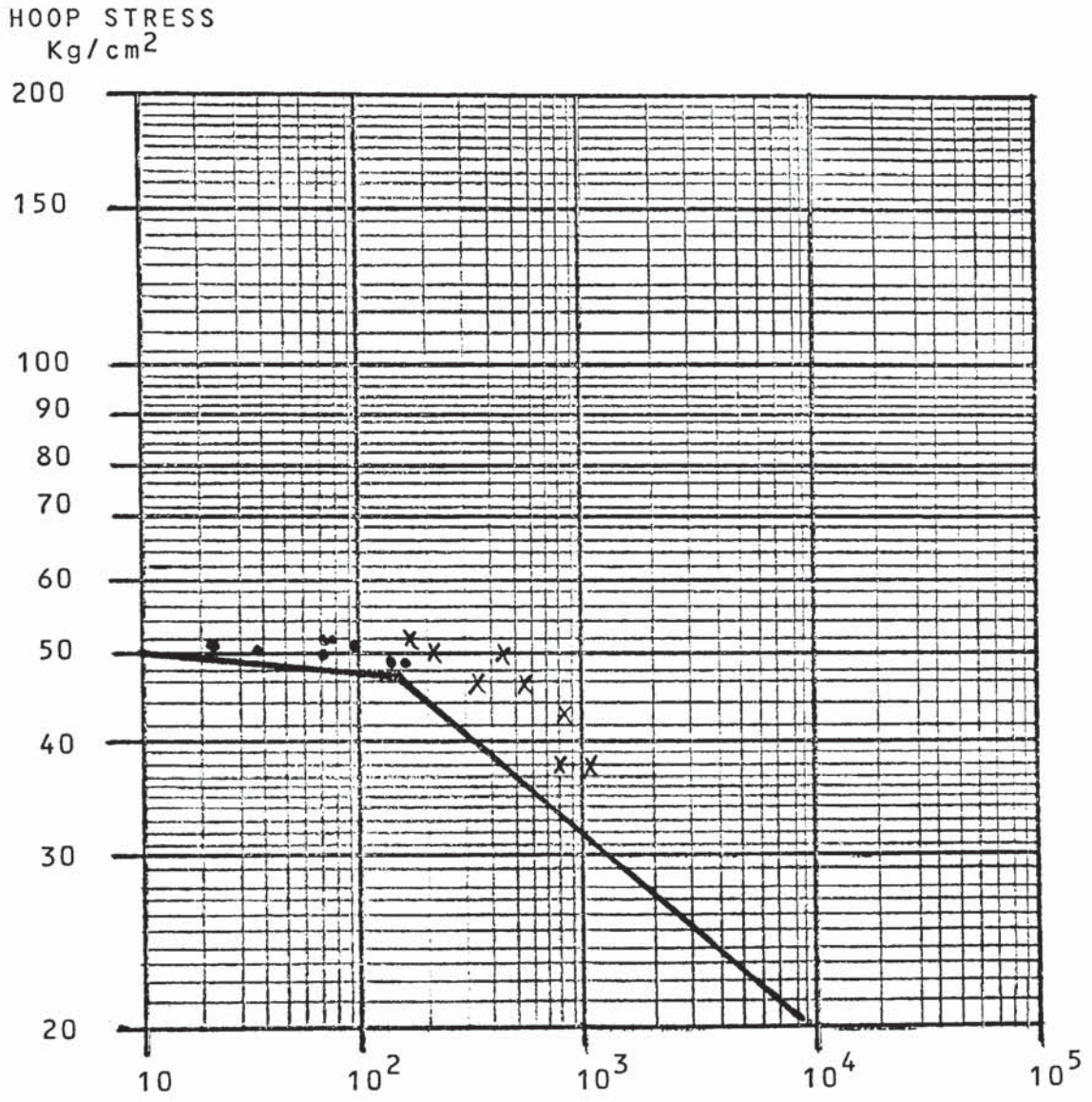

Fig. 5.28 Data Points and 95% LCL Plot for Phillips Black Medium Molecular Weight Ethylene-Hexene Copolymer at 90°C

Ductile Region

At 23°C $h = (80.94541 - 37.72841\ f) - 0.49920\ t$

At 60°C $h = (77.882764 - 40.023868\ f) - 0.240224\ t$

At 66°C $h = (86.623272 - 44.754418\ f) - 0.46945\ t$

At 90°C $h = (83.379466 - 47.947452\ f) - 0.385790\ t$

Brittle Region

At 60°C $h = (13.459515 - 5.164243\ f) - 0.171376\ t$

At 66°C $h = (12.580251 - 4.925057\ f) - 0.199785\ t$

At 90°C $h = (10.385556 - 4.671149\ f) - 0.153737\ t$

As in the previous sections, the brittle region equations were applied to selected levels of 65, 40 and 30 Kg/cm^2. The corresponding time values predicted by these equations are tabulated below:

95% LCL Time	Stress level Kg/cm^2		
hours	65	40	40
At 60°C	5188	63667	281210
At 66°C	1698	18555	76524
At 90°C	36.48	352	1351

At the selected hoop stress level of 65 Kg/cm^2, the relationship between the computer-dervied 95% lower confidence limit time values and the different temperature levels, and thus the separation factor, is:

Temp. Range °C	Calaculated Time (hrs)	Factor Derived
90/66	36.5/1698	22.00
90/60	36.5/5188	22.34
66/60	1698/5188	23.69

At hoop stress level of 40 Kg/cm^2, the derived factors are:

Temperature Range °C	Calculated Times hours	Factor Derived
90/66	352/18555	21.78
90/60	352/63667	22.56
66/60	18555/63667	25.45

At hoop stress level of 30 Kg/cm^2, the derived factors are:

Temp. Range °C	Calculated Times (hrs)	Factor Derived
90/66	1351/76524	21.63
90/60	1351/28210	22.60
66/60	76524/28210	26.49

The factors so derived can be rearranged into the following Table:

Stress level Kg/cm^2	Temperature Range °C		
	90/66	90/60	66/60
70	22.03	22.31	23.42
65	22.00	22.34	23.69
60	21.96	22.37	23.98
55	21.92	22.39	24.29
50	21.89	22.44	24.64
40	21.78	22.51	25.45
35	21.71	22.56	25.93
30	21.63	22.60	26.49

The relationships between the high temperature data for the black compounded pipe are less consistent than those for the cadmium pigmented samples. A large part of the reason must lie with the fact that the number of sample failures included in the regression analysis at each of the three temperatures were less than that recommended by the evaluation procedure.

The average time to failure was consistently significantly longer for the black composition compared to the cadmium pigmented, Irganox stablised pipe and on this point alone some doubt must be cast on the validity of European gas pipe specifications, notably those of the United Kingdom and the Netherlands (128) which stipulate the use of yellow coloured pipe and fittings.

The average factor determined over the stress level range of 70 - 30 Kg/cm^2 is 23.013 and if this average factor is used to determine the long term pipe strength at 23°C from the data at higher temperatures then the following is obtained:

		At Stress Level of		
Predicted 23°C Failure		70 Kg/cm^2	65 Kg/cm^2	60 Kg/cm^2
From	90°C	8.712×10^6	1.349×10^7	2.106×10^7
	66°C	7.258×10^6	1.102×10^7	1.732×10^7
	60°C	7.397×10^6	1.138×10^7	1.812×10^7

Using these data, the brittle region equation at 23°C

for the black composition of the medium molecular weight high density ethylene-hexene copolymer can be determined as:

$$h = 17.455865 - 5.726116\ f$$

This equation predicts the onset of brittle fracture at a stress level of 115.68 Kg/cm^2 at 4.38×10^5 hours (50 years). This stress level is higher than the 95% lower confidence failure stress of 93.21 Kg/cm^2, predicted by the 23°C ductile equation, and there is therefore a 95% confidence that within the 50-year time period, no brittle failures will occur at 23°C. The complete hoop stress-failure time characteristic for this copolymer is shown in Fig. 5.29.

5.3.3.3 Ultra High Molecular Weight Data

The hoop stress data on the carbon black composition of Phillips P.F. ultra high molecular weight ethylene-hexene copolymer are tabulated in Tables 5.31 to 5.36 together with the computer-derived data. The respective plots of these data are shown in Figs 5.30 to 5.32.

In summary the computer-derived equations from these data are:

Ductile Region:

At 23°C $h = (58.16346 - 26.53109\ f) - 0.38828\ t$
At 60°C $h = (1.92068 - 0.01231\ f) - 0.00277\ t$
At 80°C $h = (90.062900 - 48.67031\ f) - 0.712147\ t$

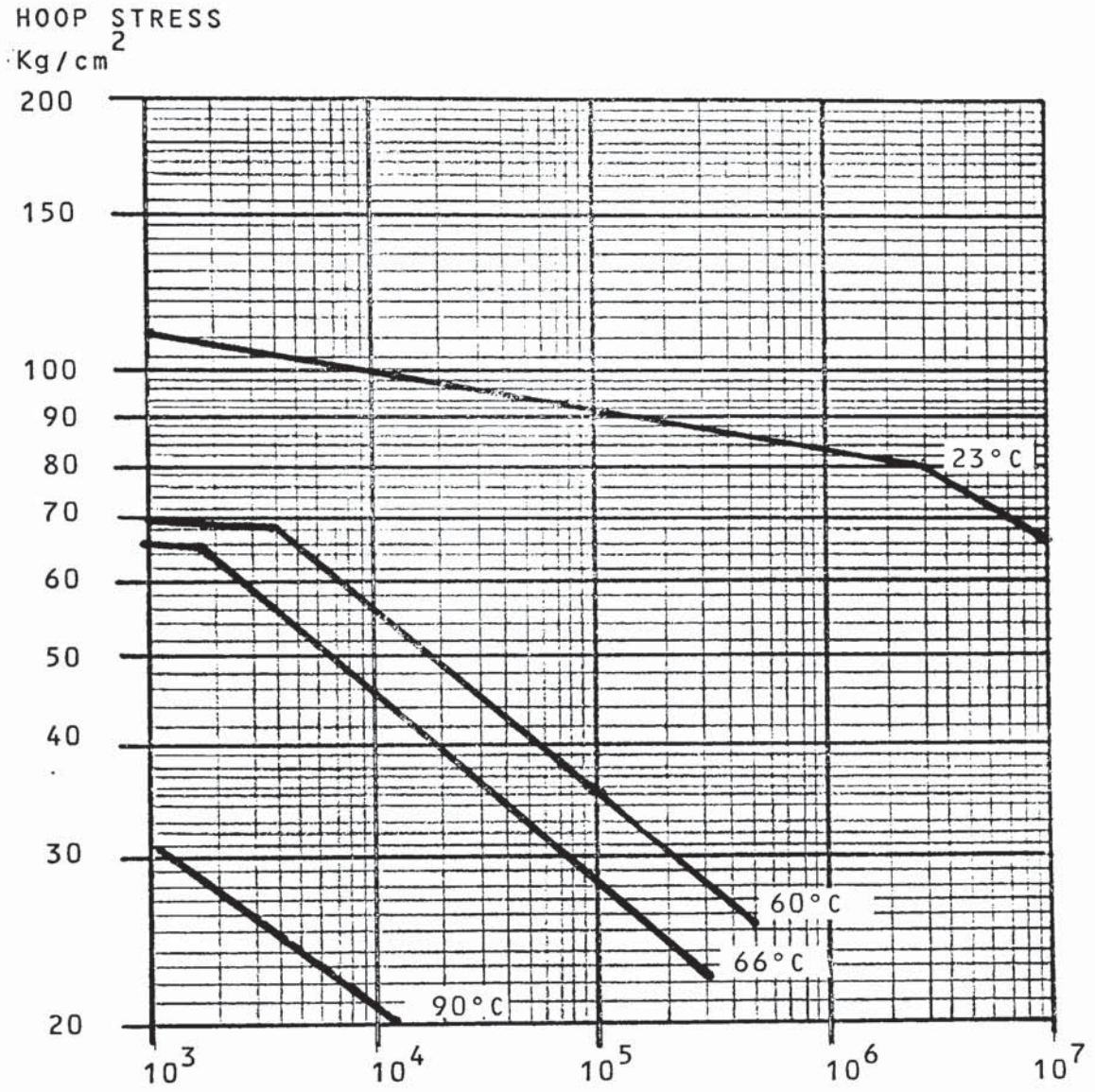

Fig. 5.29 Complete Hoop Stress - Failure Time Characteristic for Phillips Black Medium Molecular Weight Ethylene-Hexene Copolymer

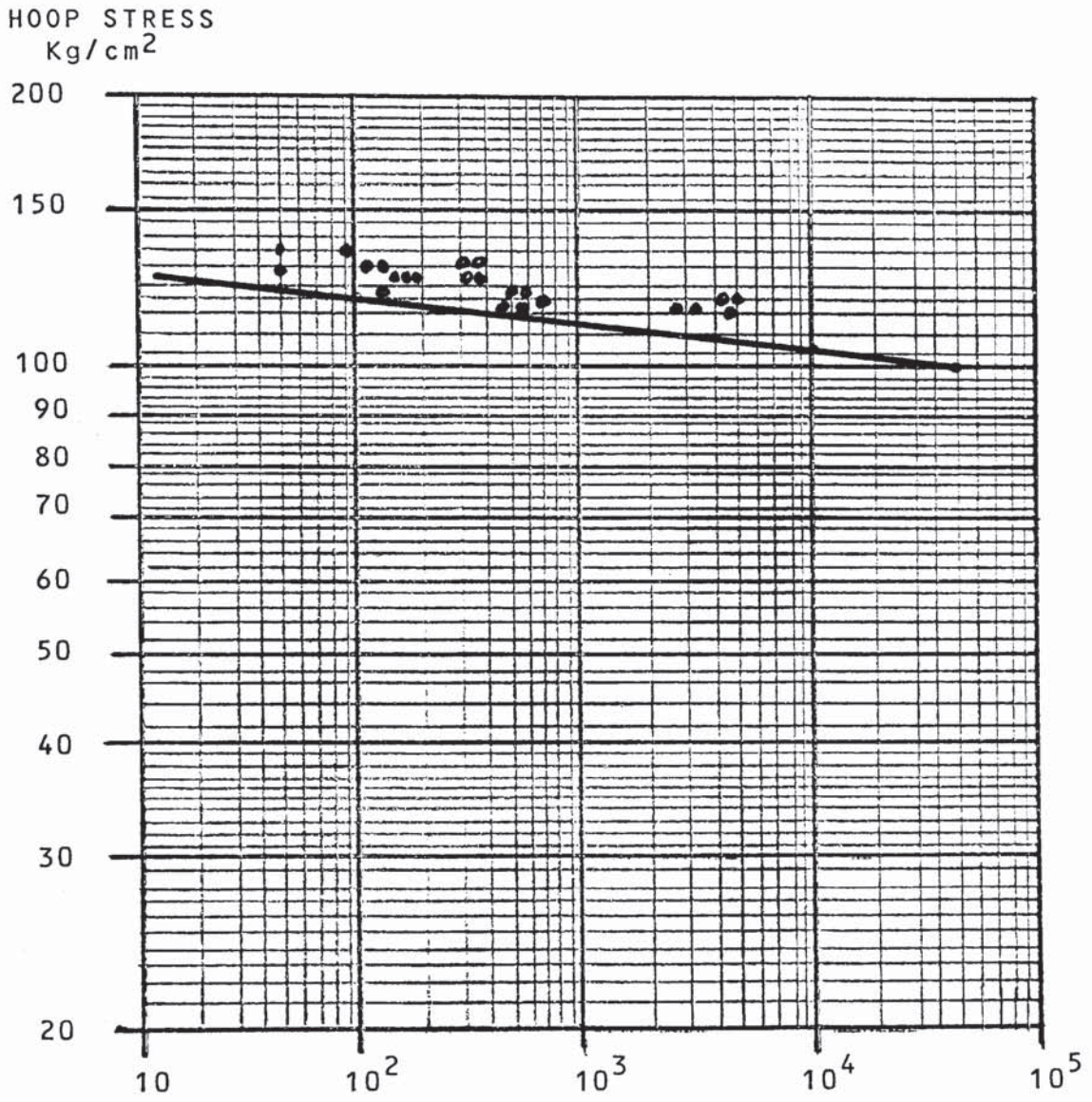

Fig. 5.30 Data Points and 95% LCL Plot for Phillips Ultra High Molecular Weight Ethylene-Hexene Copolymer at 23°C

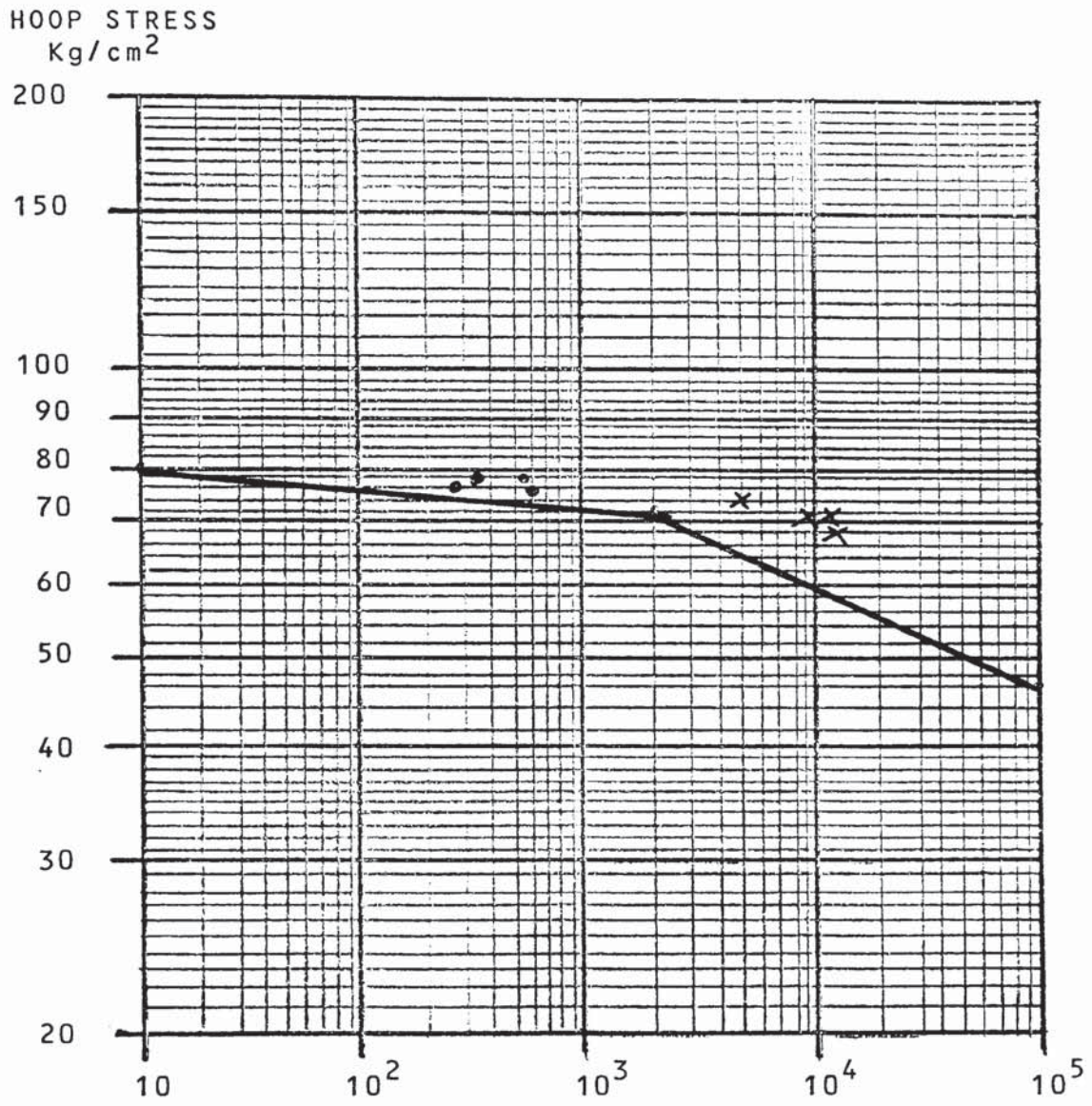

Fig. 5.31 Data Points and 95% LCL Plot for Phillips Ultra High Molecular Weight Ethylene-Hexene Copolymer at 60°C

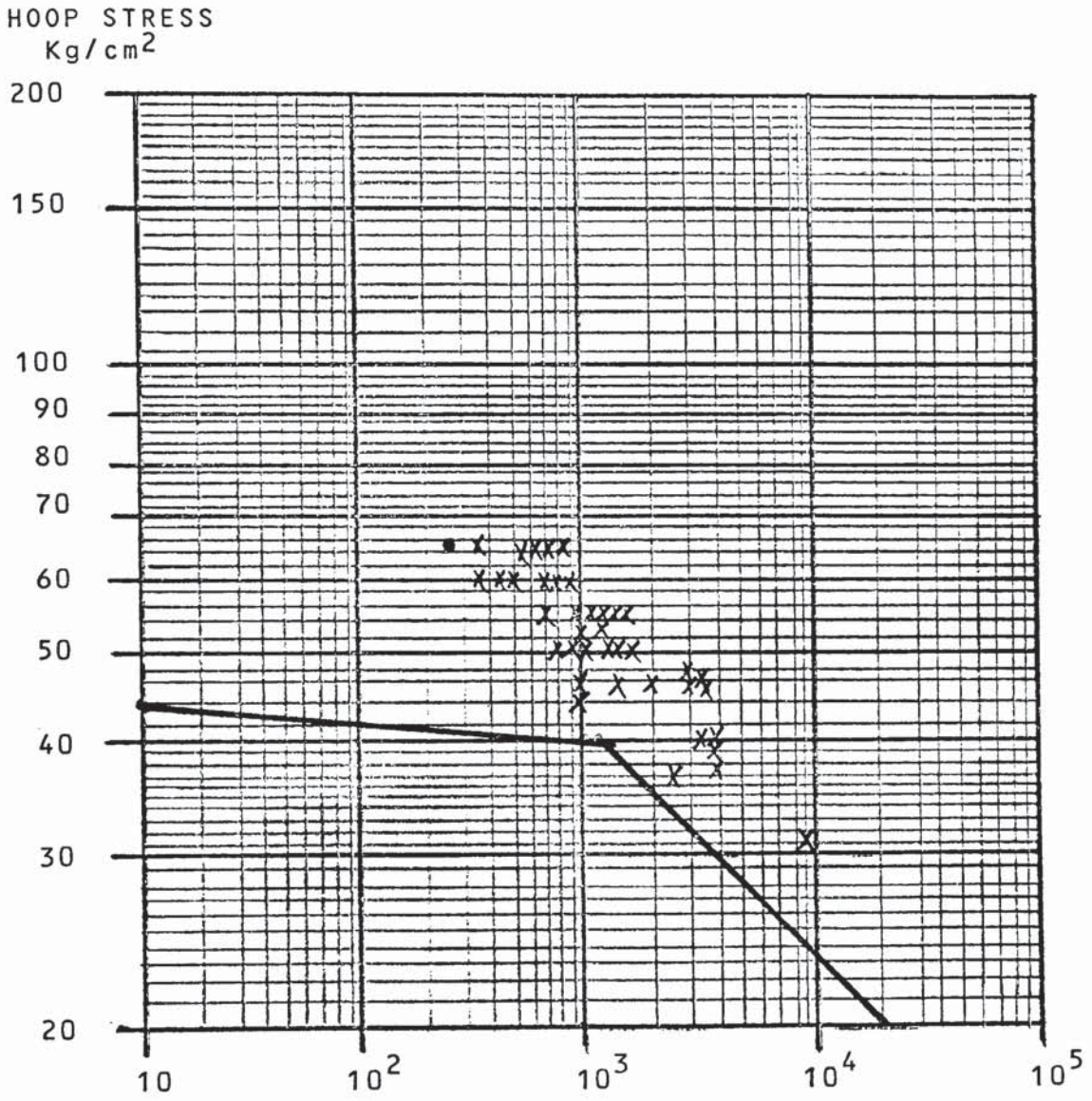

Fig. 5.32 Data Points and 95% LCL Plot for Phillips Ultra High Molecular Weight Ethylene-Hexene Copolymer at 80°C

Brittle Region

At 60°C $h = (20.843373 - 0.150033\ f) - 0.13050\ t$

At 80°C $h = (9.389510 - 3.669072\ f) - 0.166017\ t$

The brittle region equations were applied to selected stress levels of 65, 60 and 55 Kg/cm^2 respectively, as being representative of the range over which the majority of the test results were obtained. The corresponding time values calculated from these equations are tabulated below:

95% LCL Time hours	Stress Level Kg/cm^2		
	65	60	55
At 80°C	252	338	466
At 60°C	4943	10282	22795

At the three hoop stress levels, the relationship between the computer-derived time values and the two different temperature levels 80°C and 60°C is:

Stress Level	Calculated Time	Factor Derived
65 Kg/cm^2	252/4943	19.12
60 Kg/cm^2	338/10282	22.17
55 Kg/cm^2	466/22795	25.46

It is submitted that the variation in the derived factor is due entirely to the very small number of brittle failures obtained at 60°C and thus included in the regression analysis.

The average factor derived over these three stress levels is 22.25 and if this factor is used to determine the long term strength at 23°C from the data at 60°C and 80°C, the following is obtained:

Stress Level Kg/cm^2	Failure Time at		
	60°C	80°C	23°C
65	4943	-	8.65×10^6
	-	252	1.41×10^7
60	10282	-	1.97×10^7
	-	338	1.99×10^7
55	22795	-	4.38×10^7
	-	446	2.78×10^7

These data are used to establish the brittle equation at 23°C for the ultra high molecular weight high density ethylene-hexene copolymer. Using the method of least squares, this equation is determined to be:

$$h = 20.057566 - 7.177989\ f$$

Using this equation, the commencement of brittle failure is predicted to be at a stress level of 101.95 Kg/cm^2, after a time period of 50 years. This is a lower stress level than predicted by the ductile region, which predicts a stress value of 102.31 Kg/cm^2. The performance of this polymer at 23°C is thus described by both equations. However, the brittle equation at

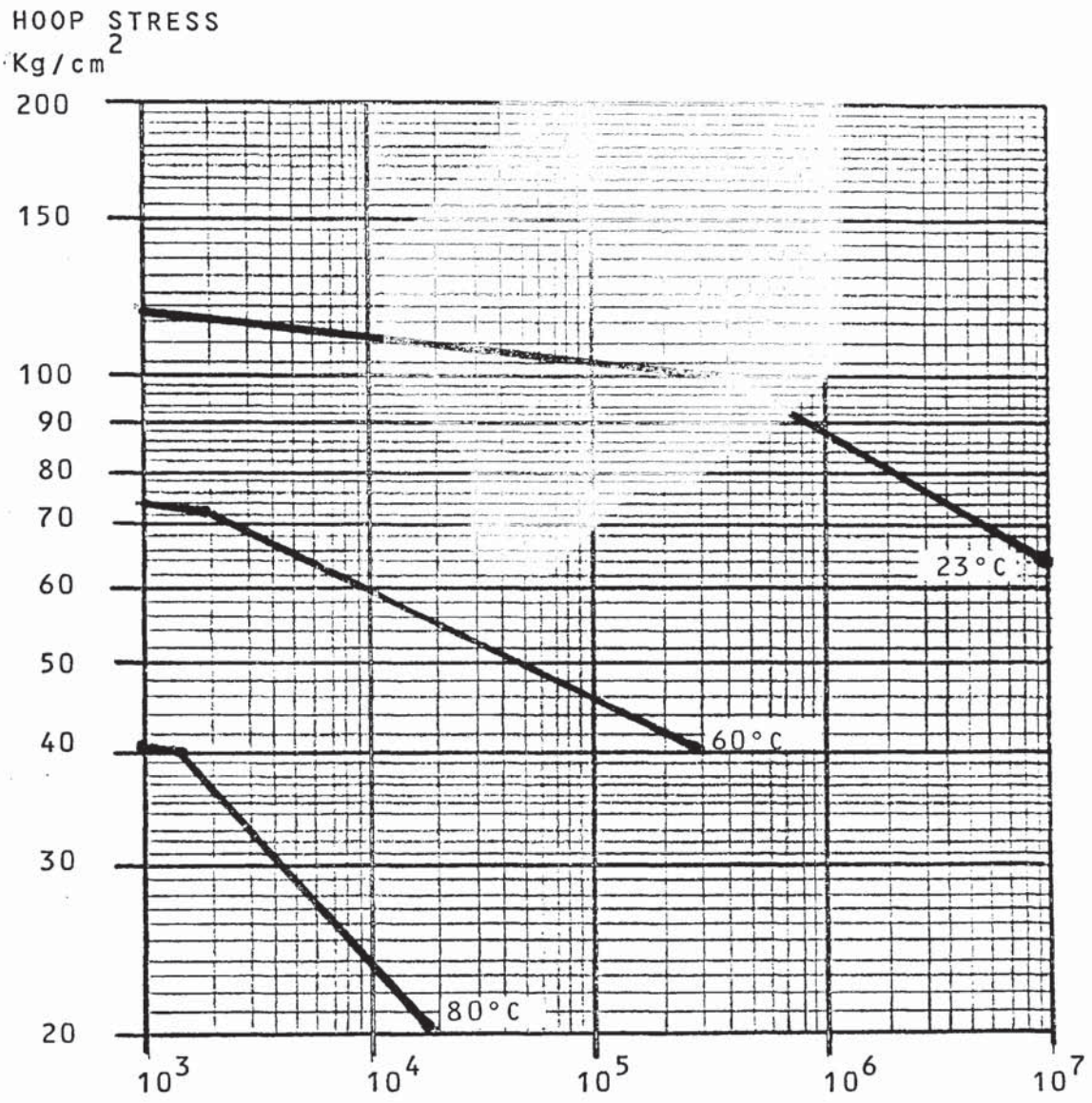

Fig. 5.33 Complete Hoop Stress - Failure Time Characteristic for Phillips Ultra High Molecular Weight Ethylene-Hexene Copolymer

23°C is derived somewhat conservatively and in view of the performance of the ultra high molecular weight ethylene-butene copolymer, a 50-year long-term stress value greater than 130 Kg/cm^2 would have to be expected.

The complete hoop stress-failure time characteristic for this copolymer is shown in Fig. 5.33

TABLE 5.1 Data Points for Ziegler High Molecular Weight Ethylene-Butene Copolymer at 80°C

Hoop Stress Kg/cm^2	Failure Times - hours	
	Ductile	Brittle
70.8	0.4 - 0.7	-
70.5	0.5 - 1.7	-
70.2	1.8 - 4	-
70.0	0.5	-
69.7	0.2 - 0.8	-
69.5	1.5	-
69.2	0.3 - 4.1	-
66.7	12	-
66.4	3 - 12 - 16	25
66.0	1.3 - 2.1 - 3.1 - 4.8	-
65.7	8 - 9	-
63.8	10 - 13	-
63.5	-	71 - 74
63.3	-	71
63.0	-	57 - 65

TABLE 5.1 Cont'd

Hoop Stress Kg/cm^2	Failure Time - hours	
	Ductile	Brittle
62.9	-	54
62.5	-	71
57.5	-	43
57.3	-	58 - 61
57.0	-	88 - 95
56.5	-	52 - 70 - 94
56.2	-	55
52.0	-	165 - 179 - 208
51.8	-	162 - 207 - 215
51.6	-	141 - 152
51.4	-	81
51.2	-	77 - 91
50.0	-	75
49.5	-	96
48.8	-	121 - 264
48.6	-	85 - 115 - 183
48.4	-	42 - 106
48.2	-	418 - 478
47.9	-	65 - 166
41.4	-	601
40.9	-	226 - 1181
40.8	-	189
40.6	-	312 - 534
40.5	-	206

TABLE 5.1 Cont'd

Hoop Stress Kg/cm^2	Failure Time - hours	
	Ductile	Brittle
40.2	-	1243
40.0	-	177 - 537
39.9	-	585
39.0	-	135 - 195
31.0	-	1060
30.8	-	1140
30.3	-	377 - 591 - 955
30.2	-	954
30.0	-	490 - 529 - 545
29.9	-	785
29.8	-	631 - 858
29.6	-	535
29.7	-	506

TABLE 5.2 Computer-Derived Data from Table 5.1

	Ductile Region	Brittle Region
Sh	= 8.857455	= 151.94415
$(Sh)^2$	= 78.454510	= 23087.02573
Sh^2	= 10.894541	= 353.87134
Sfh	: 16.076919	= 249.539185
H	= 0.369061	= 2.23447
Sf	= 43.955146	= 112.953083
$(Sf)^2$	= 1932.054838	= 12758.39886
Sf^2	= 80.507421	= 188.379586
F	= 1.831464	= 1.661074
N	= 24	= 68
U	= 0.005136	= 0.756073
W	= -0.145195	=-2.8514104
V	= 7.625603	= 15.356257
a	= 52.146926	= 8.49895
b	= -28.271292	=-3.77134
$/\overline{s}$	= 0.400043	= 0.264077

TABLE 5.3 Data Points for Phillips Ultra High Molecular Weight Ethylene-Butene Copolymer at 23°C

Hoop Stress Kg/cm^2	Failure Time - hours
130.0	26 - 27 - 28
126.6	312 - 384
123.7	112 - 136 - 186 - 208
120.9	189 - 217 - 281
120.2	859 - 929 - 953
119.5	552 - 1320
117.8	674 - 1053
117	1151 - 1173 - 1337 - 1364
116.7	504 - 1584
114.6	1101
113.8	1313 - 1407 - 1459 - 1512
112.8	7248 - >11,500
111.4	3120
110.4	2350 - 2536 - 2638 - 2800 - 2881
109.0	3240 - 4632 - 15,064
108.3	35,768 - 36,500 - 39,768
106.2	> 11,500
105.8	34,880 - > 45,000

TABLE 5.4 Computer-Derived Data from Table 5.3

Ductile Region

Sh	=	146.58841
$(Sh)^2$	=	21488.16194
Sh^2	=	487.389895
Sfh	=	301.831002
H	=	3.118902
Sf	=	97.04847
$(Sf)^2$	=	9418.405529
Sf^2	=	200.419860
F	=	2.064861
N	=	47
U	=	0.028253
W	=	-0.853698
V	=	30.19496
a	=	65.51111
b	=	-30.21618
$/\overline{s}$	=	0.31268

TABLE 5.5 Data Points for Phillips Ultra High Molecular Weight Ethylene-Butene Copolymer at 60°C

Hoop Stress Kg/cm^2	Failure Time - Hours	
	Ductile	Brittle
87.7	25 - 55	-
84.4	30 - 120 - 192	-
84.0	29 - 45 - 69	-
83.7	30 - 57 - 552 - 984	-
81.0	312 - 480 - 1560	-
80.5	360 - 432	-
80.1	168 - 288 - 480	-
78.9	600	-
78.1	382 - 600	-
78.0	312 - 480 - 1630 - 1632 - 2592	
77.3	2112 - 2712 - 2760	3648
76.8	744 - 984 - 2712	4128 - 5232
75.6	1528 - 2326	-
73.4	-	3744 - 4056 - 6888 - 1100
73.0	-	4056 - 4440 - 4608
70.3	-	5520 - 6984 - 7416 - 11064 - >11500
69.95	-	3984 - 4704 - 4944 - 6625 - 5520 - 6624 - 6984 - 7416 - 7896 - 7920
67.2	-	6624

TABLE 5.5 Cont'd

Hoop Stress Kg/cm^2	Failure Time - hours	
	Ductile	Brittle
66.8	-	7896 - 7920 - 8352 - >11,000
66.4	-	4920 - 5472 - 7056
63.7	-	8784 - 10,008
63.3	-	7320 - >11,500

TABLE 5.6 Computer-Derived Data from Table 5.5

	Ductile Region		Brittle Region
Sh	= 87.16173	Sh	= 141.02702
$(Sh)^2$	= 7597.16766	$(Sh)^2$	= 19888.62037
Sh^2	= 237.71853	Sh^2	= 538.32818
Sfh	= 165.870335	Sfh	= 259.873219
H	= 2.56358	H	= 3.811541
Sf	= 64.82652	Sf	= 68.19844
$(Sf)^2$	= 4202.47797	$(Sf)^2$	= 4651.027218
Sf^2	= 123.61271	Sf^2	= 125.721827
F	= 1.9066623	F	= 1.843201
N	= 34	N	= 37
U	= 0.0104168	U	= 0.0183887
W	= -0.3176542	W	=-0.067937
V	= 14.272422	V	= 0.797899

TABLE 5.6 Cont'd

Ductile Region		Brittle Region	
a	= 60.706325	a	= 10.621224
b	= -30.494517	b	= -3.694487
$/\overline{s}$	= 0.3785558	$/\overline{s}$	= 0.125004

TABLE 5.7 Data Points for Phillips Ultra High Molecular Weight Ethylene-Butene Copolymer at 66°C

Hoop Stress Kg/cm^2	Failure Time - hours	
	Ductile	Brittle
84.4	4.8 - 5 - 17	-
80.9	43 - 125	-
77.3	48 - 84 - 154 - 191 - 908	1482
70.3	452 - 888 - 1392	1512 - 2544
68.6	1368 - 1512	1848
66.7	1392	2568 - 2856 - 4920 - 5472
65.1	-	2476 - 2836
63.3	-	3168 - 3216 - 3600 - 3624 - 3744 - 3888
56.2	-	6200 - 6300 - 7536
49.2	-	6830 - 8360 - 12,300

TABLE 5.8 Computer-Derived Data from Table 5.7

Ductile Region		Brittle Region	
Sh	= 35.579667	Sh	= 78.81571
$(Sh)^2$	= 1256.912693	$(Sh)^2$	= 6211.916143
Sh^2	= 90.252379	Sh^2	= 283.621004
Sfh	= 66.464717	Sfh	= 141.181986
H	= 2.223729	H	= 3.582532
Sf	= 30.073462	Sf	= 39.47563
$(Sf)^2$	= 904.41311	$(Sf)^2$	= 1558.325344
Sf^2	= 56.544369	Sf^2	= 70.891069
F	= 1.879591	F	= 1.794347
N	= 16	N	= 22
U	= 0.0185499	U	= 0.058099
W	= -0.4105185	W	= -0.240733
V	= 11.1328356	V	= 1.261179
a	= 43.82000	a	= 11.017409
b	= - 22.130495	b	= -4.143500
$/\overline{s}$	= 0.3824598	$/\overline{s}$	= 0.114826

TABLE 5.9 Data Points for Phillips Ultra High Molecular Weight Ethylene-Butene Copolymer at 80°C

Hoop-Stress Kg/cm^2	Failure Time - hours	
	Ductile	Brittle
72.0	10 - 12	-
70.8	76 - 82	-
69.5	122	174
67.8	121	-
65.3	-	249 - 292
62.0	-	296
61.2	-	722
60.0	-	567 - 585
54.7	-	1147 - 1241 - 1303
50.0	-	1329
49.3	-	1403
45.1	-	1897 - 5760
43.0	-	2131 - 2365
39.8	-	1755 - 1787
38.0	-	2170 - 2408
34.7	-	2210 - 2417
32.0	-	3191 - 3202

TABLE 5.10 Computer-Derived Data from Table 5.9

	Ductile Region		Brittle Region
Sh	= 12.28350	Sh	= 74.18399
$(Sh)^2$	= 150.8843722	$(Sh)^2$	= 5503.2643723
Sh^2	= 23.075720	Sh^2	= 232.868298
Sfh	= 22.666033	Sfh	= 123.557206
H	= 1.754786	H	= 3.091000
Sf	= 12.92991	Sf	= 40.23861
$(Sf)^2$	= 23.883755	$(Sf)^2$	= 1619.1457347
Sf^2	= 167.1825726	Sf^2	= 67.719425
F	= 1.847130	F	= 1.676609
N	= 6	N	= 24
U	= 0.0005300	U	= 0.2550190
W	= -0.0231880	W	= -0.8203210
V	= 1.5208100	V	= 3.5656160
a	= 82.56844	a	= 8.48415
b	= -43.75093	b	= -3.21670
$/\overline{s}$	= 0.31803	$/\overline{s}$	= 0.20526

TABLE 5.12 Computer-Derived Data from Table 5.11

Brittle Region

$Sh = 45.31338$

$(Sh)^2 = 2053.302407$

$Sh^2 = 137.362544$

$Sfh = 75.692196$

$H = 3.020892$

$Sf = 25.07423$

$(Sf)^2 = 628.71701$

$Sf^2 = 41.932806$

$F = 1.671615$

$N = 15$

$U = 0.018339$

$W = -0.054345$

$V = 0.475717$

$a = 7.97447$

$b = -2.96335$

$/\overline{s} = 0.15559$

TABLE 5.14 Computer-Derived Data from Table 5.13

Ductile Region

$Sh = 205.14043$

$(Sh)^2 = 42082.596021$

$Sh^2 = 530.575942$

$Sfh = 423.976171$

$H = 2.413417$

$Sf = 176.03591$

$(Sf)^2 = 30988.64161$

$Sf^2 = 364.59990$

$F = 2.071011$

$N = 85$

$U = 0.027647$

$W = -0.871856$

$V = 35.486577$

$a = 67.72331$

$b = -31.53527$

$/\bar{s} = 0.31031$

TABLE 5.15 Data Point for Phillips Pigmented Medium Molecular Weight Ethylene-Hexene Copolymer at 60°C

Hoop Stress Kg/cm^2	Failure Time - hours	
	Ductile	Brittle
78.4	21 - 28	-
77.3	3.4 - 4.9 - 5.6 - 32 - 41 - 48 - 96 - 317	-
75.5	120 - 1464	-
74.8	48 - 96 - 192	-
73.8	96 - 139 - 167 - 216 - 240 - 264 - 576 - 648 - 840 - 864 - 1152	-
73.1	216	-
72.4	-	3432 - 4728 - 5046
71.0	-	3360
70.3	-	4056 - 8040
69.6	-	3214
67.5	-	8112
67.2	-	3204 - 9400
66.4	-	5400 - 5592 - 8496 - 9700
64.3	-	5001 - 7400
64.0	-	6276
62.3	-	11616

TABLE 5.16 Computer-Derived Data from Table 5.15

Ductile Region		Brittle Region	
Sh	= 55.12958	Sh	= 67.674503
$(Sh)^2$	= 3039.270591	$(Sh)^2$	= 4579.838439
Sh^2	= 125.709186	Sh^2	= 254.982554
Sfh	= 103.361419	Sfh	= 123.872848
H	= 2.041836	H	= 3.759695
Sf	= 50.68426	Sf	= 32.956821
$(Sf)^2$	= 2568.8942117	$(Sf)^2$	= 1086.152029
Sf^2	= 95.146909	Sf^2	= 60.348642
F	= 1.877195	F	= 1.830934
N	= 27	N	= 18
U	= 0.002679	U	= 0.006863
W	= -0.127543	W	-0.034734
V	= 13.143609	V	= 0.547085
a	= 91.41214	a	= 13.026467
b	= -47.60843	b	= -5.061226
$/\overline{s}$	= 0.53185	$/\overline{s}$	= 0.152333

TABLE 5.17 Data Points for Phillips Pigmented Medium Molecular Weight Ethylene-Hexene Copolymer at 66°C

Hoop Stress Kg/cm^2	Failure Time - hours	
	Ductile	Brittle
77.3	20 - 48 - 96 - 148 - 298	-
73.8	240 - 576 - 648 - 864	-
70.3	-	952 - 1536 - 2664 - 2904 - 2992 - 3864 - 4896
66.8	-	1800 - 3360
63.3	-	3864 - 4176 - 5208

TABLE 5.18 Computer-Derived Data from Table 5.17

Ductile Region		Brittle Region	
Sh	= 30.00085	Sh	= 41.512479
$(Sh)^2$	= 900.051001	$(Sh)^2$	= 1723.285887
Sh^2	= 79;316166	Sh^2	= 144.138317
Sfh	= 56.100803	Sfh	= 76.02371
H	= 2.500071	H	= 3.459373
Sf	= 22.47512	Sf	= 21.982467
$(Sf)^2$	= 505.131019	$(Sf)^2$	= 483.228861
Sf^2	= 42.096882	Sf^2	= 40.27355
F	= 1.872927	F	= 1.831872
N	= 9	N	= 12
U	= 0.00263	U	= 0.004478
W	= -0.088589	W	= -0.021848
V	= 4.211916	V	= 0.531159
a	= 65.58778	a	= 12.396427
b	= -33.68402	b	= -4.878645
$/\bar{s}$	= 0.35041	$/\bar{s}$	= 0.206051

TABLE 5.19 Data Points for Phillips Pigement Medium Molecular Weight Ethylene-Hexene Copolymer at 80°C

Hoop Stress Kg/cm^2	Failure Time - hours	
	Ductile	Brittle
58.0	4	
57.4	1	
57.0	0.3 - 3 - 28	
56.7	3.4	
56.5	0.5 - 3.3 - 10 - 32	
56.3	3.3	
56.1	3.3 - 3.5	
56.0	2.9 - 3.1 - 3.5 - 4 - 7 - 10 - 24	
54.7	3 - 9	
54.0	94	
53.5	60	
53.0	25	
52.8	14 - 16 - 17	
52.6	32 - 35 - 47 - 48 - 125 - 154	
52.5	59 - 87 - 142 - 176 - 206	
52.4	63	
52.3	23 - 70 - 199	
52.2	141	

TABLE 5.19 Cont'd

Hoop Stress Kg/cm^2	Failure Time - Hours	
	Ductile	Brittle
52.0	88 - 122 - 155 - 194 - 197 - 228 - 197	
51.9	112	
51.8	140 - 157 - 172 - 215	
51.7	152 - 190	
51.6	90 - 124 - 211	
51.4	194	
51.3	152 - 179 - 328	
51.0	67	
50.8	-	3299
50.6	786 - 862	2290
50.0	-	596 - 834 - 862 - 1230 - 1340 - 1901 - 3297 - 3390
49.8	284	862
49.5	-	540 - 738 - 3180
49.1	-	1272 - 1950 - 1952
48.9	-	1013 - 2752 - 3299
48.8	-	581 - 1662 - 2011
48.7	-	2434 - 3297

TABLE 5.19 Cont'd

Hoop Stress Kg/cm^2	Failure Time - hours	
	Ductile	Brittle
48.5	-	1993 - 2004 - 2668
48.2	-	1086
47.5	-	4767
47.3	-	3683 - 3939 - 5354
47.1	-	4056 - 5383 - 5391
47.0	-	1857
46.9	-	4607 - 4880 - 5399
46.8	-	4775 - 5107
46.6	-	1808 - 1820
46.4	-	1991
46.3	-	2034
46.0	-	1813 - 2009
45.9	-	1627
44.9	-	1950 - 2539
44.7	-	1776
43.0	-	2449 - 3361
42.0	-	1954
40.4	-	4104 - 6138 - 6883
40.2	-	4240 - 6072

TABLE 5.19 Cont'd

Hoop Stress Kg/Cm^2	Failure Time - hours	
	Ductile	Brittle
40.1	-	5516 - > 6883
40.0	-	6289 - > 6883
39.8	-	> 6883
35.6	-	6527
35.0	-	7986 - 8151
31.2	-	9971

TABLE 5.20 Computer-Derived Data from Table 5.19

Ductile Region		Brittle Region	
Sh =	109.10800	Sh =	238.4541814
$(Sh)^2$ =	11904.555664	$(Sh)^2$ =	56860.39665
Sh^2 =	216.989987	Sh^2 =	821.733995
Sfh =	187.645896	Sfh =	395.2029044
H =	1.604529	H =	3.406488306
Sf =	117.44127	Sf =	116.2282846
$(Sf)^2$ =	13792.451899	$(Sf)^2$ =	13509.01413
Sf^2 =	202.849622	Sf^2 =	193.138511
F =	1.727077	F =	1.660404065
N =	68	N =	70
U =	0.019447	U =	0.1525948803
W =	-0.792076	W =	-0.7273887897
V =	41.922992	V =	9.442618813
a =	71.94832	a =	11.3212874
b =	-40.72997	b =	-4.766790967
$/\overline{s}$ =	0.38261	$/\overline{s}$ =	0.2964323215

TABLE 5.21 Data Points for Phillips Pigmented Medium Molecular Weight Ethylene-Hexene Copolymer at 90°C

Hoop Stress Kg/cm^2	Failure Time - hours	
	Ductile	Brittle
48.0	1.6 - 1.7 - 1.8 1.9 - 2.0 - 2.2 2.3 - 2.9	-
46.0	1.4 - 2.6 - 3.5 6.3 - 38 - 44 76	161
43.3	-	375 - 380 - 358
43.0	-	252 - 376
40.0	-	513 - 537 - 629 683 - 727 - 740 783 - 813 - 830
38.4	-	840 - 1440 - 1560
35.4	-	478 - 600 - 1680
35.1	-	792 - 836 - 864 900

TABLE 5.22 Computer-Derived Data from Table 5.21

Ductile Region		Brittle Region	
Sh =	9.444717	sh =	70.08830244
$(Sh)^2$ =	89.202681	$(Sh)^2$ =	4912.370139
Sh^2 =	10.652747	Sh^2 =	197.835164
Sfh =	15.749329	Sfh =	111.551505
H =	0.629648	H =	2.803532
Sf =	25.089244	Sf =	39.838944
$(Sf)^2$ =	629.470181	$(Sf)^2$ =	1587.141426
Sf^2 =	41.965956	Sf^2 =	63.515336
F =	1.672616	F =	1.593558
N =	15	N =	25
U =	0.001277	U =	0.029679
W =	-0.048058	W =	-0.138252
V =	4.705902	V =	1.340358
a =	63.575265	a =	10.226699
b =	-37.633029	b =	-4.658235
$/\overline{s}$ =	0.472022	$/\overline{s}$ =	0.173999

TABLE 5.23 Data Points for Phillips Black Medium Molecular Weight Ethylene-Hexene Copolymer at 23°C

Hoop Stress - Kg/cm^2	Failure Time - hours
126.5	17 - 18 - 45 - 75
125.0	40 - 73 - 170 - 180 - 250 - 260 - 510
123.0	49 - 50 - 55 - 56-130-132-150-510-580
121.0	40 - 45 - 47 - 115 - 132 - 151 - 155 160 - 216 - 220 - 362 - 580 - 2200 - 2300
120.0	102 - 645
119.5	32 - 49 - 69 - 70 - 72 - 98 - 130 - 150 - 210 - 450 - 552 - 912 - 1056 - 1100 - 1200 - 1300 - 1400 - 1520 - 1600 - 3200
118.0	98 - 150 - 240 - 270 - 408 - 450 - 552 - 912 - 930 - 1056 - 1100 - 1200 1300 - 1400 - 1520 - 1600 - 3200
117.0	408 - 840
116.0	75 - 180 - 250 - 260 - 470 - 648 - 740 760 - 850 - 888 - 1344 - 1500 - 3336 - 12000
114.0	550 - 850 - 1200 - 1400 - 2520 - 5200 6120 - 7704 - 7968 - 8700 - 13000 - > 20000
112.5	520 - 550 - 2328 - 3432 - 3800 - 5112 6400 - 6936 - 13176 - 14000 - 23280

TABLE 5.23 Cont'd

Hoop Stress - Kg/cm^2	Failure Time - hours
111.0	3700 - 5400 - 7800 - 8600 - 22700
110.0	> 9000
109.0	> 10000
107.0	10300 - > 20000
105.5	> 30000
98.4	> 30000

TABLE 5.24 Computer-Derived Data from Table 5.23

Ductile Region

$Sh = 335.38113$

$(Sh)^2 = 112480.502360$

$Sh^2 = 1021.264582$

$Sfh = 693.256118$

$H = 2.818329$

$Sf = 246.42229$

$(Sf)^2 = 60723.945009$

$Sf^2 = 510.318196$

$F = 2.070776$

$N = 119$

$U = 0.032944$

$W = -1.242925$

$V = 76.050276$

$a = 80.94541$

$b = -37.72841$

$/\overline{s} = 0.49920$

TABLE 5.25 Data Points for Phillips Black Medium Molecular Weight Ethylene-Hexene Copolymer at 60°C

Hoop Stress Kg/cm^2	Failure Time - hours	
	Ductile	Brittle
77.3	163 - 172	-
75.5	336 - 624 - 840	-
73.8	2904	7278
72.1	1824	4128 - 5592 - 8160
70.3	-	8160 - 9744
68.5	-	12312 - 14232 - 16500
62.3	-	12300 - 15120 - 15969

TABLE 5.26 Computer-Derived Data from Table 5.25

	Ductile Region	Brittle Region
Sh =	19.417529	47.774221
$(Sh)^2$ =	377.040442	2282.376196
Sh^2 =	55.264785	190.699701
Sfh =	36.411143	87.643410
H =	2.773933	3.981185
Sf =	13.136210	22.024518
$(Sf)^2$ =	172.560013	485.079410
Sf^2 =	24.652125	40.431083
F =	1.876601	1.835377
N =	7	12
U =	0.000695	0.007799
W =	-0.027817	-0.040274
V =	1.401864	0.501684
a =	77.882764	13.459515
b =	-40.023868	-5.164243
$/\overline{s}$ =	0.240224	0.171376

TABLE 5.27 Data Points for Phillips Black Medium Molecular Weight Ethylene-Hexene Copolymer at 66°C

Hoop Stress Kg/cm^2	Failure Time - hours	
	Ductile	Brittle
79.1	12 - 12.3 - 14.7 - 17.8 - 55 - 80	-
77.3	144 - 192 - 720 - 808 - 956	-
73.8	552 - 648 - 720 - 1032 - 1224	-
72.1	1824	1003 - 2328 - 3624
70.3	-	3456 - 3528 - 3864 - 4728
66.8	-	1829 - 4176 - 5424 - 6984
65.1	-	3264 - 3864 - 6504
63.3	-	2894 - 4176 - 5230 - 7280 - 8136

TABLE 5.28 Computer-Derived Data from Table 5.27

Ductile Region		Brittle Region	
Sh	39.190464	Sh	68.083158
$(Sh)^2$	1535.892487	$(Sh)^2$	4635.316462
Sh^2	100.140225	Sh^2	244.843846
Sfh	73.690433	Sfh	124.331131
H	2.305321	H	3.583324
Sf	32.028245	Sf	34.708554
$(Sf)^2$	1025.80847	$(Sf)^2$	1204.683746
Sf^2	60.344914	Sf^2	63.412706
F	1.884014	F	1.826766
N	17	N	19
U	0.00323914	U	0.008298
W	-0.1449658	W	-0.040869
V	9.793608	V	0.879821
a	86.623272	a	12.580251
b	-44.754418	b	-4.925057
$/\overline{s}$	0.46945	$/\overline{s}$	0.199785

TABLE 5.29 Data Points for Phillips Black Medium Molecular Weight Ethylene-Hexene Copolymer at 90°C

Hoop Stress Kg/cm^2	Failure Time - hours	
	Ductile	Brittle
56.1	0.2 - 0.3	-
53.2	2.3 - 2.4	-
51.7	72 - 78	168
51.0	21 - 90	-
50.2	37 - 72	216 - 438
48.7	144 - 168	-
45.7	-	336 - 552
42.8	-	864
37.7	-	408 - 1065

TABLE 5.30 Computer-Derived Data from Table 5.29

Ductile Region		Brittle Region	
Sh	= 14.355193	Sh	= 21.337235
$(Sh)^2$	= 206.071566	$(Sh)^2$	= 455.277578
Sh^2	= 29.153791	Sh^2	= 57.499217
Sfh	= 24.386340	Sfh	= 35.160869
H	= 1.196266	H	= 2.667154
Sf	= 20.568317	Sf	= 13.218851
$(Sf)^2$	= 423.055680	$(Sf)^2$	= 174.738010
Sf^2	= 35.259204	Sf^2	= 57.508150
F	= 1.714026	F	= 1.652356
N	= 12	N	= 8
U	= 0.004564	U	= 0.0205119
W	= -0.218840	W	= -0.095846
V	= 11.981160	V	= 0.589520
a	= 83.379466	a	= 10.385556
b	= -47.947452	b	= -4.671149
$/\overline{s}$	= 0.385790	$/\overline{s}$	= 0.153737

TABLE 5.31 Data Points for Phillips Ultra High Molecular Weight Ethylene-Hexene Copolymer at 23°C

Hoop Stress - Kg/cm^2	Failure Time - hours
134.3	48 - 96
130.2	312 - 360
129.8	48 - 120 - 144
126.9	144 - 168 - 192 - 312 - 336
123.5	48 - 120 - 504 - 550
120.1	552 - 672
119.2	480 - 504
118.2	5304 - 5328 - 5352
116.7	2784 - 3048

TABLE 5.32 Computer-Derived Data from Table 5.31

Ductile Region

$Sh = 64.57910$

$(Sh)^2 = 4170.460157$

$Sh^2 = 176.340281$

$Sfh = 135.059363$

$H = 2.583164$

$Sf = 52.37281$

$(Sf)^2 = 2742.911227$

$Sf^2 = 109.725050$

$F = 2.094912$

$N = 25$

$U = 0.008601$

$W = -0.228194$

$V = 9.521875$

$a = 58.16346$

$b = -26.53109$

$/\overline{s} = 0.38828$

TABLE 5.33 Data Points for Phillips Ultra High Molecular Weight Ethylene-Hexene Copolymer at 60°C

Hoop Stress Kg/cm^2	Failure Time - hours	
	Ductile	Brittle
84.5	0.3 - 0.4	-
81.5	5 - 6	-
77.8	342 - 553	-
76.9	264 - 576	-
73.9	-	4314
71.0	-	9360 - 10392
66.6	-	12288

TABLE 5.34 Computer-Derived Data from Table 5.33

Ductile Region		Brittle Region	
Sh	= 15.22986	Sh	= 15.712336
$(Sh)^2$	= 231.948636	$(Sh)^2$	= 246.877513
Sh^2	= 28.995718	Sh^2	= 61.841114
Sfh	= 20.799938	Sfh	= 29.037167
H	= 1.903732	H	= 3.928084
Sf	= 11.01510	Sf	= 7.394635
$(Sf)^2$	= 121.332428	$(Sf)^2$	= 54.680632
Sf^2	= 28.953759	Sf^2	= 13.671205
F	= 1.376887	F	= 1.848658
N	= 8	N	= 4
U	= 13.787206	U	= 0.001047
W	= -0.169866	W	= -0.0096819
V	= 0.002139	V	= 0.121736
a	= 1.92068	a	= 20.843373
b	= -0.01231	b	= -9.150033
$/\overline{s}$	= 0.00277	$/\overline{s}$	= 0.130500

TABLE 5.35 Data Points for Phillips Ultra High Molecular Weight Ethylene-Hexene Copolymer at 80°C

Hoop Stress Kg/cm^2	Failure Time - hours	
	Ductile	Brittle
70.0	1	-
64.9	276	377 - 516 - 597 649 - 854
61.0	710	730
60.6	-	410 - 452 - 985
60.1	-	336 - 735 - 852 881
55.5	-	765 - 974 - 1084 1379 - 1500 - 1607
54.0	-	984
53.2	-	1773
50.8	-	704 - 707 - 709 - 1598 - 1740
49.9	-	956 - 1502 - 1560 - 1687 - 1740 - 1829
46.7	-	3145
46.2	-	2116 - 3102
45.8	-	1593 - 3030 - 3538
45.3	-	1075
44.8	-	1075
40.2	-	3530 - 3776

TABLE 5.35 Cont'd

Hoop Stress Kg/cm^2	Failure Time - hours	
	Ductile	Brittle
39.3	-	3905
38.0	-	3864
37.0	-	2604
31.0	-	9000

TABLE 5.36 Computer-Derived Data from Table 5.35

Ductile Region		Brittle Region	
Sh	= 5.292167	Sh	= 143.227065
$(Sh)^2$	= 28.007036	$(Sh)^2$	= 20513.99213
Sh^2	= 14.087711	Sh^2	= 450.418418
Sfh	= 9.513961	Sfh	= 244.101542
H	= 1.764056	H	= 3.113632
Sf	= 5.442673	Sf	= 78.682118
$(Sf)^2$	= 29.622685	$(Sf)^2$	= 6190.875699
Sf^2	= 9.876020	Sf^2	= 134.825625
F	= 1.814224	F	= 1.710481
N	= 3	N	= 46
U	= 0.001792	U	= 0.241371
W	= -0.087217	W	= -0.885607
V	= 4.752033	V	= 4.462067
a	= 90.062900	a	= 9.389510
b	= -48.670310	b	= -3.669073
$/\overline{s}$	= 712147	$/\overline{s}$	= 0.166017

TABLE 5.11 Data Points for Phillips Ultra High Molecular Weight Ethylene-Butene Copolymer at 90°C

Hoop Stress - Kg/cm^2	Failure Time - hours
52.7	528 - 744 - 768
49.2	384 - 1200 - 1246 - 1320
45.7	912 - 1488 - 1560 - 1608
42.2	1056 - 1224 - 1272 - 1608

TABLE 5.13 Data Points for Phillips Pigmented Medium Molecular Weight Ethylene-Hexene Copolymer at 23°C

Hoop Stress - Kg/cm^2	Failure Time - hours
126.5	34 - 34 - 41
125.0	54 - 56 - 63 - 100 - 146
123.5	71 - 73 - 75 - 78 - 80
122.5	16 - 16 - 17 - 21 - 22 - 24 - 29 - 35 - 46 - 76 - 152 - 245
121.0	40 - 87 - 109 - 216
120.0	90 - 192 - 240 - 500 - 864
119.5	96 - 116 - 125 - 145 - 165 - 192 - 234
118.0	338 - 1224
117.0	360 - 456 - 1224
116.0	144 - 286 - 403 - 451 - 480 - 514 - 576
114.0	399 - 426 - 431 - 463 - 470 - 490 - 520 - 569 - 618 - 652 - 674 - 681 - 694 - 766 - 940 - 981 - 983 - 995 - 1022
112.5	360 - 480 - 552 - 576 - 1056 - 1224
111.0	2904 - 3860
110.0	10700
109.0	1680
105.5	1344 - 7500 - 26000
102.2	> 10000
98.4	> 10000

CHAPTER 6: CHEMICAL ENVIRONMENTAL INFLUENCE ON HOOP STRESS

INTRODUCTION

The problem of environmental stress cracking and crazing in unplasticised PVC gas pipe lines was first encountered in Holland in 1964 (197), which subsequent research suggested was attributed to the high aromatic concentration of the town gas distributed at that time. Gas pipes which had been in service for a number of years (198) (maximum service time 10 years, minimum 6 months) were found to contain "hair line crack features" in the bore. Wolf (199) attributed these to environmental stress cracking caused by an abnormally high concentration of naphthalene in the Dutch gas grid. British gas does not contain such quantities of naphthalene (200) but Brighton and Benton (201) have shown that stress cracking of PVC occurs in the presence of the aromatic and aliphatic hydrocarbons found in most gases. However, it was considered that the use of PVC pipe in the United Kingdom, and especially pipe produced from PVC, compounded with certain impact modifiers would be satisfactory, because the concentration of aromatic hydrocarbons is so low.

It was not to be expected that natural gas, with its substantially lower concentration of aromatics, would cause similar stress cracking. The fact that the composition of natural gas has considerably changed in the course of years may be the cause that this phenomenon has also been found in PVC natural gas pipe lines in Holland (202) and that, although this has not as yet led to any calamities in practice, such calcamities cannot necessarily be ruled out.

It was therefore considered that an important aspect of this thesis was to determine to what extent the basic pipe hydrostatic data require modification for safe service of the same pipe for gas distribution purposes.

6.1 STRESS CRACKING PHENOMENON

Faulkner and Atkinson (203) and Gotham (204) make a clear distinction between "cracking" and "crazing".

i) Environmental stress cracking may be defined as the cracking which occurs when a material is stressed above some critical value when in contact with an active environment; the stress being insufficient to cause cracking in the absence of such an environment. Brighton and Benton (201) defined this phenomenon as environmental strain cracking because

of the apparent strain dependance.

ii) An environmental stress crack may be considered as two distinct polymer surfaces separated by the environment and in contact only at the tip or tips. With such a system, stress cannot be transmitted across the environment.

An environmental stress craze consists of oriented polymer bounded by two sharply defined crazed boundaries. Beyond these boundaries the polymer reverts from the unoriented (original) state to the oriented and voided (crazed) state. In this system, stress can be transmitted across the craze boundaries and crazed material.

iii) Environmental stress cracking is an irreversible process. An environmental stress craze can be considered as a reversible process as the craze can be healed by gentle heating above the glass transition temperature. The heating mechanism probably involves the reversion of crazed material back to a nearly random, original state. However, some of the larger voids present in the crazed material are not removed by this treatment and remain as cracks.

iv) Crazes are similar to cracks in that there exists a critical energy below which they do not form. Menges and Schmidt (205) regarded crazing as a phenomenon analogous to that of steel and other metals in

the supercritical stress range where dislocation and slip mechanisms in the crystal planes are observed.

6.2 SITUATIONS CAUSING STRESS

The calculation for the minimum dimensions of wall thickness of a pipe and its fittings assembly is based on only the tangential stress arising from internal pressure. In a buried pipeline, however, wall stress may be increased by such factors as soil load, inaccurate assembly, temperature differentials, soil movement and superficial mechanical damage.

Stress in the plastics pipeline will cause an elongation in the material. In practice, the elongation caused by internal pressure can be neglected since most operating lines are less than 4 bar pressure. Soil load and traffic loads may cause deformations in the region of 2-3% which, dependent on the pipe diameter, will give elongations corresponding to these deformations of between 0.3 - 0.5% (197). Bends elastically formed in the field will give similar elongation values. The largest elongation and deformation will appear in the pipe at the point of the joints and branching saddles. Dependent on the type of branching saddle, the elongation may vary between 0.5 to 2%. Elongation also occurs as a result of the installation techniques employed, although proper

adherence to the codes of practice should ensure that such induced stresses are kept to a minimum and can be estimated as a maximum elongation of 1.5% (197). Thus in practice, stress situations can arise which result in material elongation of between 0.5 - 1% on average.

6.3 INCIDENCE OF CHEMICAL ENVIRONMENT

Tests at Batelle Memorial Institute (206) have shown that the long-term strength of pipe when tested with natural gas was equal to, or better than, the stress rupture curves of the same plastics materials when water was used as the test medium. Similar studies (207) have shown that the results obtained with methane and water are essentially the same; the data results in water being slightly lower and explained by a slight absorption of the water by plastics materials imparting a plasticising effect as demonstrated in creep, modulus, tensile strength and impact tests.

However, there are constituents in some natural gases, either present originally or added prior to use, which can have a pronounced deleterious effect on the performance of the gas distribution system. Various compositions of natural condensates (197, 200, 208, 209) which have been found to exist in various concentrations are reproduced in Tables 6.1 - 6.3.

TABLE 6.1 Approximate Composition of U.K. Gases[13]

Constituent Vol. %	Natural Gas	Coal Gas	Reformer Gas
Nitrogen	0.4 - 8.9	10	0 - 3.5
Carbon Dioxide	0.01- 0.66	2.5 - 3.5	0 -19
Oxygen	-	0.5	-
Hydrogen	-	48	33 -65
Carbon Monoxide	-	8 -16	2.5 -14.2
Methane	82 - 95	21 -28	1.7 - 5.6
Ethane	2.6 - 8.6	-	-
Propane	0.4 - 2.4	-	0 - 0.5
Butane	0.2 - 0.9	-	6.4 - 8.5
Pentane	0.66-0.17	-	0.2 - 0.8
Benzene	0.03-0.04	0.2 - 1.0	-
Toluene	0.01	0.2 - 1.0	-

TABLE 6.2 Hungarian (Pecs) Town Gas Composition

Hydrogen	48	- 50	Volume percent
Nitrogen	14	- 12	
Methane	5	- 10	
Carbon Monoxide	3.5	- 5.5	
Oxygen	0.5		
Ethane - Ethylene	2	- 3	
Propane-Propylene	0.9	- 0.5	
Butane-Butylene	0.1	- 0.2	
Pentanes	0.7	- 1.0	
Hexanes	0.6	- 0.5	
Heptanes	0.2	- 0.4	
Benzene	0.4	- 0.2	
Toluene	0.1	- 0.2	

TABLE 6.3 Typical Composition of Natural Gas Condensate

	DUTCH	GERMAN
Paraffines	76.0% by vol	78.0% by vol
Naphthenes	13.0%	12.0%
Aromatics	6.0%	8.0%
Cyclic olefins, alkenes and diolefins	5.0%	2.0%
Aniline Point	57.2°C	57.9°C

These condensates are found in the distribution lines through a process of retrograde condensation. Retrograde condensation occurs at the pressure reduction at the well-head where the condensation of hydrocarbons increases with a decrease in pressure, until a maximum condensation has occurred at which point the condensation diminishes. The so formed condensate travels through the main transmission lines in the form of a fog of approximate particle size of 10 microns. This fog is difficult to remove by filters and thus passes over into the distribution network and is of prime concern where the distance between well-head and consuming area is small, such as in Holland. Concentration and composition of these condensates vary with distance due to periodical condensation and vapourisation, but a typical content from the Groningen Natural Gas Field would be between 2 to 50 mg/m^3.

In addition to natural gas condensates in the distribution and service lines, old cast iron pipe lines through which town gas has been distributed, may contain deposits of naphthalene and these deposits may evaporate into the drier natural gas and may thus be transported to the plastics service lines connected to the old cast iron network.

Brighton and Benton (201) have pointed out that an aromatic impurity of concentration of as little as one percent in n-hexane could result in a 15% variation in the critical strain for the environmental stress cracking of PVC. They also showed that results obtained in a liquid environment would be similar to those obtained in a gaseous environment of the same chemical activity. In addition to the aromatic constituents in natural gas, odourants are added in the distribution lines. In the U.K., a blend of various mercaptans are used, whilst in general, on the Continent, tetrahydrothiophene THT at a level of 18 mg/m^3 is used. At the point of injection, the overodourisation may reach a concentration of up to 100 mg/m^3. In the high pressure network, methanol is injected to precent hydration. This methanol may penetrate in vapour form into the low pressure distribution networks in concentrations up to 1.4 mg/m^3 (197).

6.4 EXPERIMENTAL RESULTS

The initial test carried out by Tansley (210) using water, gas and gas mixture with various aggressive media yielded the conclusions that there was insignificant difference between gas and water in the long term hydrostatic test at 80°C, that the effect of benzene and toluene were equally aggressive but less so than trimethylbenzene and that liquid phase contact was far more aggressive than vapour phase contact.

6.4.1 Condensate Absorption

In order to determine both the rate of absorption and the saturation level, condensate absorption curves were determined for two representative materials.

i) Ziegler polymerised high molecular weight high density ethylene-butene copolymer

ii) Phillips' polymerised medium molecular weight medium density ethylene-hexene copolymer.

Test pieces of 3 mm thick coupons cut from a pressed sheet were weighed before being immersed in gas condensate for set time periods at each of four temperature levels. The samples were weighed regularly during the test to determine the percentage increase in weight. These results are shown graphically in Figs 6.1 and 6.2.

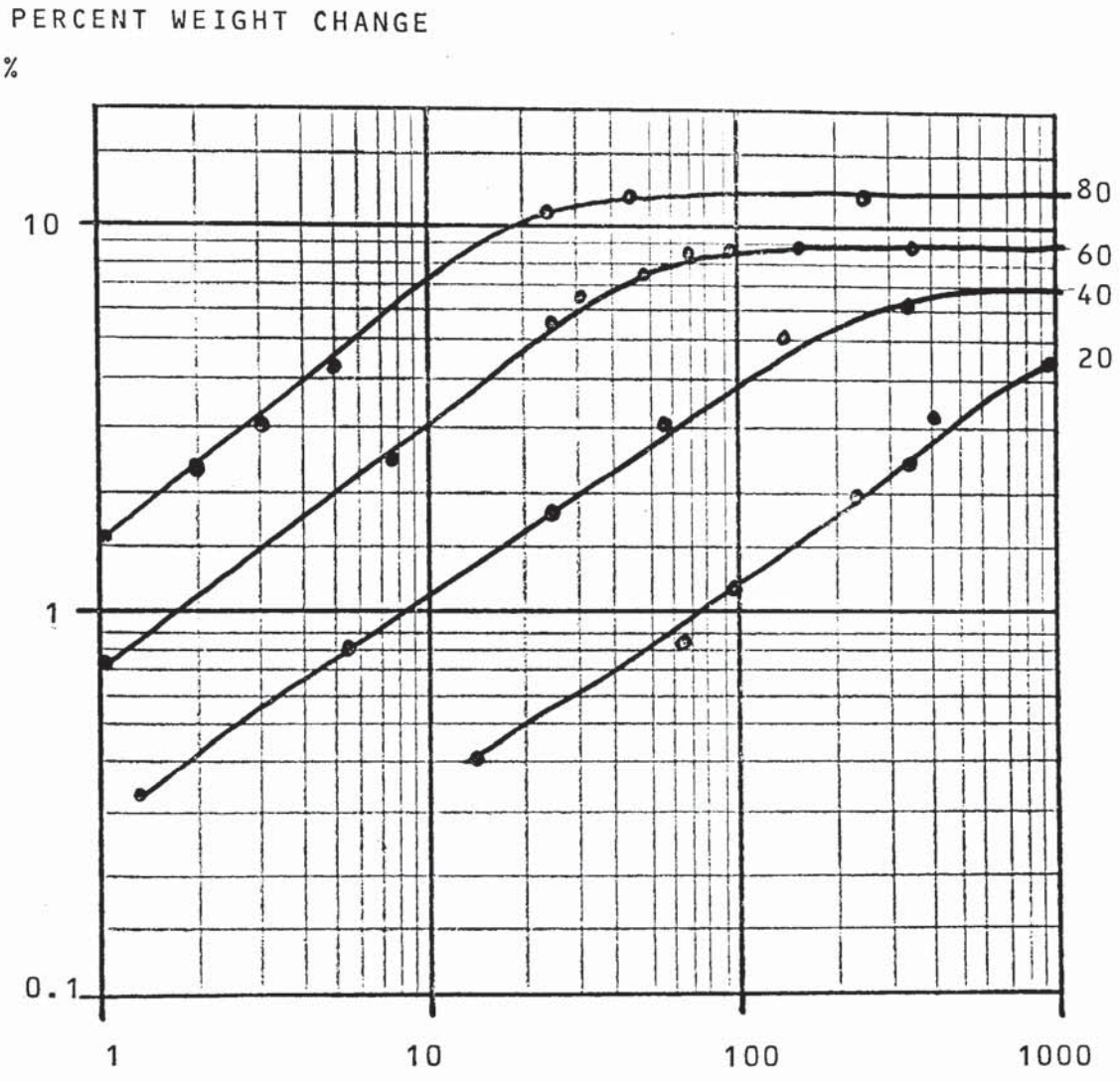

Fig. 6.1 Rate of Gas Condensate Absorption for Ziegler Polymerised High Molecular Weight Ethylene-Butene Copolymer

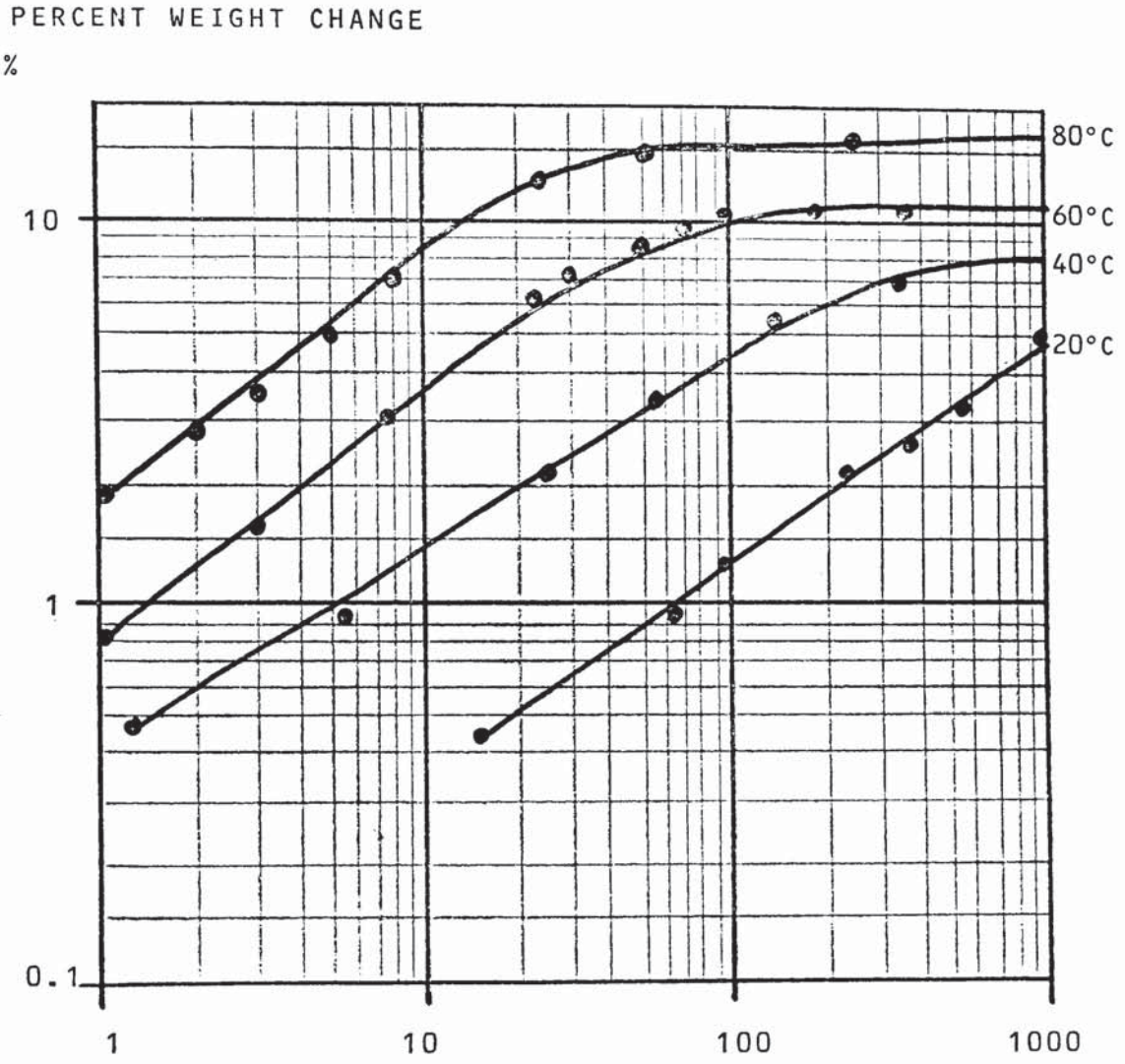

Fig. 6.2 Rate of Gas Condensate Abosrption for Phillips Polymerised Medium Molecular Weight Ethylene-Hexene Copolymer

In all cases, the absorption by the higher density (0.948 G/cc) material is less than the medium density material. It is thus to be concluded that both rate of absorption and the saturation point, irrespective of temperature, are related to the amount of non-crystalline polymer in the samples studied.

6.4.2 Condensate Desorption

The condensate level in natural gas will not only vary in normal circumstances, but can also be expected to vary with the season; even to the extent that during the low gas usage during the Summer months, desorption of the condensate from the inner pipe wall would occur.

This has been studied by submitting tensile coupons cut from pipe samples to condensate immersion for 68 hours at 80°C and then cooling the samples down to room temperature in air prior to reweighing. From these samples, one set was reheated in air at 80°C for three hours before cooling at room temperature and reweighing and a second set heated in air at 80°C for 70 hours before cooling to room temperature and reweighing.

The initial condensate immersion time was chosen as being in excess of the saturation point for both materials, whilst the desorption times were selected arbitrarily as short and long time periods.

After three hours desorption at 80°C, the Ziegler polyethylene copolymer has given up 30% of the absorbed condensate; whilst the Phillips' polyethylene copolymer has given up almost 40% (Table 6.4). After 70 hours desorption, the respective values are 91.3% and 90.1%, showing that although the rate of desorption is higher for the lower-density hexene copolymer, both materials reach an equilibrium point at which some 10% of the condensate absorption remains within the sample, even after extended desportion has taken place. It may thus be concluded that within the boundaries of this simple test, complete desorption of condensate from the inner walls of a polyethylene gas distribution line is unlikely to occur; or, expressed in another way, once subjected to condensate absorption the inner pipe line walls remain in contact with some condensate for extended time periods, even after the condensate source has been removed.

The samples originating from the previous evaluation were tensile tested at a crosshead separation speed of 50 mm/min and the tensile yield stress, ultimate stress and ultimate elongation determined. For ease of reference, the results in Table 6.5 are expressed as a percentage of the tensile properties of a blank specimen for both materials (sample 1). The sample 2 was used as a second control to study the effect of

heating at 80°C for 70 hours. In both cases, due to the annealing effect, the tensile properties are significantly higher; the increase in crystallinity due to annealing being more pronounced for the high density butene copolymer.

Condensate absorption to saturation reduces the tensile strength of both materials by 25% Desorption for 3 hours has very little influence even though the condensate level has been significantly reduced. Desorption for 70 hours at 80°C brings the yield stress almost back to its original value, but both ultimate stress and elongation are still significantly affected by the residual condensate present.

TABLE 6.4 Residual Condensate After Desorption

	High mol.wt. Ziegler Ethylene-Butene Copol.	Medium mol.wt. Phillips Ethylene-Hexene Copolymer.
Original Weight g	9.15	5.708
Weight Change:		
after absorption, %	12.1	15.8
3 hrs desorption, %	8.4	9.6
70 hrs desorption, %	1.05	1.57

TABLE 6.5 Influence of Condensate Absorption and Desorption on Tensile Properties

Sample N°	Yield Stress (Kg/cm)	%	Ultimate Stress (Kg/cm)	%	Ultimate Elongation (%)	%
1.Ziegler Copolymer						
1	(220)	100	(225)	100	(690)	100
2		121		114		105
3		79		71		75
4		83		71		83
5		98		65		34
2.Phillips Copolymer						
1	(185)	100	(245)	100	(690)	100
2		110		101		108
3		81		53		77
4		86		56		75
5		103		58		75

Sample N° Code	80°C Condensate hours	80° Desorption hours
1	0	0
2	0	70
3	68	0
4	68	3
5	68	70

6.5 CONDENSATE INFLUENCE ON PIPE DESIGN STRESS

In Chapter 5 of this work, the long term hoop stress was determined for a range of copolymers and a correlation obtained for different temperatures of test. These results hold true when the pipe samples are tested with water as the internal and external medium.

It is to be expected that, for pipelines in gas distribution and service use, certain constituents of the transmitted gas and specifically the aromatic components will have a deleterious effect on the long-term strength characteristics of the polyethylene pipe. As a consequence, similar hoop stress testing to that of the previous chapter was performed, but using gas condensate as the internal pressure medium instead of water.

6.5.1 Influence of Preconditioning

The data in Section 6.4 showed that saturation of pipe wall was time dependent. In order to arrive at a meaningful test procedure, three preconditioning steps for the pipe samples were evaluated at test temperatures of 80°C and 60°C, the steps differing in the condensate contact time prior to pressurisation. The applied hoop stress - time to failure results for the medium molecular weight high density ethylene-hexene

copolymer are tabulated in Tables 6.6 - 6.9, together with details of the preconditioning.

All the pipe failures obtained were of a ductile nature, which is in complete contrast to the same tests made using water as the internal pressure medium. Closer examination of the failure area shows the point of burst to be larger and more circular in shape in contrast to the circumferential direction split obtained previously. From this it is concluded that the condensate has a plasticising effect on the copolymer and since the failure results fall into the characteristic double-sloped plot, the burst failures must be considered as being conventional ductile failures at the higher stress levels, but plasticised-brittle failures at the lower stress - longer time to failure - levels.

When the failure points are plotted as the 95% lower confidence limit (Figs 6.3 and 6.4) the failures, irrespective of type of preconditioning, tend towards a central downwards slope.

TABLE 6.6 Influence of Preconditioning in Condensate on Medium Molecular Weight Ethylene Hexene Copolymer at 80°C

Hoop Stress Kg/cm^2	Failure Time - hours		
	A	B	C
45.0	4.1		1.5 - 1.8
42.0			4.3
40.0	8.8		3.0 - 3.4 - 3.9
37.0		2.0	13.0
35.0	9.9 - 14.9	3.5 - 5.1 - 5.3	5.8 - 6.8 - 9.2
32.0		8.8	15.5
30.0	20.4-20.8	6.1 - 7.5 13.0-13.6	11.3 - 11.6 - 15.0
27.0		30.0	27.1
25.0	38.3	26.8-39.6 50.0	28.8 - 33.2 - 102.2
23.0			60.0 - 163

Preconditioning:

A. One hour with condensate in pipe at 80°C prior to pressurisation

B. 24 hours with condensate in pipe at 80°C prior to pressurisation.

C. One month with condensate in pipe at room temperature followed by one hour at 80°C prior to pressurisation

TABLE 6.7 Computer-Derived Data from Table 6.6

Preconditioning	A	B	C
Sh	7.93698	13.3312	21.23541
Sh^2	9.59414	15.8727	28.4352
$(Sh)^2$	62.9956	177.7215	450.9428
H	1.13385	1.0255	1.06177
V	0.59477	2.20186	5.88814
N	7	13	20
Sf	10.69559	19.2392	30.2214
Sf^2	16.3860	28.51623	45.84389
$(Sf)^2$	114.3956	370.1478	913.3338
F	1.52794	1.4799	1.51107
U	0.04377	0.0433	0.17721
Sfh	11.96962	19.4363	31.1207
W	- 0.1576	- 0.2931	- 0.9675
b	- 3.6006	- 6.769	- 5.4597
a	6.6354	11.04302	9.31171
$/\overline{s}$	0.07379	0.14105	0.18347

TABLE 6.8 Influence of Preconditioning in Condensate on Medium Molecular Weight Ethylene -hexene Copolymer at 60°C

Hoop Stress Kg/cm^2	Failure Time - hours	
	X	Y
60.0		2.3 - 2.4
55.0		7.8
50.0	5.3 - 7.0	14.6 - 14.9 - 15.5
47.0		5.0 - 13.3 - 18.5
45.0	13.3 - 16.0	25.0 - 35.2 - 41.1
42.0		29.2 - 30.6
40.0	30.6	29.8 - 35.7 - 41.7
37.0		48.6 - 218
35.0		78.6 - 121.6 - 187.6
32.0		2242

Preconditioning:

X. One week with condensate in pipe at 60°C prior to pressurisation

Y. One month with condensate in pipe at room temperature followed by one hour at 60°C prior to pressurisation.

TABLE 6.9 Computer-Derived Data from Table 6.8

Preconditioning	X	Y
Sh	5.38306	34.03767
Sh^2	6.15908	59.7387
$(Sh)^2$	28.9774	1158.5626
H	1.07661	1.47989
V	0.36360	9.36646
N	5	23
Sf	8.30642	37.69594
Sf^2	13.8058	61.90514
$(Sf)^2$	68.9967	1420.98369
F	1.66129	1.63895
U	0.00648	0.12325
Sfh	8.89516	54.81476
W	- 0.04764	- 0.97139
b	- 7.3542	- 7.88167
a	13.29409	14.39759
$/\overline{s}$	0.0664	0.2854

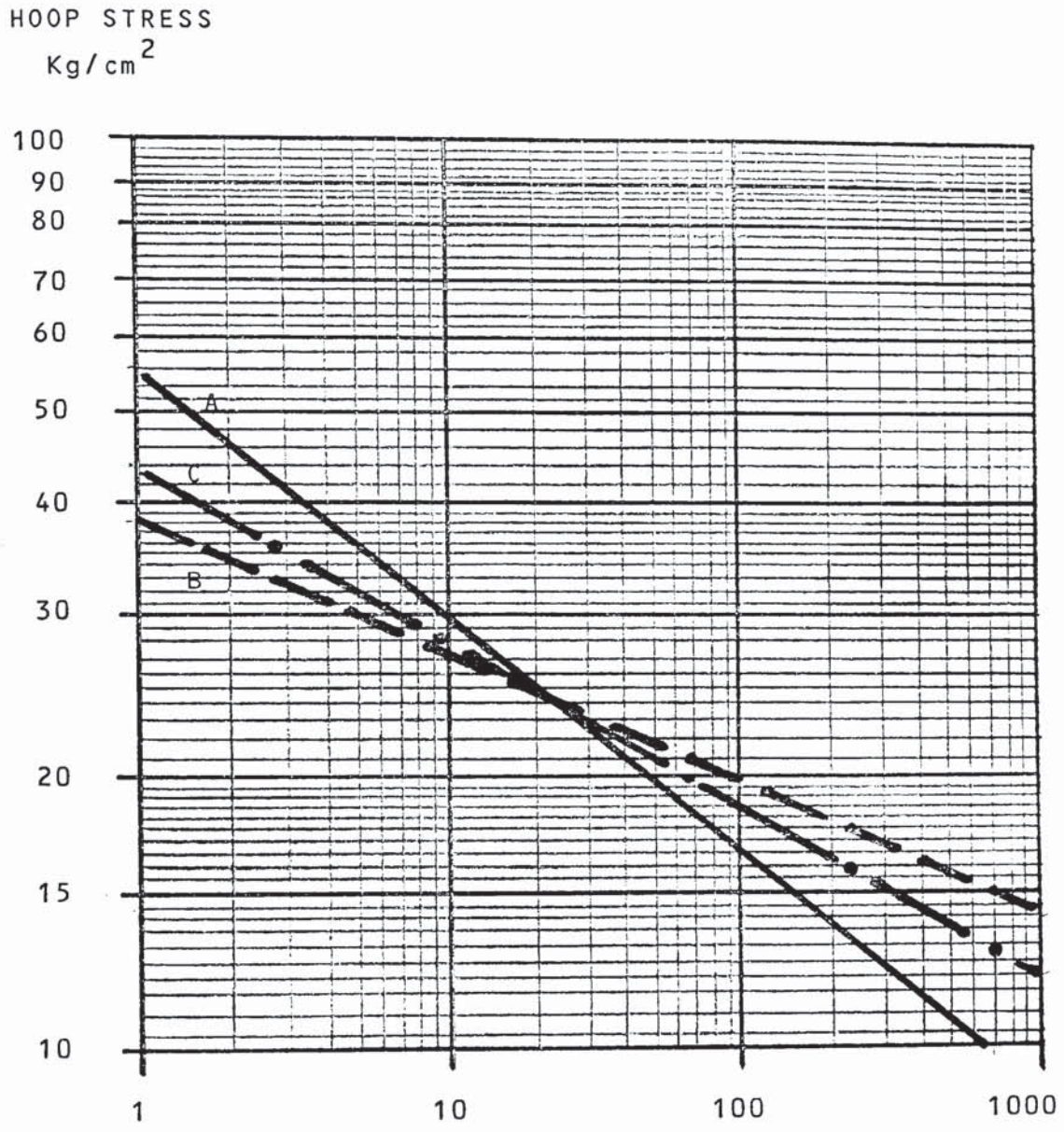

Fig. 6.3 Influence of Preconditioning in Condensate on Medium Molecular Weight Ethylene-Hexene Copolymer at 80°C

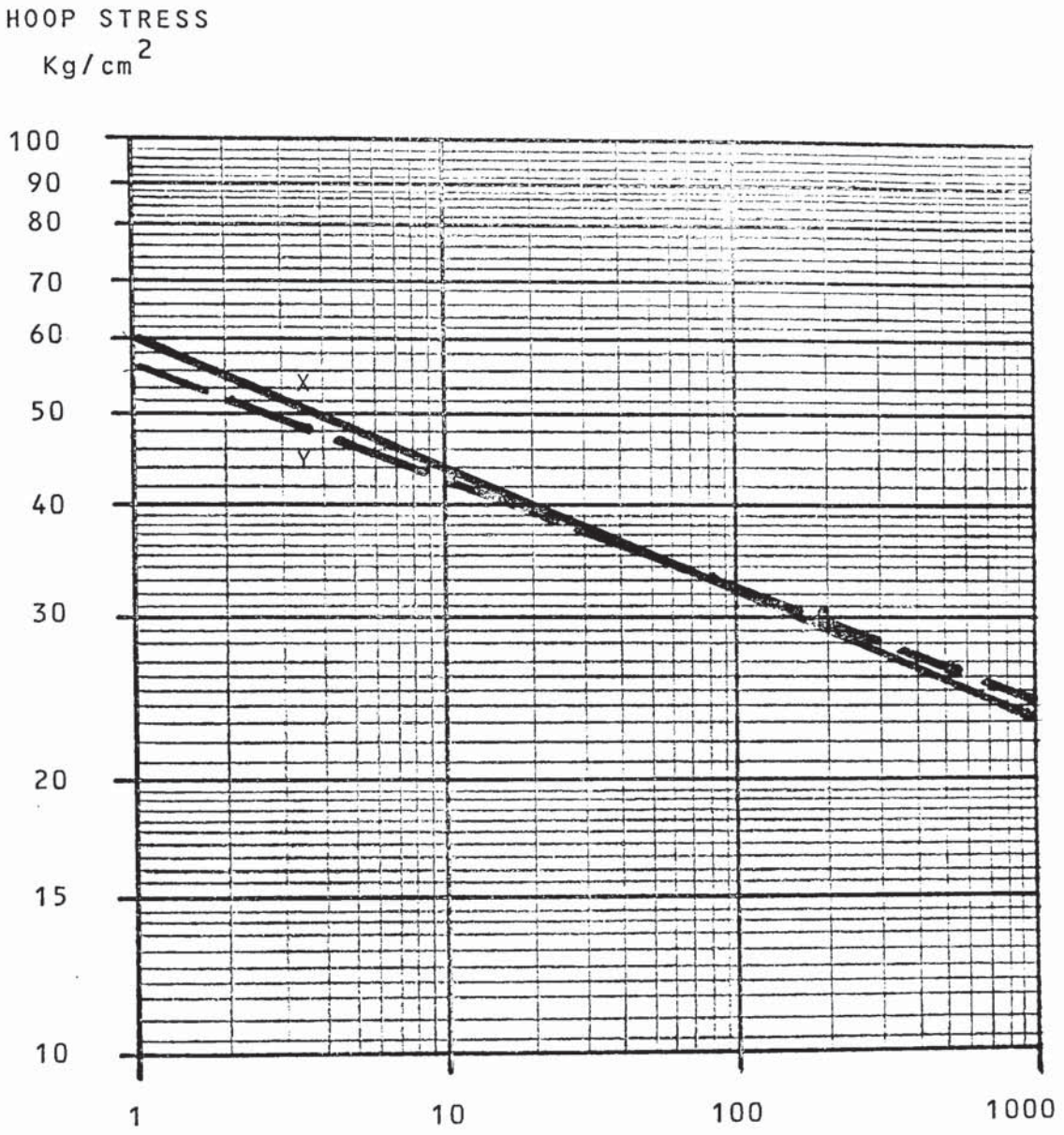

Fig. 6.4 Influence of Preconditioning in Condensate on Medium Molecular Weight Ethylene-Hexene Copolymer at 60°C

It is considered that the preconditioning influence is limited to the shorter time failures where condensate saturation has yet to occur. However, these unsaturated results will strongly bias the calculated line of lower confidence limit. As such, at both the 80°C and 60°C test temperature it was found to be more meaningful to standardise the condensate hoop stress test by conditioning the pipe samples at room temperature for 1000 hours with condensate inside the pipe followed by one hour at test temperature prior to pressurisation.

6.5.2 Influence of Pipe Wall Thickness

A separate evaluation was made to determine the influence of wall thickness on the long-term failure stress. Two series of medium molecular weight ethylene-hexene copolymer pipe samples - one set having a 50% larger wall thickness that the other - were hoop stress tested with condensate after standard preconditioning. The results are tabulated in Table 6.10.

At the high stress levels, the time to failure is longer for the thicker walled samples, although on the composite plot Figure 6.5 the failure points of both sets of pipe samples converge at the lower hoop stress values.

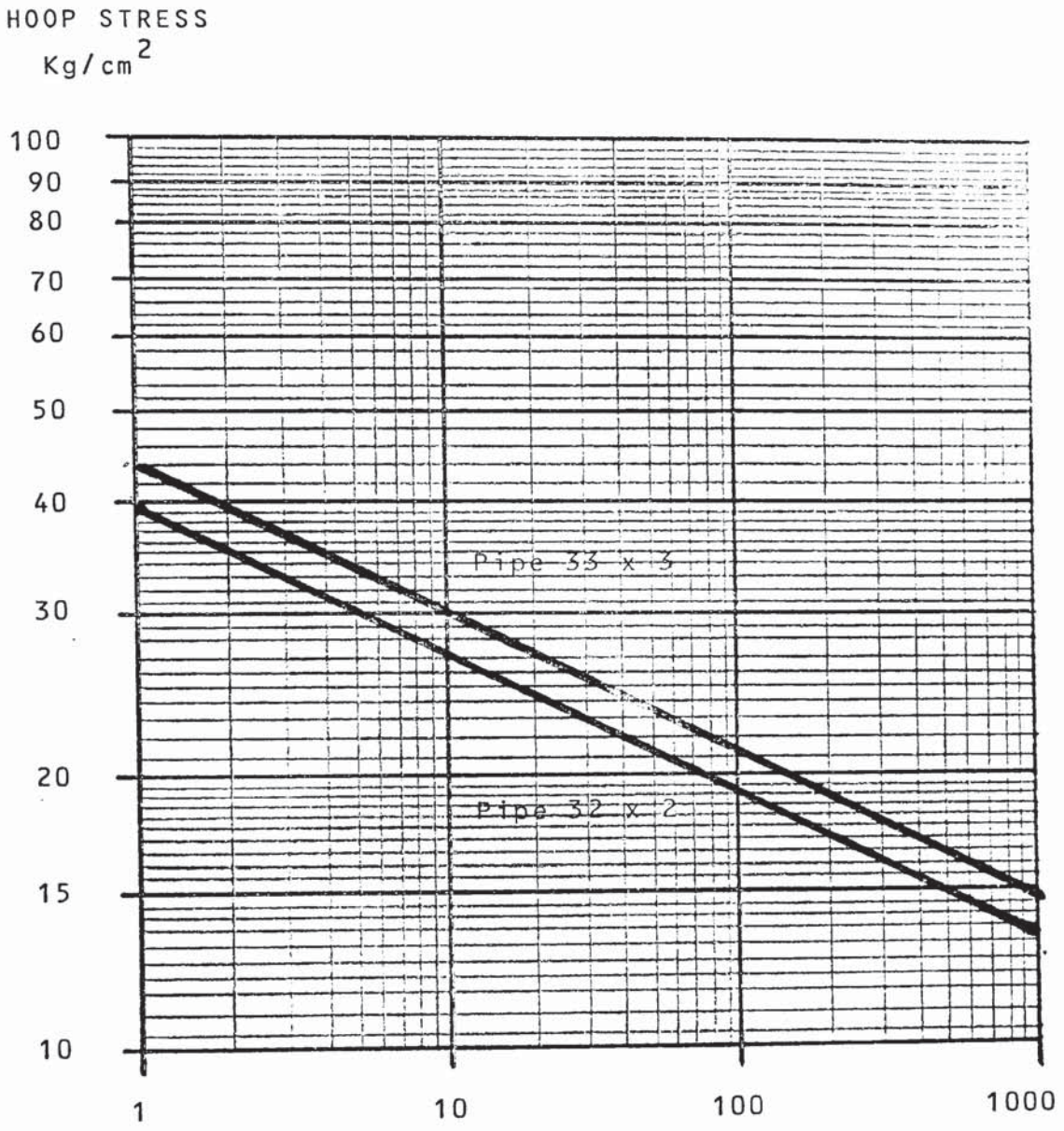

Fig. 6.5 Influence of Pipe Wall Thickness on Medium Molecular Weight Ethylene-Hexene Copolymer in Condensate at 80°C

It can therefore be concluded that, irrespective of pipe wall thickness, absorption of the gas condensate in the pipe line will occur and lead, over a period of time, to saturation of the pipe wall with a corresponding deleterious effect on the hoop stress resistance and therefore, on the long-term strength characteristics of the polyethylene pipe.

TABLE 6.10 Influence of Pipe Wall Thickness on Medium Molecular Weight Ethylene-Hexene Copolymer in Condensate at 80°C

Hoop Stress Kg/cm^2	Failure Time - hours	
	33 x 3.0mm (pipe dimension)	32 x 2.0mm
60	0.8	
55	0.03	
52	0.1	0.06
50	0.8 - 1.2	0.2
47	2.5	
45	1.8 - 5.0	0.3 - 1.5 - 1.8
42		4.3
40	12.5 - 13.1 - 18.7	3.0 - 3.4 - 3.9
37	13.0	13.0
35	22.3 - 22.5 - 23.3	5.8 - 6.8 - 9.2
33	20.9	
32		15.5
30	40.6 - 50.7	11.3 - 11.6 - 15.0
28	41.7 - 46.6	

TABLE 6.10 Cont'd

Hoop Stress Kg/cm^2	Failure Time - hours	
	33 x 3.0mm	32 x 2.0mm
27	60.2	27.1
25	74.7	28.8 - 33.2 - 102.2
24	242.1	
23	144.5	60.9 - 163.0

Preconditioning: One month with condensate in pipe at room temperature, followed by one hour at 80°C prior to pressurisation.

6.5.3 Hoop Stress Evaluation in Condensate Medium

Pipe samples of the medium molecular weight hexene copolymer and both the high and ultra high molecular weight butene copolymers were subjected to hoop stress testing at 80°C and 60°C using gas condensate as the internal medium. Due to the need for special test apparatus, these tests were performed using the facilities at the Dutch Gas Institute in Rijswijk in Holland. For these tests, preconditioning was standardised at 1000 hours contact with condensate in the pipe samples at room temperature followed by one hour at either 80°C or 60°C prior to pressurisation. The times to failure are tabulated in Tables 6.11 - 6.13 and the results plotted as lines of 95% lower confidence limit in Figures 6.6 - 6.8. For the purposes

of plotting, only the plasticised-brittle failures were considered. From these data, and employing the Larson-Miller relationship, the separation factors between the two temperatures were used to construct the gas condensation plot at 23°C. The very significant reduction in pipe hoop stress performance which could occur when polyethylene pipe is used to convey substances other than water, is illustrated by comparison of these 23°C data with the corresponding data established in a water environment (Figures 5.12, 5.18 and 5.19). These comparisons are illustrated in Figures 6.9 - 6.11.

Such condensate in a gas distribution pipeline is only likely to be present, if at all, in small quantities and thus the water and condensate hoop stress curves represent the two extremes of what is likely to be found in practice.

Mutter (211) has demonstrated that Miner's superposition law can be applied to predict the hoop stress failure plot when the pipe is exposed to natural gas condensate for only part of the time and for the remainder to natural gas, the influence of which is taken to be the same as for water.

This superposition law is:

$$\frac{Ec}{tc} + \frac{E}{t} = 1$$

Where Ec is time of contact in condensate environment

E is time of contact in water environment

Ec + E is total life of pipe

tc is time to failure in condensate environment

t is time to failure in water environment

Although the British Gas Corporation are of the opinion that gas condensates do not exist in the U.K. natural gas grid, the Dutch Gas Institute have concluded that natural gas, originating from the Groningen field, gives a condensate contact exposure time of approximately two months per year, accounting for 16.7% of the total design lifetime of the pipeline (212). Taking this value as a reference point, Fig. 6.12 presents the calculated 95% lower confidence limit long-term hoop stress (LTS) for the three polyethylene copolymers. These long-term stress data are used as the basis for design consideration in Chapter 7.

TABLE 6.11 Data Points for Ziegler High Molecular Weight Ethylene-Butene Copolymer in Condensate at 80°C

Hoop Stress Kg/cm2	Failure Time - hours
55	0.1
52	0.4
50	1.4 - 2.0
47	1.4
45	2.4 - 5.6
40	8.0 - 8.4
35	14 - 15
30	32 - 43
25	91 - 144

TABLE 6.12 Data Points for Phillips Ultra High Molecular Weight Ethylene-Butene Copolymer in Condensate at 80°C

Hoop Stress Kg/cm^2	Failure Time - hours
60	0.2 - 0.4
55	1.2 - 1.4
50	4.0 - 4.9
45	7.2 - 8.1 - 8.5
40	14.6 - 14.8 - 15.1
35	23.7 - 23.7 - 24.2
30	42.8 - 45.4 - 45.8 47.7
25	263 - 313 - 331

TABLE 6.13 Data Points for Phillips Medium Molecular Weight Ethylene-Hexene Copolymer in Condensate at 80°C

Hoop Stress Kg/cm^2	Failure Time - hours
52.0	0.1
50.0	0.8 - 1.2
48.6	2 - 3.5
47.0	2.5
46.0	24
45.0	2 - 5
44.4	12 - 18
40.3	35
40.0	12 - 13 - 18
37	13
36.4	20
35.0	22 - 23 - 40
33.0	21
32.0	30
30.0	29 - 35 - 40 - 50
29.8	82 - 92
28.0	41 - 44 - 46
27.0	60
25.0	75 - 77
24.8	96 - 120
24.0	242
23.0	144
21.0	480

Conditioning - 1000 hours at room temperature, followed by one hour at 80°C

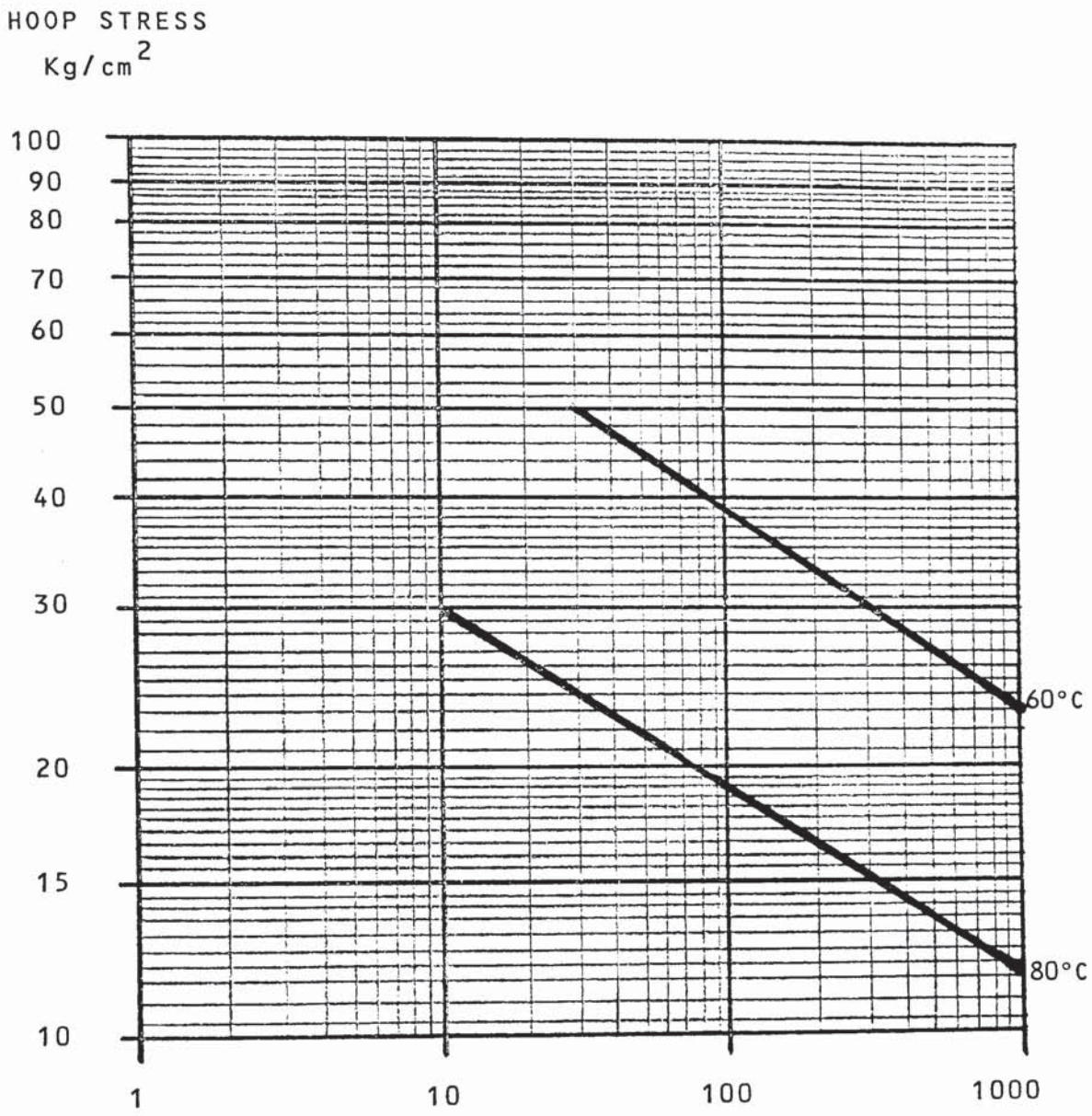

Fig. 6.6 95% LCL Plots for Ziegler High Molecular Weight Ethylene-Butene Copolymer in Condensate at 80°C and 60°C

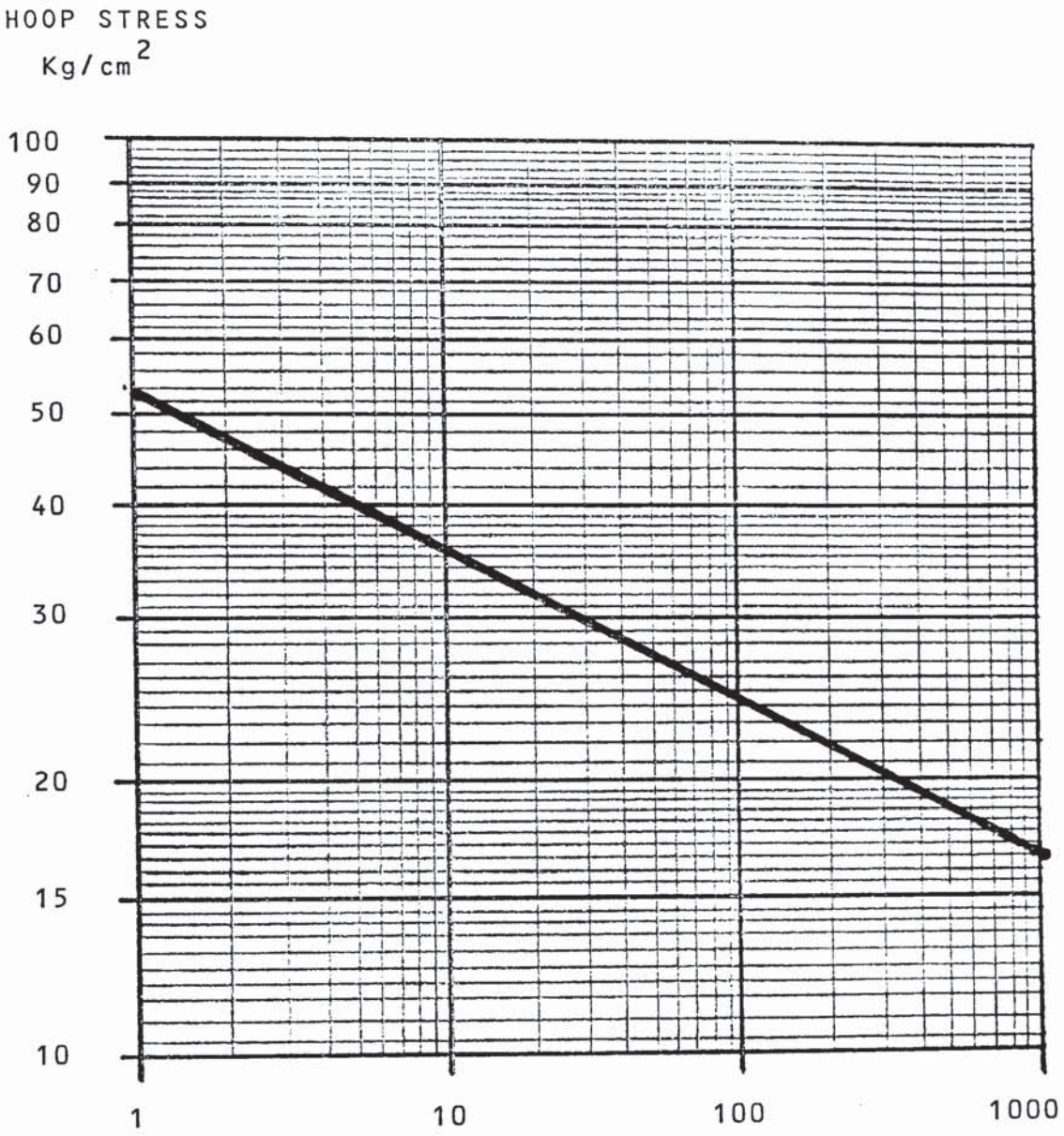

Fig. 6.7 95% LCL Plot for Phillips Ultra High Molecular Weight Ethylene-Butene Copolymer in Condensate at 80°C

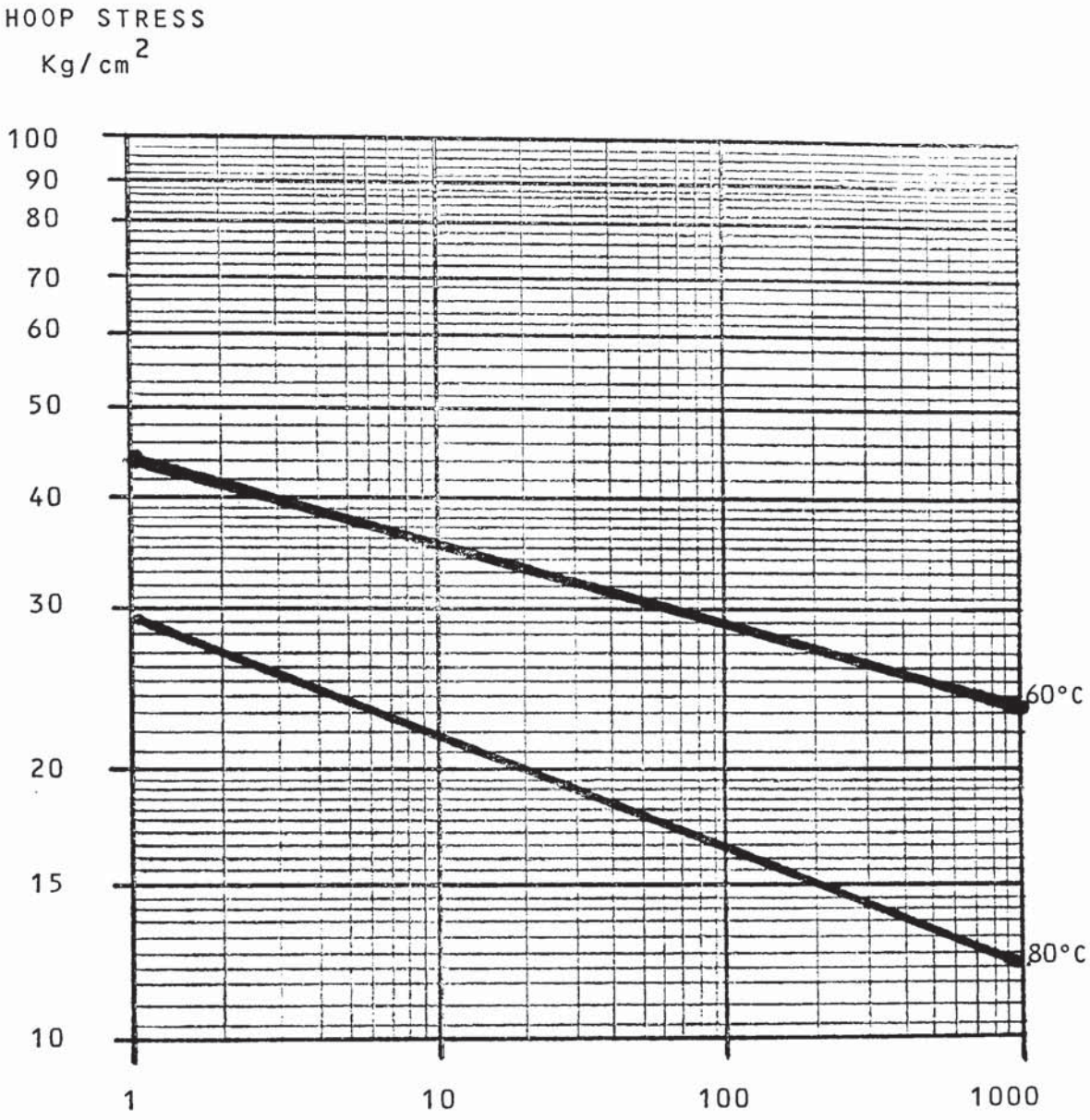

Fig. 6.8 95% LCL Plots for Phillips Medium Molecular Weight Ethylene-Hexene Copolymer in Condensate at 80°C and 60°C

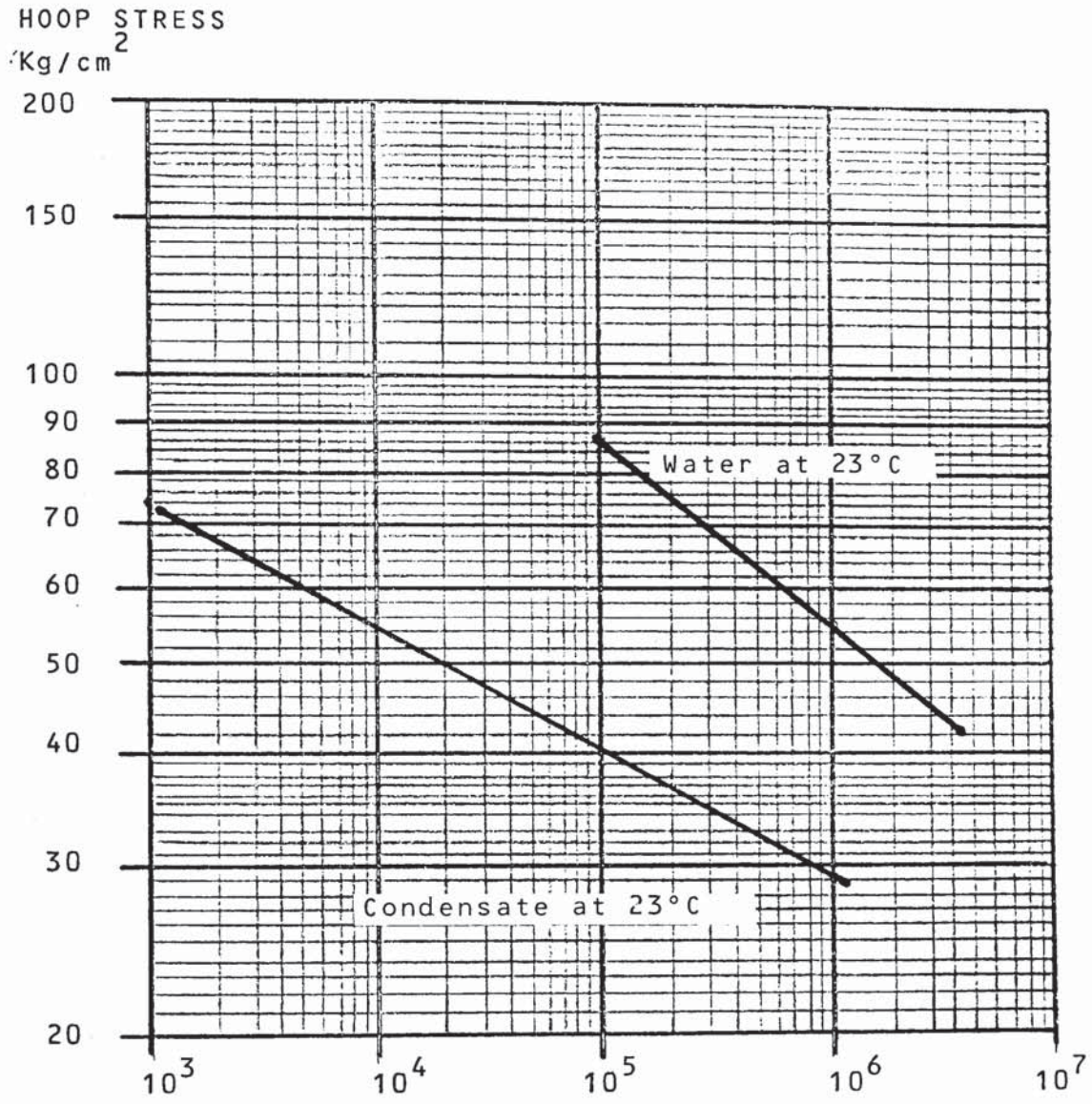

Fig. 6.9 Extrapolated 23°C Water and Condensate 95% LCL Data for Ziegler High Molecular Weight Ethylene-Butene Copolymer

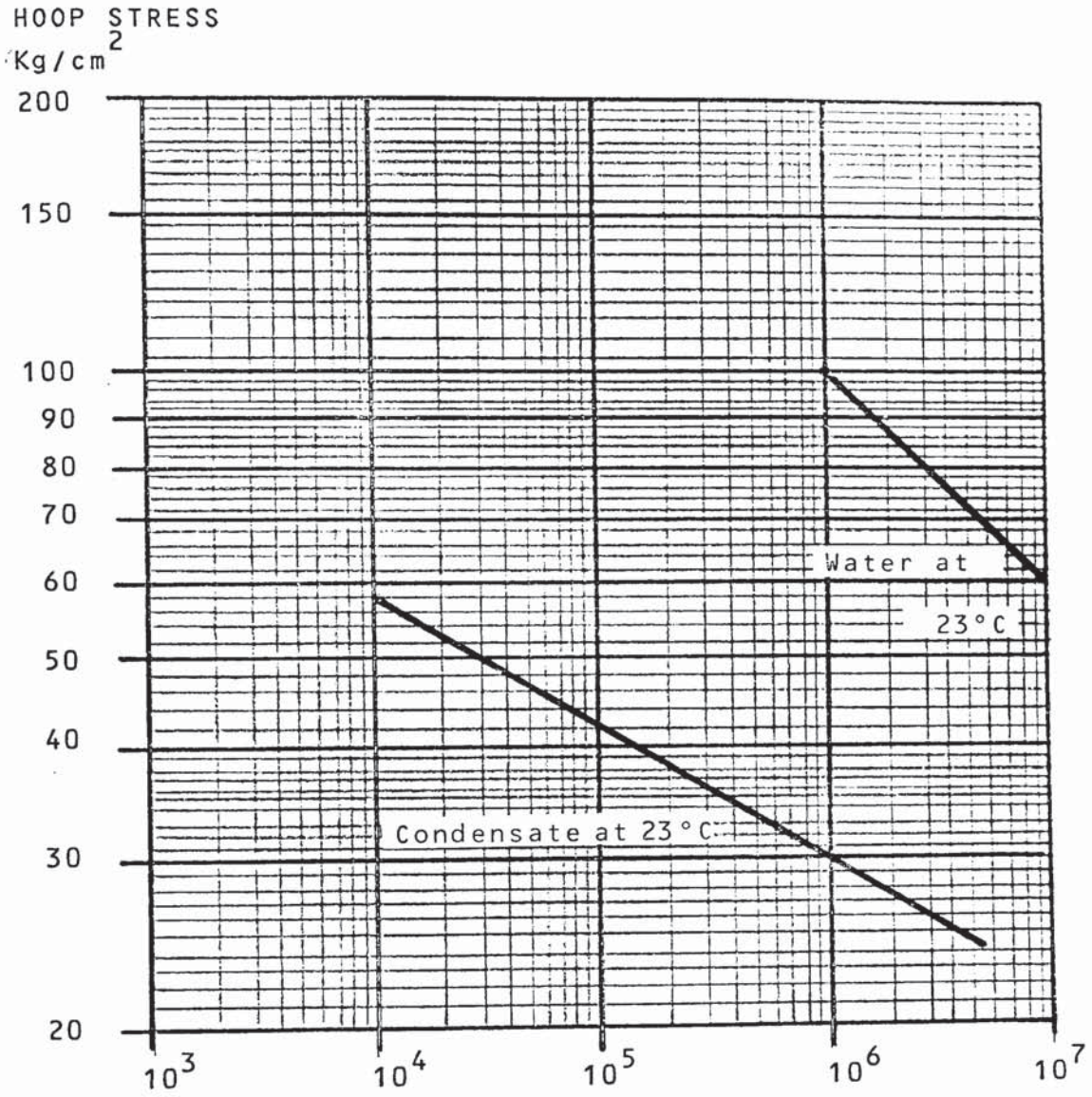

Fig. 6.10 Extrapolated 23°C Water and Condensate 95% LCL Data for Phillips High Molecular Weight Ethylene-Hexene Copolymer

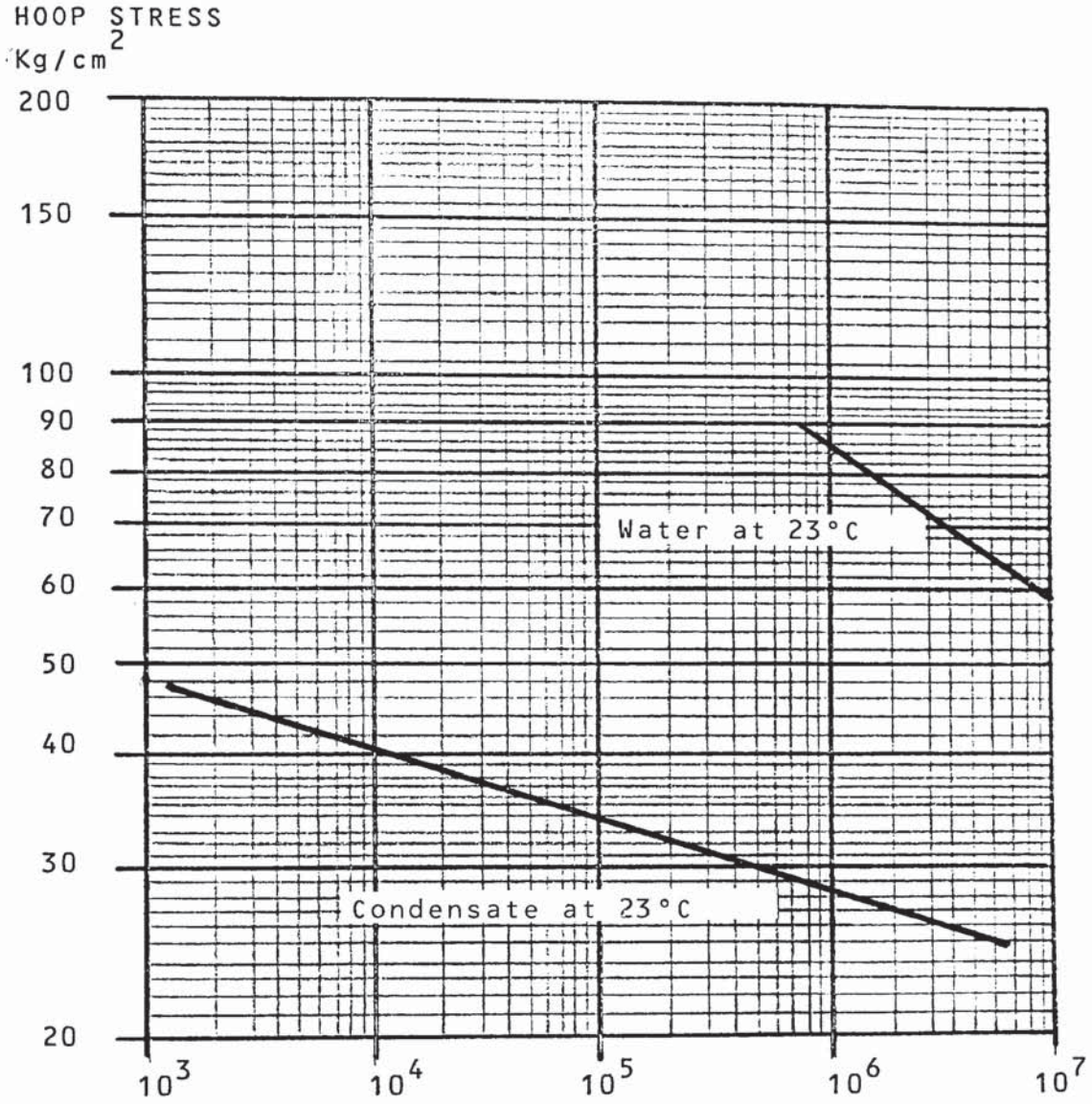

Fig. 6.11 Extrapolated 23°C Water and Condensate 95% LCL Data for Phillips Medium Molecular Weight Ethylene-Hexene Copolymer

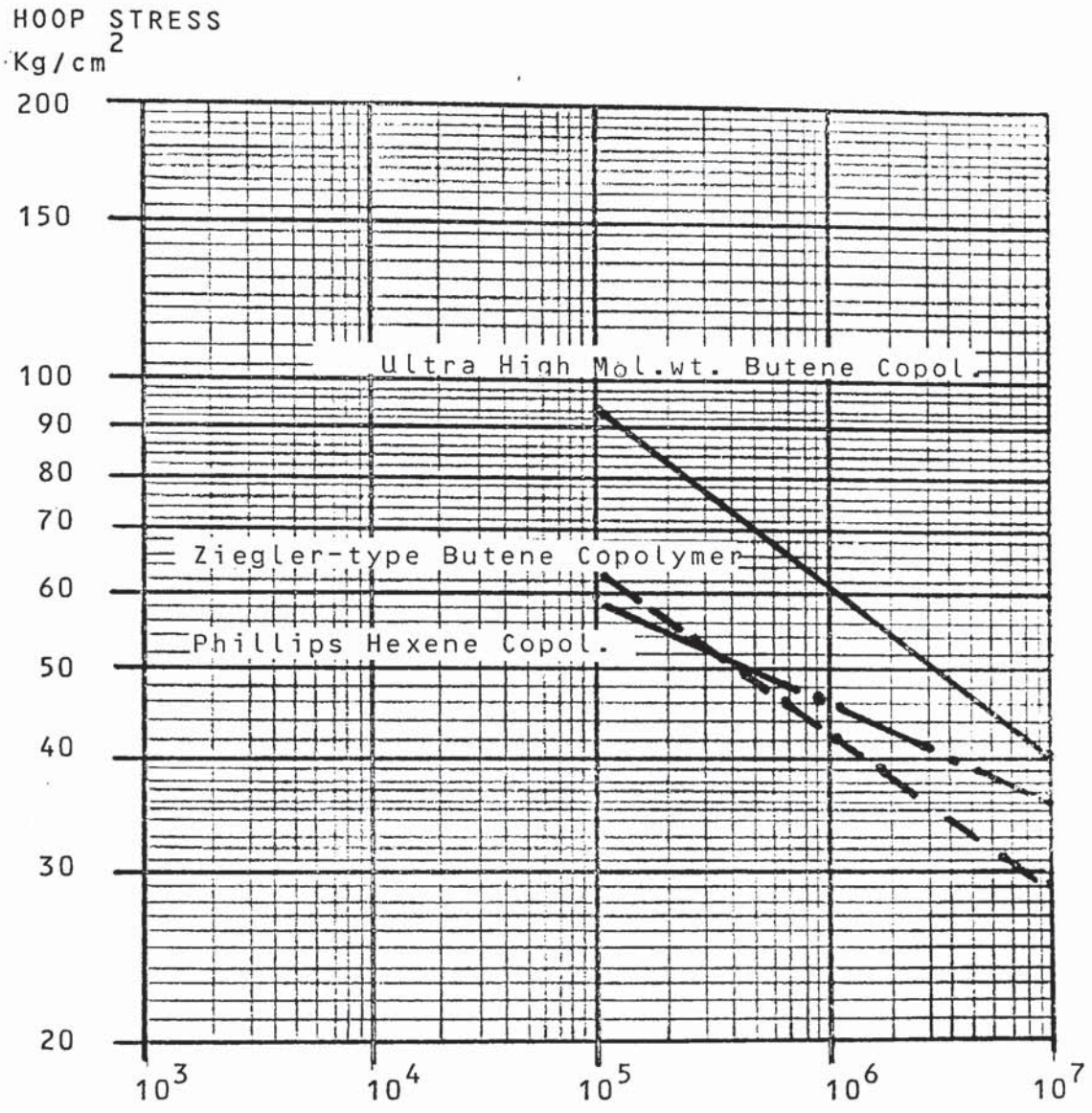

Fig. 6.12 Extrapolated 95% LCL Plots for Various Polyethylene Copolymers Subjected to Condensate for 16.7% of their Lifetime

CHAPTER 7: APPLICATION OF THE RESULTS TO PIPELINE DESIGN AND CONCLUSIONS

INTRODUCTION

The results given in the preceding chapters of this work have clearly shown that both molecular weight and type of comonomer in a copolymer can have a significant influence on the residual pipe performance characteristics and, most importantly, on the long term hoop stress resistance of the pipe extrapolated to a period of 50 years; the time period being an internationally accepted figure by municipal authorities, to allow for amortisation of pipeline costs.

Pipelines produced from thermoplastics materials can be expected to gain much further penetration into the total pipe market, not only due to their inherent advantages over the more traditional metal materials, but also - and perhaps more significantly nowadays - due to the reduction in total energy requirement to produce the pipe. In 1977 some 900,000 MT of plastics pipe were produced in Europe, accounting for a total energy requirement of 9×10^{13} Joules (213). The equivalent pipeline length in metal would have required 8 million MT of steel for a total energy requirement five times larger. The resulting energy saving of 3.4×10^{14} Joules is equivalent to 56 million

barrels of oil. The West European plastic pipe usage is projected to grow to 1.3 million MT by 1985 (214).

Much of this growth will be in the area of pressure pipe for the conveyance of potable water, natural gas and a variety of other substances, including coal slurries. The suitability or otherwise of a pipeline is, to a large extent, determined on the permissible pipe diameter to wall thickness ratio and the maximum allowable working stress, both of which are determined from the long-term strength characteristics of the pipe material.

7.1 LONG-TERM DESIGN STRENGTH

The strength characteristics of several ethylene homopolymers and copolymers have been determined in a water environment and the extrapolated long-term performance at 23°C calculated with a 95% lower confidence limit. However, these derived long-term strength values are based on consideration of only the tangential stress occuring from the internally applied pressure in the pipe. In actual usage, a buried pipe line will be subjected to additional stresses due to a variety of factors, such as soil load, inaccurate joint assemblies, soil movements, temperature differences, or even reduction of wall thickness by mechanical damage during the laying operation. Since these

additional stresses are not easily amenable to calculation, except in selected prescribed situations, it is necessary to resort to the use of a safety factor which is applied to the 95% lower confidence limit of the pipe performance. The numerical value of these safety factor components will depend not only on the knowledge available of the uncertainties to be safeguarded, but also on the consequences if pipeline failure should occur.

Data are available (215 - 217) which recommend a figure of 1.3 for the various safety factor components and thus the stress rating of the pipeline is found by dividing the long-term strength value by this composite safety factor. For the polyethylene materials under study, the stress ratings therefore become:

Polymer	Long Term Strength Kg/cm2	Stress Rating Kg/cm^2
Med. mol.wt. homopolymer	14.5	11.1
High mol.wt. homopolymer	18.0	13.8
Med. mol.wt. butene copol.	51.0	39.2
High mol.wt. butene copol.	65	50
Ultra high mol.wt. copolymer	89.8	69
Med. mol.wt. hexene copolymer	93.2	71.5
Ultra High mol.wt. hexene copolymer	101.9	78.5

7.2 APPLICATION OF STRESS RATING

The International Standards Organisation has established a recommendation (217, 218) which refers to the use of preferred numbers and of series of preferred numbers to be used for design stress ratings. The actual numbers of interest in this area of study are:

10	50
25	65
32	80

Thus the stress rating used for pipe design purposes and hence the design stress rating, is the number from the series of preferred numbers which is the closest below the value of the actually derived stress rating. The design stress ratings of the polymers and copolymers evaluated in this study are therefore:

Polymer	Stress Rating Kg/cm^2	Design Stress Kg/cm^2	Additional Safety Factor %
Med. mol.wt. homopol.	11.1	10	11
High mol.wt. homopol.	13.8	10	13.8
Med. mol.wt. butene copolymer	39.2	32	22.5
High mol.wt. butene copolymer	50.2	50	-
Ultra high mol.wt. butene copolymer	69	65	6.2
Med. mol.wt. hexene copolymer	71.5	65	10
Ultra mol.wt. hexene copolymer	78.5	65	20.8

The additional safety factor is derived from the percentage difference of the actual stress rating over the derived design stress rating. The so-derived design stress rating is then used as the basis for pipeline dimensioning according to the modified Boiler Formula:

$$\text{Design Stress} = \frac{\text{Allowable Pressure x min. pipe diameter}}{2 \text{ x minimum wall thickness}}$$

Thus, for normal service at fixed pressure levels, the use of a polymer of a higher design stress rating has an economic significance in that a pipe of higher standard dimension Ration SDR (ratio of the nominal external diameter to the nominal specified wall thickness) can be used which, with the smaller wall thickness, gives a pipe material cost savings and at fixed external diameter, the larger pipe bore of the higher SDR pipe allows a higher transmitted volume.

The applicational differences of the polymers studied are illustrated by an example where pipeline pressure is a fixed value, as is the case in water distribution pipe and an example where the maximum allowable pressure is to be found. To emphasize the differences, actual stress ratings as opposed to design stress ratings are used in the modified formula.

7.2.1 At Standard Pressure Level

At standardised pressure level of 6 Kg/cm^2, a nominal 110 mm diameter pipe would have the following wall thickness for each of the polymers studied.

Polymer Type	Wall Thickness mm	Pipe Weight/Meter Kg
Med. mol.wt. homopolymer	23.40	3.61
High mol.wt. homopolymer	19.64	3.09
Med. mol.wt. butene copolymer	7.82	1.30
High mol.wt. butene copol.	6.23	1.05
Ultra high mol.wt. butene copolymer	4.58	0.78
Med. mol.wt. hexene copolymer	4.43	0.75
Ultra high mol.wt. hexene copolymer	4.05	0.69

7.2.2 Maximum Allowable Pressure

The maximum allowable pressure for a pipe of standard dimensions of 110 mm outside diameter wall thickness would be

Polymer Type	Maximum Allowable Pressure - Kg/cm^2
Med. mol.wt. homopolymer	2.22
High mol.wt. homopolymer	2.76
Med. mol.wt. butene copolymer	7.84
High mol.wt. butene copol.	10.0
Ultra high mol.wt. butene copol.	13.8
Med. mol.wt. hexene copolymer	14.3
Ultra high mol.wt. hexene copol.	15.7

The differences in the performance characteristics of the different polymers and copolymers studied are hence most significant and advantage can be taken of this fact by either running the pipelines at higher pressure for the same pipeline diameter, or reducing the wall thickness of the pipeline for a fixed permissable pressure level, or using the pipeline under standard conditions, but operating at a significantly increased safety factor.

7.3 APPLICATION OF STRESS RATING TO GAS PIPE

The previous comments apply when the conveyed medium has little or no effect on the pipeline material. However, the data established and reported in Chapter 6 show that some of the constituents found in natural gas distribution pipelines can, and do, have a profound effect on the pipeline performance. It is thus essential that the long-term strength and design stress rating established in a water environment, be downrated when the same polymer is to be used for natural gas distribution purposes.

The 50 year, 95% lower confidence limit, design hoop stress rating (DSR) for gas use for the three copolymers of prime interest, is calculated by applying the composite safety factor of 1.3 to the long-term hoop stress figures obtained in a gas condensate environ-

ment (Fig. 6.9 - 6.11). These values are summarised in Table 7.1

TABLE 7.1 Design Hoop Stress Ratings for Ethylene Copolymers

	LTS-Water Kg/cm^2	DSR-Water Kg/cm^2	LTS-Gas Kg/cm^2	DSR-Gas Kg/cm^2
High mol.wt. butene copolymer	65	50	32.5	25
Ultra high mol.wt. butene copolymer	89.8	69	33	25.4
Med. mol.wt. hexene copolymer	93.2	71.5	29	22.3

If it is accepted that direct pipeline contact with the natural gas condensate will not occur for more than two months per year throughout the 50 years lifetime, then the long-term strength values of Fig. 6.12 will apply and the values become those as tabulated in Table 7.2:

TABLE 7.2 Ethylene Copolymer Ratings for Gas Use With 16.7% Contact Limit

	LTS - 16.7% Contact	DSR - 16.7% Contact
High mol.wt. butene copolymer	50.5	38.8
Ultra high mol.wt. butene copol.	73	56.2
Med. mol.wt. hexene copolymer	50.75	39

7.4 BASIS OF IMPROVED PERFORMANCE

Because of their relative simplicity of structure, the long, flexible chain molecules of linear polyethylene assume a planar zig-zag conformation. The individual molecules may be related to each other in a completely amorphous manner; looped, coiled or entangled with each other, or in the orderly pattern of a crystalline region. In the crystalline region, like portions of chain segments are nested together so that a repeating geometric pattern in space results. The level of crystallinity as determined (219) by X-ray studies or by nuclear magnetic resonance techniques for a polyethylene of 0.96 g/cc density will be 93%. In the case of low density polyethylene, where polymerisation is by a free radical mechanism, the chain transfer reactions lead to considerable branching in the molecular chains and these irregularities reduce the chain packing ability such that the degree of crystillinity for a polymer of 0.92 g/cc density is only 65%. The higher degree of crystallinity of the higher density product results in a higher melting point, higher tensile strength, higher flexural modulus, lower permeability and greater hardness than for the product of lower density.

Polyethylene is composed of both crystallites and amorphous regions with a given molecule extending

through more than one crystilline region and the intervening amorphous regions. Strong primary atomic bonds hold the elements of the chains together and, since polyethylene is non-polar, the intermolecular attraction between the chains is due to Van der Waals forces. Creep of such material involves rupture or interchange of these forces, resulting from stress (220). This action permits the molecules as a whole or molecular segments to slide past one another.

The high creep resistance of the more crystalline polyethylenes results from the reduced mobility of the bulk polymer. The mobility of chain segments in a crystallite is very small at a given stress compared to that in the amorphous region. Thus creep of a partially crystalline material occurs entirely in the amorphous regions and the crystallites merely rotate or deform elastically under small strain creep. Creep involving larger strains may result in increased crystallinity due to orientation of molecular segments (221).

Due to the non-polarity and comparatively low intermolecular forces of attraction, when polyethylene chains are under stress they tend to slip and untangle. This results in creep and cracking failures of the types found in pressure pipe and in environmental

stress cracking. Since it is more difficult for long molecules to be completely accommodated in the crystallites, owing to the greater degree of entanglement it follows that as molecular weight is increased, density and density dependant properties will decrease but also chain slippage and untanglement will be more difficult giving rise to better creep properties and higher environmental stress cracking resistance and is the basis of the improved performance tabulated in Table 3.2 of Chapter 3.

The freedom from chain branching in high density polyethylene results in a high crystallinity. This freedom from branching gives high values for density related properties such as short term tensile strength but less satisfactory performance in long term creep dependent properties since the linear chains can more easily untangle themselves. The introduction of a controlled, small number of random, short chain branches during the polymerisation of high density polyethylene does not dramatically change the long chain structure of the polymer, but does have a very noticeable effect in reducing the crystallinity and hence the properties dependent upon crystallinity. On a mole basis, the larger butyl branch (hexene-1 comonomer) is more effective in reducing crystallinity that the ethyl branch (butene-1 comonomer) which

itself is more effective than the smaller methyl branch (propylene comonomer). The influence of reducing crystallinity on the mechanical properties is shown in Table 3.1 of Chapter 3 and further discussed in Section 3.5.3. The effect of the comonomer on the basic linear polymer chain is to disrupt the order. In Section 3.2.4 it was stated that 21 methyl branches per 1000 carbon atoms were equivalent to 14 ethyl branches insofar as lowering of crystallinity is concerned. As the side group introduced through copolymerisation increases in size in the homologous series ethylene to propylene to butene-1 to hexene-1, the number of branches necessary to reduce overall crystallinity diminishes. At equivalent molecular weight this leaves a correspondingly longer length of side chain to become independently included in two or more different crystals.

Hayes and Webster (222) propose that these branches reduce crystallinity with some loss of desirable density dependent properties such as stiffness and softening point, but make chain slippage and disentanglement more difficult and therefore improve creep properties. Although this explains the improved performance of a copolymer over an ethylene homopolymer, the explanation is not quite so satisfactory when applied to the improvements shown by the copolymers

of the higher homologues such as ethylene-hexene copolymers compared to the ethylene-propylene and ethylene-butene copolymers.

7.5 BASIS OF IMPROVED HOOP STRESS RESISTANCE

At low stresses, very little creep at short times occurs and molecular movement is considered to be limited to movement of some segments in favourable positions. However, rotation of other segments into favourable positions probably also occurs since at longer test duration there is a marked change in the creep rate at low stresses (223). At higher stresses, a second mechanism involving a more complete intermolecular movement dominates and thus superposition of the complete hoop stress curve, consisting of both ductile and brittle failure portions, must be individually performed.

Reference was made in Chapter 3 to a structural model for polyethylene. Meyer and Funck (224) propose that the polyethylene molecules or chains fold back on themselves and each other to form layers that are stacked one on another and essentially randomly oriented throughout the pipe wall. In the areas of tie-chains, some of the molecular chains go through one layer of folds into the next one, and in this area the two are tied together.

During the pipe extrusion process, the hot molten polymer passes through a cooling unit where the outside of the pipe wall is rapidly cooled and the inner pipe wall is cooled more slowly. This will result in the modulus and crystallinity of the outer wall material being lower than that of the inner wall; the modulus gradient depending upon the pipe wall thickness. In addition, it is to be expected that the orientation arising from the extrusion process would confer a higher creep modulus in the longitudinal direction and a lower modulus in the circumferential direction. However, for the pipe sizes studied in this work, Moore and Turner (225) showed that the modulus anisotropy was low. In addition, Cash (226) had demonstrated that at an extrusion linear speed of 5 metres/min, the inner pipe wall of a pipe of wall-thickness 3.3 mm will have a temperature below the crystallisation temperature within the first metre length of the cooling unit. Thus, in the pipe samples evaluated, the overall anisotropy can be considered as being low.

When the pipe samples are stressed with a high instantaneous loading, the strain response to the applied tensile stress is so large that a gross decrease of cross-section occurs locally in the specimen. The failure by this mechanism is always in the radial

direction and gives rise to the characteristic ductile failures shown in the photograph of Fig. 5.3. The elongation of partially crystalline polymers produces orientation of crystallites and orientation of molecules in the non-crystalline portions of the polymer (227). In the case of the highly crystalline homopolymers, there is insufficient time for chain slippage to occur and thus the folded chains lengthen by unfolding. The high elongation thus converts crystals consisting of folded chains to bundle-like crystals as illustrated in Figure 7.1.

Taylor (227) has proposed in a study on the strength of glass under constant load that the slow process preceeding fracture is taken to be the orientation of the atomic network contained in an elementary prism. Additionally, Bucknall (228) has shown that crazing is accompanied by a small, but measurable, elongation and that in order to fracture a glassy polymer it is necessary to expand a thin layer of the material to form a craze and then to extend the crazed layer to its breaking point.

The pipe hoop stress ductile failure is thus determined by the tensile yield stress which itself is determined by density or level of crystallinity. At the shorter time periods, the more crystalline homo-

polymers will have a higher failure stress than the less crystalline copolymers and this has been shown to be true in Chapter 5. The higher than expected failure stresses for the copolymers are explained on the same basis as that for the mechanism of craze formation (229). The effect of copolymerisation of ethylene with minor amounts of a higher butyl group being more effective than the smaller ethyl and methyl groups. The relatively larger proportion of non-crystalline zones act as local drawability zones. Fibril-type, threadlike molecules are withdrawn, when under stress, out of the unorientated amorphous zones and are orientated in the direction of the greatest occurring tensile stress. As such, it is to be expected that the copolymers would show a lower initial failure stress than homopolymer polyethylene but that the gradual formation of the orientated fibrils would maintain the stress resistance over a longer time period and this again has been shown to hold true in Chapter 5. Failure always occurs at the point of the highest tensile stress, which is the stress in the hoop direction and thus the failure point as in the case of the homopolymers will be orientated perpendicular to the pipe axis (in the case of pure internal pressure).

The time which elapses between stress application and

pipe failure increases as the applied stress decreases. At lower stresses, instead of a ductile failure, cracks develop, after which the intervening material yields. At still lower stresses, the failure is more directly due to the growth of cracks rather than a true yield phenomenon. At these low levels of stress, chain slippage becomes the dominant mechanism. Failure is by a separation along the boundaries between the layers of chains and in this mechanism of failure (Fig. 7.2) there is no prior elongation. The failure appears as a small slit in the axial direction as illustrated in the photograph of Fig. 5.4.

The transition in failure mode from ductile to brittle is clearly the point at which the chain slippage mechanism predominates. This transition point for all the polymers investigated has been shown to be controlled by the temperature of testing. During elevated temperature testing an annealing process occurs in the pipe specimen. Differential scanning calorimeter studies (230) on virgin pipe material and a pipe sample exposed at 80°C gave a much narrower endotherm for the exposed pipe sample. The narrower, taller, peak suggests that the crystal structure is more uniform and regular than the virgin material which gave a broader peak. It is proposed that this is the result of the increase in crystallinity during anneal-

ing by the testing process and therefore corresponds to the reduction in volume of the amorphous regions as polymer chains from the amorphous region are drawn into the spherulites as the fold length of the lamellae increases during annealing.

The extent to which annealing can occur is determined by the original structure. Higher molecular weight polymers and copolymers with longer side branches will have more difficulty in being accommodated into the spherulites than the polymer chains of lower molecular weight homopolymers or short side branched copolymers.

7.6 BASIS FOR ESTIMATION OF SEPARATION FACTOR

The separation factor C determined and used in this work was found to lie between 21.6 - 22.2 for most of the results where an adequate number of pipe samples were tested. The value of the separation factor C can be estimated for a specific polymer from the average number of effective molecules per mole and the concentration of polymer in gramme - moles per unit volume. Assuming that the rate of rupture of the molecules is proportional to the concentration of polymer present and that the maximum value of the rate corresponds to Avogadros Number,

$$\text{then rate } K = \frac{P}{t}$$

where P is the contentration in gramme-moles per unit volume

t is the time

and separation factor C = log Ko = log P

Where Ko is average number of effective molecules per mole.

Applying this to the three polymers studied, Ziegler polymerised ethylene butene copolymer, Phillips polymerised high molecular weight ethylene butene copolymer and the Phillips polymerised ethylene hexene copolymer gives:

	Copolymer type		
	Ziegler butene	Phillips butene	Phillips hexene
Base resin density g/cc	0.945	0.943	0.939
Number average mol.wt.	50,000	27,000	17,000
Average number of $-ch_2$ units per chain	3,571	1,929	1,214
Ko x 10^{20}	1.686	3.121	4.958
Concentration gramme-moles	0.019	0.035	0.055
Separation factor C	21.95	21.95	21.95

7.7 CONCLUSIONS

In the survey of the European market for the use of ethylene copolymers for the distribution and service lines for natural gas, usage is projected to increase at an average annual growth rate of 17.7% from an

estimated volume of 19,000 MT in 1980, to 43,000 MT by 1985. This estimated volume will represent some 30% of the total high density polyethylene pipe consumption of 1985.

The performance requirements for natural gas distribution pipelines, because of the hazardous nature of the transported medium, should be more severe than those for the distribution of potable water. With this in view, the work presented here sets out a comparison between ethylene homopolymers and various copolymers and their suitability or otherwise for this market, on the basis of hoop stress performance.

The influence of copolymerisation is adequately demonstrated by comparison of the extrapolated long-term strength of the homopolymers in Section 5.3.1 with the strength of the ethylene-butene and ethylene-hexene copolymers of the subsequent sections.

On an approximately equivalent molecular weight basis this comparison becomes:

	50 year Hoop Stress Value
Homopolymer	18.0 Kg/cm^2
Ethylene-butene copolymer	51.0 Kg/cm^2
Ethylene-hexene copolymer	93.21 Kg/cm^2

The influence of molecular weight is adequately demonstrated in each of the three categories studied: homopolymers, ethylene-butene copolymers, and ethylene-hexene copolymers. The extrapolated 50-year room temperature hoop stress value shows a marked increase in each case for the higher molecular weight polymer or copolymer. In addition, it is shown that the combination of increased molecular weight with copolymerisation has a synergistic effect on the long-term stress value as shown below.

Polymer type	Melt Index dg/min	50-year Stress Value Kg/cm^2
Homopolymer	0.8	14.5
	0.2	18.0
Ethylene-butene copolymer	0.3	51.0
	14.0 (HLMI)	65.0
	2.0 (HLMI)	89.84
Ethylene-hexene copolymer	0.3	93.21
	2.0 (HLMI)	102.31

The hoop stress performance characteristic at different temperatures for all of the polymers studied has been shown to be related by a separation factor of approximately 22 for the brittle portion of the curve.

With respect to performance, both the hoop stress evaluation and weathering test data demonstrate the superiority of black compositions and thus some

reservation should be placed on the stipulation that natural gas distribution pipelines be coloured yellow. A much safer approach would be to use a correctly dispersed black composition which is then subsequently colour-coded during the extrusion process.

The incidence of constituents found in some distributed natural gases have been shown to have a significant deleterious effect on the hoop stress resistance and thus for design purposes, it is essential that this effect be taken into consideration. Although not extensively examined, there is sufficient indication to show that complete desorption of condensate is unlikely to occur.

The evaluationary results demonstrate that the most suitable polymer for natural gas distribution pipelines would be a higher molecular weight ethylene hexene-1 copolymer. Assuming that the average contact time with gas condensate is no more than two months per year, the design strength rating used for design purposes should be 39 Kg/cm^2 for materials in the molecular weight range of 150 - 200,000, and 55 Kg/cm^2 for higher molecular weight polymers.

7.8 SUGGESTED FURTHER WORK

7.8.1 The results presented in this work have been related to the evaluation of pipe samples. Pipelines of necessity, also contain fittings and valve assemblies, the intricate design of which must result in highly-localised moulded-in stresses. There is thus scope to evaluate the long-term resistance of such mouldings and to investigate the influence of the service conditions on the method of jointing such mouldings to the pipe.

7.8.2 The evaluations made on pipe samples in this work have centred on both a water and a gas condensate environment. Since some considerable quantities of plastics pipelines are used in the chemical industry, the scope of this work could be expanded to include other environments found in such industries. In addition to chemical pipework, a newer industry will be slurry pipelines.

7.8.3 The separation factor determined in this work was found to lie between 21.6 - 22.2. Theoretical considerations would indicate that the figure should be 21.95. It is thus proposed that a considerably larger number of pipe samples be tested over a longer time duration and at more temperature intervals, to verify the value of the separation factor.

7.8.4 This work has concentrated on the ethylene copolymers of high density. There is in Denmark (231) a proposal to use low density polyethylenes for natural gas distribution. The advent of linear low density polyethylenes has also broadened the scope of the polyolefin types available and their overall suitability for natural gas distribution purposes should be evaluated.

7.8.5 A point of further concern is that the testing procedures employed in this work used static conditions. In practice the medium continually passes through the installed pipe and this would contain more oxygen than the laboratory model. This factor is of significant importance for such applications as domestic hot water distribution or domestic central heating systems, where the resistance to oxidation at temperatures approaching 95°C by air dissolved in the water is of utmost importance.

7.8.6 It is considered of interest to investigate the change in crystalline nature of pipe samples and to monitor this change in nature during elevated temperature testing and also to compare the results from pipe with significant service life.

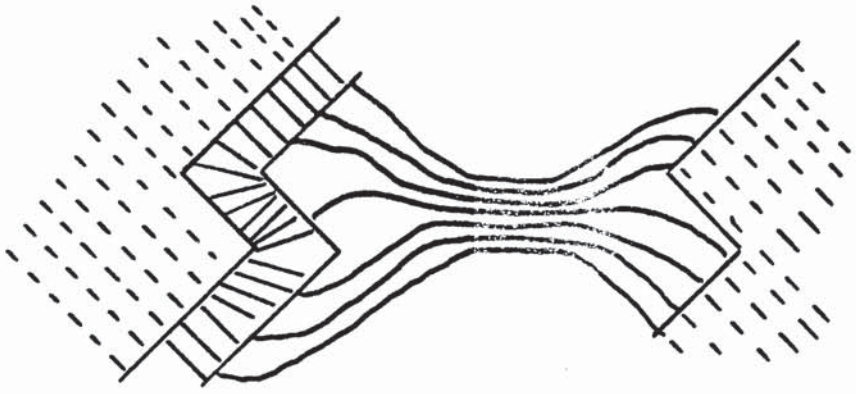

Fig. 7.1 Scheme of Conversion of Folded Chains to Bundle-like Crystals

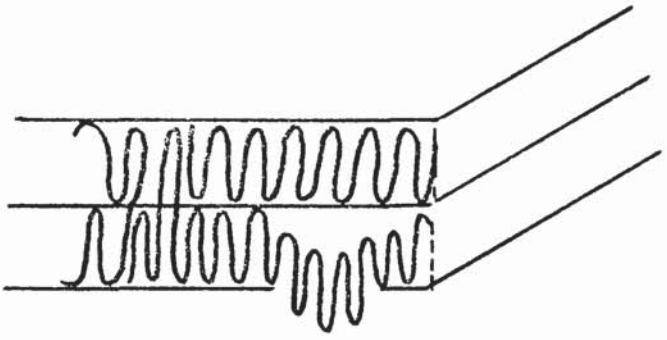

Fig. 7.2 Boundary Separation Between Layers of Folded Chains

CHAPTER 8: APPENDICES

8.1 METHODS OF TEST

The methods of test used to determine the results presented in Chapter 3 can be found in the Annual book of ASTM Standards, Part 35. The more relevant methods are summarised below.

8.1.1 Density

Test made in accordance with ASTM D 1505-75, using a density gradient column prepared from an isopropanol-water mixture. Density of a specimen is determined by observing the level to which it sinks in the liquid column in comparison with standards of known density.

8.1.2 Vicat Softening Temperature

Test made in accordance with ASTM D 1525-76 and covers the determination of the temperature at which a flat-ended needle of $1mm^2$ circular cross-section will penetrate the specimen to a depth of 1mm under a load of 1 Kg and using a uniform rate of temperature rise of 50°C/hour.

8.1.3 Melt Index

Test made in accordance with ASTM D 1238-73 and covers the measurement of the rate of extrusion of molten polymer at 190°C through a die of 2.095mm in diameter

and 8mm in length and under an applied load of 2.16 Kg (Melt Index) or 21.6 Kg (high load Melt Index).

8.1.4 Bell E.S.C.R.

Test made in accordance with ASTM D 1693-75 and covers the determination of the susceptibility of the material to environmental stress cracking when bent specimens, each having a controlled imperfection, are exposed to the action of a surface active agent at elevated temperatures.

8.2 COMPUTER PROGRAMME

The computer programme used to establish the 95% lower confidence limit data of the hoop stress - time to failure results of Chapters 5 and 6, is reproduced below.

```
LIS


HOLL        03:54CST    02/05/79

100         OPTION NOCHECK,NOWARN
105         IMPLICIT DOUBLE PRECISION (A-Z)
110         DIMENSION FH(500),H2(500),F2(500)
115         DIMENSION MEAN(2)
120         REAL T(500),S(500),X(500),R(3),YMIN,YSTEP
125         DIMENSION TE(500),TB(50,8),HE(500),H(500),F(500),TST(3)
126 STRING FT
130         ALPHA Q(16),Q6(6),TAB(4),MES(2)
135         INTEGER IT(500),NP,JT,I2,I,J,K,L,ND
137         INTEGER I1
138         FD(Y,ND)=DINT(10.D0^ND*Y+5.D-1)/10.D0^ND
140         CALL LECTURE(T,S,NP,FT)
145         CALL QUICKI(NP,T,IT)
147         JT=1
150         MP=NP
155    155  SH=0.D0
160         SF=0.D0
165         SH2=0.D0
170         SF2=0.D0
175         SFH=0.D0
180         DO 235 I=1,NP
190         H(I)=FD(DLOG10(T(I)),5)
195         F(I)=FD(DLOG10(S(I)),5)
200         H2(I)=FD(H(I)*H(I),6)
205         F2(I)=FD(F(I)*F(I),6)
210         FH(I)=FD(F(I)*H(I),6)
215         SH=SH+H(I)
220         SF=SF+F(I)
```

```
225         SH2=SH2+H2(I)
230         SF2=SF2+F2(I)
235    235  SFH=SFH+FH(I)
240         MEAN(1)=FD(SH/MP,6)
245         MEAN(2)=FD(SF/MP,6)
246         YMIN=AINT(SNGL(10.^MEAN(2)+.5))-25.
247         YSTEP=1.
260         SHH=FD(SH*SH,7)
265         SFF=FD(SF*SF,7)
270         U=SF2-FD(SFF/MP,6)
275         V=SH2-FD(SHH/MP,6)
280         W=SFH-FD(FD(SF*SH,5)/MP,6)
285         B=FD(W/U,5)
290         A=FD(MEAN(1)-FD(B*MEAN(2),6),5)
295         IF(B.LE.0.D0)GOTO 310
300         PRINT 640,MES(1)
305         GOTO 755
310    310  VAR=(1.D0/(MP-2.D0)*FD(V-FD(FD(W*W,6)/U,6),6))
315         STD=FD(DSQRT(VAR),6)
320         DO 330 I=1,NP
325         HE(I)=FD(A+B*F(I),6)
330    330  TE(I)=FD(10.D0^HE(I),0)
332         IF(JT.EQ.0)GOTO 395
335         PRINT 750,NP-2
340         INPUT 705,TST
345         PRINT 735
347         INPUT 705,TAB
355    355  IF(TAB(1).NE."YES ")GOTO 395
356  PRINT,' <<< '+FT+' >>>'
360         PRINT645
365         PRINT 710
370         DO 390 J=1,NP
```

```
375         I=IT(J)
380         PRINT 645,I,T(I),S(I),H(I),F(I),FH(I),H2(I),F2(I),HE(I),TE(I)
385         IF(MOD(J,5).EQ.0)PRINT645
390    390 CONTINUE
395    395 IF(TAB(2).NE."YES ")GOTO 410
396 PRINT,' <<< '+FT+' >>> '
400         PRINT 650,SHH,SFF,SH2,SF2,SH,SF,MEAN(1),MEAN(2),NP,SFH
405         PRINT 665,U,V,W,A,B,VAR,STD
410    410 IF(TAB(4-JT).NE."YES ")GOTO 590
412         PRINT,"INPUT MINIMUM & STEP"; INPUT, XMIN,XSTEP
413         XMIN=XMIN-XSTEP
425         DO 530 I1=1,5
426         DO 530 I2=1,10
427         I=I2+10*(I1-1)
437         TB(I,1)=DBLE(XMIN+FLOAT(I)*XSTEP)
440         IF(XSTEP.NE.0.)GO TO 456
445         TB(I,1)=(1+MOD(I-1,9))*10^IFIX((I-1)/9)
455    456  TB(I,2)=FD(DLOG10(TB(I,1)),5)
460         D=TB(I,2)-MEAN(1)
480    480 DO 530 J=1,3
485         K=J*2
490         L=K-1
495         TB(I,K+2)=A+B*TB(I,2)-STD*TST(J)
500         TB(I,L+2)=FD(10.D0^TB(I,K+2),0)
530    530 CONTINUE
535         IF(JT.EQ.0)PAUSE"POSITION TO A NEW PAGE AND PRESS 'RETURN'"
540         PRINT 675,Q(2),(Q(1),J=1,9)
545         PRINT 680,Q(6),Q(6),Q6,Q(5),FT,Q(4),Q(5),Q6,Q(7),(Q6,Q(6),J=1,3),Q(5),Q(3),Q(4),Q(3),
550        &Q(3),Q(13+JT),Q(15+JT),Q(3),Q(3),Q(4),Q(5),Q(14-JT),Q(16-JT),Q(4),Q6,Q(6),Q6,Q(6),Q6,
555        &Q(5),Q(5),Q(3),Q(4),(R(J),Q(4),J=1,3),Q(5),(Q6,Q(7),J=1,3),Q6,Q(5),Q(5),Q(8+JT),Q(4),
560        &Q(12),Q(10+JT),Q(4),(Q(9-JT),Q(4),Q(12),Q(11-JT),Q(4),J=1,3),Q(5),(((Q6(J),J=1,3),Q(7),
565        &I=1,2),K=1,3),(Q6(J),J=1,3),Q(7),(Q6(J),J=1,3),Q(5)
```

```
      DO 580 I=1,50
  575 PRINT 695,Q(5),(TB(I,K),Q(4),K=1,8)
  580 CONTINUE
      PRINT 700,(Q6,J=1,4),Q6(1),Q6(1)
  590 JT=JT-1
      IF(JT.LT.0)GOTO 755
      CALL CMOVE(T,X,500)
      CALL CMOVE(S,T,500)
      CALL CMOVE(X,S,500)
      GOTO 155
      DATA R/0.,97.5,99.5/
      DATA Q6/6*0055055055055/
      DATA Q/003306100000,003306200000,001100000000,001117400000,017400000000,
     &005500000000,005300000000,011011712512 2,011311111411 7,015015716516 2,015315115415 7,
     &011415714705 4,004012312412 2,004004012411 1,010512312304 0,011510504004 0/
      DATA MES/016316515116 4,016214515415 1/
      DATA TAB/4*"YES "/
  640 FORMAT(1X,"The data are un",A4,"able for evaluating materials")
  645 FORMAT(1H ,I4,1X,2(2X,F7.1,1X),2(2X,F9.5,1X),4(1X,F10.6,1X),2X,F7.0)
  650 FORMAT(1H-,9X,"(Sh)2=  ",F14.7,4X,"(Sf)2=  ",F14.7,//,10X,"  Sh2=  ",F13.6,5X,
     &"  Sf2=  ",F13.6,//,10X,"   Sh=    ",F10.5,5X,"    Sf=    ",F10.5,//,11X,"   H=    ",
     &F11.6,5X,"    F=    ",F11.6,//,10X,"    N=    ",I4,12X,"  Sfh=  ",F13.6,//)
  665 FORMAT(1H-,10X,"   U=  ",F14.7,5X,"   V=  ",F14.7,5X,"    W= ",F14.7,///,1H ,9X,
     &"    A=    ",F10.5,5X,"     B=    ",F10.5,9X,"VAR="3X,F10.5,8X,"STD="4X,F10.5/1H-)
  675 FORMAT(1H ,A2,/1H-8XA2,4(12X,A2,13XA2))
  680 FORMAT(1H 2A1,6A4/1XA1,2X,A14,2X,A2,"KILO=kgf/cm2",/1XA1,4(6A4,A1)/1X2A1,A2,2A1,8X,
     &2A4,2A1,A2/1XA1,8X2A4,A2,3(6A4,A1)/1X2A1,A2,3(6X,4HLCL ,F5.1,A2)/1XA1,4(6A4,A1)/1XA1,4X,
     &A4,A2,2X,2A4,A2,3(4X,A4,A2,2X,2A4,A2)/1XA1,2(2(2A4,A3,A1,3A4,A1)))
  695 FORMAT(1H ,A1,4(F10.1,A2,F11.5,A2))
  700 FORMAT(1H .4(6A4).A4,A1/1H-)
```

```
705    705 FORMAT(V)
710    710 FORMAT(1H ," DATA"4X"TIME"5X"STRESS"6X"TIME"7X"STRESS"8X"f.h"9X"h2"10X"f2"10X"h'"9X"H'",
715       &1H ,"POINT"4X"hour"5X"kilo"6(9X"Log")7X"hour"/1H ,5(1H-),2(2X,8(1H-)),6(2X,10(1H-))2X,
720       &3(1H-)/1H-)
735    735 FORMAT(1X,"DO YOU WISH THE 'Calculations' AND THE 'Statistics'",/,
740       &1X"AND THE LCL FOR 'Stress to Time' AND 'Time to Stress'  (YES,YES,YES,YES) ")
750    750 FORMAT(1X"ENTER THE THREE VALUES OF t FOR ",I4," DEGREES OF FREEDOM")
755    755 CALL EXIT
760        STOP
765        END
770        SUBROUTINE LECTURE(T,S,J,FT)
775        REAL T(500),S(500),R(500)
776 STRING FT
777        FILENAME FINP
778      PRINT,"ENTER FILENAME ";INPUT,FINP
780        READ(FINP,845,END=785,ERR=860)FT,R
781 PRINT,FT
785    785 K=I+2
790        DO 830 I=K,500
795        IF(R(I).EQ.0.)GOTO 820
800        J=J+1
805        S(J)=R(K-1)
810        T(J)=R(I)
815        GOTO 830
820    820 IF(R(I+1).EQ.0.)GOTO 875
825        GOTO 785
830    830 CONTINUE
835        PRINT 850
840        STOP
845    845 FORMAT(V)
850    850 FORMAT(1H ,"THERE ARE TOO MANY DATA.TYPE :"/1HO"CHANGE /(500)/(1000)/ *",
```

8.3 P.R.I. CONFERENCE

paper presented at 4th Plastics and Rubber Institute International Pipe Conference, Sussex University, 28-30 March, 1979.

AN ANALYSIS OF PAST AND FUTURE MARKETS FOR THERMOPLASTICS PIPES.

P. F. McNally
Phillips Petroleum Chemicals N. V. Belgium.

Production and Consumption data for the major European pipe producing nations are given and the major pipe markets for PVC and the Polyolefins are identified. Comparison is made with market data from the United States. Projections for the future of the European pipe industry are offered.

INTRODUCTION

Transportation by pipeline represents the cheapest mode of product transport today, as evidenced by the data (1) in Table 1. Amongst the proliferation of various pipeline materials, it is only right that Plastics should participate in this market; although, equally, it is to be recognised at the outset that plastics materials do not have any divine right to a monopoly at the expense of the more traditional materials and that the very rapid rates of growth achieved in the past are unlikely to be maintained in the future.

Pipelines and pipeline materials represent a very broad topic and thus for the purposes of this paper, consideration is restricted to the more commodity-type thermoplastic materials, such as the Polyolefins and PVC in the applications of public services and specialised industrial usage. The penetration of plastics into these fields of application is based on the inherent properties of these materials which confer advantages in use over and above those of metals. These properties are well known and include the economics of installed cost through easier handling, transportation and simpler jointing techniques, the resistance to the chemical and physical agression of the natural environment and the strength and durability to provide long-term service under the normal internal and external stresses at economical cost. However, less publicised are some of these materials' limitations, such as poor weathering resistance, tendancy towards brittle fractures under adverse conditions and the basic viscoelastic nature of thermoplastics in general. These limitations, unless resolved by the introduction of new techniques, could be one of the restrictions to further growth.

As a percentage of the present West European thermoplastics consumption, pipe at 8% represents a relatively small outlet, but in terms of extruded product, at 1.1 million kilometres, it is still impressive.

TABLE 1 - Energy Content of Transportation:

Transportation Mode	Ton-Miles/Gallon Fuel
Road	10
Rail	125
Sea	250
Pipeline	500

THE PAST

PVC

The past, at least up to the time of the OPEC crisis, was marked by tremendous growth rates in all plastics applications and, as a consequence, has heralded in widespread expansions not only of polymerisation capacity, but also conversion capacity; the full consequences of which we have yet to suffer.

Taking first the case of PVC because it is the most established thermoplastic pipe material. West European PVC consumption has increased at an average annual growth rate of 8.8% from 1965 to 1978. In the same time period, PVC consumption for the manufacture of rigid pipe and fittings has grown from 195 KMT (16% of the total PVC consumption in 1965) to 905 KMT (25% of the total PVC consumption expected for 1978) representing an AAGR of 12.7%. The West European countries accounting for the relative shares of this growth(2, 3) are shown in Table 2:

TABLE 2 - W. European PVC Pipe Production:

	PVC Pipe Production in KTA				AAGR %	
Country	1965	1970	1973	1978	1965/73	1973/78
Benelux	32	72	109	102	16.6	(1.3)
France	23	85	185	192	29.8	0.7
Italy	30	49	80	90	13.0	2.4
Nordic Area	20	40	100	108	22.3	1.6
Spain	5	12	30	45	25.1	8.4
UK	27	68	90	98	16.2	1.7
W. Germany	55	145	255	228	21.1	(2.2)
Others	3	16	31	42	33.3	7.0
Total:	195	487	880	905	20.7	0.6
Total PVC:	1220	2356	3395	3675	13.6	1.6
% Pipe:	16.0	20.7	26.0	24.6		

There is a clear case that of all the plastics materials, the demand for PVC is the most closely tied to the cyclical economic trends and that as economic activity declines, the PVC demand declines. The building and construction industries directly or indirectly use or influence over 50% of the PVC consumption, of which one of the major components is pipe, conduit and fittings. In building and construction the rôle of ever-increasing labour costs is the key to this end use and the acceptance of PVC pipe is based not only on the lower initial costs, but also lower installation costs, due to reduced on-site labour requirements and virtual freedom from maintenance.

The principal applications are for potable water mains, rainwater and sewage systems, land drainage and conduit. Over 80% of rigid PVC piping is consumed directly or indirectly by the construction industry. Growth is still likely to occur in these market segments, due to increasing market penetration, particularly for cast-iron replacement. The principal competitive products, apart from the traditional materials of asbestos cement and ceramics, are polypropylene, ABS and the polyethylenes. Other competitive materials find favour in the more specialised, lower-volume applications, and are unlikely to have any significant influence on the future rate of growth of PVC.

The Polyolefins

Polyethylene, both the high and low density types and polypropylene constitute at present a much smaller proportion of the thermoplastics pipe market than PVC. Table 3 shows an estimate of the major producing nations in Western Europe:

TABLE 3 - Estimated Polyolefins Pipe Production KTA:

Country		1970	1973	1977
Benelux	LDPE	4.5	8.0	7.5
	HDPE	1.5	2.8	4.2
France	LDPE	15.0	29.0	25.0
	HDPE	1.0	2.5	3.0
W. Germany	LDPE	8.0	10.0	6.0
	HDPE	8.0	11.5	16.0
Nordic Area	HDPE	7.0	10.0	12.5
UK	LDPE	3.2	5.3	9.0
	HDPE	1.6	3.7	4.9
Total W. Europe	HDPE	20.0	30.0	40.0
	LDPE	35.0	59.0	-
	P.P.	-	-	5.0

The application areas of the polyolefins are more fragmented than those of PVC and the degree of importance varies from country to country. On a purely economic basis, for small diameters, low density polyethylene is preferred to high density polyethylene and polypropylene competes with ABS for higher temperature applications, such as domestic waste water outlets. High density polyethylene has been credited with much dormant potential, but the recent assistance of both national and international specifications have virtually assured its future in gas distribution piping and extrusion facilities enabling HDPE to be produced in pipe diameters up to 1,600m.m. open up new horizons, especially for insertion techniques into corroded lines for sewers, potable water and gas networks.

MARKET SEGMENTS

Historically, West Germany has been the dominant thermoplastics pipe and fittings producer accounting for a quarter of the total produced in Western Europe. The growth in pipe and fittings production is illustrated in Table 4:

TABLE 4 - W. German Plastics Pipe and Fittings Production

Year	MT	Year	MT
1963	31,500	1972	236,500
1968	105,400	1973	261,000
1969	134,500	1974	234,500
1970	167,800	1975	215,900
1971	204,500	1976	241,500

A major factor in this growth has been the use of PVC in the water supply network (Table 5) where currently some 60% of new installations are in plastics materials and notably in the areas of Niedersachsen and Nordrheim-Westfalen.

TABLE 5 - W. German Water Supply Network - %

	1968	1975
Cast Iron	70.4	62.3
Steel	10.4	7.7
Asbestos Cement	9.2	10.3
Plastics	9.0	19.0
Other	1.0	0.7

In most national potable water networks PVC is the preferred material other than for the trunk main supply lines, which are either ductile iron or asbestos cement in diameters up to 2 metres. PVC has been used in the UK since 1958 and is now installed at an annual rate of some 50,000MT. In Holland, some 85% of the total plastics pipe in the potable water network is in PVC; the use of the Polyolefins being reserved predominantly for either

house services or where river crossings or installations across dykes are necessary. In plumbing other than potable water services, one area where PVC is meeting intense competition is in hot water waste and discharge systems, where materials of higher dimensional stability are preferred. ABS has the advantage of ease of jointing with solvent cements allied to a much higher impact strength compared to Polypropylene, but both materials are less susceptible to the high water discharge temperatures from domestic appliances, such as washing machines and dishwashers. However, this is contrary to the situation in France where PVC still shows promising growth in this market segment.

TABLE 6 - French Plastics Pipe Consumption - MT:

	1973	1975	1978 Est.
Potable Water	70, 300	46, 500	57, 600
Soil Pipe	11, 000	7, 500	9, 600
DWV	59, 200	48, 600	65, 300
Conduit	37, 200	44, 200	55, 300
Other	29, 000	20, 000	21, 700
Total (PE, PVC)	206, 800	166, 800	209, 500

The main portion of electrical conduit in France, both burried and in-house, is made from foamed PVC in order to achieve a favourable price/wall-rigidity relationship. However, the in-house electrical and telephone duct is moving from PVC to expanded polyethylene and the expansion and modernisation of the telephone system heralded for France during the next five years, will call for substantial consumption of both material types.

In the drainage market segment, the storm water culverts laid alongside motorways and main roads, are necessarily of large diameter in order to rapidly remove the high volumes of surface water. The principal material used is concrete pipe with competition in the smaller sizes being PVC and vitrified clay and in the larger sizes GRP. However, for sewage applications, PVC offers a high rigidity to price ratio compared to other plastics materials and is used quite extensively in most European countries and is now some 20% of the total in Holland, although it is rarely used in diameters above 315mm. The situation in Spain is somewhat different in that, due to the cheaper raw materials and labour and the subsidised energy costs of the cement industry, concrete pipe is considerably more economic.

TABLE 7 - Indicative Spanish Pipe Prices:

External Diameter	Price Ptas/Metre
60mm concrete	98
60mm HDPE	180
400mm concrete	880
400mm HDPE	3, 500

Prices include proportional share of joints and fittings.

One area of future interest is the relining of sewer systems such as those in the west of Holland; where, due to the high water table, all such pipe lines are laid on wooden beds. When subsidence occurs, the rigid pipelines break, causing infiltration and subsequent line blockage. Although relining itself is not new, the advent of remote tapping possibilities with HDPE greatly reduce the overall costs of the operation.

The last market segment to be considered, that of gas distribution, has been the one most subject to recent change; first from the viewpoint of the advent of oil gasification and then in turn North Sea gas and secondly from the availability of complete plastic pipe and fittings systems. The declining trends for PVC, grey iron and asbestos cement are due to two prime factors: firstly, the greater preoccupation with safety and the use of tougher pipeline materials; and secondly, the trend towards higher distribution pressures at which these materials are not authorised for use. The strong tendency to change from unplasticised PVC to higher impact resistant PVC grades and HDPE is due to not only a desire for higher impact strength, but also chemical resistance, higher resistance and overall greater safety possibilities. There is also concern over the effect of the gas constituents on the plastics pipe lines and here the polyethylene has a big advantage over PVC.

The standard for cost purposes is still PVC pipe with a rubber ring push-fit joint. This system is cheap, easily and quickly made and relatively fool-proof from the point of view of installation by the contractors. Thus the modified PVC systems are well placed since, although the monolithic joint of polyethylene is psychologically good, it is approximately 40% more expensive. In many service line installations, the number of fittings and joints on a cost basis far outweighs the cost of the pipe.

THE FUTURE

The period up to 1973, conveniently called the OPEC crisis, was marked by very high increases in growth, especially the period 1970-73. Since that time, three main influences have drastically reduced the rate of growth of plastics pipe; the first being a general levelling-off of demand as the saturation point was approached, and the second being a price increase in the basic raw materials, coupled with a general malaise in the economy. Public purchasing authorities have had to effectively reduce quantities purchased in order to stay within given budgets until such time as greater credit approval has been obtained. At the same time, the downward trend of the building industry, both the public and private sectors, resulted in an overall slackening in demand for pipework. In Germany the number of new housing starts dropped from a high of 700,000 in 1974, to some 400,000 in 1977. The situation has been equally bad in the UK[4], the respective figures being:

1972	361,322	..		1974	259,739
1973	337,214			1978	155,000
		1979 Est.	135,000		

A final influence is the general decline in the intra-Europe export market as hitherto production deficient countries have become self-sufficient in production capacity and themselves entered the export market. This is particularly true of PVC where the net trade balance[6] within the common market has diminished to some 50% of the 1970 levels. Conversely, exports outside the EEC area have doubled, but these must be considered as a temporary situation considering the PVC capacity being erected in the traditional export markets, the favourable economics of feedstock and polymers in the Middle East, and the ever-increasing costs of transportation of pipe over long distances.

TABLE 8 - Net Trade Balance

	PVC		Polyethylene		
	1970	1975	1970	1973	1975
Intra EEC	8,597	4,322	1,248	2,775	2,775
Extra EEC	5,764	11,843	1,438	2,011	1,823
Total:	14,361	16,165	2,686	4,786	4,598

The greater productivity and competition among companies in resin manufacture have all exerted in the past an influence in reducing the price of the pipe resins. In the case of PVC (Table 9) the major factors have been the change from acetylene to ethylene as basic feedstock and economics of scale from larger production facilities.

TABLE 9 - Price of Suspension PVC (Base 1960 = 100)

1961	1965	1968	1978
95	85	71	105

However, prices have now dropped to a point where the return on investment is less than the prevailing interest rates, resulting in a stagnation of capital spending. Equally important is that a relatively increasing share of new investment has to be spent on pollution control hardware. It is therefore reasonable to expect an annualised escalation factor of at least 7% until the early 1980's.

Naphtha is the major feedstock of Europe's Petrochemical industry and this fact was brought home sharply when the spot price zoomed up from $22/ton in 1972 to $180/ton, then decreased to the lower 90's in early 1975. Naphtha pricing is influenced mainly by crude oil prices and the trends in refinery runs, both of which are leading towards higher monomer prices (Table 10) which in turn means higher polymer prices, in order to provide the adequate return to maintain growth in our industry.

TABLE 10 - W. Europe Monomer Price Forecast $/MT

Monomer	1st Qtr. 1976	1980
Ethylene	300	450
Propylene	200	345
Styrene	460	710
VCM	340	520

CONCLUSIONS

The West European Pipe Industry has a value today of some $1.3 milliard ($10^9$) but is entirely dependent on the state of economic affairs in the area it serves. Whilst most national economics are in a stronger position than in the recent past, capital investment remains low; unemployment is high and rising; and in strong currency areas, trade is shrinking. Taken together, these developments lead to only a small growth expectation for the medium term, leading to the Orwellian Doomsday of 1984. The construction industry upon which much of the pipe industry exists, is a function not only of the general economy, but also related to the growth in population, which is currently slowing down. It is for these reasons that major new applications for thermoplastics pipe systems need to be researched. Promising areas on the horizon include solar energy systems, involving the use of plasticised PVC, LDPE and polypropylene pipework, hot and cold plumbing which would generate sales of approximately 12-18 Kg of pipework per household (6), and the whole new area of large and very large diameter pipe. In this context must be considered the pipeline transportation by hydraulic or pneumatic means. Gradient slurry lines are not new, but more effort is being expended on pressurised slurry lines for coal transport, iron ore, clay and limestone. In addition, pilot plant facilities for transportation of capsules in pipelines are being built.

Significant developments in polymer technology will also be made; the most recent being the assignment by the United States Plastics Pipe Institute of the first 800 psi rating given to a polyethylene pipe. Such pipe offers the advantage of either higher pipeline pressures or thinner walls for standard pressures, compared to the more traditional 630 psi rated polyethylene pipe.

Finally, as shown in Table 11 the estimated 1978 consumption of plastics pipe in the major producing countries of Europe still lags behind that of the United States. It is thus reasonable to expect these countries in the near term to approach closer to the U.S. usage figures and that the other European countries will show above average growth rates as their pipe usage approaches that of the major Common Market nations.

TABLE 11 - Pipe Usage Factors

Country	PVC		HDPE	
	Kg/Capita	Kg/Km^2	Kg/Capita	Kg/Km^2
Benelux	4.3	1,512	0.18	62
France	3.7	351	0.06	5.5
UK	1.7	390	0.09	19.5
W. Germany	3.6	872	0.26	61.2
EEC	2.8	-	0.12	-
W. Europe	2.4	-	0.10	-
USA	3.9	85	1.00	22.0

REFERENCES

1. Watkins, R.K. March 1977 "Principles of Structural Performance of Buried Pipes" Utah State University.
2. Pardos, Jaques F. 1974-1978 "Plastiques Modernes et Elastomères".
3. European Chemical News 1969, October 17th.
4. U.K. House Builders Federation. 1978, Daily Telegraph 15th September, page 8.
5. EUROSTAT Nimexe 1970-75, Deel D, Hoofdstuk 39-43.
6. Heilmayer, P.F. 1976 "Plastics Engineering" January, page 26.

CHAPTER 9: REFERENCES

1. WATKINS R.K., "Principles of Structural Performance of Buried Pipes", Utah State University, March (1977).

2. FRANCK S.A., "Outlook for Energy and Chemical Feedstocks in the European Climate", EVAF Conference, Helsinki, May (1977)

3. Private Communication from Seidgas, Spain

4. Private Communication from Veg-Gasinstitut, Holland.

5. Phillips Petroleum Company Information

6. AKKERMAN W.J., BAKKER J., MUTTER F., 12° Congrès Mondial du Gaz, Nice (1973)

7. Petroleum Times, p. 37, October 19 (1976)

8. Internaitonal Standards Organisation, Document 9 of ISO/TCS/SC6/W.G.D. (1969)

9. International Standards Organisation, Document 5 of ISO/TCS/SC6/W.G.D. (1969)

10. U.K. House Builders Federation, Daily Telegraph p.8, September 15 (1978)

11. U.K. House Builders Federation, Daily Telegraph November 12 (1979)

12. HARRISON J.T., HORNE J.B., Session 1, 13 5th AGA Plastics Pipe Symposium, Houston, November (1974)

13. MUTSCHMANN J., G.W.F. 116, 7, (1975)

14. DE LA PEÑA J., Phillips Petroleum Internal Report, June (1976)

15. KOSSOFF R.M., Phillips Petroleum Internal Report, May (1977)

16. McNALLY P.G., Maintenance Eng. 4, 11, April (1967)

17. McNALLY P.F., Muanyag es Gumi 14, 1, Jan (1977)

18. McNALLY P.F., Paper 2, Petrochemistry Symposium Belgrade, 16th May (1974)

19. McNALLY P.F., Paper presented to Commission des Matières Synthetique, Brussels, 8th May (1974)

20. Phillips Petroleum Co., Technical Service Memorandum N° 243, Aug (1972)

21. GUILLOT R., "Les Matières Plastiques dans la Distribution d'Eau et Autres Fluides", (Ed. Eyrolles) Paris, (1960)

22. PETRO P.P., "Interim Report of Flow Capability of Polyethylene Pipe" (Unpublished) March (1971)

23. Plastics Pipe Institute Technical Report PP1-TR-14, March (1971)

24. DE VRIES A.J., Eurotest Technical Bulletin, XEW 663 (1970)

25. AYRES R.L., Session 5, 66-69, 3rd AGA Plastics Pipe Symposium, New Orleans, February (1971)

26. ALBRECHT R., Session 5, 78, 5th AGA Plastics Pipe Symposium, Houston, November (1974)

27. AGA Plastics Pipe Manual for Gas Service, 28-34, AGA Inc. New York, (1968)

28. ASTM D 3139-73, "Joints for Plastic Pressure Pipes Using Flexible Elastomeric Seals" (1973)

29. DE BLIEU I.K., Session 2, 17-20, 4th AGA Plastics Pipe Symposium, Denver, November (1972)

30. GRENIER G., CALDWELL R., Session 4, 84-87, 4th AGA Plastics Pipe Symposium, Denver, November (1972)

31. WITHERS W.B., Session 4, 82-83, 4th AGA Plastics Pipe Symposium, Denver, November (1972)

32. WILKINSON D.G., HALLIWELL F.B., Paper 5, 1-10, 3rd BPF Plastics Pipe Symposium, Southampton, September (1974)

33. WOLNIK M.A., Session 4, 78-81, 4th AGA Plastics Pipe Symposium, Denver, November (1972)

34. TURNER S., Trans. J. Plastics Inst., 95, August (1965)

35. DIETER G., "Mechanical Metallurgy", Chapter 4, 107, McGraw-Hill, Tokyo (1976)

36. DIETER G., "Mechanical Metallurgy", Chapter 1, 6, McGraw-Hill, Tokyo (1976)

37. BAWN C.E.H., Pl & Polymers, 373, October (1969)

38. ONYON P.F., "Physics of Plastics", Chapter 1, 9, (Ed. P.D. Ritchie) Iliffe, London (1965)

39. MILLER M.L., "The Structure of Polymers", Chapter 6, 257, Reinhold, New York (1966)

40. BULL A.L., Paper presented at Plastics and Rubber Institute Conference, Brussels (1976)

41. THORSTAD T., European Rubber Journal 161, 15-21, July (1979)

42. PIRRET D.J., European Rubber Journal 161, 11-15, July (1979)

43. MIERAS H., WILSON E., Journal IRI, 72-79, April (1973)

44. HAAF F., Information Chimie, 188, 215-227, April (1979)

45. KARAS G.C., WARBURTON B., Trans. J. Plastics Inst. 207, June (1962)

46. MASCIA L., University of Aston in Birmingham, M.Sc. notes.

47. BUCKNALL C.B., British Plastics, 84-86, December (1967)

48. KRAUS G., "Polymer Blends" (Ed. D.R. Paul and S. Newman) Academic Press, New York (1976)

49. BUCKNALL C.B., British Plastics, 121-122, November (1967)

50. WILLIAMS J.G., Trans. J. Plastics Inst., 119, June (1966)

51. TURNER S., Trans. J. Plastics Inst., 127, June, (1966)

52. FERRY J.D., "Viscoelastic Properties of Polymers" Chapter 2, 52, Wiley, New York (1970)

53. GOTHAM K.V., Plastics & Polymers, 309, August (1969)

54. RIDDEL M.N., Plastics Eng., 71, April (1974)

55. MILLER M.L., "The Structure of Polymers" Chapter 6, 237, Rheinhold, New York (1966)

56. VINCENT P.I., "Physics of Polymers" Chapter 2, 87-90 (Ed. P.D. Ritchie) Iliffe, London (1965)

57. TRELOAR L.R., "The Physics of Rubber Elasticity" Oxford University Press, London (1958)

58. SCHMIEDER K., WOLF K., Kolloid-Z, 134, 149 (1953)

59. HOFF E.A., ROBINSON D.W., WILLBOURN A.H., J. Polym Sci., 18, 161, (1955)

60. THURN H., Exakt Naturw., 31, 22, (1959)

61. SCHMIEDER K., WOLF K., Kolloid-Z, 127, 65, (1952)

62. KLINE D.E., SAUER J.A., WOODWARD A.E., J. Polym Sci., 22, 445, (1956)

63. McNALLY P.F., Phillips Petroleum Co. Internal Report, January (1978)

64. BAILEY G.C., REID J.A., (to Phillips) U.S. Patents 2581228, January (1952) and 2606940 August (1952)

65. CLARK A., HOGAN J.P., BANKS R.L., LANNING W.C., Ind & Eng Chem, 48, 7, July (1956)

66. Phillips Petroleum Company information

67. RENFREW A., MORGAN P., "Polyethylene", Iliffe, London (1960)

68. Phillips Petroleum Co., British Patent 862985 March (1963)

69. DOAK K.W., SCHRAGE A., "Crystalline Olefin Polymers", Chapter 8, 360, (Ed. A. Raff & K.W. Doak) Interscience, New York (1964)

70. FRIEDLANDER H.N., "Crystalline Olefin Polymers" Chapter 6, 222, (Ed. A. Raff & K.W. Doak) Interscience, New York (1964)

71. COSSEE P., VAN REIJEN L.L., Actes du 2ème Congrès Int. de Catalyse, 1679-1695, Techniq, Paris (1960)

72. SMITH D.C., Ind. & Eng. Chem., 48, 1162, July (1956)

73. HOGAN J.P., BANKS R.L., (to Phillips) U.S. Patent 2825721, March (1958)

74. BAWN C.E., Trans J. Plastics Inst., 337, February (1967)

75. BAWN C.E., Trans J. Plastics Inst., 374, October (1969)

76. KELLER A., Plastics & Polymers, 18, February (1975)

77. HOWARD J.B., Polym. Eng. & Sci., 127, July (1965)

78. BOYER R.F., Plastics & Polymers, 16, February (1973)

79. PRITCHARD J.E., MARTINOVICH R.J., BOEKE P., Plastics Techn., 6, 31, (1960)

80. PRITCHARD J.E., McGLAMERY R.M., BOEKE P., Modern Plastics, October (1959)

81. Phillips Petroleum Co. Technical Information Bulletin N° 20

82. SPERATI C.A., FRANTA W.A., STARKWEATHER H.W., J. Am. Chem. Soc., 75, 6127, (1953)

83. READING F.P., J. Polym. Sci., 32, 487, (1958)

84. PEARSON R.G., Plastics & Rubber, 1, 21, February (1976)

85. FLORY P.J., "Principles of Polymer Chemistry" 568-573, Cornel, New York (1953)

86. READING F.P., LOVELL C.M., J. Polym. Sci., 21, 157, (1956)

87. WALTER E.R., REDING F.P., J. Polym. Sci., 21, 561, (1956)

88. EICHHORN R.M., J. Polym. Sci., 31, 197, (1958)

89. BOYER R.F., Plastics & Polymers, 15, February (1973)

90. McCRUM N.G., READ B.E., WILLIAMS G., "Anelastic and Dieletric Effects in Polymeric Solids", 376, Wiley, New York (1967)

91. REDING F.P., FAUCHER J.A., WHITMAN R.D., J. Polym. Sci., 57, 483, (1962)

92. FAUCHER J.A., REDING F.P., Crystalline Olefin Polymers, Chapter 13, 686, (Ed. R.A.Raff & K. Doak) Interscience, New York (1965)

93. International Standards Organisation, Document 5 of ISO/TC 138/WG 5 (1973)

94. BAGLEY E.B., J. Appl. Physics, 28, 624, (1957)

95. BRAGEW C.G., Modern Plastics, 33, 199, (1956)

96. DECOSTE J.B., MALN F.S., WALLDER V.T., Ind. & Eng. Chem., 43, 117, (1957)

97. CAREY R.H., ASTM Bulletin N° 167, 56, July (1950)

98. RICHARDS R.B., J. Appl. Chem.; 1, 370, (1951)

99. BOCKHOFF F.J., NEUMANN J.A., S.P.E.J., 10, 17, May (1974)

100. REISS J.H., LONGRA V.L., Wire & Wire Products, 33, 1182, October (1958)

101. HOWARD J.B., Polym. Eng. & Sci., 125, July (1965)

102. REBINDER P.A., Physik, 72, 191, (1931)

103. GILROY H.M., Bell Telephone Laboratories Internal Report

104. GIEWIEWSKI C., HOWARD J.B., "Engineering Design for Plastics", 764-768 (Ed. Baer) Rheinhold, New York (1964)

105. AYRES R.L., MARTINOVICH R.J., Unpublished Work

106. STANNETT V., YASUDA H., "Crystalline Olefin Polymers" Chapter 4, 138, (Ed. R.A. Raff & K. Doak) Interscience, New York, (1964)

107. British Gas Corporation, Engineering Research Station, Private Communication

108. HAWKINS W.L., WINSLOW F.H., "Crystalline Olefin Polymers" Chapter 8 (Ed. R.A. Raff & K. Doak) Interscience, New York (1964)

109. SCOTT G., Macr. Chem., 8, 319, (1973)

110. AMIN M., SCOTT G., TILLEKERATNE L., Eur. Polym.J. 10 (1974)

111. SCOTT G., American Chem. Soc. Symposium Series 25 (1976)

112. WRIGHT B., Plastics, 4-6, November (1963)

113. SCHAAF R., Verein Deutscher Ingenieure Symposium, 154-155, Baden-Baden, November (1979)

114. Phillips Petroleum Co. Technical Information Bulletin N° 26

115. BREDERECK P., "Recycling of Thermoplastic Waste" 120-121 (Ed. M.S. Welling) VDI-Verlag, Dusseldorf (1979)

116. KING A., Plastics & Polymers, 195, June (1968)

117. BRYDSON J.A., "Plastics Materials" Chapter 5, 77-78, Iliffe, London (1966)

118. SEDRIKS W., Stanford Research Institute Report N° 115, 13-33, August (1977)

119. LE BRASSEUR G., NICCO A., Informations Chemie, 177, 156, May (1978)

120. ESTEVEZ J.M., Trans J. Plastics Inst., 91, June (1965)

121. SCOTT G., "Atmospheric Oxidation and Antioxidents" 68, Elsevier, Amsterdam (1965)

122. MARTINOVICH R.J., Plastic Techn., 9, 45, November (1963)

123. MARTINOVICH R.J., HILL G.R., Appl. Polym. Symposia N° 4, 141-154 (1967)

124. MARTINOVICH R.J., Phillips Petroleum Co. Technical Information Bulletin N° 18 (1964)

125. VENN R.G., Trans J. Plastics Inst., 602, August (1967)

126. LATHM D.H., LEASHON J.A., Plastics & Polymers, 351, October (1971)

127. MARTINOVICH R.J., HILL G.R., Phillips Petroleum Co. Technical Information Bulletin N° 18 (1973)

128. International Standards Organisation, Document 64 of ISO/TC 138/WG 4, February (1973)

129. MARTINOVICH R.J., HILL G.R., SPE-Retec, Philadelphia, October (1972) and ISO Recommended Method R 879 "Resistance of Plastics to Xenon Arc", April (1973)

130. International Standards Organisation Recommended Method ISO R 527 (1966)

131. ASTM D 2565 "Operating Xenon Arc Exposure Apparatus" (1970)

132. ISO Draft 4892 "Plastics Exposure to Laboratory Light Sources", March (1976)

133. McNALLY P.F., Document 133 of ISO/TC 138/WG4/TG1 October (1974)

134. Private Communication from Uccle Observatory, Belgium

135. CARTIER H., Document 132 of ISO/TC 138/WG4/TG1, September (1974)

136. TANSLEY A.V., Document 120 of ISO/TC 138/WG4/TG1 May (1974)

137. International Standards Organisation. Document 97 of ISO/TC 138/WG4/TG1, September (1973)

138. For example, British Gas Standard BGC/PS/PL2 November (1976)

139. MULLER W., Document 51 of ISO/TC 138/WG4/TG1 November (1972)

140. ASTM D 2837 "Obtaining Hydrostatic Design Basis for Thermoplastic Pipe Materials" November (1969)

141. TAYLOR J., Appl. Physics, 18, 943, (1947)

142. MACHLIN et al., Am. Inst. of Mining & Metallurgical Engineers Bulletin, 2137 (1947)

143. RATNER et al., Inst. of Chem. Engineers N° 1, 2, 18 (1962)

144. CAREY et al., SPE J, 21, March (1956)

145. LARSON F.R., MILLER J., Trans A.S.M.E., 75, 765 (1952)

146. FISHER J.C., MacGREGOR C.W., Trans A.S.M.E., 67, 824 (1945)

147. FISHER J.C., MacGREGOR C.W., Trans A.S.M.E., 68, 11 (1946)

148. HOLLOMAN J.H., LUBAHN J.D., General Electric Review, 50, 28 (1947)

149. HOLLOMAN J.H., ZENER C., J. Appl. Physics, 17, 69 (1946)

150. DUSHMAN S., Proc. ASTM 29, 7 (1929)

151. SEITZ F., "Physics of Metals" 137-142, McGraw-Hill, New York (1943)

152. GUARNIERI G., MILLER J., Trans A.S.M.E., 41, 167, (1949)

153. HOLLOMAN J.H., JAFFE L.C., Trans A.I.M.E., 162, 223, (1945)

154. KANTER J.J., Trans A.S.M.E., 75, 772, (1952)

155. KANTER J.J., Trans A.I.M.E., 131, 385, (1938)

156. GOLDFEIN S., Modern Plastics, 139, May (1960)

157. FERRY, "Viscoelastic Properties of Polymers" Chapter 11, 294-301, Wiley, New York (1961)

158. SMITH J., J. Polym. Sci., 32, 99, (1958)

159. SMITH J., J. Polym. Sci., 42, 391, (1960)

160. CHANG F., 27th SPE-ANTECH., 15, Chicago, May (1969)

161. DIETER G.E., "Mechanical Metallurgy", 318-319, McGraw-Hill, Tokyo (1976)

162. CHANG F., J. Polym. Sci., 57, 949, (1962)

163. GOLDFEIN S., "Testing of Polymers", Vol. 4, 121, (Ed. Brown) Interscience, New York

164. REINHART F.W., Polym. Eng. & Sci., 285, October (1966)

165. RICHARD K., GAUBE E., DIEDRICH G., Kunstoffe 49, 516-525, (1959)

166. GLOOR E., Kunstoffe, 49, 120, (1959)

167. WHYMAN A.D., SZPAK E., S.P.E. J, 29, 77, (1973)

168. VAN DER VEGT A.K., Svenska Plastforeningen, Sektion OB, 3-4, (1960)

169. DUKES W.A., Brit. Plastics, 34, March (1961)

170. HARRISON J.T., SMITH T.R., Pipe Line Industry, May (1973)

171. HARRISON J.T., SMITH T.R., Session 2, 30-41, 4th AGA Plastics Pipe Symposium, Denver, November (1972)

172. EWING L., Document 102 of ISO/TC 138/WG4 (1975)

173. MARSHALL G.P., WILLIAMS J.G., Paper, 3rd Plastics Symposium, Southampton, September (1974)

174. PLATI E., WILLIAMS J.G., Polym. Eng. & Sci., 15, 470, June (1975)

175. PRICE J.B., Document 167 of ISO/TC 138/WG4/TG1 (1976)

176. WALKER E.F., MAY M.J., BISRA Open Report MG/E/307/67 (1967)

177. RICHARD K., GAUBE E., DIEDRICH G., Kuntstoffe, 49, 517, October (1959)

178. DIETER G.E., "Mechanical Metallurgy", Chapter 2, McGraw-Hill, Tokyo (1976)

179. Hoechst Plastics Bulletin, August (1971)

180. GAIKHORST G., 9ème Union de l'Ind. du Gaz IGU/D 2-64 (1964)

181. HARRISON J.T., HORNE J.B., Session 1, 14, 5th AGA Plastic Pipe Symposium, Houston, November (1974)

182. COONEY J.L., J. Appl. Polym. Sci., 8, 1889 (1964)

183. RICHARD K., GAUBE E., DIEDRICH G., German Plastics Digest, 49, 16, October (1959)

184. BS 4728, Procedure for Testing Thermoplastic Pipe (1971)

185. ASTM D 1598.63, Time to Failure of Plastics Pipe Under Long-Term Hydrostatic Pressure (1963)

186. DIN 8075, Specification for Hard PE-50 Polyethylene Pipe

187. AGA Plastics Pipe Manual for Gas Service, Appendix A, 1-10, AGA Inc., New York (1968)

188. BOWLES R.L., WOLFF G., "Computer Programmes for Plastics Engineers", N° 8 (Ed. Klein & Marshal) Rheinhold, New York

189. THONON L., General Electric Technical Centre, Brussels (1978)

190. For example, "Factoren t" Nederlands Normalisatie Instituut, NEN 1047, December (1967)

191. ISO Test Method 2506 "Polyethylene Pipes - Determination of Longitudinal Reversion"

192. Veg-Gasinstituut Specification "Hard P.E.-50 Buizen voor Gas" (1967)

193. McGLAMERY R.M., Phillips Petroleum Report 2601-60R (1960)

194. GAUBE E., DIEDRICH G., MULLER W., Kunstoffe, 66, 1, (1976)

195. BARTON S.J., CHERRY B.W., Polym. Sci. & Eng., 19, 8, June (1979)

196. CHERRY B.W., HOLMES C.M., British J. Appl. Physics, 2, 828, February (1969)

197. MUTTER F., BENJAMIN P., Paper 2.6, 3rd Plastics Pipe Symposium, Southampton, September (1974)

198. MUTTER F., Document 101 of ISO/TC 138/WG4/TG1, September (1973)

199. WOLF J., Nederlandse Gas, 87, 433, November (1967)

200. CLEREHUGH G., Paper 6, Plastics Service Pipe Symposium, Darlington, February (1969)

201. BRIGHTON C.A., BENTON J.L., Inst. Gas Eng. J., 419, July (1968)

202. MIERAS H.J., Shell Special Series Report DTSR 0014.73, March (1974)

203. FAULKNER P.G., ATKINSON J.R., Plastics & Polymers 109-117, June (1972)

204. FOTHAM K.V., Plastics & Polymers, 309, August (1969)

205. MENGES G., SCHMIDT H., Plastics & Polymers, 13-19, February (1970)

206. BRADFIELD S.A., Paper 4, 4th AGA Plastics Pipe Symposium, Dnever, November (1972)

207. REINHART F.W., Paper 5, 4th AGA Plastics Pipe Symposium, Denver, November (1972)

208. KUHLMANN H.W., WOLTER F., SOWELL S., SMITH R.B., Second Summary Report AGA Project ID-3-1 (1970)

209. Private Communication from PEMU, Solymer, Hungary (1976)

210. TANSLEY A.V., Document 50 of ISO/TC 138/WG4/TG1 (1972)

211. MUTTER F., TAKENS W., HAGAN M., Nederlandse Gas, 11, 3, November (1972)

212. International Standards Organisation Document 85 of ISO/TC 138/WG4/TG1 (1972)

213. Modern Plastics International, 9, 27, July (1979)

214. McNALLY P.F., Paper 1, 6, 4th PRI International Pipe Conference, Sussex, March (1979)

215. ALBRECHT R., Session 5, 79, 3rd AGA Plastics Pipe Symposium, New Orleans, February (1971)

216. LINDNER H., Paper 10, 3, 4th PRI International Pipe Conference, Sussex, March (1979)

217. International Standards Organisation, Recommendation R.17

218. International Standards Organisation, Document 207 of ISO/TC 138/WG4, March (1978)

219. HAYES R., WEBSTER W., Trans. J. Plastics Inst., 221, June (1964)

220. FINDLEY W.N., Trans J. Plastics Inst., 148, June (1962)

221. FINDLEY W.N., Trans J. Plastics Inst., 149, June (1962)

222. HAYES R., WEBSTER W., Trans J. Plast. Inst., 224-225, June (1964)

223. BRODY H., Plastics & Polymers, 24, February (1969)

224. MEYER D.D., FUNCK D.L., Session 3, 44, 3rd AGA Plastics Pipe Symposium, New Orleans, February (1971)

225. MOORE D.R., TURNER S., Plastics & Polymers, 44, February (1974)

226. CASH F.M., "Processing of Thermoplastics Materials", Chapter 4, 288-293, (Ed. E.C. Bernhardt) Rheinhold, New York (1958)

227. TAYLOR N.W., J. Appl. Physics, 18, 43, (1947)

228. BUCKNALL C.B., British Plast., 118-119, November (1967)

229. MENGES G., SCHMIDT H., Plastics & Polymers, 18, (1970)

230. SCHONEFELD G., WINTERGERST S., Kunstoffe, 61, 15, January (1971)

231. MAEGAARD S., Document 198 of ISO/TC 138/WG4/TG1 August (1977)